

MULTI-SITE PHOSPHORYLATION OF HEPATOCYTE Gi-2

NICHOLAS JAMES MORRIS

A thesis submitted to the University of Glasgow for the degree of Doctor of Philosophy

January, 1994.

Department of Biochemistry
University of Glasgow
Scotland

ProQuest Number: 13818749

All rights reserved

INFORMATION TO ALL USERS

The quality of this reproduction is dependent upon the quality of the copy submitted.

In the unlikely event that the author did not send a complete manuscript and there are missing pages, these will be noted. Also, if material had to be removed, a note will indicate the deletion.



ProQuest 13818749

Published by ProQuest LLC (2018). Copyright of the Dissertation is held by the Author.

All rights reserved.

This work is protected against unauthorized copying under Title 17, United States Code
Microform Edition © ProQuest LLC.

ProQuest LLC.
789 East Eisenhower Parkway
P.O. Box 1346
Ann Arbor, MI 48106 – 1346

Thesis
9776
copy 1



TO MY PARENTS

Acknowledgement

I am indebted to my supervisor Prof. Miles D. Houslay for his help and guidance during the preparation of this thesis, and I would also like to thank my industrial supervisor Dr. Paul Young at SmithKline Beecham, Epsom, Surrey for his assistance and helpful comments.

My thanks to Prof. C. A. Fewson, head of the Department of Biochemistry at Glasgow University, for providing the research facilities, and to the SERC and SmithKline Beecham for their financial support.

I would also like to thank the members of the Department of Biochemistry at Glasgow University and at SmithKline Beecham who helped create a lively and productive working environment. In particular I must thank at Glasgow University Dr. Mark Bushfield for his initial help with the project, Dr. Anne Savage for the hepatocytes and proof-reading, Li Zeng for hepatocytes, Gary Sweeney for the PKC antibodies, and Drs Margaret Lobban and Yasmin Shakur for the non-scientific conversations. At SmithKline Beecham I would like to thank Dr Greg Murphy for helping with the transition from a University to an industrial laboratory, and Gary Moore, Helen Chapman and Martin Hughes for the dosing of the Zucker rats. I must also thank rabbit 1867 without whose antisera for the immunoprecipitation of α -G_{i-2} this project would not have been possible.

Finally, my thanks goes to Peter Thetford and Richard Lovett for allowing me to stay at the house in Teddington whilst working at SmithKline Beecham, to Judith Hourston who was almost there at the beginning but did not make it to the end, and to my other friends and family for their support and encouragement during the period of study.

MULTI-SITE PHOSPHORYLATION OF HEPATOCYTE G_{i-2}

N. J. MORRIS, GLASGOW UNIVERSITY

Submitted for the degree of Doctor of Philosophy,
January 1994.

ABSTRACT

The phosphorylation of the heterotrimeric guanine nucleotide binding proteins has received increasing attention as a possible mode of controlling intracellular signalling. Here further evidence is submitted which helps to confirm the occurrence of such phosphorylation events in rat hepatocytes, to identify the phosphorylation site in $\alpha-G_{i-2}$, to examine the effects of insulin on the phosphorylation and to investigate any changes in the phosphorylation characteristics in animal models of type I and type II diabetes.

Using the antiserum 1867 it was possible to immunoprecipitate specifically the phosphorylated form of guanine nucleotide binding protein $\alpha-G_{i-2}$ from rat hepatocytes. By carrying out two dimensional phosphopeptide mapping and phosphoamino acid analysis of the protein it was found that phosphorylation occurred at two different serines and that one of the sites was most probably a protein kinase C (PKC) phosphorylation site whilst the other, although being protein kinase A (PKA)-dependent, was phosphorylated by an unknown kinase. By the use of the enzymes trypsin and *Staphylococcus aureus* V8, and theoretical analysis of possible phosphopeptides and their migration in the two-dimensional chromatography, it was possible to predict the phosphorylation site for the PKC-mediated phosphorylation as either serine 47 or serine 144, with serine 144 being the most likely candidate. The identification of the other phosphorylation site was not possible from the data produced. These sites were also found to occur in $\alpha-G_{i-2}$ from hepatocytes in streptozotocin-treated Sprague Dawley rats and in both lean and obese Zucker rats.

The incubation of hepatocytes from Sprague Dawley rats with insulin produced both a time and concentration dependent inhibition of the ^{32}P -labelling of $\alpha-G_{i-2}$ with the inhibition becoming significant after 2 minutes and insulin being effective at 1 nM. As it is known that the phosphorylation of $\alpha-G_{i-2}$ in rat hepatocytes is under the control of a futile cycle the point of action of insulin was investigated by the use of a range of ligands that interacted with the inositol phosphate and cAMP signalling pathways and hence stimulated the phosphorylation of $\alpha-G_{i-2}$. From these studies it was found that insulin was able to inhibit some of the ligand-induced phosphorylation of $\alpha-G_{i-2}$ and this indicated that insulin interacted with at least two components of the cycle, that is a kinase and a phosphatase. Interestingly, insulin also enhanced the phosphorylation induced by glucagon and the insulin inhibition of phosphorylation was reversed by amylin which also caused a cAMP-dependent phosphorylation. Evidence was also found that a cAMP-dependent phosphorylation of $\alpha-G_{i-2}$ may occur even when the cAMP system is not being stimulated.

The induction of type I diabetes in Sprague Dawley rats with streptozotocin caused a loss of the insulin-induced inhibition of $\alpha-G_{i-2}$ phosphorylation and also reduced the levels of phosphorylation of $\alpha-G_{i-2}$ achieved by 8-bromo-cAMP, PMA and glucagon and abolished the insulin enhancement of glucagon stimulated phosphorylation.

In the obese Zucker rat model of type II diabetes and their lean litter mates, insulin did not effect the phosphorylation of $\alpha-G_{i-2}$ and the enhancement of glucagon stimulated phosphorylations was lost. The compound BRL 49653, which normalises glucose handling in animal models of diabetes, did not effect the ligand induced phosphorylations of $\alpha-G_{i-2}$ other than abolishing the significant insulin inhibition of glucagon stimulated phosphorylation in the lean animals.

In conclusion, the activated insulin receptor does interact with $\alpha-G_{i-2}$ and although the result of this interaction on cellular signalling is not known it does seem likely that it is not involved in the control of glucose homeostasis but some other aspect of insulin signalling.

Table of Contents

Chapter One: Introduction	1
1.1 General Introduction	1
1.2 Cellular Signalling	1
1.2.1 Receptors	1
1.2.2 Mediators - the G-proteins	2
1.2.2.1 Mode of activation of heterotrimeric G-proteins	6
1.2.2.2 Heterotrimeric G-protein isoforms and interaction with effectors	9
1.2.3 Effector systems and secondary messenger generation	11
1.2.3.1 Adenylyl Cyclase and cAMP production	11
1.2.3.2 Phospholipase and inositol phosphates	12
1.2.3.3 Secondary messenger system crosstalk	15
1.2.4 Protein kinases and phosphatases	15
1.2.4.1 Protein kinase A	16
1.2.4.2 Protein kinase C	17
1.2.4.3 Protein phosphatases	20
1.3 Cellular signalling and disease	21
1.3.1 Diabetes	22
1.4 The insulin receptor	23
1.4.1 Insulin	23
1.4.2 Insulin receptor structure	24
1.4.2.1 The α -subunit	24
1.4.2.2 The β -subunit - structure and function	24
1.4.3 Insulin signalling - the activated receptor	25
1.4.3.1 Insulin receptor tyrosine kinase activity and the insulin receptor substrate	29
1.4.3.2 Secondary messenger production and the interaction of the insulin receptor with G-proteins	33
1.5 Aims	36
Chapter Two: Materials and Methods	37
2.1 Materials	37
2.1.1 Animals	37
2.1.2 Chemicals	37
2.2 Methods	37
2.2.1 Antibody production	37
2.2.2 Hepatocyte preparation	38
2.2.3 Phosphorylation of α -G _{i-2}	38
2.2.4 Solubilisation of cells and immunoprecipitation of α -G _{i-2}	39
2.2.5 SDS-PAGE	39
2.2.6 Elution of ³² P-labelled α -G _{i-2} from polyacrylamide gels	40
2.2.7 Precipitation and oxidation of eluted proteins	40
2.2.8 Proteolytic cleavage and desalting	41
2.2.9 Separation of ³² P-labelled enzymatic cleavage products	41
2.2.10 Recovery of peptides and secondary digests	44
2.2.11 Phosphoamino acid analysis	45
2.2.12 Prediction of enzyme cleavage products and mass charge ratios	45
2.2.13 Preparation of plasma membranes from rat hepatocytes	48

2.2.14	Protein determination	48
2.2.15	Western blotting	48
	2.2.15.1 Immunostaining of Western blots	48
2.2.16	Enzyme linked immuno - assay (ELISA)	49
2.2.17	Statistical analysis	49
Chapter Three: Multiple phosphorylation sites of α -G _{i-2}		50
3.1	Introduction	50
3.1.1	Phosphorylation of G-proteins	50
3.1.2	Kinase motifs	51
3.1.3	Protein structure	54
	3.1.3.1 Primary sequence of α -G _{i-2}	54
	3.1.3.2 Secondary structure of α -G _{i-2}	54
	3.1.3.3 Tertiary structure of α -G _{i-2}	58
3.1.4	Enzymatic cleavage, prediction of peptides and their movement in two-dimensional chromatography	61
	3.1.4.1 Prediction of tryptic cleavage products of α -G _{i-2}	62
	3.1.4.2 Prediction of V8 cleavage products	62
	3.1.4.3 Prediction of a-chymotrypsin cleavage products	62
3.2	Aims	63
3.3	Results	
3.3.1	Production and characterisation of polyclonal rabbit anti- α -G _{i-2} antisera	63
3.3.2	Two-dimensional thin layer analysis of phosphopeptides derived from α -G _{i-2}	67
	3.3.2.1 Trypsin digestion products	67
	3.3.2.2 V8 digestion of the tryptic peptides	74
	3.3.2.3 V8 digestion	91
	3.3.2.4 α -chymotrypsin	91
3.3.3	Phosphoamino acid analysis of peptides C1, C2, C3 and AN	91
3.3.4	Prediction of enzymatic digestion products of phosphorylated α -G _{i-2} and associated mass-charge ratios	91
3.3.5	Prediction of the secondary structure of α -G _{i-2}	91
3.4	Discussion	98
Chapter Four: Phosphorylation of α -G _{i-2} in hepatocytes from Sprague Dawley rats: Effects of insulin, amylin and streptozotocin induced diabetes		110
4.1	Introduction	110
4.1.1	Streptozotocin induced diabetes - type I model	110
4.1.2	Glucagon and amylin	111
4.2	Aims	113
4.3	Results	113
4.3.1	Effects of insulin on α -G _{i-2} phosphorylation - time course and dose response	113
4.3.2	Examination of ligand mediated phosphorylation of rat hepatocyte α -G _{i-2} and the effects of insulin	113
4.3.3	Amylin and the phosphorylation of α -G _{i-2} in Sprague Dawley rat hepatocytes	119
4.3.4	Effects of streptozotocin induced diabetes on the phosphorylation of α -G _{i-2} in Sprague Dawley rat hepatocytes	142

4.3.5	Two-dimensional phosphopeptide mapping of tryptic peptides of α -G _{i-2} from ligand treated hepatocytes from 'normal' and streptozotocin treated Sprague Dawley rats	148
4.4	Discussion	181
Chapter Five:	Phosphorylation of α -G _{i-2} in hepatocytes from lean (Fa/+) and obese (Fa/Fa) Zucker rats: Effects of various agents, insulin and BRL 49653	189
5.1	Introduction	189
5.1.1	The Zucker rat model of 'type II' diabetes	191
5.1.2	The thiazolidinediones and BRL 49653	192
5.2	Aims	197
5.3	Results	197
5.3.1	Treatment of Zucker rats with BRL 49653	197
5.3.2	Phosphorylation of α -G _{i-2} in lean (Fa/+) and obese (Fa/Fa) Zucker rat hepatocytes	198
5.3.3	Effects of chronic dosing of lean (Fa/+) and obese (Fa/Fa) Zucker rats with BRL 49653 on the phosphorylation of α -G _{i-2} in hepatocytes	198
5.3.4	Two-dimensional phosphopeptide mapping of tryptic peptides of α -G _{i-2} from lean (Fa/+) and obese (Fa/Fa) Zucker rats	210
5.3.5	Phosphoamino acid analysis of ligand stimulated phosphorylation of α -G _{i-2} in hepatocytes from lean (Fa/+) Zucker rats	215
5.3.6	Examination of the levels of α -G _{i-2} expression in lean (Fa/+) and obese (Fa/Fa) Zucker rat hepatocytes, membrane cytosol distribution and the effects of BRL 49653	215
5.3.7	Examination of the levels of PKC-isoform expression in lean (Fa/+) and obese (Fa/Fa) Zucker rat hepatocytes, membrane cytosol distribution and the effects of BRL 49653	215
5.4	Discussion	238
Chapter Six:	General conclusions	247
Appendix		255
References		277

List of figures

Chapter One:	Introduction	
1.1:	Phylogenetic trees of the heterotrimeric guanine nucleotide binding protein subunits	4
1.2:	Diagrammatic representation of the activation of heterotrimeric G-proteins	8
1.3:	Diagrammatic representation of the insulin receptor	27
1.4:	Diagrammatic representation of the interaction of the activated insulin receptor and the insulin receptor substrate	31
Chapter Two:	Materials and Methods	
2.1:	Diagrammatic representation of t.l.c. plate template used for two-dimensional chromatography analysis of phospho - peptides	43
2.2:	Template for the layout of t.l.c. plates used for phospho-amino acid analysis	47
Chapter Three:	Multiple phosphorylation sites of α -G _{i-2}	
3.1:	The primary sequence of rat α -G _{i-2}	56
3.2:	Tertiary structure of α -G _{i-2}	60
3.3:	Immunoprecipitation of ³² P labelled α -G _{i-2} with antisera 1867, 1868, 2394 and 1432	66
3.4:	Specificity of the immunoprecipitation of α -G _{i-2} by antisera 1867	69
3.5:	Phosphopeptide map of α -G _{i-2} from Sprague Dawley rat hepatocytes incubated with vehicle solution and then digested with trypsin	71
3.6:	Phosphopeptide map of α -G _{i-2} from Sprague Dawley rat hepatocytes incubated with PMA and then digested with trypsin	73
3.7:	Phosphopeptide map of α -G _{i-2} from Sprague Dawley rat hepatocytes incubated with 8-bromo-cAMP and then digested with trypsin	76
3.8:	Phosphopeptide map of α -G _{i-2} from Sprague Dawley rat hepatocytes incubated with vehicle solution and then digested with trypsin: shortened digestion period	78
3.9:	Phosphopeptide map of α -G _{i-2} from Sprague Dawley rat hepatocytes incubated with vehicle solution and then first digested with trypsin followed by V8	80

3.10:	Phosphopeptide map of α -G _{i-2} from Sprague Dawley rat hepatocytes incubated with vehicle solution and digested with trypsin: Digestion of tryptic peptide C1 with V8 to give C2'	82
3.11:	Phosphopeptide map of α -G _{i-2} from Sprague Dawley rat hepatocytes incubated with vehicle solution and digested with trypsin: Digestion of tryptic peptide C2 with V8 to give C2' and C2''	84
3.12:	Phosphopeptide map of α -G _{i-2} from Sprague Dawley rat hepatocytes incubated with vehicle solution and digested with trypsin: Digestion of tryptic peptide C3 with V8 to give C3'	86
3.13:	Phosphopeptide map of α -G _{i-2} from Sprague Dawley rat hepatocytes incubated with 8-bromo-cAMP and digested with trypsin: Digestion of tryptic peptide AN with V8 to give AN'	88
3.14:	Phosphopeptide map of α -G _{i-2} from Sprague Dawley rat hepatocytes incubated with 8-bromo-cAMP and digested with trypsin followed by V8	90
3.15:	Phosphopeptide map of α -G _{i-2} from Sprague Dawley rat hepatocytes incubated with vehicle solution and digested with V8	93
3.16:	Diagrammatic representation of the peptide distribution after two-dimensional chromatography	95
3.17:	Phosphoamino acid analysis of tryptic peptides C1, C2, C3 and AN	97
3.18:	The location of the seven proposed sites of serine phosphorylation shown in conjunction with predicted secondary structure and protein features of α -G _{i-2}	100
Chapter Four:	Phosphorylation of α -G _{i-2} in hepatocytes from Sprague Dawley rats: Effects of insulin, amylin and streptozotocin induced diabetes	
4.1:	Typical insulin time course auto-radiograph	116
4.2:	Time course of insulin induced phosphorylation of α -G _{i-2}	121
4.3:	Typical insulin dose response curve auto-radiograph	123
4.4:	Dose response curve for the insulin induced phosphorylation of α -G _{i-2} in Sprague Dawley rat hepatocytes	125
4.5:	A typical auto-radiograph of ³² P phosphorylated α -G _{i-2} from Sprague Dawley rat hepatocytes that have been challenged with vehicle solution, 8-bromo-cAMP, PMA, glucagon, insulin, 8-bromo-cAMP and insulin, glucagon and insulin, PMA and insulin, and vehicle solution	127
4.6:	Percentage phosphorylation of α -G _{i-2} in Sprague Dawley rat hepatocytes: Effects of 8-bromo-cAMP, PMA, glucagon, and insulin	129

4.7:	Percentage inhibition of ligand induced α -G _{i-2} phosphorylation in Sprague Dawley rat hepatocytes: Effects of insulin on 8-bromo-cAMP, PMA and glucagon induced phosphorylations	129
4.8:	Percentage phosphorylation of α -G _{i-2} in Sprague Dawley rat hepatocytes: Effects of forskolin, IBMX, and insulin	131
4.9:	Percentage inhibition of ligand induced α -G _{i-2} phosphorylation in Sprague Dawley rat hepatocytes: Effects of insulin or IBMX on forskolin, and IBMX induced phosphorylations	131
4.10:	Percentage phosphorylation of α -G _{i-2} in Sprague Dawley rat hepatocytes: Effects of forskolin, HA1004, and insulin	133
4.11:	Percentage inhibition of ligand induced α -G _{i-2} phosphorylation in Sprague Dawley rat hepatocytes: Effects of insulin or HA1004, on forskolin and HA1004 induced phosphorylations	133
4.12:	Percentage phosphorylation of α -G _{i-2} in Sprague Dawley rat hepatocytes: Effects of okadaic acid, HA1004, and insulin	135
4.13:	Percentage inhibition of ligand induced α -G _{i-2} phosphorylation in Sprague Dawley rat hepatocytes: Effects of insulin, on okadaic acid and HA1004 induced phosphorylations	135
4.14:	Percentage phosphorylation of α -G _{i-2} in Sprague Dawley rat hepatocytes: Effects of okadaic acid, PMA, and insulin	137
4.15:	Percentage inhibition of ligand induced α -G _{i-2} phosphorylation in Sprague Dawley rat hepatocytes: Effects of insulin or okadaic acid, on okadaic acid and PMA induced phosphorylations	137
4.16:	A typical auto-radiograph of immunoprecipitated α -G _{i-2} from hepatocytes from Sprague Dawley rats: Dose response for amylin, 10 ⁻¹² to 10 ⁻⁶ M	139
4.17:	Dose response curve for the amylin induced phosphorylation of α -G _{i-2} in Sprague Dawley rat hepatocytes	141
4.18:	Percentage phosphorylation of α -G _{i-2} in Sprague Dawley rat hepatocytes: Effects of amylin, PMA, glucagon, and insulin	145
4.19:	Percentage inhibition of ligand induced α -G _{i-2} phosphorylation in Sprague Dawley rat hepatocytes: Effects of amylin or insulin on amylin, PMA and glucagon induced phosphorylations	145
4.20:	Percentage phosphorylation of α -G _{i-2} in hepatocytes from 'normal' and streptozotocin treated Sprague Dawley rats: Effects of 8-bromo-cAMP, PMA, glucagon, and insulin	147
4.21:	Percentage inhibition of ligand induced α -G _{i-2} phosphorylation in hepatocytes from 'normal' and streptozotocin treated Sprague Dawley rats: Effects of inulin or insulin on 8-bromo-cAMP, PMA and glucagon induced phosphorylations	147

4.22:	Phosphopeptide map of α -G _{i-2} from Sprague Dawley rat hepatocytes incubated with insulin and then digested with trypsin	150
4.23:	Phosphopeptide map of α -G _{i-2} from Sprague Dawley rat hepatocytes incubated with glucagon and then digested with trypsin	152
4.24:	Phosphopeptide map of α -G _{i-2} from Sprague Dawley rat hepatocytes incubated with 8-bromo-cAMP and insulin and then digested with trypsin	154
4.25:	Phosphopeptide map of α -G _{i-2} from Sprague Dawley rat hepatocytes incubated with glucagon and insulin and then digested with trypsin	156
4.26:	Phosphopeptide map of α -G _{i-2} from Sprague Dawley rat hepatocytes incubated with forskolin and then digested with trypsin	158
4.27:	Phosphopeptide map of α -G _{i-2} from Sprague Dawley rat hepatocytes incubated with IBMX and then digested with trypsin	160
4.28:	Phosphopeptide map of α -G _{i-2} from Sprague Dawley rat hepatocytes incubated with forskolin and IBMX and then digested with trypsin	162
4.29:	Phosphopeptide map of α -G _{i-2} from Sprague Dawley rat hepatocytes incubated with forskolin and insulin and then digested with trypsin	164
4.30:	Phosphopeptide map of α -G _{i-2} from Sprague Dawley rat hepatocytes incubated with okadaic acid and then digested with trypsin	166
4.31:	Phosphopeptide map of α -G _{i-2} from Sprague Dawley rat hepatocytes incubated with amylin (1 μ M) and then digested with trypsin	168
4.32:	Phosphopeptide map of α -G _{i-2} from Sprague Dawley rat hepatocytes incubated with amylin (0.1 pM) and then digested with trypsin	170
4.33:	Phosphopeptide map of α -G _{i-2} from streptozotocin treated Sprague Dawley rat hepatocytes incubated with vehicle solution and then digested with trypsin	172
4.34:	Phosphopeptide map of α -G _{i-2} from streptozotocin treated Sprague Dawley rat hepatocytes incubated with 8-bromo-cAMP and then digested with trypsin	174
4.35:	Phosphopeptide map of α -G _{i-2} from streptozotocin treated Sprague Dawley rat hepatocytes incubated with PMA and then digested with trypsin	176
4.36:	Phosphopeptide map of α -G _{i-2} from streptozotocin treated Sprague Dawley rat hepatocytes incubated with glucagon and then digested with trypsin	178

4.37:	Phosphopeptide map of α -G _{i-2} from streptozotocin treated Sprague Dawley rat hepatocytes incubated with insulin and then digested with trypsin	180
Chapter Five:	Phosphorylation of α -G _{i-2} in hepatocytes from lean (Fa/+) and obese (Fa/Fa) Zucker rats: Effects of various agents, insulin and BRL 49653	
5.1:	Chemical structures of ciglitazone, CS-045, pioglitazone, englitazone (CP 68722) and BRL 49653	194
5.2:	A typical auto-radiograph of ³² P phosphorylated α -G _{i-2} from lean (Fa/+) Zucker rat hepatocytes that have been challenged with vehicle solution, 8-bromo-cAMP, PMA, glucagon, insulin, 8-bromo-cAMP and insulin, glucagon and insulin, PMA and insulin, and vehicle solution	200
5.3:	A typical auto-radiograph of ³² P phosphorylated α -G _{i-2} from obese (Fa/Fa) Zucker rat hepatocytes that have been challenged with vehicle solution, 8-bromo-cAMP, PMA, glucagon, insulin, 8-bromo-cAMP and insulin, glucagon and insulin, PMA and insulin, and vehicle solution	202
5.4:	Percentage phosphorylation of α -G _{i-2} in lean (Fa/+) and obese (Fa/Fa) Zucker rat hepatocytes: Effects of 8-bromo-cAMP, PMA, glucagon, and insulin	204
5.5:	Percentage inhibition of ligand induced α -G _{i-2} phosphorylation in lean (Fa/+) and obese (Fa/Fa) Zucker rat hepatocytes: Effects of insulin on 8-bromo-cAMP, PMA and glucagon induced phosphorylations	204
5.6:	A typical auto-radiograph of ³² P phosphorylated α -G _{i-2} from hepatocytes from BRL 49653 dosed lean (Fa/+) Zucker rats that have been challenged with vehicle solution, 8-bromo-cAMP, PMA, glucagon, insulin, 8-bromo-cAMP and insulin, glucagon and insulin, PMA and insulin, and vehicle solution	206
5.7:	A typical auto-radiograph of ³² P phosphorylated α -G _{i-2} from hepatocytes from BRL 49653 dosed obese (Fa/Fa) Zucker rats that have been challenged with vehicle solution, 8-bromo-cAMP, PMA, glucagon, insulin, 8-bromo-cAMP and insulin, glucagon and insulin, PMA and insulin, and vehicle solution	208
5.8:	Percentage phosphorylation of α -G _{i-2} in lean (Fa/+) and BRL 49653 dosed lean (Fa/+) Zucker rat hepatocytes: Effects of 8-bromo-cAMP, PMA, glucagon, and insulin	212
5.9	Percentage inhibition of ligand induced α -G _{i-2} phosphorylation in lean (Fa/+) and BRL 49653 dosed lean (Fa/+) Zucker rat hepatocytes: Effects of insulin on 8-bromo-cAMP, PMA and glucagon induced phosphorylations	212

5.10:	Percentage phosphorylation of α -G _{i-2} in obese (Fa/Fa) and BRL 49653 dosed obese (Fa/Fa) Zucker rat hepatocytes: Effects of 8-bromo-cAMP, PMA, glucagon, and insulin	214
5.11	Percentage inhibition of ligand induced α -G _{i-2} phosphorylation in obese (Fa/Fa) and BRL 49653 dosed obese (Fa/Fa) Zucker rat hepatocytes: Effects of insulin on 8-bromo-cAMP, PMA and glucagon induced phosphorylations	214
5.12:	Phosphopeptide map of α -G _{i-2} from lean (Fa/+) Zucker rat hepatocytes incubated with vehicle solution and then digested with trypsin	217
5.13:	Phosphopeptide map of α -G _{i-2} from lean (Fa/+) Zucker rat hepatocytes incubated with PMA and then digested with trypsin	219
5.14:	Phosphopeptide map of α -G _{i-2} from lean (Fa/+) Zucker rat hepatocytes incubated with 8-bromo-cAMP and then digested with trypsin	221
5.15:	Phosphopeptide map of α -G _{i-2} from obese (Fa/Fa) Zucker rat hepatocytes incubated with vehicle solution and then digested with trypsin	223
5.16:	Phosphopeptide map of α -G _{i-2} from obese (Fa/Fa) Zucker rat hepatocytes incubated with PMA and then digested with trypsin	225
5.17:	Phosphopeptide map of α -G _{i-2} from obese (Fa/Fa) Zucker rat hepatocytes incubated with 8-bromo-cAMP and then digested with trypsin	227
5.18:	Phosphoamino acid analysis of phosphorylated α -G _{i-2} from lean (Fa/+) Zucker rat hepatocytes incubated with 8-bromo-cAMP, PMA and insulin	229
5.19:	Level of α -G _{i-2} present in hepatocytes from lean (Fa/+) and obese (Fa/Fa) Zucker rat hepatocytes	231
5.20:	Membrane and cytosol distribution of α -G _{i-2} in Zucker rat hepatocytes	231
5.21:	Level of δ -PKC present in hepatocytes from lean (Fa/+) and obese (Fa/Fa) Zucker rat hepatocytes	234
5.22:	Membrane and cytosol distribution of δ -PKC in Zucker rat hepatocytes	234
5.23:	Level of ϵ -PKC present in hepatocytes from lean (Fa/+) and obese (Fa/Fa) Zucker rat hepatocytes	237
5.24:	Membrane and cytosol distribution of ϵ -PKC in Zucker rat hepatocytes	237
5.25:	Level of γ -PKC present in hepatocytes from lean (Fa/+) and obese (Fa/Fa) Zucker rat hepatocytes	240
5.26:	Membrane and cytosol distribution of γ -PKC in Zucker rat hepatocytes	240

5.27: Level of ζ -PKC present in hepatocytes from lean (Fa/+) and obese (Fa/Fa) Zucker rat hepatocytes	242
5.28: Membrane and cytosol distribution of ζ -PKC in Zucker rat hepatocytes	242

List of tables

Chapter One:	Introduction	
1.1	Isoforms of G-protein subunits	5
1.2	Isoforms of protein kinase C	19
1.3	Cellular responses to insulin and their respective time courses	28
Chapter Three:	Multiple phosphorylation sites of α -G _{i-2}	
3.1	The occurrence of protein kinase recognition motifs in α -G _{i-2}	52
3.2	Antibodies raised for the detection and immunoprecipitation of α -G _{i-2} from rat hepatocytes	64
3.3	Summary of the seven potential phosphorylation sites, associated kinase motifs and occurrence in other G-proteins	106
Chapter Four:	Phosphorylation of α -G _{i-2} in hepatocytes from Sprague Dawley rats: Effects of insulin, amylin and streptozotocin induced diabetes	
4.1	Time course of percentage insulin (10 μ M) induced phosphorylation of α -G _{i-2} in Sprague Dawley rat hepatocytes	114
4.2	Induced levels of α -G _{i-2} phosphorylation by insulin in Sprague Dawley rat hepatocytes	114
4.3	Percentage stimulation of the phosphorylation of α -G _{i-2} in Sprague Dawley rat hepatocytes	118
4.4	Percentage inhibition of ligand induced phosphorylation of α -G _{i-2} in Sprague Dawley rat hepatocytes	119
4.5	Effects of different concentrations of amylin on the phosphorylation of α -G _{i-2} in Sprague Dawley rat hepatocytes	142
4.6	Ligand induced percentage stimulation of the phosphorylation of α -G _{i-2} in 'normal' and 'type I' diabetic Sprague Dawley rat hepatocytes	143
4.7	Percentage inhibition by insulin of ligand induced phosphorylation of α -G _{i-2} in 'normal' and 'type I' diabetic Sprague Dawley rat hepatocytes	148

Chapter Five:	Phosphorylation of α-G_{i-2} in hepatocytes from lean (Fa/+) and obese (Fa/Fa) Zucker rats: Effects of various agents, insulin and BRL 49653	
5.1	Percentage stimulation of the phosphorylation of α -G _{i-2} in lean (Fa/+) and obese (Fa/Fa) Zucker rat hepatocytes and the effects of BRL 49653	209
5.2	Percentage inhibition of ligand induced phosphorylation of α -G _{i-2} from lean (Fa/+) and obese (Fa/Fa) Zucker rat hepatocytes and the effects of BRL 49653 on the inhibition.	210
5.3	Summary of ELISA results for the detection of α -G _{i-2} and PKC-isoforms in whole cell preparations of hepatocytes from lean (Fa/+) and obese (Fa/Fa) Zucker rats, and the effects of BRL 49653	232
5.4	Cellular distribution of α -G _{i-2} and PKC-isoforms in lean (Fa/+) and obese (Fa/Fa) Zucker rat hepatocytes and the effects of BRL 49653	235

Abbreviations

ADP	Adenosine 5'-diphosphate
ATP	Adenosine 5'-triphosphate
BRL 49653	5-(4-[2-(N-methyl-N-(2-pyridyl)amino)ethoxy]benzyl)-thiazolidine-2,4-dione
cAMP	Cyclic adenosine 3', 5'-monophosphate
CP68722	(±)-5-[(3,4-dihydro-2-phenylmethyl-2H-1-benzopyran-6-yl)methyl]-thiazolidine-2,4-dione
CS-045	(±)-5-[4-(6-hydroxy-2,5,7,8-tetramethyl-chroman-2-yl-methoxy)-benzyl]-2,4-thiazolidinedione
DAG	Diacylglycerol
DNP	Dinitrophenyl
EDTA	Ethylene diaminetetraacetic acid
ELISA	Enzyme linked immuno-assay
G-protein	GTP binding protein
GABA	4-aminobutyric acid
GDP	Guanosine 5'-diphosphate
G _i	Inhibitory G-proteins
G _s	Stimulatory G-protein
GTP	Guanosine 5'-triphosphate
HA1004	N-(2'-guanidinoethyl)-5-isoquinoline-sulfonamide
IBMX	3-isobutyl-1-methylxanthine
IDDM	Insulin-dependent diabetes mellitus (type I diabetes)
Ins(1,4,5)P ₃	Inositol 1,4,5-trisphosphate
InsP	Inositol phosphate
IRS1	Insulin receptor substrate 1
m _r	Mass-charge ratio
NIDDM	Non-insulin-dependent diabetes mellitus (type II diabetes)
PDE	Phosphodiesterase
PI	Phosphatidyl inositol

PIP ₂	Phosphatidylinositol 4,5-bisphosphate
PKA	cAMP-dependent protein kinase (protein kinase A)
PKC	Protein kinase C
PKG	Cyclic guanosine 3'5'-monophosphate-dependent protein kinase
PLA ₂	Phospholipase A ₂
PLC	Phospholipase C
PLD	Phospholipase D
PMA	Phorbol 12-myristate 13-acetate
PTPase	Phosphotyrosine phosphatase
SDS-PAGE	Sodium dodecyl sulphate polyacrylamide gel electrophoresis
SEM	Standard error of the mean
SH2	src homology domain 2
SH3	src homology domain 2
TPCK	Tosylphenylalanylchloromethane
Tris	2-amino-2-hydroxymethyl-propane-1,3-diol

Publications by the author related to this thesis

Bushfield, M., Savage, A., Morris, N.J., and Houslay, M.D. (1993) A mnemonical or negative co-operativity model for the activation of adenylyl cyclase by a common G-protein coupled CGRP/amylin receptor. *Biochemical Journal* 293 229-236

Morris, N.J., Bushfield, M., Lavan, B.E., and Houslay, M.D. (1994) Multi-site phosphorylation of the inhibitory guanine nucleotide regulatory protein Gi-2 occurs in intact hepatocytes. *Journal of Biological Chemistry* (submitted for publication)

Chapter 1

Introduction

1.1 *General Introduction*

Recent years have seen an explosion in the knowledge and understanding of the transfer of information between cells, and from extra- to intracellular signals. Techniques such as receptor binding assays, patch clamping, secondary messenger assays, molecular biology, computer imaging, and monoclonal antibody technology have provided the means to probe what are now known to be complicated, subtle, and intricate systems of intracellular communications.

The interaction of biologically active compounds with cell surface receptors can effect cellular responses in three possible ways (see Martens, 1992; Michell, 1987). The effects can be produced by the opening of ion channels, the phosphorylation of intracellular proteins (see section 1.2.4) or the generation of a secondary messenger such as inositol phosphates (InsP) or cyclic nucleotides (e.g. adenosine 3',5'-monophosphate [cAMP]; see sections 1.2.3.2 and 1.2.3.1) which again can lead to the phosphorylation of proteins. The procedure for the production of secondary messengers requires three components namely; receptors (see section 1.2.1); mediators (see section 1.2.2); and effectors (see section 1.2.3; e.g. see Berridge & Irvine, 1989; Gilman, 1987; Neer & Clapham, 1988; Neubig & Thomsen, 1989; Rana & Hokin, 1990; see also Rodbell, 1992). The effectors then produce the intracellular secondary messengers (i.e. cAMP [see section 1.2.3.1] or InsP / DAG [see section 1.2.3.2]) which in turn can activate a series of dependent kinases (e.g. cAMP-dependent PKA [see section 1.2.4.1] and DAG-dependent PKC [see section 1.2.4.2]) resulting in the phosphorylation of intracellular proteins.

1.2 *Cellular Signalling*

1.2.1 *Receptors*

Cell surface receptors can be divided broadly into four classes and each class can then be further subdivided. The four receptor classes are those which form ligand gated ion channels (e.g. nicotinic acetylcholine, GABA, glycine), G-protein linked receptors (e.g. adrenergic, muscarinic), species expressing tyrosine kinase activity (e.g. insulin [see section 1.4], insulin-like growth factor, epidermal growth factor, platelet derived growth factor) and guanylate cyclase expressing receptors (e.g. atrial natriuretic peptide; see Neubig & Thomsen, 1989).

The ligand gated ion channel receptors are multi-subunit membrane spanning proteins which, upon the binding of a specific ligand, undergo a conformational change that allows a channel between the subunits to open and specific ions to flow across the cell membrane (see Michell, 1987; Neubig & Thomsen, 1989).

The G-protein (see section 1.2.2) linked receptors share a common structure. The receptor protein is folded to form seven transmembrane domains with the N-terminal on the extracellular face and the C-terminal on the intracellular surface (see Findlay & Eliopoulos, 1990; Iismaa & Shine, 1992; Martens, 1992; Reithmann, Gierschik & Jakobs, 1990). The receptor contains a ligand binding site formed from the transmembrane loops and a G-protein interaction site formed by a specific sequence of amino acids in the third intracellular loop (see Martens, 1992).

The G-protein linked receptors can be divided into several sub-groups depending on the cellular responses that are mediated by the G-protein they activate (see section 1.2.2; Neubig & Thomsen, 1989).

1.2.2 Mediators - the G-proteins

The G-proteins are a super-family of proteins which bind guanosine 5'-triphosphate (GTP) and have GTPase activity to produce the diphosphate form (GDP; see Linder & Gilman, 1992; Egan & Weinberg, 1993). Many such proteins have now been identified and these can be divided into two basic groups by molecular weight and structure. Both groups are involved in the transduction of extracellular signals but their composition and modes of action are different (see Reithmann *et al.*, 1990). One group consists of a family of closely related heterotrimeric proteins which are formed from α (17 different subunits, 36 - 52 kDa), β (4 different subunits, 35 - 37 kDa) and γ (5 different subunits, 6 - 8 kDa) subunits giving a protein of a final molecular weight in the range of 77 - 87 kDa (see section 1.2.2.2, table 1.1 and figure 1.1; see Gilman, 1987; Reithmann *et al.*, 1990; Taylor, 1990; Yamane & Fung, 1993). The other group does not have a heterotrimeric structure and because of their molecular weight (20 - 30 kDa) and tertiary structure have been termed 'small', 'mini' or monomeric G-proteins. Indeed, more than fifty 'small' G-proteins have been found in mammalian tissues (see Bokoch, 1993; Yamane & Fung, 1993).

Based on sequence homology, the 'small' G-proteins have been divided into four families *ras*, *rho*, *rab* and *arf* (see Bokoch, 1993). The *ras* family are involved in receptor mediated signalling, controlling cell proliferation and differentiation. The *rho* family in cytoskeletal assembly and the *rab* and *arf* proteins in the regulation of transport vesicles (see Balch, 1990; Bokoch, 1993; Egan & Weinberg, 1993).

Both the heterotrimeric and 'small' G-proteins can undergo covalent modifications, such as ADP-ribosylation, prenylation, acylation and phosphorylation (Jakobs, Bauer & Watanabe, 1985; Lounsbury *et al.*, 1993; Morris *et al.*, 1994; Sagi-Eisenberg, 1989) which are critical for their activity and cellular distribution (see Parenti *et al.*, 1993; Yamane & Fung, 1993).

Figure 1.1: Phylogenetic trees of the heterotrimeric guanine nucleotide binding protein subunits

Phylogenetic trees of α , β and γ subunits of the heterotrimeric guanine nucleotide binding proteins (taken from Birnbaumer, 1992).

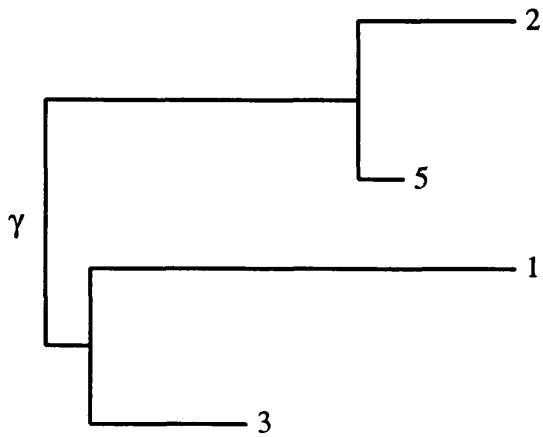
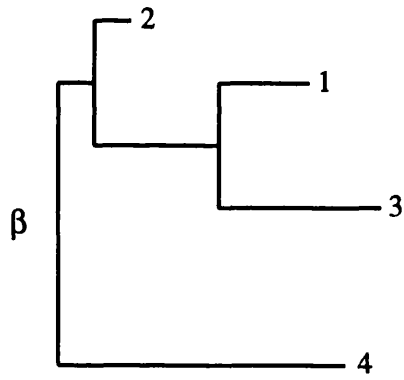
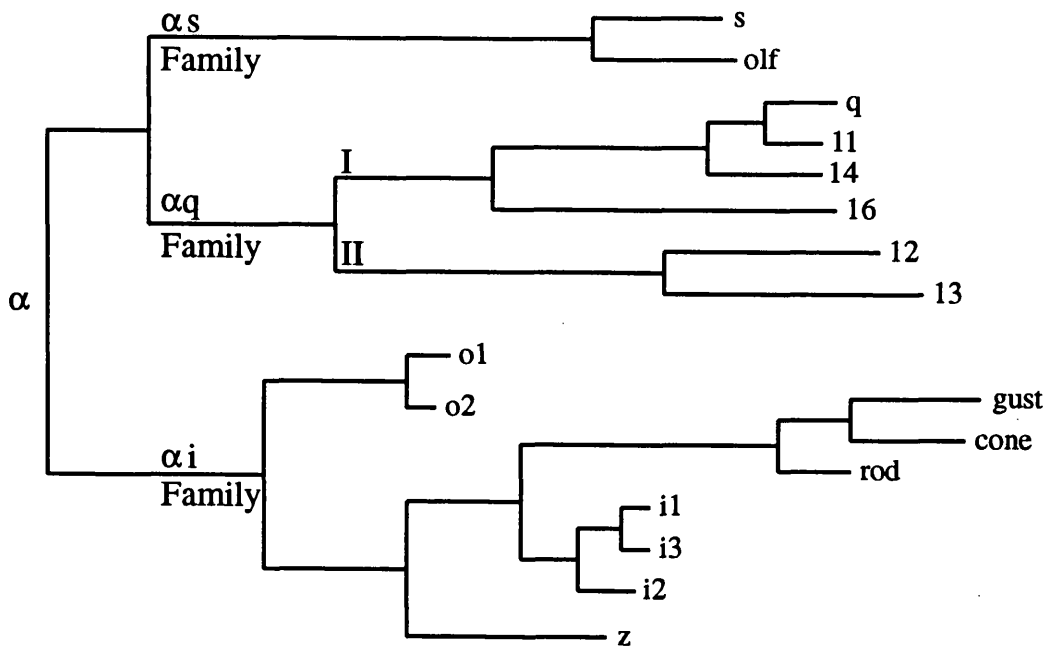


Table 1.1: Isoforms of G-protein subunits.

F	cDNA	MW	Toxin	SDS	AC	PLC	Effector PDE	K ⁺	Ca ²⁺	Intracellular Messenger	Location
α_s	s	46.5	CT	52	+			+Ca	+L	\uparrow cAMP \downarrow MP	Ubiquitous
α_s	olf	44.5	CT	45	+					\uparrow cAMP	Olfactory
α_q	q			42		$+\beta$				\uparrow IP ₃ \uparrow DAG	Ubiquitous
α_q	11	41.4		42		$+\beta$				\uparrow IP ₃ \uparrow DAG	Ubiquitous
α_q	14	41.5		42		$+\beta$				\uparrow IP ₃ \uparrow DAG	Ubiquitous
α_q	16	43.5		43		$+\beta$				\uparrow IP ₃ \uparrow DAG	Ubiquitous
α_q	12	44.0		43		?				?	Ubiquitous
α_q	13	44.0		43		?				?	Ubiquitous
α_i	o1	40.0	PT	39		$+\beta$			-L,N	\downarrow MP	Brain
α_i	o2	40.0	PT	39		$+\beta$			-L,N	\downarrow MP	Brain
α_i	gust		PT				+A			\downarrow cAMP	Taste buds
α_i	t-cone	40.1	PT	40			+G			\downarrow cGMP	Retinal cones
α_i	t-rod	40.0	PT	39			+G			\downarrow cGMP	Retinal rods
α_i	i1	40.4	PT/CT	41	-			+ir,A		\downarrow cAMP \uparrow MP	Ubiquitous*
α_i	i2	40.5	PT/CT	40	-			+ir,A		\downarrow cAMP \uparrow MP	Ubiquitous
α_i	i3	40.5	PT/CT	41	-			+ir,A		\downarrow cAMP \uparrow MP	Ubiquitous
α_i	z	40.9		41	-					\downarrow cAMP	Brain
β	1	37.4	-	36							Ubiquitous
β	2	37.3	-	35							Ubiquitous
β	3	37.2		36?							Ubiquitous
β	4			36?							Brain
γ	1	8.4	-	8							Retina
γ	2	7.9		6							Ubiquitous
γ	3			8							Brain
γ	4			5-10							?
γ	5										

F = G-protein family (see figure 1.1); cDNA = cDNA clone, o1 and o2 are splice variants of α_o ; MW = predicted molecular weight (kDa) based on genetic sequence; Toxin = toxin sensitivity of the protein, PT = pertussis toxin sensitive, CT = cholera toxin sensitive, CT/PT = cholera and pertussis toxin sensitive; SDS = observed molecular weight (kDa) on SDS-PAGE; Effectors: AC = adenylyl cyclase, PLC = phospholipase C ($+\beta$, activation of β isoform; $+\beta$, activates PLC but isoform is unknown; ?, effects PLC but effects unknown), PDE = phosphodiesterase (A = cAMP, G = cGMP), K⁺ = potassium channel (Ca = calcium activated, ir = inwardly rectifying potassium channel, A = ATP-inhibited potassium channel), Ca²⁺ = calcium channel (L = L-type, N = N-type) [$+$ = positive effect (activation); $-$ = negative effect (inhibition)]; Intracellular messenger, IP₃ = D-myo-inositol 1,4,5-trisphosphate, DAG = diacylglycerol, cAMP = cyclic adenosine 3',5'-monophosphate, cGMP = cyclic guanosine 3',5'-monophosphate, MP = membrane potential [\uparrow increases, \downarrow decreases]; Location, tissue distribution of the isoforms (* not in hepatocytes); $\beta\gamma$ -subunits form non-dissociating subunit which can activate adenylyl cyclases II and IV, inhibit adenylyl cyclase I, activate phospholipases C and A₂, and stimulate the phosphorylation of receptors (see Birnbaumer, 1992; Conklin & Bourne, 1993; Reithmann *et al.*, 1990).

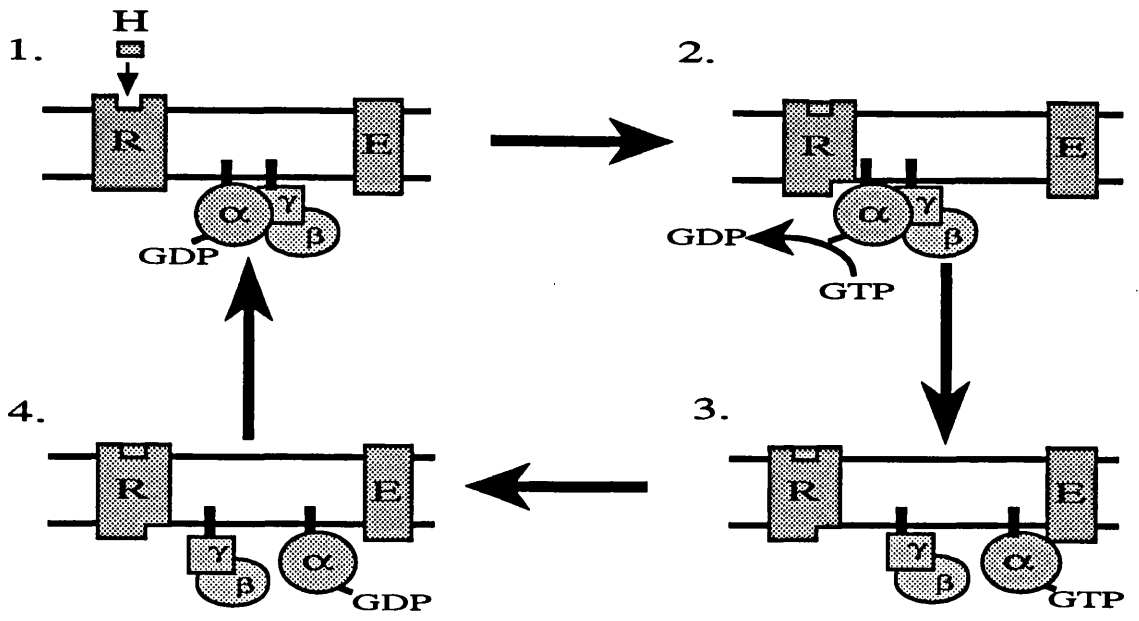
1.2.2.1 Mode of activation of heterotrimeric G-proteins

The heterotrimeric G-proteins are found associated with the cytoplasmic face of the plasma membrane (see Spiegel *et al.*, 1991). The exact orientation of the heterotrimer within the membrane is unknown and initially it was thought that the β -subunit of the protein provided the main anchorage (see Neer & Clapham, 1988; Reithmann *et al.*, 1990) but there is now evidence that it is the α and γ -subunits that provide attachment (Spiegel *et al.*, 1991). The α -subunit possess the ability to bind guanosine 5'-triphosphate (GTP) and exhibits GTPase activity to produce the diphosphate form (GDP; see Reithmann *et al.*, 1990). The binding of a ligand to its cell surface receptor produces a conformational change in the receptor leading to activation of a G-protein. The activated G-protein then interacts with its effector molecules (see section 1.2.3). One ligand / receptor complex can activate several G-proteins which in turn can activate a number of effectors and so produce signal amplification (see Birnbaumer, Abramowitz & Brown, 1990; Neer & Clapham, 1988; Reithmann *et al.*, 1990; Yamane & Fung, 1993; Lamb & Pugh Jr, 1992). Initially it was thought that the termination of the G-protein signal, namely the hydrolysis of GTP, was under the control of the GTPase activity of the α -subunit but recent evidence indicates that the effector may also play a role in termination of the signal. Early experiments on GTP hydrolysis by the α -subunit in reconstituted systems indicated that the rate of hydrolysis was slower than would be expected for the physiological processes that were being controlled but it has now been found that if the hydrolysis rates are measured in the presence of the effector then the rates are significantly increased so reducing hydrolysis times to a physiological level (see figure 1.2; see Bourne & Stryer, 1992).

In the inactive state, GDP is bound to the α subunit, and this gives the G-protein a high affinity for $\beta\gamma$ subunits the binding of which increases the α -subunit's affinity for GDP. Interaction with the activated receptor results in the release of GDP from the α -subunit producing an α -subunit with an empty nucleotide binding site. In the absence of GTP, the activated receptor binds tightly to the $\alpha\beta\gamma$ complex. This then precipitates the binding of GTP to the α -subunit, which then undergoes a conformational change causing it to dissociate rapidly from the $\beta\gamma$ -subunits and the receptor (see Conklin & Bourne, 1993). The GTP- α subunit has a low affinity for receptors and $\beta\gamma$ -subunits, but a high affinity for its effector (e.g. ion channels, adenylyl cyclase, phospholipase C [see section 1.2.3; see Reithmann *et al.*, 1990). The $\beta\gamma$ subunits represent a stable heterodimer that does not dissociate under physiological conditions. After dissociation of the heterotrimer, the $\beta\gamma$ -subunit remains associated with the membrane. In contrast, the activated α -subunit either remains associated with the plasma membrane (Buss *et al.*, 1987) or released into the cytoplasm (see Crouch & Hendry, 1993; Rodbell, 1985; Spiegel *et al.*, 1991). The α -subunit is deactivated as a result of the hydrolysis of GTP to GDP. The GDP-bound α -subunit has a high affinity for $\beta\gamma$ -subunits, with which it re-associates, and a low affinity for effectors and receptors (see Reithmann *et al.*, 1990).

Figure 1.2: Diagrammatic representation of the activation of heterotrimeric G-proteins

Diagrammatic representation of the activation of heterotrimeric G-proteins. Panel 1 show the binding of hormone / transmitter (H) to the receptor (R). The G-protein ($\alpha\beta\gamma$) is in an inactive state with GDP bound to the α -subunit. Panel 2: Hormone (H) has bound to the receptor (R) which undergoes a conformational change. The receptor (R) interacts with the G-protein ($\alpha\beta\gamma$) and catalyses the exchange of GDP for GTP. Panel 3: The GTP bound α -subunit dissociates from the $\beta\gamma$ -subunit and interacts with the effector (E). Panel 4: The α -subunit hydrolyses GTP to GDP and dissociates from the effector (E). Panel 1: The GDP bound α -subunit binds to the $\beta\gamma$ -subunit.



There is evidence that one type of α -subunit may interact with different receptors and that an effector can interact with several different classes of G-proteins (see Iismaa & Shine, 1992). Membrane binding or interaction of the α -subunit with the cytoskeleton may produce compartmentalisation and so prevent interaction with non-localised effectors (see Neer & Clapham, 1988; Rodbell, 1992).

1.2.2.2 Heterotrimeric G-protein isoforms and interaction with effectors

Initially, within the cell, at least two major classes of G-protein were identified and the different activities of the G-proteins was thought to be mainly associated with the α subunit. The first class of G-protein was defined as having a stimulatory effect on adenylyl cyclase and was called G_s . The second class was defined as having an inhibitory effect on adenylyl cyclase and was called G_i . However, it is now known that G_s can also affect K^+ and Ca^{2+} ion channels and G_i can regulate K^+ channels (see table 1.1; see Birnbaumer, 1992; Conklin & Bourne, 1993; Reithmann *et al.*, 1990). Indeed, several forms of each of these G-proteins have so far been identified. These include three isoforms of G_i , namely G_{i-1} , G_{i-2} , and G_{i-3} , and four splice variants of G_s (see table 1.1 and figure 1.1; see Birnbaumer, 1992; Birnbaumer *et al.*, 1990; Reithmann *et al.*, 1990; Conklin & Bourne, 1993). The G-protein classes, G_i and G_s , can be distinguished from one another not only by their activity but also their interaction with cholera and pertussis toxins (from *Vibrio cholera* and *Bordetella pertussis*, respectively; see Yamane & Fung, 1993). G_s proteins are affected by cholera toxin and G_i by pertussis toxin, although G_i can also be affected by cholera toxin in a receptor-dependent manner (see Reithmann *et al.*, 1990; Yamane & Fung, 1993). Both toxins cause a NAD^+ -dependent ADP-ribosylation of the α -subunit. The pertussis toxin site on the α -subunit of G_i is at a cysteine four amino acids from the C-terminal of the protein whilst the cholera toxin site in α - G_s is just before the guanine nucleotide binding domain (Arg187/188; see Yamane & Fung, 1993). ADP-ribosylation results in a persistent activation of the stimulatory α subunit (α_s) and an inhibition of the effects of the inhibitory α subunit (α_i).

The mode of action of the G_s is clear in that the α_s subunit directly interacts with and activates adenylyl cyclase (Gilman, 1987; Reithmann *et al.*, 1990), although there is now evidence that some isoforms of adenylyl cyclase can also be activated by $\beta\gamma$ -subunits (see section 1.2.3.1; Tang & Gilman, 1991; see Birnbaumer, 1992; Lefkowitz, 1992; Yamane & Fung, 1993; Choi *et al.*, 1993). The mode of action of G_i is more complex. It is conceivable that the α_i subunit interacts with adenylyl cyclase and hence prevents its activation (see Reithmann *et al.*, 1990) or the release of $\beta\gamma$ subunits from G_i may prevent the dissociation of G_s , and so modulate adenylyl cyclase activity (see Gilman, 1987; Reithmann *et al.*, 1990) and as different experimental systems produce different results it is possible that both mechanisms may play a role in the inhibition of adenylyl cyclase (see Reithmann *et al.*, 1990).

Early work suggested that the biological activity of the heterotrimeric G-proteins was associated only with the α -subunits but there is now evidence that the $\beta\gamma$ subunits may also have a role in signal transduction such as activating phospholipase A2 (see section 1.2.3.2), phospholipase C (see section 1.2.3.2; Camps *et al.*, 1992; Smrcka & Sternweis, 1993), adenylyl cyclase (see section 1.2.3.1; Tang & Gilman, 1991; see Birnbaumer, 1992; Lefkowitz, 1992; Yamane & Fung, 1993) and the stimulation of receptor phosphorylation (e.g. β -AR kinase; Kameyama *et al.*, 1993; Koch *et al.*, 1993). Both the β and γ -subunit families consist of four isoforms (see table 1.1) and with both families containing at least four subunits this gives a possible sixteen $\beta\gamma$ subunits but recent evidence has suggested that not all the β and γ isoforms may be able to combine to form functional $\beta\gamma$ subunits (Schmidt *et al.*, 1992).

In addition to α -G_s and α -G_i further members of the α -G_s and α -G_i families have been identified and another α -G-protein family has also been described, namely that of α -G_q (see table 1.1 and figure 1.1; see Birnbaumer, 1992). The α -G_s family contains four splice variants of α -G_s with an additional member identified as α -G_{olf}, which occurs in the olfactory epithelium. The α -G_i family contains the three α -G_i's, together with α -G_{o1} and α -G_{o2} (splice variants of α -G_o), α -G_z, α -G_{gust}, α -G_{tr} and α -G_{tc}. The third α -G-protein family is α -G_q and contains α -G_q, α -G₁₁, α -G₁₄, α -G₁₆, α -G₁₂ and α -G₁₃ (see table 1.1; and figure 1.1; see Birnbaumer, 1992; Sternweis & Smrcka, 1992; Birnbaumer, 1992; Conklin & Bourne, 1993).

G_o (other G-protein) is found in the brain where it is associated with neurite growth cones and with growth associated protein (GAP-43, Strittmatter *et al.*, 1990). G_o inhibits the actions of Ca²⁺ channels and may be involved in the activation of phospholipase C (see section 1.2.3.3). G_z (or G_x), can inhibit adenylyl cyclase, is the only member of the G_i family that cannot be ADP-ribosylated by pertussis toxin (Fong *et al.*, 1988; Matsuoka *et al.*, 1988) and has been shown to have one of the slowest GTPase activity of any of the G-proteins. This has led to the suggestion that it may be involved in long term signal responses (Casey *et al.*, 1990). G_{gust} is found in the taste buds and activates a cAMP specific phosphodiesterase (see section 1.2.3.2). α -G_{tr} and α -G_{tc}, originally called α -G_t, are associated with the photoreceptors with α -G_{tr} being found in the rods and α -G_{tc} in the cones. Both are sensitive to cholera and pertussis toxin (Lerea *et al.*, 1986) and are not activated by hormones or transmitters but by the action of light on rhodopsin. The α _t subunits can activate cyclic-GMP specific phosphodiesterase (Fung, Hurley & Stryer, 1981; Kohnken, Eadie & McConnell, 1981) and phospholipase A2 (Jelsema & Axelrod, 1987). The α -G_q family is ubiquitously expressed, not effected by pertussis or cholera toxins and except for α -G₁₂ and α -G₁₃, is involved in the activation of PLC β (see table 1.1 and figure 1.1; see Birnbaumer, 1992; Conklin & Bourne, 1993; Reithmann *et al.*, 1990; Sternweis & Smrcka, 1992).

1.2.3 Effector systems and secondary messenger generation

The activated G-protein, α or $\beta\gamma$ subunits, finally conveys the 'message' to its effector system. To date it has been shown that activated G-proteins can interact with at least three different effector systems, adenylyl cyclase (see section 1.2.3.1), resulting in the stimulation or inhibition of cAMP production; phospholipases (see section 1.2.3.2); or ion channels.

1.2.3.1 Adenylyl Cyclase and cAMP production

The first report of agonist-induced stimulation of cAMP production, on which the whole concept of secondary messengers was developed, was in 1960 by Sutherland and Rall (see Sutherland & Rall, 1960).

cAMP is produced from ATP and the reaction is catalysed by the Mg^{2+} -dependent enzyme adenylyl cyclase. Cell surface receptors can either stimulate or inhibit cAMP production and these effects are mediated by two different classes of G-proteins (see section 1.2.2.2 and table 1.1) with the two signalling systems co-existing in the same cell type (see Reithmann *et al.*, 1990).

The catalytic subunit of adenylyl cyclase was first purified from heart in 1985 and brain in 1986 and had molecular weights of 150 kDa and 120 kDa respectively (see Reithmann *et al.*, 1990). To date at least six distinct families (types I - VI) have been reported which contain up to eight isoforms, and although the enzymes have similar structures there is evidence that they possess different regulatory properties and show different tissue distributions (see Glatt & Snyder, 1993; Hellevuo *et al.*, 1993; Pleroni *et al.*, 1993; Yoshimura & Cooper, 1993; Choi *et al.*, 1993; Tang & Gilman, 1992).

Types I and III are stimulated by Ca^{2+} in the presence of calmodulin, type VI is inhibited by Ca^{2+} and types II, V and IV are insensitive to Ca^{2+} (see Yoshimura & Cooper, 1993; Choi *et al.*, 1993). In addition, types II and IV are stimulated by G-protein $\beta\gamma$ subunits, type I is inhibited, and types III, V and VI are insensitive (Choi *et al.*, 1993). All six adenylyl cyclases catalytic subunits have a predicted molecular weight of 120 - 130 kDa and contain twelve transmembrane sequences and two large cytoplasmic domains (Choi *et al.*, 1993; Tang & Gilman, 1992). It has been suggested that the hydrophilic domains contain the nucleotide binding domains and hence the catalytic site (see Reithmann *et al.*, 1990).

The cAMP system has four main components (Ross & Gilman, 1980): the receptors (see section 1.2.1), the G-proteins (see section 1.2.2; Rodbell *et al.*, 1971), adenylyl cyclase, and phosphodiesterase. Control, or modification, of the system can be achieved at any of the four levels and by changes in the rate of cAMP leaving the cell.

Interaction of ligands with cell surface receptors results in the dissociation of the G-protein heterotrimer (see section 1.2.2) which in turn can activate, or inhibit, adenylyl cyclase. One ligand / receptor complex can interact with several G-proteins, which in turn

can activate a number of adenylyl cyclase molecules, and each adenylyl cyclase molecule can produce many cAMP molecules. The resulting raised levels of intracellular cAMP causes the activation of cAMP dependent protein kinases (PKA, see section 1.2.4.1).

Adenylyl cyclase can be stimulated in cells by a naturally occurring diterpene, forskolin (isolated from *Coleus forskohlii*). Forskolin has also been demonstrated to inhibit the activity of a number of membrane transporter proteins, such as the glucose transporters, by a cAMP-independent mechanism (see Laurenza, McHugh Sutkowski & Seamon, 1989).

The effects of cAMP mediated cellular signalling can be modulated and finally deactivated by a group of enzymes that hydrolyse cAMP (see Beavo, 1990). These enzymes are called phosphodiesterases (PDE) and the cAMP specific PDEs are part of a family of enzymes that can also hydrolyse cGMP (see Beavo, 1990). The PDE family can be divided into five sub-groups, determined by the characteristics of the enzyme, with each subgroup being further divided (see Beavo, 1990). Group I contains the Ca²⁺ - calmodulin dependent PDEs; group II the cGMP - stimulated PDEs; group III the cGMP - inhibited PDEs; group IV the cAMP - specific PDEs, and group V the cGMP - specific PDEs. The different isoforms of PDEs exhibit a range of molecular weights from 58 - 110 kDa (see Beavo, 1990), as well as different modes of activation, substrate specificities, tissue distributions and inhibition characteristics (see Beavo, 1990) but all can be inhibited by IBMX (3-isobutyl-1-methylxanthine; see Corda, Luini & Garattini, 1990).

Many reviews have appeared on G-protein structure and the function of the adenylyl cyclase signal transduction system which have been summarised above (see Baumgold, 1992; Choi *et al.*, 1993; Reithmann *et al.*, 1990; Tang & Gilman, 1991; Tang & Gilman, 1992; Gilman, 1987; Levitzki, 1988; Neer & Clapham, 1988; Styer & Bourne, 1986).

1.2.3.2 Phospholipase and inositol phosphates

Over the past few years many excellent reviews have appeared on the generation of inositol phosphate (InsP) secondary messengers (see Abdel-Latif, 1986; Berridge, 1987a, 1987b; Berridge, 1993; Berridge & Irvine, 1989; Osborne, Tobin & Ghazi, 1988; Rana & Hokin, 1990).

The first description of phospholipid turnover as a result of agonist stimulation was by Hokin and Hokin (Hokin & Hokin, 1955a, 1955b) but it was not until 1974 (Hokin-Neaverson, 1974; Michell, 1975) that the components of the system were identified as phosphatidyl inositol and phosphatidic acid.

There are now recognised to be three families of phospholipases; phospholipases A₂, C and D; with each family containing several isozymes. The phospholipases can act on different phospholipids to produce a range of secondary messengers and precursors for other signalling molecules.

Phospholipases A₂ (PLA₂) catalyse the hydrolysis of many different phospholipids giving products which may serve as intracellular messengers or precursors for other messenger molecules (see Mayer & Marshall, 1993). The PLA₂ family can be split into four subgroups (I - IV). Groups I, II, and III are found in the extracellular fluids, will cleave most phospholipids, require Ca²⁺ for activation and have a molecular weight of 14 kDa. These PLA₂s are also referred to as the non-pancreatic or secretory. Group IV PLA₂s are intracellular, will only cleave arachidonic acid containing phospholipids, also require Ca²⁺ for activation and have a molecular weight of 85 kDa (see Glaser *et al.*, 1993; Mayer & Marshall, 1993).

The preferred substrate for phospholipase D (PLD) is phosphatidylcholine which it cleaves to produce phosphatidic acid and choline. Phosphatidic acid can then be further metabolised by phosphatidic phosphohydrolase to produce diacylglycerol. Again PLD, like PLC, can be found in cytosolic and membrane fractions and this is thought to reflect different isozyme distribution (see Billah, 1993).

Phospholipase C (PLC) produces two secondary messenger from phosphatidylinositol 4,5-bisphosphate (PIP₂), namely diacylglycerol (DAG) which activates protein kinase C (PKC; see section 1.2.4.2; see Huang, 1989; May Jr *et al.*, 1985; Nishizuka, 1984; Wolf *et al.*, 1985; Cook & Wakelam, 1992) and D-myo-inositol 1,4,5-trisphosphate (Ins(1,4,5)P₃) which mobilises Ca²⁺ from intracellular stores (see Berridge, 1993; Berridge & Irvine, 1989). Two pathways have now been identified by which the enzyme can be activated and hydrolyse PIP₂. One pathway does not require a mediator between the receptor but relies on tyrosine phosphorylation of the enzyme whilst the other is G-protein dependent (see Cockcroft & Thomas, 1992).

Early studies on PLC indicated that such an activity was predominantly associated with the cytosol which did not appear consistent with a role as an effector in the inositol phosphate signalling pathway (Fukui, Lutz & Lowenstein, 1988; Homma *et al.*, 1988; Rebecchi & Rosen, 1987) although some activity was found associated with the membrane (Banno & Nozawa, 1987; Banno, Yada & Nozawa, 1988; Cockcroft, Baldwin & Allan, 1984). It has also been shown that in permeabilised cells that the diffusion of PLC from the cytosol into the surrounding medium is very slow (Stutchfield & Cockcroft, 1988) and this suggests that the enzyme is not found exclusively in the cytoplasm.

To date three PLC isozymes have been identified based on sequence homology (β , γ and δ) and four families based on enzyme purification data (α , γ , δ and ϵ ; see Cockcroft & Thomas, 1992; Guillon, Mouillac & Savage, 1992). The sequence data set can be further sub-divided to give β 1, β 2, β 3, γ 1, γ 2, δ 1, δ 2, and δ 3. The phospholipases have been shown to have different tissue distributions and different modes of activation. PLC- β , β 1 and ϵ have been shown to be regulated by G_q family of G-proteins (see table 1.1 and section 1.2.2.2) whilst PLC- γ 1 and γ 2 have been shown to be activated by tyrosine kinase-mediated phosphorylation (see Cockcroft & Thomas, 1992). In addition there is now

evidence that PLC may also be regulated by G-protein $\beta\gamma$ subunits (Camps *et al.*, 1992; Smrcka & Sternweis, 1993).

The substrate for PLC, namely PIP₂, is produced from phosphatidyl inositol (PI) which is synthesised at the rough and smooth endoplasmic reticulum (Williamson & Morre, 1976) before being transferred, by a carrier protein (Somerharju, Paridon & Wirtz, 1983), to the plasma membrane and further phosphorylated. The hydrolysis of PIP₂, besides producing Ins(1,4,5)P₃ and DAG, may also result in the production of a small quantity of D-myo-inositol (1:2-cyclic,4,5)-trisphosphate (see Hawkins *et al.*, 1986; Ishii *et al.*, 1986; Wilson *et al.*, 1985).

The metabolic fate of Ins(1,4,5)P₃ is to be either phosphorylated to Ins(1,3,4,5)P₄ or dephosphorylated to Ins(1,4)P₂. These InsPs can then be further phosphorylated to produce a range of inositol polyphosphates (up to InsP₆) or dephosphorylated to finally give inositol which can then be recycled to produce PIP₂. The route for the metabolism of Ins(1,4,5)P₃ is dependent on cell type, and not all of the metabolites of Ins(1,4,5)P₃ have been found in all cells studied.

The inositol phosphates can be divided into two groups; those whose levels rise as a result of agonist-induced stimulation and those which are agonist insensitive (e.g. Ins(1,3,4,5,6)P₅ and InsP₆). It has been suggested (see Berridge & Irvine, 1989) that only three of the agonist sensitive metabolites of PIP₂ assert any function as secondary messengers (namely Ins(1,4,5)P₃, Ins(1,3,4,5)P₄ and DAG) and that the other agonist sensitive metabolites are breakdown products. The wide array of breakdown products may represent cellular control in preventing an increase in the levels of a biologically active InsP (e.g. Ins(1,4,5)P₃) as a result of the breakdown of another InsP (e.g. dephosphorylation of Ins(1,3,4,5)P₄ not producing the biologically active Ins(1,4,5)P₃ (see Berridge & Irvine, 1989).

Ins(1,4,5)P₃ has been identified as mobilising Ca²⁺ from non-mitochondrial Ca²⁺ pools (see Berridge, 1993; Berridge & Irvine, 1989; Putney *et al.*, 1989; Schulz, Thevenod & Dehlinger-Kremer, 1989; Streb *et al.*, 1983). These stores are now known to contain three components: pumps for the recovery of released calcium, binding proteins such as calsequestrin and calreticulin to store the calcium and Ins(1,4,5)P₃ receptor (IP₃R) or ryanodine receptors to control release into the cytoplasm. There are now known to be at least five IP₃R (IP₃R1a, IP₃R1b, IP₃R2, IP₃R3, and IP₃R4; [see Berridge, 1993]). The receptors contain four subunits with each subunit possessing a C-terminal membrane spanning region and a N-terminal Ins(1,4,5)P₃ binding domain. Although the receptors contains four Ins(1,4,5)P₃ binding sites it is not known whether all four sites have to be occupied or if occupancy of one site is enough to evoke Ca²⁺ release (see Berridge, 1993). It is now thought that the receptors are located on specialised regions of the ER (see Berridge, 1993).

Diacylglycerol is involved in the activation of protein kinase C (PKC; see section 1.2.4.2; see Nishizuka, 1984) and cellular levels may only rise briefly as DAG can be readily metabolised to PIP₂, via phosphatidic acid (see Berridge, 1987b), or converted to arachidonic acid (see O'Flaherty, 1987) which can be used for the production of thromboxanes, prostaglandins, and leukotrienes which can have localised actions. DAG can also be produced by the agonist induced breakdown of phosphatidylcholine (Billah *et al.*, 1988; Pelech & Vance, 1989; see Exton, 1990) by phospholipase D, or from inositol containing glycolipids (Chan, Chao & Saltiel, 1989).

1.2.3.3 Secondary messenger system crosstalk

Recent years have seen a growing body of evidence for the 'cross talk' between receptors linked to different secondary messenger pathways (see Houslay, 1991a; Geny, Stutchfield & Cockcroft, 1989; Hill & Kendall, 1989; Sagi-Eisenberg, 1989). Briefly, the above authors have described 'cross talk' as either an enhancement, or attenuation, of normal agonist induced secondary messenger levels by the action of another (or even the same) agonist on a different receptor which is linked to a different secondary messenger system. An example is the decrease in the accumulation of cAMP by a phosphodiesterase (see section 1.2.3.2) which is activated by Ca²⁺ released as a result of Ins(1,4,5)P₃ production by muscarinic receptor activation (see section 1.2.3.2). Phorbol esters have been shown to increase cAMP levels, in the presence of cAMP agonists, by the activation of protein kinase C (see section 1.2.4.2) which phosphorylates adenylyl cyclase (see section 1.2.3.2) or a G-protein (see section 1.2.2 and 3.1.1; Sagi-Eisenberg, 1989). The InsP pathway can be affected by the cAMP system but the method, or point, of control is unknown (Hill & Kendall, 1989) although the Ins(1,4,5)P₃ receptor for Ca²⁺ release (see section 1.2.3.2) has been shown to be a substrate for the cAMP dependent protein kinase A (Ferris *et al.*, 1989; Supattapone *et al.*, 1988).

1.2.4 Protein kinases and phosphatases

Many cellular systems have now been shown to be regulated by the phosphorylation of specific components within the system. The result of phosphorylation can be to cause either a stimulation, or enhancement of the system or an inhibition. As the phosphorylation state of a protein can affect its activity then the processes of phosphate addition and removal have to be tightly controlled.

To date well over 100 mammalian protein kinases have been identified (see Hunter, 1991). The kinases seem to consist of a modular structure with the segment responsible for the catalytic activity of the enzyme being highly conserved and the other modules introducing functional properties to the molecule (see Taylor, Buechler & Yonemoto, 1990). The kinases can be broadly divided into three categories based on their phosphorylation sites. One group of kinases (e.g. activated insulin receptor, see section

1.4) phosphorylate on tyrosines, another group phosphorylate on serines and / or threonines (e.g. protein kinase A [see section 1.2.4.1] and protein kinase C [see section 1.2.4.2]) and the third, and least common, group have been reported to phosphorylate on histidine, lysine and arginine (see Hunter, 1991; Taylor *et al.*, 1990).

The tyrosine and serine / threonine kinases can be further subdivided depending upon their method of activation, although this kind of categorisation is flawed as the method of activation of some kinases is still not understood (see Hunter, 1991). This has led to the subdivision of some of the members of the serine / threonine kinases into families such as the cyclic nucleotide-regulated protein kinases (e.g. cAMP-dependent protein kinases [PKA]; see section 1.2.4.1); calmodulin-regulated protein kinases (e.g. the myosin light chain kinases) and a family of diacylglycerol-regulated protein kinases (e.g. PKC; see section 1.2.4.2; see Hunter, 1991; Taylor *et al.*, 1990).

The removal of phosphates from proteins is carried out by a group of enzymes called phosphatases and these can be divided into two groups, the protein-serine / threonine phosphatases and the protein-tyrosine phosphatases, which can also be further sub-divided (see section 1.2.4.3).

1.2.4.1 Protein kinase A

Protein kinase A is a cAMP dependent serine kinase which was first described in 1968 (see Johnson & Barford, 1993). The kinase consists of four subunits, two of which are regulatory (R) and two catalytic (C; see Døskeland, Maronde & Gjertsen, 1993). The mechanism of activation of PKA is unusual in that cAMP binds to the regulatory subunit which causes the subunits to dissociate and release two active catalytic subunits (see Døskeland *et al.*, 1993; Johnson & Barford, 1993).

Three isoforms of the catalytic subunit have been identified ($C\alpha$, $C\beta$, $C\gamma$; see Døskeland *et al.*, 1993; Hanks & Quinn, 1991; Hunter, 1991) with alternative splice variants of $C\alpha$ ($C\alpha 1$ and $C\alpha 2$) and $C\beta$ ($C\beta 1$ and $C\beta 2$) also being detected and four isoforms of the regulatory subunit ($RI\alpha$, $RI\beta$, $RII\alpha$ and $RII\beta$; see Døskeland *et al.*, 1993; McKnight *et al.*, 1988). The three isoforms $C\alpha$, $RI\alpha$ and $RII\alpha$ are expressed in most tissues and $C\beta$, $RI\beta$ and $RII\beta$ are highly expressed in the central nervous system and at very low levels in other tissues (McKnight *et al.*, 1988).

The regulatory subunits contain four functional domains, the so called N-terminal dimerisation domain, the auto-inhibitory or hinge region, and two cAMP binding sites (see Døskeland *et al.*, 1993; Taylor *et al.*, 1990). The dimerisation domain is the region of the protein where greatest variation amongst regulatory subunit types is found and it is in this region that the interaction between two R-subunits occurs to form the R-R dimer. The auto-inhibitory, or hinge region, shows little variation between R-subunit types and it is this region that contains the pseudo-substrate motif (arginine-arginine-x-serine [where x is any amino acid]) to which the kinase domain of the C-subunit binds (see Døskeland *et al.*, 1993;

Taylor *et al.*, 1990). In addition, mutation studies of the catalytic site of the C-subunit and the hinge region of the R-subunit have shown that the R-subunit is still able to interact with the C-subunit. This demonstrates that there must also be another R-C-subunit interaction site (Orellana *et al.*, 1993; Wang *et al.*, 1991). The two cAMP binding regions (A and B) consist of a conserved structure which gives the regions a three α -helix, eight stranded anti-parallel β -barrel cAMP binding domain. The binding of cAMP to one of the sites, either A or B, causes an increase in the affinity of the empty site for cAMP. Once the second site is occupied this increases the probability of the dissociation of the R-C complex although occupation of all four sites is required for the release of the catalytic subunits (see Døskeland *et al.*, 1993; Orellana *et al.*, 1993; Taylor *et al.*, 1990).

To date little is known about the functions of the different C-subunits or even why there are different R-subunits, although the R-subunits may provide differential cAMP control and cellular localisation of the C-subunits (Bregman, Bhattacharyya & Rubin, 1989; Bregman, Hirsch & Rubin, 1991; see Døskeland *et al.*, 1993). It has been demonstrated that C α and C β have similar substrate specificities but C γ seems to prefer histone (see Døskeland *et al.*, 1993).

In addition to the R-subunit mediated inhibition of the activity C-subunit a second cellular control mechanism has been described which uses a 75 amino acid specific protein kinase inhibitor (PKI). Two isoforms of PKI have been identified and like the R-subunits they contain a pseudo-substrate motif and a second point of interaction with the C-subunit (Orellana *et al.*, 1993).

A range of PKA inhibitors are becoming available for experimental use and one of these is HA1004 (N - (2'-guanidinoethyl) - 5 - isoquinoline - sulfonamide; available from LC Services Corporation) which, although at high concentrations is a non-specific protein kinase inhibitor (see section 1.2.4), can show specificity for PKA with a reported inhibitor potency of 2.3 μ M. For the other kinases it has been reported as 1.3 μ M for PKG (cGMP activated protein kinase; Asano & Hidaka, 1984; Hidaka *et al.*, 1984) and 40 μ M for PKC (see section 1.2.4.2).

1.2.4.2 Protein kinase C

The activation of cell surface receptors linked to the InsP pathway (see section 1.2.3.2) results in the production of two intracellular messengers, the cytosolic InsPs and membrane bound diacylglycerol (DAG). The intracellular rise of Ins(1,4,5)P₃ and the subsequent rise of Ca²⁺ levels can last for many minutes but the increase in DAG is transient and it is rapidly recycled back into the InsP pathway or further metabolised (see section 1.2.3.2). In some cell types a second increase of DAG occurs which arises from agonist induced breakdown of phosphatidylcholine (Billah *et al.*, 1988; Pelech & Vance, 1989; see Exton, 1990) by phospholipase D (see section 1.2.3.3), or from inositol containing glycolipids (Chan *et al.*, 1989). It has been shown that the membrane bound

DAG, when complexed with phosphatidylserine and Ca^{2+} , activates a specialised protein kinase, protein kinase C (PKC), and increases its affinity for Ca^{2+} (May Jr *et al.*, 1985; Wolf *et al.*, 1985; see Huang, 1989). The Ca^{2+} released by $\text{Ins}(1,4,5)\text{P}_3$ may not be required by PKC for its activation as physiological levels of Ca^{2+} may be sufficient (Castagna, 1987), or the PKC isoform may not require Ca^{2+} (Ha & Exton, 1993). Upon activation, some isoforms of PKC can translocate from the cytosol to the membrane (see table 1.2; Harrison & Mobly, 1990; Hirota *et al.*, 1985; Kraft & Anderson, 1983; Osborne *et al.*, 1991; Tapley & Murray, 1984) with the correct orientation of PKC in the membrane being insured by the hydrophobic domain of DAG (see Huang, 1989).

PKC has a predicted molecular weight of 67 - 84 kDa (Huang *et al.*, 1987; Huang & Huang, 1986; Stabel & Parker, 1993) and can be divided by proteolysis to give 48 kDa and 38 kDa portions which represent the catalytic and regulatory sites of the enzyme (Huang & Huang, 1986). It has been shown that PKC is associated with many different tissues (Kikkawa *et al.*, 1988) and that it can be isolated in both membrane and cytosolic fractions. It has been shown that the enzyme can exist in multiple forms of closely related structure as a result of interaction of the same species of PKC with different cofactors (Huang, 1989).

Nine species of PKC have now been identified, α , βI , βII , δ , ϵ , γ , η , ζ and θ with a possible further two subspecies, ϵ' and ζ' , based on alternative mRNA splicing of ϵ and ζ respectively (see table 1.2; see Hug & Sarre, 1993; Stabel & Parker, 1993). The PKC species α , βI , βII , δ , ϵ and ζ show a heterogeneous tissue distribution, γ is found exclusively in the central nervous system, η in the skin and lungs, and θ in the muscle (see table 1.2; Hug & Sarre, 1993). The PKC isozymes can be divided into two groups, A and B or cPKC and nPKC, on the basis of the conservation of the protein sequence (Considine & Caro, 1993; Huang *et al.*, 1987; Huang, 1989; Ono *et al.*, 1988) and Ca^{2+} sensitivity (see Hug & Sarre, 1993). Group A, consists of α , βI , βII and γ , are Ca^{2+} dependent, and contain five variable regions separated by four highly conserved regions. Group B (Ca^{2+} independent, δ , ϵ , η , ζ and θ) shows similarities to group A in two of the conserved regions but completely lacks one of the conserved sequence of group A PKCs (Ono *et al.*, 1988; see Hug & Sarre, 1993). The PKCs within one group display similar characteristics but PKCs from different groups exhibit different characteristics (see Huang, 1989). It has been shown that the PKC species exhibit a range of affinities for DAG (Huang *et al.*, 1988b), hence DAG, and phorbol esters, may have different effects on different species of PKC or on the same species of PKC under altered cellular conditions (see table 1.2; Huang, 1989). In addition, PKC activated by phorbol esters or by DAG show different phosphorylation products (see Castagna, 1987).

A wide variety of substrates have been identified for PKC both *in vivo* and *in vitro* (see Nishizuka, 1986). It has been shown to phosphorylate both membrane bound proteins (e.g. receptors; see Nishizuka, 1986); G-proteins, (see Jakobs *et al.*, 1985;

Lounsbury *et al.*, 1993; Morris *et al.*, 1994; Sagi-Eisenberg, 1989; see section 3.1.1); adenylyl cyclase, (Olianas & Onali, 1986); and cytosolic proteins (e.g. intermediate filaments; vimentin, Huang, Devanney & Kennedy, 1988a).

Table 1.2: Isoforms of protein kinase C.

Family	PKC	Tissue	MW	SDS	Ca ²⁺	DAG/PE	Auto	Location	Trans	Down
A	α	Ubiquitous*	76.8	80-81	+	+	+S	C	Y	Y
A	βI	Ubiquitous	76.8	79-80	+	+	+T	C	Y	Y
A	βII	Ubiquitous	76.9	80	+	+	+ST	C	Y	Y
A	γ	Brain	78.4	77-84	+	+	+			
B	δ	Ubiquitous	77.5	74-79	-	+	+	C/M	-	Y
B	ε	Ubiquitous*	83.5	89-96	-	+	+	C/M	-	Y/N
B	(ε-)	-								
B	ζ	Ubiquitous	67.7	76-80	-	-	+S	C	?	?
B	(ζ-)	-								
B	η	Skin/Lung	77.9	82-86	-	+	+	NUC	ND	N
B	θ	Muscle	81.6	79	ND	ND	+	M	ND	

Nine isoforms have been identified, plus two subspecies based on alternative mRNA splicing (shown in parenthesis). "Family" indicates which family the different isoforms belong (A or B); tissue indicates their tissue distribution; MW = predicted molecular weight (kDa) based on cDNA clone; SDS = observed molecular weight (kDa) in SDS-PAGE; Ca²⁺, "+" indicates isoform requires Ca²⁺ for activation, "-" indicates that it does not; DAG/PE indicates whether the isoform is activated by diacylglycerol or phorbol esters; "Auto" = autophosphorylation, S if the site is serine, T for threonine; "Location" is the cellular distribution in unstimulated cells, C = cytosol, M = membrane, C/M = cytosol or membrane (i.e. dependent on cell type), NUC = nucleus; Trans, Y the isoform is translocated, "-" indicates that it depends on cell type, ? unknown; Down, Y = the isoform is down regulated on chronic exposure to phorbol esters, Y/N, down regulation depends on cell type, ? data inconclusive; ND = not determined; * not in hepatocytes (see Azzi, Boscoboinik & Hensey, 1992; Hug & Sarre, 1993).

An increasingly wide range of artificial activators and inhibitors of PKC are available. PKC can be activated by 4-amino pyridine and the tumour promoting phorbol esters. The phorbol esters interact with DAG binding site on the regulatory domain of PKC (see Blumberg *et al.*, 1984; Sharkey, Leach & Blumberg, 1984). The inhibitors of PKC can be divided into two groups (Huang, 1989). One group interacts at the catalytic (kinase) site of the enzyme by competing with ATP or other substrates (e.g. H7, see Hidaka & Hagiwara, 1987; Nakadate, Jeng & Blumberg, 1988); or by binding directly to the catalytic site (e.g. staurosporine, Nakadate *et al.*, 1988). The catalytic site inhibitors tend to show an inhibitory effect on other kinases due to interactions with the similar catalytic sites. The other group of inhibitors interacts with the regulatory site of PKC and so prevents the activation of the enzyme by competing with the activator for the binding site (e.g. Polymixin B; Huang, 1989). These inhibitors can be very specific for PKC if they interact with DAG or phorbol ester binding site, but interaction at the acid phospholipid binding site will tend to make the inhibitor less specific (see Huang, 1989).

Phorbol esters possess structures similar to DAG and their mode of action of the phorbol esters is similar to that of DAG in that they can insert into the cell membrane, bind to the regulatory site of the enzyme, increase its affinity for Ca^{2+} , and hence activate the enzyme (see Blumberg *et al.*, 1984; Castagna, 1987). Unlike DAG, phorbol esters are long lived in biological systems and are not readily metabolised.

1.2.4.3 Protein phosphatases

Protein phosphatases can be split into two main groups; one group removes phosphate groups from the amino acid tyrosine, whilst the other group is described as threonine / serine specific phosphatases.

The first tyrosine phosphatase was purified in 1988 (PTPase 1B; see Pot & Dixon, 1992) and so far some 42 PTPases have been identified. It was found that PTPase 1B did not have any sequence similarities to the serine / threonine phosphatases but it did possess sequence homology with lymphocyte cell surface protein called CD45 (see Pot & Dixon, 1992). CD45 is a 'receptor-like' molecule found on the surface of lymphocytes and it is an intracellular portion of the molecule which contains the region that is highly conserved between both CD45 and PTPase 1B. This has led to the idea that the protein tyrosine phosphatase family can be divided into two groups, the so called receptor-like tyrosine phosphatases and the non-receptor-like. The receptor-like phosphatases, with the exception of PTPase- β and DPTP10D, contain two 200 amino acid cytosolic tyrosine phosphatase domains and a transmembrane spanning region whilst the non-receptor-like phosphatases contain only one 200 amino acid phosphatase domain and no trans-membrane spanning region (see Pot & Dixon, 1992).

The serine / threonine phosphatases can be divided into two main groups, type 1 and type 2. Phosphatases were classed as type 1 (PP1) if they could dephosphorylate the β -subunit of phosphorylase kinase and were inhibited by nanomolar concentrations of two small inhibitory proteins called inhibitor 1 (I-1) and inhibitor 2 (I-2; also called modulator). Type 2 (PP2) phosphatases dephosphorylate the α -subunit of phosphorylase kinase and are insensitive to I-1 and I-2 (see Bollen & Stalmans, 1992; Cohen, 1991; Kemp & Pearson, 1991). The type 2 phosphatases can be further sub-divided into three groups, PP2A, PP2B and PP2C, in a number of ways but the most simply based on divalent cation requirement. PP2A is partially active in the absence of cations, PP2B requires Ca^{2+} and PP2C requires Mg^{2+} (see Bollen & Stalmans, 1992; Cohen, 1991). The system of classification of the phosphatases has now been complicated by reports of phosphatases that may only fit one of the criteria to place them in a particular group (see Bollen & Stalmans, 1992). Examination of mammalian phosphatases has shown that both type 1 and type 2 phosphatases are widely distributed amongst different tissues, have a wide range of substrate specificities *in vitro*, and appear to be involved in the regulation of many cellular processes (see Cohen, 1991). By the use of cDNA cloning it has now been found that there are at least two isoforms of PP1, PP2A and PP2B present in mammalian tissues. These isoforms are distinguished in the literature by the inclusion of α or β after the phosphatase type. In addition the phosphatases can also be described not only by their type but also by other proteins to which they are found complexed (e.g. in the muscle; glycogen [PP1_G], myofibrillar [PP1_M] or inactive [PP1_I]) or by elution from protein separation columns (see Bollen & Stalmans, 1992; Cohen, 1991; Hubbard & Cohen, 1991).

The phosphatases can be inhibited by an increasing range of commercially available inhibitors. One such inhibitor is okadaic acid which is a polyether fatty acid secreted by dinoflagellates (Okadaic acid used in these studies was from *Prorocentrum lima*, although it was originally isolated from the marine sponge, *Halichondria okadaii*) and is a potent inhibitor of the PP1 and 2A, and has also been reported to inhibit phosphatase 2B at high concentrations. Okadaic acid has not been shown to inhibit protein tyrosine phosphatases or any of the kinases (see Cohen, 1991; Hardie, Haystead & Sim, 1991; Haystead *et al.*, 1989).

1.3 Cellular signalling and disease

It has long been recognised that in many disease states the fault lies in some element of signal transduction. In some instances this may be as a result of the over production of hormones or neurotransmitters (e.g. possible over production of dopamine in schizophrenia) in which case the disease may be treated by the use of receptor specific antagonists or by inhibiting the transmitter production system; or it may be an under-production of a transmitter (e.g. Parkinson's disease; type I diabetes [see section 1.3.1]) hence the transmitter levels may be increased (e.g. injections of insulin in type I diabetes) or

by stimulating the production system (e.g. sulphonylureas stimulating insulin release from the pancreas; also see section 5.1.2).

Some disease states and illnesses may be the result of a post - receptor dysfunction of the signal transduction system (e.g. type II [insulin independent] diabetes; see section 1.3.1), and this has now become the target of research for drugs that may be able to interact specifically at that level and so correct the problem (see section 5.1.2).

1.3.1 Diabetes

Diabetes is a condition when the body is no longer able to maintain blood glucose levels between the normal physiological levels. The term diabetes mellitus is derived from the observation that the urine contains sugar and is therefore sweet (diabetes, Greek meaning siphon; mellitus is Latin for honeyed) and one of the earliest recorded descriptions of this complaint was in 15th century BC Egypt (see Bottazzo, 1993). The 'sweet-urine' (glycosuria) results from an increased blood glucose level above the kidney threshold and so excess glucose is excreted. Diabetes is diagnosed in non-pregnant adults if they are found to meet one of the following criteria: 1. Random plasma glucose ≥ 11.1 mM (plus symptoms such as polydipsia, polyuria, polyphagia and weight loss). 2. Fasting plasma glucose levels ≥ 7.8 mM on more than two occasions. 3. Fasting glucose levels < 7.8 mM plus elevated plasma glucose levels (≥ 7.8 mM) during two or more oral glucose tolerance tests (If the plasma glucose level is ≥ 7.8 mM at two hours, and at least one other sample between 0 and 2 hours, after the administration of 75 g of glucose then a lack of glucose tolerance is observed; see Ruoff, 1993; Tattersall & Gale, 1990).

The condition of diabetes can be divided into two forms, so called insulin-dependent diabetes mellitus (IDDM), early onset, juvenile or type I, and non-insulin-dependent diabetes mellitus (NIDDM), late onset, or type II. Type I diabetes is characterised by a failure of the β -cells of the pancreas to produce insulin in response to increased blood glucose levels. This form is usually treated with insulin therapy in the form of injections. Type I diabetes is an auto-immune disease and it is thought that it may be a modern disease that has only become prominent in the last two centuries (see Bottazzo, 1993).

Type II diabetes represents a more intriguing dysfunction of the system. The disease state is characterised by both abnormalities in insulin secretion and in insulin resistance at the target tissues (i.e. liver, fat and muscles; see DeFronzo, 1992; Häring, 1991). The insulin resistance can occur as a result of a change in insulin binding characteristics, changes in the tyrosine kinase activity of the receptor (see section 1.4), mutations in the receptor, or from a combination of the above (see Coccozza *et al.*, 1992; Häring, 1991; O'Rahilly & Moller, 1992). Events such as mutations of the receptor are very rare and therefore do not explain all the cases of type II diabetes. It is still not known whether the altered rates of insulin production are the cause or a symptom of the disease

because as the body becomes insulin resistant and blood glucose levels rise the pancreas compensates by increasing insulin production and such elevated levels of production may finally cause the pancreas to fail resulting in abnormal insulin production. The disease is characterised by a failure of insulin to reduce glycogen storage in the muscle and to suppress normal hepatic glucose output. Treatment of type II diabetes has tended to concentrate on modifications of diet, increased physical activity, oral hyperglycaemic agents and insulin (see Ruoff, 1993). Clearly a better understanding of the normal functioning of the insulin receptor (see section 1.4) and the post-insulin binding events (see section 1.4) would be useful in determining the selective malfunction that occurs and thus for the treatment of type II diabetes.

Both forms of diabetes can lead to long and short term health problems. In the short term poor control of blood glucose can result in hypoglycaemia if glucose levels fall below 2.5 mM or ketoacidosis (results from lack of insulin and hence reduced glucose uptake) if glucose levels rise above 15 mM (hyperglycemia) for long periods (see Watkins, Drury & Taylor, 1990). Both problems can eventually result in death if not treated promptly (see Watkins *et al.*, 1990). Long term problems resulting from lack of control are nephropathy, neuropathy, retinopathy, coronary heart disease and stroke (see Ruoff, 1993; Nathan, 1993).

1.4 The Insulin Receptor

Although recent years have seen a great increase in our knowledge and understanding of the function of the activated insulin receptor it is clear that the complete signal transduction system has not been fully described.

1.4.1 Insulin

Insulin is a fifty-one amino acid poly-peptide hormone which is secreted from the β -cells of the pancreas. The secretion is regulated by the interaction of a variety of nutrients, hormones and neurotransmitters but glucose is the predominant trigger. The ability of the cells to secrete insulin depends on the metabolism of glucose and the generation of a range of intermediates which results in membrane depolarisation and Ca^{2+} entry (see Cook, Satin & Hopkins, 1991; Wang *et al.*, 1993). It is also a process in which G-proteins may play a role (see Robertson, Seaquist & Walseth, 1991). The biosynthetic precursor of insulin is proinsulin which is a single-chain poly peptide containing 81 - 86 amino acids with a molecular weight of ~9 kDa. The precursor is kept in storage granules where it has a connecting peptide enzymatically removed to produce two polypeptide chains (A and B) linked by disulphide bridges (final molecular weight ~6 kDa; see Wang & Tsou, 1991) which is stored in crystallin hexameric form complexed with zinc (see Brader & Dunn, 1991).

1.4.2 *Insulin Receptor Structure*

In the 1950s it was thought that the receptors for insulin were part of a matrix surrounding the target cells and that insulin binding caused a disturbance which was propagated throughout the tissue (see Rodbell, 1992). It is now known that the insulin receptor is located in the plasma membrane of the target cells and that it consists of two subunits (α and β), and the full receptor complex has two α and two β subunits (molecular weight 450 kDa). The subunits are the product of a single gene which has 22 exons and is located on chromosome 19 in humans. The precursor poly-peptide contains 1343 or 1355 amino acids preceded by a 27 amino acid leader sequence which is cleaved during the processing of the receptor. During processing the precursor poly-peptide has oligo-saccharide side chains added to specific glycosylation sites, two monomers associate to form a dimeric structure and a four amino acid sequence is removed from each monomer to yield a receptor that consists of two α and two β subunits joined by disulphide bonds (see figure 1.3). This results in a modular protein that contains several functional domains and has a specific membrane orientation (see Hollenberg & Jacobs, 1990; Olefsky, 1990). The receptor is orientated such that the α subunits of the receptor are located on the extra-cellular face of the plasma membrane with the β subunit providing the membrane spanning portion of the receptor.

1.4.2.1 *The α -subunit*

The α subunit (135 kDa [82 kDa before glycosylation]) contains the insulin binding site which consists of a cysteine rich site with at least two other regions of the α subunit contributing to the binding domain. Although each receptor contains two α subunits, and hence two insulin binding sites, the occupancy of one site inhibits the binding of insulin to the second. When both sites are unoccupied the α subunits exerts a tonic inhibition on the biological activity of the β subunit. As stated above the polypeptide chain can have either 1343 or 1355 amino acids. The extra 12 amino acids can be found associated with the α subunit where they have been shown to cause a decrease in the receptors affinity for insulin. The α subunits are linked by disulphide bonds to each other and to the β subunit (see Häring, 1991; Olefsky, 1990; see figure 1.3).

1.4.2.2 *The β -subunit - structure and function*

The β subunit has a molecular weight of 90 kDa (70 kDa before glycosylation) and consists of two globular domains joined by a single α helix (see figure 1.3). The function of the extracellular domain, other than binding the α subunit and transmitting the insulin signal, is unknown. The function of the α helix, which joins the two globular domains, is to provide membrane anchorage for the receptor and to transmit the insulin signal between the domains. The result of insulin binding to the α -subunit is to produce a conformational change in the C-terminal of the β -subunit with any further conformational

changes resulting from subsequent phosphorylation of the subunit (Baron *et al.*, 1992; see section 1.4.3). The biological effects of insulin are produced by the intracellular portion of the β subunit. This region contains the tyrosine kinase domain, several phosphorylation sites (Tavaré *et al.*, 1988), which are both stimulatory and inhibitory on receptor function, and a C-terminal which has a number of insulin-receptor-specific sequences (see figure 1.3; Avurch *et al.*, 1990; Begum, Olefsky & Draznin, 1993; Hollenberg & Jacobs, 1990; Houslay & Siddle, 1989; Olefsky, 1990). The tyrosine kinase domain becomes active as a result of the autophosphorylation, or transphosphorylation, of tyrosines 1146, 1150 and 1151 in the regulatory region and tyrosine 960 in the juxtamembrane region of the β subunit (see Feener *et al.*, 1993; Denton *et al.*, 1992; Avurch *et al.*, 1990; Häring, 1991; Tavaré *et al.*, 1988) with the phosphorylation event occurring asymmetrically with more phosphate being incorporated into the β -subunit that is not bound to the insulin bound α -subunit (Lee *et al.*, 1993). In addition phosphorylation has also been reported on tyrosines 1316 and 1322 (see Denton *et al.*, 1992; Häring, 1991). It appears that some of the sites undergo an insulin independent phosphorylation and dephosphorylation whilst the other sites are insulin dependent (Argetssinger & Shafer, 1992). Recent reports have emerged in which type II diabetes (see section 1.3.1) has been observed in patients that have exhibited a point mutation near an autophosphorylation site of the receptor and although this does not effect insulin binding or insulin-independent kinase activity it does result in a receptor that is no longer able to phosphorylate its substrates (Formisano *et al.*, 1993).

The β -subunit also possess serine (1293 and 1294) and threonine (1336) phosphorylation sites (see figure 1.3) which when phosphorylated attenuated the receptor's kinase activity (see Denton *et al.*, 1992; Chin *et al.*, 1993; Considine & Caro, 1993; Hollenberg & Jacobs, 1990; Häring, 1991). These phosphorylations appear to be carried out by PKC, PKA, and some additional kinases (see section 1.2.4; Ahn, Donner & Rosen, 1993; Smith, King & Sale, 1988; see Grunberger, 1991). In addition there is evidence that the insulin signal transduction system can activate PKC and it is by this mechanism that insulin may produce some of its responses. This kinase has also been implicated in type II diabetes (see Chin *et al.*, 1993; Considine & Caro, 1993).

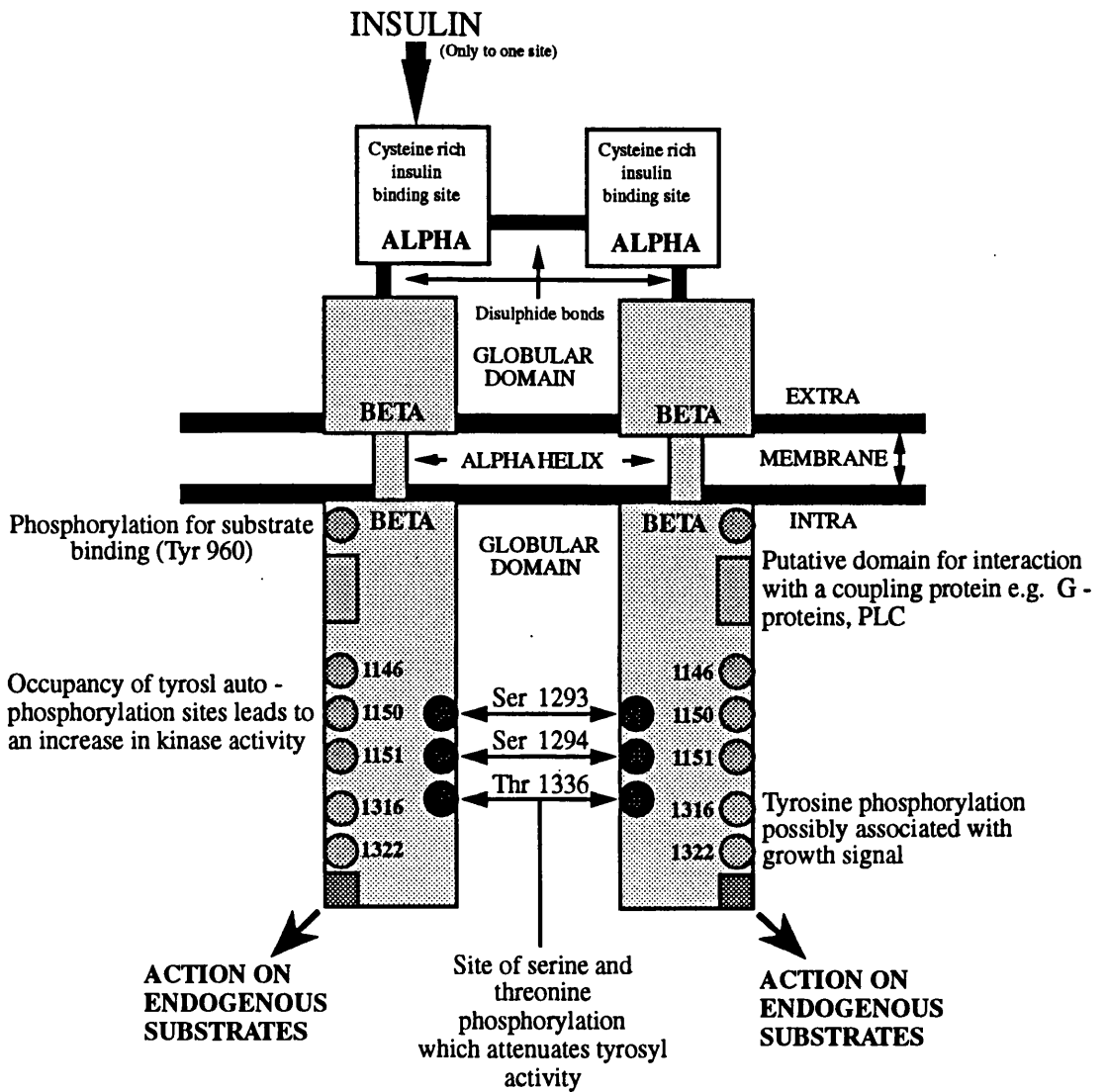
1.4.3 *Insulin signalling - the activated receptor*

The interaction of insulin with its receptor is not easily understood. Firstly, the binding characteristics of insulin are confusing and complex; secondly, interaction of insulin with its receptor results in a diverse range of cellular responses which can occur over time-courses from milliseconds to tens of hours (see table 1.3; see Hollenberg & Jacobs, 1990; Houslay & Siddle, 1989).

The earliest effect of insulin binding with its receptor is seen in muscle where it produces a change in membrane potential within milliseconds. In general, the first response is an increase in receptor auto-phosphorylation at specific tyrosine residues on the β subunit

Figure 1.3: Diagrammatic representation of the insulin receptor

Diagrammatic representation of the insulin receptor showing receptor orientation, phosphorylation sites (number indicating position in primary sequence; Tavaré *et al.*, 1988; Häring, 1991), and putative receptor - effector coupling site. The insulin receptor contains two sub-units (α and β), and the full receptor complex has two α and two β subunits linked by disulphide bonds. This results in a modular protein that contains several functional domains (see Olefsky, 1990) and has a specific membrane orientation. The receptor contains two insulin binding sites which when they are both unoccupied exerts a tonic inhibition on the biological activity of the β subunit. The β subunit the tyrosine kinase domain, several autophosphorylation sites (tyrosines 960, 1316, 1322, 1146, 1150, and 1151) which stimulate receptor activity, and several serine / threonine phosphorylation sites (serines 1293 and 1294, and threonine 1336) which are inhibitory on receptor function. The receptor also has a C-terminal which has a number of insulin-receptor-specific sequences (see Hollenberg & Jacobs, 1990; Houslay & Siddle, 1989; Olefsky, 1990).



which results in an increase of its tyrosine kinase activity (see section 1.4.2.2; Avurch *et al.*, 1990; Rothenberg *et al.*, 1990). The activated receptor then forms microclusters before being endocytosed. After internalisation, insulin dissociates from the receptor as a result of the acidified environment of the endosome and is degraded. The receptor bearing endosomes can then either fuse with lysosomes, which results in the receptors' being degraded, or the receptors can be recycled to the plasma membrane (see Carpentier, Gorden & Lew, 1992; Hollenberg & Jacobs, 1990). The initial internalisation of the insulin receptor is Ca^{2+} independent but the subsequent processing and recycling to the plasma membrane has been shown to be Ca^{2+} dependent (Carpentier *et al.*, 1992). It is thought that the early responses to insulin binding are triggered as a result of the formation of the microclusters of activated receptors and that the prolonged actions are initiated after the receptors are internalised (see Hollenberg & Jacobs, 1990; Olefsky, 1990) although it has also been reported that internalisation of the receptor is not required for it to produce its responses (McClain, 1990). An alternative to the receptor recycling is that they are redistributed to internal membranes, but this has not been fully demonstrated (see Hollenberg & Jacobs, 1990; Olefsky, 1990).

Table 1.3: Cellular responses to insulin and their respective time courses.

Response	Time Course
Regulation of ion flux (Na^+ , K^+ , Ca^{2+})	Milliseconds to seconds
Stimulation of receptor tyrosine kinase	Seconds to minutes
Stimulation of receptor-substrate phosphorylation	Minutes
Stimulation of glucose transport	Minutes
Stimulation of enzyme activity	
Glycogen synthase	Minutes
Pyruvate dehydrogenase	Minutes
Acetyl-CoA-carboxylase	Minutes
Stimulation of amino acid transport	Tens of minutes
Stimulation of protein synthesis	Tens of minutes to hours
Regulation of gene transcription	Tens of minutes to hours
Stimulation of cell division	Tens of hours

Taken from: Hollenberg, 1990

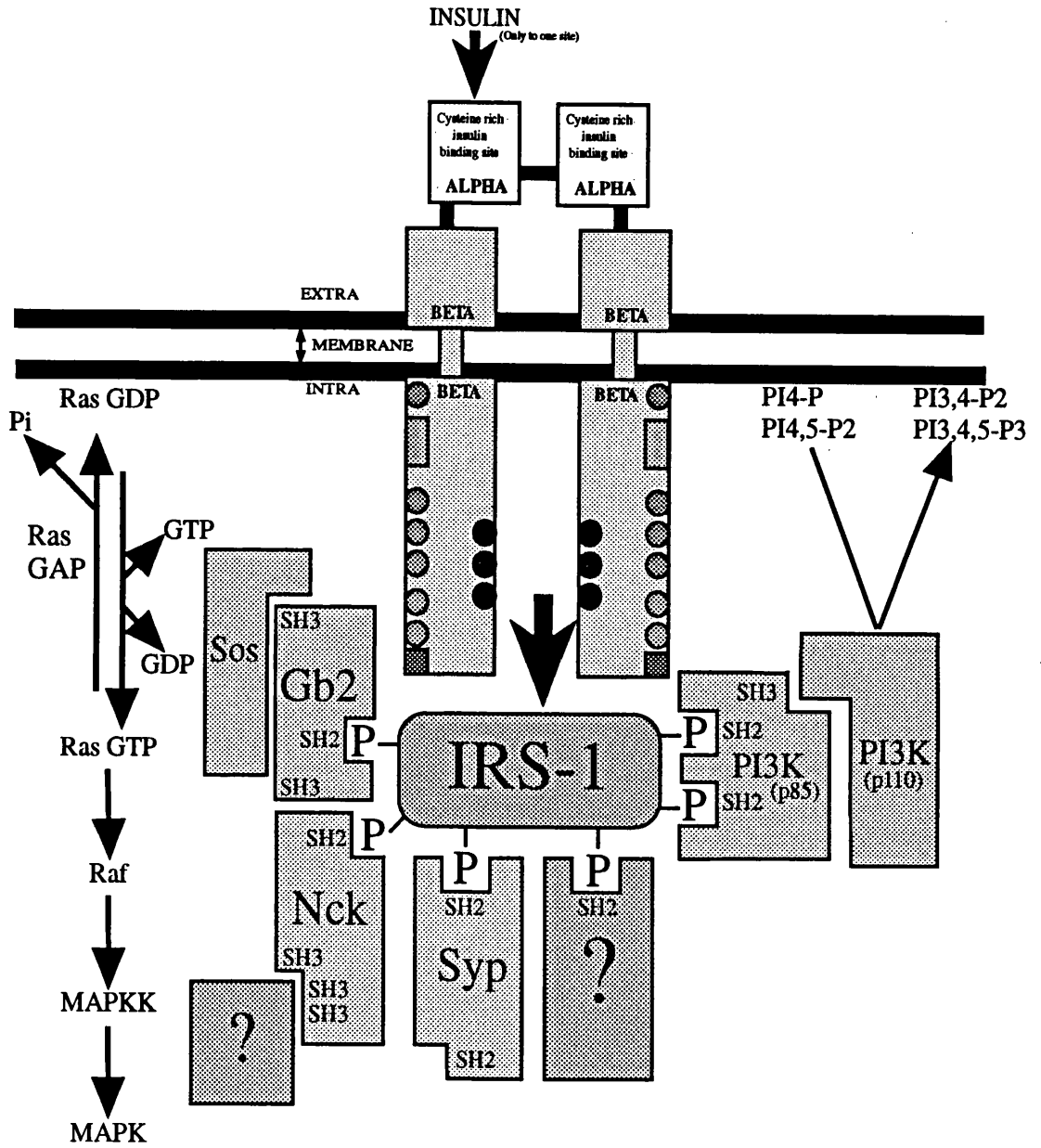
1.4.3.1 Insulin receptor tyrosine kinase activity and the insulin receptor substrate

As outlined in table 1.3 the insulin receptor mediates a range of cellular responses, yet the method, or methods, by which all the effects are produced is unknown. One of the best characterised responses of the receptor is its tyrosine kinase activity. The kinase activity has been examined and several intracellular insulin-dependent-phosphoproteins identified (see Avurch *et al.*, 1990; Dent *et al.*, 1990; Denton, 1990; Häring, 1991; Hollenberg & Jacobs, 1990; Pillion *et al.*, 1992). The most prominent insulin-dependent phosphotyrosine protein described, other than the β subunit of the receptor, has a molecular weight of 160-185 kDa and has now been called insulin receptor substrate 1 (IRS1; Avurch *et al.*, 1990; Dent *et al.*, 1990; Denton, 1990; Hollenberg & Jacobs, 1990; Keller & Lienhard, 1993; Rothenberg *et al.*, 1990; see Myers & White, 1993). It has also been found that this protein can be phosphorylated by insulin-like growth factor-I receptor (Giorgetti *et al.*, 1993; Myers *et al.*, 1993). Conversely it has been shown that the activated receptor can also cause the dephosphorylation of several cellular proteins. This has led to the proposal that the receptor initiates a phosphorylation / dephosphorylation cascade (Avurch *et al.*, 1990; Dent *et al.*, 1990). In this cascade, which is involved in the metabolism of glycogen, several of the component enzymes have been identified (Dent *et al.*, 1990). It has been shown that the cascade is dependent on the tyrosine kinase activity of the receptor and the link between the receptor and the first identified enzyme in the cascade may be via IRS1 (see figure 1.4; see Klarlund *et al.*, 1993; Tobe *et al.*, 1993).

IRS1 was first described in 1985 but it was not known if there were one or more of these proteins as the molecular weights reported ranged from 160 to 185 kDa. In 1991 the protein was cloned and the situation was resolved to show only one protein which was subsequently named IRS1 (see figure 1.4; see Keller & Lienhard, 1993). The protein has now been cloned from several different tissues, and species, and although it does not have extended homology with any other known proteins its conservation between the species examined is greater than 90% (Keller *et al.*, 1993). IRS1 has a predicted molecular weight of 131 kDa, is very hydrophilic and possesses numerable phosphorylation sites (see Keller & Lienhard, 1993). The protein is rich in sites for threonine and serine phosphorylations and contains twelve sites (out of thirty-four) that have good tyrosine kinase recognition motifs (Shoelson *et al.*, 1992). Several of these tyrosines are also in sequences that makes them good src homology 2 (SH2) binding domain recognition sites and it is via these sites that IRS1 binds to at least four SH2 domain containing proteins (see Keller & Lienhard, 1993; Myers & White, 1993). It has been reported that the protein has phosphotyrosine phosphatase activity associated with it (Goren & Boland, 1991) and no tyrosine kinase

Figure 1.4: Diagrammatic representation of the interaction of the activated insulin receptor and the insulin receptor substrate

Diagrammatic representation of the interaction of the activated insulin receptor (see figure 1.3) and the insulin receptor substrate (IRS1; see Keller & Lienhard, 1993). (GAP, GTPase activating protein; MAPK, mitogen-activated protein kinase; MAPKK, mitogen-activated protein kinase kinase; PI3K, phosphatidylinositol 3-kinase [p85 = regulatory domain, p110 = catalytic domain]; SH2 and SH3 are src homology domains binding domains 2 and 3; ?, unknown protein; Syp, tyrosine phosphatase; Nck, protein of unknown function although likely to be an adapter protein; Grb2, growth factor receptor-bound protein; Sos, Son of sevenless)



activity (Goren, Boland & Fei, 1993). Increased phosphorylation of IRS1 has been detected in the insulin induced regeneration of hepatocytes indicating its role in transmitting the insulin signals to intracellular regulators of growth (Sasaki *et al.*, 1993) but, in contrast, constant stimulation of the insulin signalling pathway causes an increase in the rate of degradation of IRS1 (Rice, Turnbow & Garner, 1993).

The four proteins that have so far been reported as binding to IRS1 are phosphatidylinositol 3-kinase (PI 3-kinase; Backer *et al.*, 1993; Backer *et al.*, 1992; Hadari *et al.*, 1992; Kelly & Ruderman, 1993; Okamoto *et al.*, 1993; Myers & White, 1993); growth factor receptor-bound protein 2 (Grb2; Skolnik *et al.*, 1993a, see Keller & Lienhard, 1993; Skolnik *et al.*, 1993b; Tobe *et al.*, 1993; Myers & White, 1993); Nck (see Keller & Lienhard, 1993); and Syp (or SH PTP2; Kuhné *et al.*, 1993; see Myers & White, 1993). It has been demonstrated that tyrosine phosphorylated IRS1 possesses more than one protein / protein interaction site as it can bind one or more of these proteins at a time (see figure 1.4; Keller & Lienhard, 1993; Skolnik *et al.*, 1993b; Tobe *et al.*, 1993).

PI 3-kinase was shown to be associated with IRS1 as immunoprecipitates of IRS1 from insulin stimulated cells also contained PI 3-kinase activity (Folli *et al.*, 1992; Kelly & Ruderman, 1993; Sung & Goldfine, 1992). PI 3-kinase consists of two subunits, a 85 kDa regulatory (p85) and a 100 kDa catalytic (p110) subunit and it is via the SH2 domains in p85 that IRS1 and PI 3-kinase interact. The result of the interaction is an activation of the enzyme and an increase of PI 3,4-bisphosphate and PI 3,4,5-trisphosphate levels in the membrane (Lamphere *et al.*, 1993). An alternative method of activation of PI 3-kinase by insulin is by the direct tyrosine phosphorylation of the 85 kDa regulatory subunit by the insulin receptor (Hayashi *et al.*, 1992; Hayashi *et al.*, 1991; Hayashi *et al.*, 1993).

Grb2, also known as abundant src homology (ASH), also co-immunoprecipitates with IRS1. The protein has a molecular weight of 23 kDa and contains one SH2 domain and two SH3 domains (see Keller & Lienhard, 1993). The presence of the SH domains indicates that it acts as an adapter protein with the SH2 domain binding to IRS1 and the SH3 domains interacting with other proteins. Biochemical evidence indicates that Grb2 is involved in the activation of *ras* (see section 1.2.2; Gale *et al.*, 1993) through an additional protein. The link protein between Grb2 and the activation of *ras* is Sos (son of sevenless) which is a guanine nucleotide-releasing protein for *ras* (see Baltensperger *et al.*, 1993; Keller & Lienhard, 1993; Li *et al.*, 1993; Rozakis-Adcock *et al.*, 1993; Skolnik *et al.*, 1993a; Skolnik *et al.*, 1993b).

Nck is a 47 kDa protein that has been found associated with the tyrosine phosphorylated form of IRS1. The function of the protein is unknown but as it contains one SH2 domain and three SH3 domains it would appear that it may function as an adapter protein (see Keller & Lienhard, 1993).

If the function of tyrosine phosphorylated IRS1 is to act as an initiator for some of the insulin receptor stimulated signalling pathways then a method for dephosphorylation, and hence deactivation, of the protein must exist. Failure to regulate the level of phosphorylation of IRS1, and its rate of dephosphorylation, could lead to the development of diabetes. It has already been demonstrated that insulin activates a serine phosphatase, protein phosphatase 1 (PP-1), by means of a C-terminal domain on the receptor (Begum *et al.*, 1993; see Bollen & Stalmans, 1992) but a method for dephosphorylation of the tyrosine residues of the receptor and IRS1 still has to be demonstrated. Insulin regulation of phosphotyrosine phosphatase activity has been reported (Meyerovitch *et al.*, 1992) but the phosphatase was only shown to dephosphorylate the insulin receptor *in vitro*. Work by Mooney and Bordwell (Mooney & Bordwell, 1992) has shown that a rapid turnover of phosphate does occur on the insulin receptor and IRS1 upon activation of the receptor, and that IRS1 is the most sensitive to phosphatase action. In addition it has been shown that tissue specific changes in phosphatase activity do occur in diabetes which indicates the importance of phosphatase activity in the correct processing of the insulin signal (Begum, Sussman & Draznin, 1991; Goldstein, 1992; Goren & Boland, 1991; Hauguel *et al.*, 1993). Goren (Goren & Boland, 1991) has shown that pp180 (IRS1) had, when immunoprecipitated, tyrosine phosphatase activity associated with it and it maybe that the phosphatase responsible for the termination of the IRS1 and insulin signals and pp180 were co-immunoprecipitated. An alternative method for the dephosphorylation of the receptor that has been proposed is a phosphatase-independent dephosphorylation (Gruppuso *et al.*, 1992).

A candidate protein for the phosphatase involved in the deactivation of the insulin receptor and IRS1 is the fourth protein that has been identified as binding to IRS1, Syp. This is a ubiquitously expressed phosphotyrosine phosphatase that contains two SH2 domains (Ahmad *et al.*, 1993; Freeman, Plutzky & Neel, 1992). It has been shown that Syp will bind to, and be phosphorylated by, activated EGF and PDGF receptors (Feng, Hui & Pawson, 1993), but not the insulin receptor (Kuhné *et al.*, 1993). The IRS1 / Syp complex was co-immunoprecipitated in insulin treated 3T3-L1 adipocytes (Kuhné *et al.*, 1993) and association of the two proteins was found to be dependent upon IRS1 being tyrosine phosphorylated. The formation of the complex may result in the activation of the phosphatase and ultimately in the dephosphorylation of IRS1 and the insulin receptor. The dephosphorylation of IRS1 by Syp has been demonstrated *in vitro* (G.E. Lienhard, personal communication).

1.4.3.2 Secondary messenger production and the interaction of the insulin receptor with G - proteins

An alternative method by which insulin may produce some of its intracellular signals is if the autophosphorylation of the receptor produces a conformational change such

that it can interact with G-proteins, or directly with enzymes such as PLC and adenylyl cyclase (see Hollenberg & Jacobs, 1990; Houslay & Siddle, 1989; Olefsky, 1990).

As insulin is able to produce such a range of metabolic effects the production of 'classical' secondary messengers by the receptor has been examined. A number of candidates have been put forward as secondary messengers of insulin, namely, cGMP, Ca²⁺ and inositol-glycans (see Romero, 1991); it has also been shown that the receptor can attenuate the production of cAMP (see Hollenberg & Jacobs, 1990; Houslay & Siddle, 1989; Olefsky, 1990; Saltiel, Cuatrecasas & Jacobs, 1990).

The production of inositol-glycans is believed to be mediated by an isoform of PLC (see section 1.2.3.2; see Saltiel *et al.*, 1990). It has been shown that insulin does not cause the production of inositol polyphosphates as a result of PLC activation but it has been demonstrated in adipose tissue that it can cause an increase in the rate of incorporation of inositol into PI 3,4-bisphosphate and PI 3,4,5-trisphosphate levels in the membrane by the activation of PI-3 kinase (Lamphere *et al.*, 1993; see sections 1.4.3.1 and 1.2.3.2; see figure 1.4; see Hollenberg & Jacobs, 1990). As in the classic inositol phosphate cycle (see section 1.2.3.2; see Berridge, 1993; Berridge & Irvine, 1989), the production of inositol -glycans is coupled to the production of another secondary messenger DAG (see sections 1.2.3.2 and 1.2.4.2). There is no clear evidence as to whether the inositol-glycan is produced on the intra- or extracellular face of the plasma membrane. It has been suggested that the glycan regulates the activity of some of the enzymes which are known to be affected in some way by insulin (see Houslay & Siddle, 1989; Saltiel *et al.*, 1990).

It has been shown that insulin can increase the concentration of DAG. This could arise either as a result of inositol-glycan production or from *de novo* synthesis (see Houslay & Siddle, 1989; Luttrell *et al.*, 1990). DAG is known to be an activator of PKC (see section 1.2.4.2; see Huang, 1989; Nishizuka, 1984) and it may be it is by the activation of this enzyme that insulin mediates some of its effects.

The activated insulin receptor can only attenuate the production of cAMP if the cAMP system is being stimulated (see sections 1.2.2, and 1.2.3.1; see Hollenberg & Jacobs, 1990; Houslay & Siddle, 1989). There is no evidence that insulin can change the rate of release of cAMP from the cell (see Houslay & Siddle, 1989), but there are indications that the attenuation may be produced by modifications of the G-proteins (see section 1.2.2), by the inhibition of adenylyl cyclase (see section 1.2.3.1) or by the stimulation of specific species of cAMP - PDE (see section 1.2.3.1; see Houslay, 1990). The insulin mediated change in PDE activity is a result of the activation of two specific species of PDE. The two species involved are the peripheral plasma membrane PDE (PPM-PDE) and the 'dense-vesicle' PDE (DV-PDE). The PPM-PDE is activated by phosphorylation (Kilgour, Anderson & Houslay, 1989) but the mode of activation of the DV-PDE is unknown (see Houslay, 1990).

Inhibition of adenylyl cyclase by insulin has not been shown to be mediated by G_i but caused either by the action of a unique G-protein or possibly by the phosphorylation of adenylyl cyclase itself. Alternatively the attenuation of the cAMP system may be achieved by the modification of G-proteins as a result of phosphorylation (see Häring, 1991). The direct involvement of G_i in the attenuation of adenylyl cyclase has been discounted in experiments which show that in diabetic animals, which exhibit G_i depleted hepatocyte plasma membranes and show a loss of cAMP attenuation, the attenuation can be restored by a drug, metformin, which does not effect G_i levels (see Houslay, 1990). This raises the possibility that as G_i levels are reduced in diabetes, and that they do not appear to be involved with adenylyl cyclase inhibition, that they may play some other role in the insulin signal transduction system such as glucose transport and metabolism (Moises & Heidenreich, 1990).

There have been reports of a 40 kDa GTP-binding site in adipocytes which is activated by the insulin receptor and is distinct from $\alpha-G_s$ (Kellerer *et al.*, 1991; see Häring, 1991) and may (Jo *et al.*, 1992) or may not (Kellerer *et al.*, 1991) be $\alpha-G_i$. There has also been a report of an insulin-dependent binding of GTP to a 66 kDa protein which has been partially purified from human placenta (G_{iR} ; Srivastava & Singh, 1990). The interaction of GTP γ S (non-hydrolysable analogue of GTP) with this protein inhibits the binding of insulin to its receptor (Srivastava & Singh, 1990) and it has also been shown that GTP γ S can inhibit insulin receptor function via a novel G-protein that is not G_s , G_i or G_o (Davis & McDonald, 1990). In addition, a pertussis toxin sensitive 40 kDa G-protein (see section 1.2.2.2) in myocytes has been implicated in the insulin signal transduction system where it has been demonstrated that pertussis toxin treatment attenuates the insulin-dependent production of DAG (see section 1.2.3.2) and inositol-glycans, but not the phosphorylation of the receptor and IRS1, and in membrane preparations insulin also increases the GTPase activity and GTP γ S binding (Luttrell *et al.*, 1990). The 'small' G-protein, (see section 1.2.2) p21^{ras}, and some other membrane proteins have been implicated in the transduction of the insulin signal (see section 1.4.3.1; see figure 1.4; see Hollenberg & Jacobs, 1990; Houslay, 1990). How the activated insulin receptor interacts or activates the heterotrimeric G-proteins is not known but *in vitro* studies have shown that $\alpha-G_i$ and $\alpha-G_o$ provide good substrates for insulin-promoted tyrosine-phosphorylation and $\alpha-G_s$ and $\alpha-G_t$ do not (Krupinski *et al.*, 1988) although the $\alpha-G_t$ data is contradicted by Zick *et al.* (1986).

Although it has not been conclusively shown that the insulin receptor is coupled to the second messenger systems by heterotrimeric G-proteins there is increasing evidence that the activated receptor can modify the action of some other G-protein coupled systems. For example, p21^{ras} inhibits the autophosphorylation of the receptor and insulin can inhibit the ADP-ribosylation of G_i in preparations of hepatocyte membranes (Rothenberg & Kahn, 1988; Rothenberg *et al.*, 1990; see Häring, 1991; Morris, N.J. unpublished results).

The possible sites of interaction between G-protein-coupled-receptors and G-proteins have been characterised (see Regoli & Nantel, 1990). The receptor G-protein-binding site shows a degree of sequence conservation, and in the sites that have been sequenced all have been shown to contain basic amino acids and to be in close proximity to the plasma membrane. This motif has been demonstrated in the insulin-like growth factor (IGF)-1 receptor. Examination of the amino acid sequence of the β -subunit of the insulin receptor has revealed no direct correlation with this motif, but it does contain regions which may possess the necessary properties to interact with G-proteins.

1.5 Aims

Activation of the insulin receptor is known to produce a wide array of responses in the target tissue with time periods varying from milliseconds to tens of hours. One of the earliest effects of receptor activation is the autophosphorylation of the receptor which results in the activation of its tyrosine kinase activity. It has been suggested that the phosphorylation may also result in a conformational change of the receptor such that it is able to interact with membrane proteins (e.g. phospholipase C, G-proteins) or that the activated receptor could modulate some of its effects via G-proteins. Possible interactions of the activated receptor with G-proteins have been demonstrated but no direct link between the receptors and G-proteins has been established. It is therefore proposed to further demonstrate whether any such interactions occur and to examine whether any changes occur in the signal transduction system as a result of diabetes.

The aim of the study was to examine the phosphorylation of the guanine nucleotide binding protein α -G_{i-2}, to identify the phosphorylation sites by peptide mapping, to investigate the effects of insulin on the phosphorylation events and to explore any changes in the phosphorylation characteristics in diabetic models. If any changes were observed in the models of type II diabetes it was proposed to use a development drug from SmithKline Beecham, which had been shown to be beneficial in treatment of animal models, to see if it had any effect on the phosphorylation event.

Chapter 2

Materials and Methods

2.1 *Materials*

2.1.1 *Animals*

Animals were obtained from stocks kept either at the University of Glasgow or at SmithKline Beecham, Epsom, Surrey. They were kept in similar conditions (unless stated otherwise in the text) of day-light / dark cycles with free access to food and water.

2.1.2 *Chemicals*

Inorganic [³²P] phosphate was purchased from Amersham International, UK. Phorbol 12-myristate 13-acetate (PMA) was from Cambridge Bioscience, UK. Insulin and protein A-agarose were bought from Sigma, UK. Cellulose t.l.c. plates were from Eastman Kodak Company, Rochester, N.Y., USA. Tosylphenylalanylchloromethane (TPCK)-treated trypsin, α -chymotrypsin, collagenase and *Staphylococcus aureus* V8 were purchased from Lorne Laboratories Ltd, Reading, Berks, UK. Okadaic acid from Mona Bioproducts, Hawaii, USA. Glucagon, Boehringer Ltd, UK. and amylin from Bachem Ltd, UK. Peptides were produced by either Biomac, Department of Biochemistry, Glasgow University, Glasgow, Scotland or the Department of Virology, Glasgow University, Glasgow, Scotland. All other biochemicals were from Boehringer Ltd, UK and other chemicals, unless stated otherwise, were of AR grade from BDH Ltd, UK or from Sigma, Poole, Dorset, England.

2.2 *Methods*

2.2.1 *Antibody Production*

Peptide conjugates were prepared using a method based on Reichlin (Reichlin, 1980). The peptides were coupled to hemocyanin (KLH; from Keyhole limpets, *Megathura crenulata*) using glutaraldehyde. 20 mg of KLH were dissolved in 2 ml of 0.1 M sodium phosphate buffer, pH7, and dialysed overnight. To the dialysed KLH 6 mg of peptide were added and dissolved. To the resulting solution 1.0 ml of 21 mM glutaraldehyde, dissolved in 0.1 M sodium phosphate buffer (pH7), was added drop-wise over an 8 hour period. The procedure was carried out at room temperature with constant stirring. The coupled peptide was stored in 100 μ l aliquots at -80°C until required.

Conjugated peptides were prepared for injection by diluting one aliquot of conjugated peptide (100 μ l, 0.2 mg of peptide) to 0.5 ml with phosphate buffered saline (PBS, see Appendix 1). This was then mixed with 0.5 ml Freund's adjuvant (complete Freund's for primary injections and incomplete for boosters) and placed in a sonicating water bath for two 15 second pulses. The solution was then mixed further by inversions of the

tube until the adjuvant was completely dispersed. The rabbits were injected at five or six sites on the back.

Bleeds were taken from all animals before the primary injection and the serum collected. Animals were given a booster injection 30 days after the initial immunisation and a test bleed was taken 10 days later. A final booster was given 50 days after the initial injection and a final bleed collected 10 days later.

For the preparation of rabbit serum blood was collected in 25 ml glass bottles, allowed to coagulate overnight at 4°C and the blood clots spun down at 500 - 700 × g in a bench centrifuge. The supernatant was collected (serum) and 0.1% (w/v) sodium azide added. The serum was aliquoted and stored at -80°C until required.

2.2.2 *Hepatocyte preparation*

Hepatocytes were prepared from male Sprague-Dawley, Zucker or diabetic Sprague Dawley rats (see Appendix 2) by using a modification of the methods of Berry, Elliott and Heyworth (Berry & Friend, 1969; Elliott & Pogson, 1977; Heyworth & Houslay, 1983). Sprague-Dawley rats (220-250g) or Zucker rats were given an intraperitoneal injection of pentobarbitone (Sagatal, 60 mg/ml) at 0.4 ml per 250g rat. Once the animal had become fully unconscious, determined by loss of the blink reflex, a laparotomy was performed. The viscera were displaced from the abdominal cavity and the inferior vena cava cannulated with a 15 gauge needle filled with heparin (see Appendix 2), and the liver perfused, via the hepatic portal vein, with 100 ml of stock Krebs buffer plus EDTA (see Appendix 2) which was allowed to drain to waste. Whilst the blood was flushed from the tissue the superior vena cava was clamped. Next, the liver was perfused with 80 ml Krebs / glucose buffer (see Appendix 2), which also drained to waste, before a final perfusion with 100 ml of recirculating Krebs / glucose buffer containing 0.5 - 1.0 mg collagenase per ml. The liver was perfused for 30 minutes or until the tissue showed signs of digestion such as excessive 'leakiness'. The liver was removed into 30 ml of Krebs, roughly chopped with scissors, and filtered through gauze before being centrifuged in two pre-warmed 50 ml centrifuge tubes at 100 × g in a bench centrifuge for 2 minutes. The supernatant was aspirated and the pellets washed twice with Krebs buffer. Finally the cells were washed in Krebs / Ca²⁺ (see Appendix 2) and cells needed for phosphorylation studies resuspended in low phosphate Krebs (see Appendix 3). All perfusion and wash buffers were gassed with 95% O₂ / 5% CO₂ and at 37°C.

2.2.3 *Phosphorylation of α -G_{i-2}*

The method followed was as outlined in Bushfield *et al.*, 1990a and Bushfield *et al.*, 1990b. Hepatocytes (see section 2.2.2) were diluted to 10⁶-10⁷ cells / ml in low phosphate Krebs buffer (see Appendix 3). The cells were aliquoted 1 ml per 25 ml siliconised conical flasks (see Appendix 3) and pre-incubated, with continuous shaking, for

65 min at 37°C in the presence of 0.2 mCi ^{32}P / ml. The cells were gassed every 10 minutes for 30 seconds with O_2/CO_2 (19:1). Ligands were added for the last 5 - 15 minutes of the incubation before the reaction was stopped by transferring the cells to ice and adding 10 ml of ice - cold low phosphate Krebs (see Appendix 3). The cells were harvested by centrifugation ($100 \times g$; 2 minutes). The cells were then solubilised and the protein immunoprecipitated (see section 2.2.4).

2.2.4 Solubilisation of cells and immunoprecipitation of $\alpha\text{-G}_{i-2}$

The method used for the immunoprecipitation of $\alpha\text{-G}_{i-2}$ is as outlined in Bushfield *et al.*, 1990a and Bushfield *et al.*, 1990b. To pelleted cells (see section 2.2.3) 1 ml of ice cold solubilising buffer was added (see Appendix 4) and vortexed. The cells were left on ice for 60 minutes before the solution was transferred to eppendorfs and centrifuged at $14,000 \times g$ for 10 minutes at 4°C. The supernatant was then transferred to clean eppendorfs and 50 μl of antiserum added. The tubes were then left overnight at 4°C.

The antibody was precipitated by adding 50 μl of protein A agarose and the tubes incubated at 4°C, with occasional inversions, for 90 - 120 minutes. The protein A agarose was then pelleted at low speed in a microfuge at 4°C and given two washes with 1 ml of Wash buffer + SDS and one wash with Wash buffer - SDS (wash buffers at 4°C; see Appendix 4). In all washes the pellet was resuspended by inversion and gentle shaking. After the final wash the pellet was resuspended in Laemmli buffer (Laemmli, 1970; see Appendix 5), boiled for 3 minutes and centrifuged at $14,000 \times g$ for 5 minutes at room temperature before the proteins were separated by SDS-PAGE (see section 2.2.5).

2.2.5 SDS-PAGE

The discontinuous buffer method of Laemmli (1970) was used. Gels, 10% (w/v), were poured into dry, clean, glass plates separated with 1.5 mm spacers (see Appendix 5). The main gel was overlaid with a small quantity of water saturated isobutanol and the gel allowed to polymerise. Polymerisation usually took 20 - 30 minutes at room temperature. Polymerised gels were used immediately and, where possible, long term storage was avoided. Prior to the addition of the stacking gel and the insertion of the well former, the layer of water / isobutanol was removed. Once the stacking gel had polymerised the well former was removed and the gel apparatus reservoirs filled with Running buffer (see Appendix 5). The samples (as prepared in section 2.2.4) were loaded (with care to avoid any protein A agarose pellet) and the gels run at 50 mA per gel (with cooling, run time 3 - 4 hours), or 7 mA per gel overnight, until the dye front had just run off the end of the gel. Gels were either used for Western blotting (see section 2.2.15) or dried, without fixing, at 65°C using a Biorad gel dryer. Dried gels were stapled to pre-flashed X-ray film (Fuji RX, see Appendix 6) and put down for autoradiography at -80°C (immunoprecipitates of phosphorylated $\alpha\text{-G}_{i-2}$ only required overnight exposure using one

intensifying screen). The autoradiography was either quantified using a Shimadzu CS-9000 densitometer or by removal of the identified bands from the gel and radioactivity determined by Cerenkov counting.

2.2.6 Elution of ^{32}P -labelled $\alpha\text{-G}_{1-2}$ from polyacrylamide gels

The method of Boyle, van der Geer & Hunter, 1991 was used. Poly-acrylamide gel chips, from unfixed gels, containing the samples were rehydrated in 500 μl of freshly prepared 50 mM ammonium bicarbonate (see Appendix 7) for 5 minutes at room temperature before being Cerenkov counted. The gel chips were then homogenised using disposable plastic pestles and homogenisation was judged to be complete when the sample was small enough to pass through the tip of a 50 - 200 μl pipette. The homogenate was then transferred to a clean screw top microfuge tube and the pestle, and its accompanying tube, given two washes with 250 μl of buffer. The final volume of homogenate was 1 ml and to this 50 μl of 2 β - mercaptoethanol and 10 μl of 10% (w/v) SDS solution was added before the sample was mixed and boiled for 5 minutes. The samples were then incubated for 90 minutes at 37°C with constant shaking to elute the protein.

After incubation the samples were centrifuged at low speed in a microcentrifuge at room temperature to pellet the gel pieces. The supernatant was transferred to clean tubes and a second volume of ammonium bicarbonate, plus 2 β - mercaptoethanol and SDS, was added to the gel pieces so that a final total volume of 1.2 ml of supernatant could be collected. The samples were mixed and boiled for 5 minutes before a second elution at 37°C for 60 minutes. A second volume of eluate was collected and pooled with the first and the total eluate (~1.2 ml) was clarified by centrifugation for 10 minutes at 14,000 \times g. The samples were then Cerenkov counted. From a typical elution procedure 80 - 90% of the counts in the original gel chip could be recovered in the eluate, if the figure was found to be less than 80% the elution procedure was repeated. Gloves were worn throughout the elution procedure and subsequent protein handling steps to avoid contamination with 'skin proteases'. Eluted proteins were either immediately precipitated and oxidized (see section 2.2.7) or stored overnight at -80°C. Only one gel chip was processed per tube and if samples required pooling for analysis this was done after the desalting in section 2.2.8.

2.2.7 Precipitation and oxidation of eluted proteins

To ice cold protein elutes 20 $\mu\text{g/ml}$ carrier protein (BSA) and TCA (final concentration 20% (w/v)) were added. The samples were then left on ice for 1 hour to allow the protein to precipitate and the protein collected by centrifugation at 14,000 \times g for 10 minutes at 4°C. The supernatant was aspirated and the samples briefly centrifuged and any remaining supernatant removed. The pellet was given one wash with ice cold acetone, the protein pelleted and the supernatant removed. All collected supernatants were kept.

The pellet was allowed to air dry at room temperature before being Cerenkov counted. The recovery from precipitation and acetone wash should be at least 70% of the original counts. If the counts were less than 70% the TCA precipitate and acetone wash supernatants were examined for radioactivity. If the radioactivity was found still to be in the supernatants the solutions were reprocessed to recover the maximum counts.

The air dried protein pellet was placed on ice and then oxidised for 60 minutes by dissolving it in 50 μ l of ice-cold performic acid (performic acid was prepared by mixing nine parts of 98% formic acid with one part 30% hydrogen peroxide and incubating for 1 hour at room temperature). Oxidation was stopped by the addition of 400 μ l of ice cold water and the samples lyophilised. At no stage of the oxidation was the sample allowed to warm as this would result in the occurrence of side reactions and so prevent good separation of the peptides by thin layer chromatography. Lyophilised samples were stored at -80°C before being digested as outlined in section 2.2.8.

2.2.8 *Proteolytic cleavage and desalting*

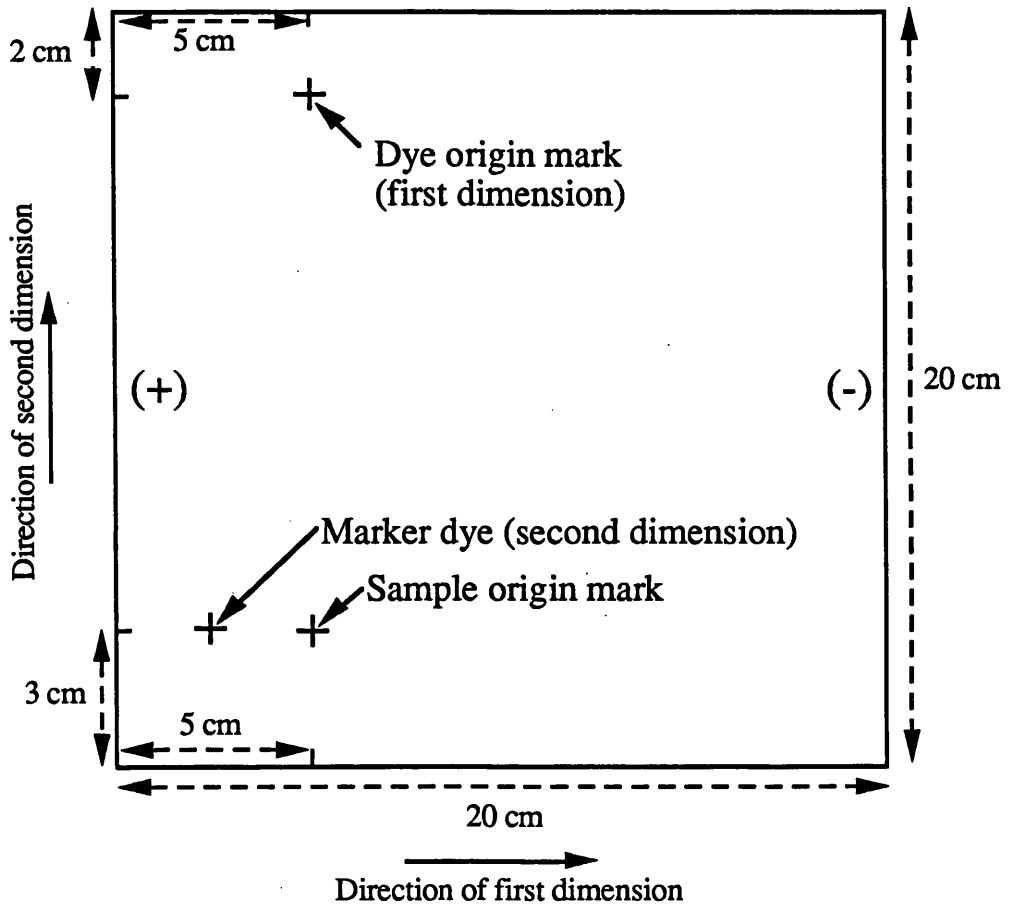
The lyophilised samples were resuspended in 50 μ l of 50 mM ammonium bicarbonate (pH 8 [ammonium bicarbonate solution prepared the day before should have drifted to this pH]; see Appendix 7), vortexed and briefly centrifuged to return the liquid to the bottom of the tube. To each tube 10 μ l of the appropriate enzyme was added and the tubes typically incubated at 37°C for 5 hours. The tubes were then vortexed for 40 seconds and centrifuged to collect the liquid in the bottom of the tube. A further 10 μ l of enzyme was added and the samples incubated for another 5 hours. The reaction was stopped by the addition of 400 μ l of water and the sample lyophilised. The samples were then repeatedly resuspended in 300 μ l of water and re-lyophilised until the salt content had been reduced to a minimum which would normally take three to four rounds of freeze drying. After the penultimate lyophilisation the samples were dissolved in 300 μ l of water, centrifuged at $14,000 \times g$ for 2 minutes at room temperature and the supernatant transferred to a new tube. The sample was then lyophilised and stored at -80°C until required for analysis. The enzymes that were used for digestion were TPCK-trypsin, α -chymotrypsin and *Staphylococcus aureus* V8. Stock solutions of 1 mg/ml were made up at the start of digestion and stored at -20°C until required. Trypsin was made up in 0.1 mM HCl and α -chymotrypsin and V8 in water (see Carrey, 1989). Occasionally longer periods of digestion were used and any variations are indicated in the results.

2.2.9 *Separation of ^{32}P -labelled enzymatic cleavage products*

Digested samples were Cerenkov counted, resuspended in 10 μ l of pH1.9 electrophoresis buffer (see Appendix 7) and vortexed for 1 minute. A 20×20 cm cellulose t.l.c. plate was overlaid on a template constructed to the measurements shown in figure 2.1 and sample and marker dye application positions marked with a soft lead pencil. The

Figure 2.1: Diagrammatic representation of t.l.c. plate template used for two dimensional chromatography analysis of phospho - peptides

Diagrammatic representation of t.l.c. plate template used for two dimensional chromatography analysis of phospho - peptides. (+) and (-) indicate the orientation of the electric field in the first dimension.



samples were then applied at the sample origin in 0.5 - 1.0 μl aliquots, with cold air drying between applications (see figure 2.1). After the last application the tube was re-counted and if more than 10% of the counts remained, the sample was re-dissolved and the procedure repeated. To the dye origin mark (first dimension) 5 μl of marker dyes (see Appendix 7) were applied in 0.5 μl aliquots. The marker dye contained ϵ - dinitrophenyl (DNP) lysine (yellow, positively charged at pH1.9); DNP-DL-glutamic acid (yellow, neutral charge at pH1.9); xylene cyanol FF (blue, negatively charged at pH1.9).

Before electrophoresis the plates were made damp with pH1.9 electrophoresis buffer. This was achieved by using a plate blotter which consisted of a 25 cm \times 25 cm sheet of 3MM filter paper with two 8 - 10 mm diameter holes cut in it so that when it was laid on a t.l.c. plate the holes were directly over the sample and dye origins. The blotter was laid over the t.l.c. plate and, using a shaving brush dampened with pH1.9 buffer, the holes were circled to encourage a flow of buffer towards the centre of the hole thus concentrating the sample. The rest of the filter paper was then brushed to dampen the plate. Correctly dampened plates had a dull grey appearance with no obvious shiny patches of excess buffer. If areas of excess buffer existed these were carefully removed using dry 3MM filter paper. The t.l.c. plates were run for 2 hours at 400 v in pH1.9 electrophoresis buffer (see Appendix 7) in a flat bed electrophoresis tank with the electric field orientated as shown in figure 2.1. After running the plates were air dried and 5 μl of marker dye (see Appendix 7) applied to the marker dye (second dimension) origin. The second dimension, ascending chromatography was then carried out in a 3MM filter paper lined chromatography tank containing phospho-chromatography buffer (see Appendix 7) with the buffer deep enough to cover only the bottom 0.5 - 1.0 cm of the plate. The plates were run until the solvent front was about 3 - 4 cm from the top of the plate which would normally take 3 - 4 hours. The labelled peptides were identified by autoradiography on pre-flashed film at -80°C (see Appendix 6) with exposure times of 6 - 10 days.

2.2.10 Recovery of peptides and secondary digests

Where secondary digests of peptides were required the samples would be scraped from t.l.c. plates and pooled. The resulting powder was Cerenkov counted, resuspended in 300 μl of distilled water and vortexed for 1 minute. The samples were then centrifuged at $14,000 \times g$ for two minutes at room temperature. The supernatant was collected and the pellet resuspended in 200 μl of distilled water, vortexed and centrifuged. The supernatant was collected and pooled with the first. Total volume recovered was approximately 400 μl which normally contained more than 80% of the counts in the original powder. If the counts recovered were lower than 80% the procedure was repeated.

The solution was freeze dried, resuspended in ammonium bicarbonate buffer (see Appendix 7) and the digestion and desalting carried out as described in section 2.2.8 and the digestion products separated as outlined in 2.2.9.

2.2.11 Phosphoamino acid analysis

The method used for phosphoamino acid analysis was as outlined in Boyle *et al.*, 1991 with the following changes. Samples were collected from t.l.c. plates as described in section 2.2.10 and freeze dried. The samples were dissolved in 500 μ l of 6 N HCl, sealed under vacuum and heated to 105°C for 90 minutes. The resulting solution was allowed to cool, collected and lyophilised using a freeze drier fitted with a NaOH trap. The samples were dissolved in pH1.9 electrophoresis buffer and applied to a 20 \times 20 cm t.l.c. plate which had sample application origins marked using the dimensions shown in figure 2.2. The plates were dampened with pH1.9 buffer (see section 2.2.9; Appendix 7) and run at 400 v for 30 minutes at pH1.9 (see Appendix 7) in the first dimension with the electric field orientated as shown in figure 2.2 and air dried. The plate was rotated through 90° and carefully made damp with pH3.5 electrophoresis buffer (see Appendix 7) with care taken to avoid the samples which were now 'streaked' out from the application points. The plate was run at 400 v for 30 minutes at pH3.5 (see Appendix 7) in the second dimension with the electric field orientated as shown in figure 2.2. Markers of phosphoserine, phosphothreonine and phosphotyrosine were included with the samples and these were visualised by staining with 0.25% (w/v) ninhydrine in acetone. Plates were put down on pre-flashed film (see Appendix 6) at -80°C for 10 - 14 days.

2.2.12 Prediction of enzyme cleavage products and mass charge ratios

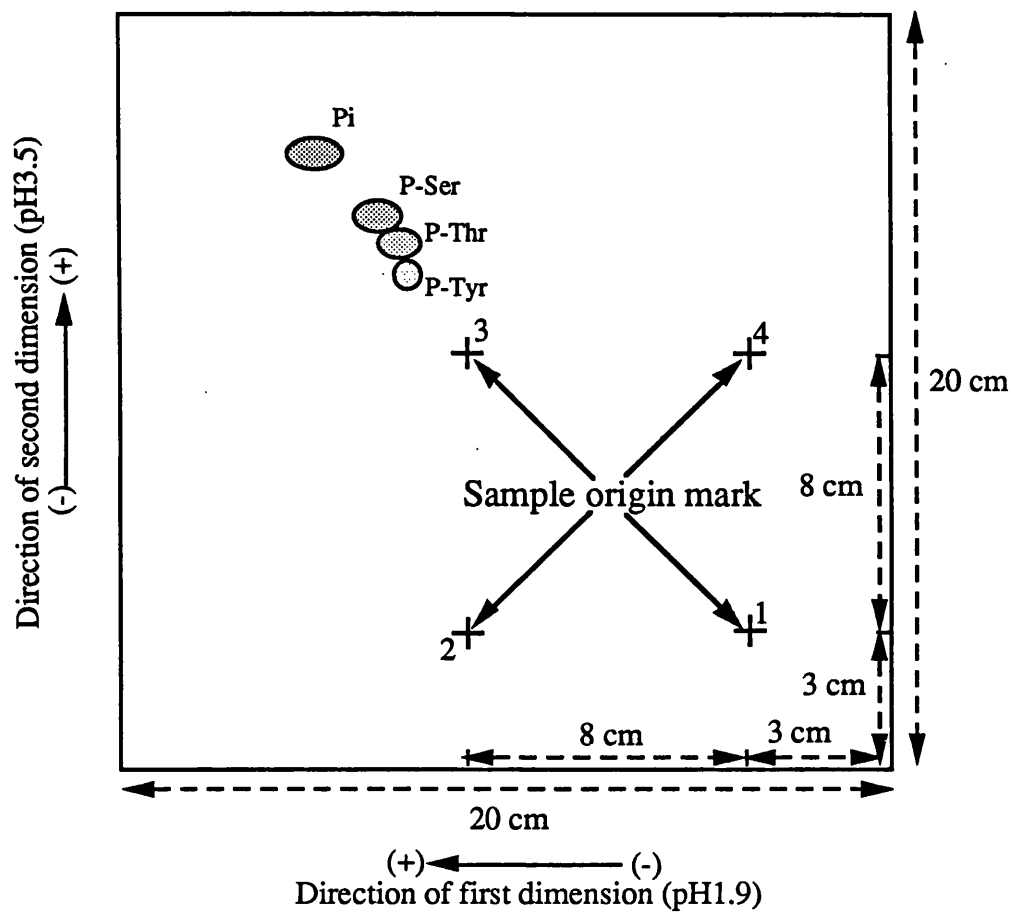
The prediction of peptide fragments produced by enzymatic cleavage and estimations of their mass-charge ratios was based on the methods outlined in Offord, 1966 and Boyle *et al.*, 1991 (see Chapter 3, section 3.1.4). The peptides produced by the enzymes can be predicted and the mass-charge ratio calculated from:

$$m_r = keM^{-2/3}$$

Where m_r = mass-charge ratio, k = constant, e = charge on the peptide, and M = molecular weight of the peptide (plus any added phosphate groups). The charge of the peptide can be calculated from the sum of the charges at pH1.9 of its constituents where the N-terminal and the amino acids arginine, histidine and lysine had a charge of +1, cysteine a charge of approximately -1 and phospho-serine a charge of -1. Mass charge ratios were calculated using a macro written for Excel (see Appendix 8).

Figure 2.2: Template for the layout of t.l.c. plates used for phospho-amino acid analysis

Template for the layout of t.l.c. plates used for phospho-amino acid analysis. The template shows the dimensions for marking out the plate for the application of four samples and the orientation of the electric fields. Spots marked Pi, P-Ser, P-Thr and P-Tyr show the final position of inorganic phosphate, phospho-serine, phospho-threonine and phospho-tyrosine, respectively, from a sample applied to position 3.



2.2.13 Preparation of plasma membranes from rat hepatocytes

A plasma membrane containing fraction was prepared from hepatocytes (see section 2.2.2) using the following method.

The hepatocytes were collected by centrifugation ($100 \times g$, 2 minutes room temperature) and resuspended in 3 volumes (approx. 20 ml) of ice cold Buffer A (see Appendix 9). The cells were homogenised by thirty strokes of a hand-held homogeniser at 4°C and the resulting homogenate was centrifuged for 10 minutes at 4°C and $1000 \times g$. The supernatant was collected and centrifuged at 4°C for 65 minutes at $100,000 \times g$. The supernatant was discarded and the pellet resuspended in Buffer A (approximately 5 ml) and snap frozen in 100 μl aliquots. The samples were assayed for protein content (see section 2.2.14) and stored at -80°C .

2.2.14 Protein Determination

A standard protein assay procedure based on Bradford was used (Bradford, 1976). In brief, a standard curve (0 - 20 μg BSA per tube) was prepared and standards and samples diluted to 800 μl with distilled water. To each tube 200 μl of Biorad protein reagent (Biorad) was added and the tubes vortexed. Samples were read at 595 nm.

2.2.15 Western blotting

Gels were prepared and run as described in section 2.2.5 and the Western blotting method of Towbin (Towbin, Staehelin & Gordon, 1979) used. In brief, the stacking gel was discarded and the main gel equilibrated in Blot Electrode buffer (BEB, see Appendix 10) for 5 minutes. Prior to use, nitro-cellulose sheets were washed for 5 minutes in distilled water. The gel was sandwiched, with the nitro-cellulose, between two 3MM filter pads and two 'Scotch-Brite' pads. The sandwich was assembled whilst submerged in BEB and firmly clamped before being transferred to the blotting tank. Blotting was carried out overnight by the application of a constant current of 10 mA (electrodes 10 cm apart) with cooling.

2.2.15.1 Immuno-staining of Western Blots

The method of Birkett *et al.*, (1985) was used with the following modifications. Blotting sandwiches were dismantled and the nitro-cellulose sheets removed. The blots were briefly stained with Ponceau S (see Appendix 10), and the required lanes cut out. The stain was removed with several washes in BEB (see Appendix 10). After destaining the blots were given two 5 minute washes with Tris-buffered saline Tween (TBS-T, see Appendix 10) and then incubated, with constant shaking, for 90 - 120 minutes with the appropriate primary antibody diluted in TBS-T. After incubation the primary antibody solution was removed and the blots were given two 5 minute washes with TBS-T, followed by one five minute wash with High-salt Tris-buffered saline (HST, see Appendix 10). This

was followed by a further two 5 minute washes with TBS-T. The blots were then incubated for 90 minutes with the appropriate secondary antibody labelled with horseradish-peroxidase (HRP) diluted in HST. After incubation the blots were given three 5 minute washes with TBS-T, followed by a 10 minute wash with HST, and three more 5 minute washes with TBS-T. After the final wash the blots were incubated with the Developing solution (See Appendix 10) to visualise the labelled bands. Development was stopped by repeated washes with distilled water. The blots were dried before being scanned by reflectance using a Shimadzu CS-9000 densitometer. Protein bands were visualised by staining with Ponceau S (see Appendix 10).

2.2.16 Enzyme linked immuno - assay (ELISA)

The method used for ELISAs is essentially as outlined in section 2.2.15 for Western blots with the following changes. Samples were diluted in sodium carbonate buffer (see Appendix 11) to 4 µg/ml. 100 µl aliquots were placed in each well of the plate and left overnight at room temperature in a humidified container. The plates were then given two washes with TBS-T (see Appendix 10) and left incubating in TBS-T for 1 hour.

Primary antibodies were diluted in TBS-T and aliquoted at 100 µl per well. Antibodies were left on the plate for 90 minutes before the plate was subjected to a wash and secondary antibody regime as outlined in section 2.2.15.

After incubation with the secondary antibody, and the subsequent washes, the plates were developed for 20 minutes by incubating with substrate solution (100 µl per well; see Appendix 11) and the reaction then stopped by the addition of 50 µl of 4 N H₂SO₄. Plates were read at 492 nm on Titerek Multiskan.

2.2.17 Statistical analysis

Statistical significance was determined using the Student t-test available on Excel (Microsoft Corporation), or Statworks on the Macintosh, or by a Mann-Witney test (Mann & Witney, 1947) using a macro written for Excel (see Appendix 8). A value of $p < 0.05$ was taken as significantly different. Where appropriate any curves were fitted using the regression function of Cricket Graph (Cricket Software).

Chapter 3

Multiple phosphorylation sites of α -G_{i-2}

3.1 *Introduction*

Many cell-surface receptors control the activity of their effector systems through specific members of a family of guanine nucleotide-binding regulatory proteins (G-proteins; see section 1.2; see Gilman, 1989; Gilman, 1987; Milligan *et al.*, 1990; Neer & Clapham, 1988). The receptor-dependent production of cAMP is effected by adenylyl cyclases (see section 1.2.3.1) whose activities are regulated by two distinct heterotrimeric G-proteins termed G_s (stimulatory) and G_i (inhibitory; see section 1.2.2). These G-proteins are characterised by unique α -subunits which are the products of different genes (see section 1.2.2.2). The G_i family comprises of eight related proteins but only the pertussis toxin-sensitive G-proteins α -G_{i-1}, α -G_{i-2} and α -G_{i-3} are involved in the inhibition of adenylyl cyclase (see section 1.2.2.2; table 1.1). Whilst the specificity of these G_i proteins is not yet fully characterised, a number of groups have provided evidence that α -G_{i-2} can act as an inhibitory G-protein controlling adenylyl cyclase activity (Bushfield *et al.*, 1990b; Senogles *et al.*, 1990; Simmonds *et al.*, 1989; Pyne *et al.*, 1989b).

3.1.1 *Phosphorylation of G-proteins*

In various cell types the activation of PKC (see section 1.2.4.2) has been shown to result in the alterations of the regulation of adenylyl cyclase activity (see section 1.2.3.3; see Houslay, 1991a). In some instances this has enhanced basal and agonist-stimulated action but in others cases a loss of receptor-mediated stimulation has been reported and the process has been believed to involve the phosphorylation of the receptor (see Geny *et al.*, 1989; Hill & Kendall, 1989; Jakobs *et al.*, 1985; Sagi-Eisenberg, 1989). Further evidence from a number of studies has indicated that the inhibitory regulation of adenylate cyclase through α -G_i can be prevented by activation of PKC (see section 1.2.4.2; Bushfield, Lavan & Houslay, 1991; Bushfield *et al.*, 1990b; Daniel-Issakani, Spiegel & Strulovici, 1989; Katada *et al.*, 1985; Pyne *et al.*, 1989a; Pyne *et al.*, 1989b). Indeed, it has been shown that the activation of this enzyme in hepatocytes, either by phorbol esters or by hormones which stimulate phosphoinositide metabolism, can lead to the phosphorylation of α -G_{i-2} and to the loss of GTP-elicited G_i functioning (Bushfield *et al.*, 1991; Bushfield *et al.*, 1990b; Pyne *et al.*, 1989b). A loss of GTPase activity of α -G_{i-2} as a result of PKC mediated phosphorylation has also been demonstrated *in vitro* (Sauvage, Rumigny & Maitre, 1991) and PKC mediated phosphorylation of α -G_{i-1} or α -G_{i-2} has been demonstrated in platelets where it was shown to inhibit Ca²⁺ mobilisation (Yatomi *et al.*, 1992) and to abolish G_i inhibition of adenylyl cyclase (Katada *et al.*, 1985). Interestingly Carlson (Carlson, Brass

& Manning, 1989) and Lounsbury (Lounsbury *et al.*, 1991) showed that neither α -G_{i-1} or α -G_{i-2} were phosphorylated by PKC in platelets.

Treatment of intact cells with phorbol esters and *in vitro* studies have demonstrated that other G-proteins can also be phosphorylated by PKC or other kinases. In human platelets treatment with thrombin or phorbol esters leads to the phosphorylation of α -G_Z or a similar protein (Carlson *et al.*, 1989; Lounsbury *et al.*, 1991; Lounsbury *et al.*, 1993). α -G_S has been shown to be phosphorylated by PKC (Pyne, Freissmuth & Palmer, 1992; Sauvage *et al.*, 1991) and PKA (Sauvage *et al.*, 1991) *in vitro* whilst PKA has been shown not to phosphorylate α -G_i *in vitro* (Lincoln, 1991) although cAMP dependent phosphorylation of α -G_{i-2} in *Dictyostelium* has been reported but it was not demonstrated to be PKA dependent (Gundersen & Devreotes, 1990).

Incubation of intact hepatocytes with a range of ligands capable of activating PKC, including PMA (phorbol ester), vasopressin, angiotensin II, and those capable of activating cAMP-dependent protein kinase (PKA, see section 1.2.4.1), such as glucagon and 8-bromo-cyclic-AMP, resulted in the selective serine-specific phosphorylation of α -G_{i-2}, but did not affect either α -G_{i-3} or α -G_S (Bushfield *et al.*, 1990b). Indeed, exposure of hepatocytes to the phosphoprotein phosphatase (1 and 2A) inhibitor okadaic acid (see section 1.2.4.3), also caused the phosphorylation of G_{i-2} (Bushfield *et al.*, 1991). It has been suggested (Bushfield *et al.*, 1991) that the activity of this guanine nucleotide regulatory protein may be controlled, in hepatocytes, by a phosphorylation / dephosphorylation cycle. These events may be cell-type dependent as the challenge of platelets and human kidney 293 cells with phorbol esters also results in the phosphorylation of a G-protein, α -G_Z, but did not affect α -G_i (Lounsbury *et al.*, 1993), with the phosphorylation of α -G_Z occurring on serine 27.

It has been suggested that α -G_{i-2} may be phosphorylated at one site by ligands which cause activation of PKC and at a separate site which is dependent upon the activation of PKA but may not be phosphorylated directly by the kinase (Bushfield *et al.*, 1990b).

3.1.2 Kinase motifs

To date over 100 mammalian protein kinases have been described (see section 1.2.4; see Hunter, 1991). These kinases not only have different modes of activation (see section 1.2.4) but also have different substrates which possess different kinase recognition motifs (e.g. see table 3.1; Azzi *et al.*, 1992; Hug & Sarre, 1993; Kennelly & Krebs, 1991; Pearson & Kemp, 1991).

The work described in this chapter is associated primarily with the activation of two protein kinases, PKA (see section 1.2.4.1) and PKC (see section 1.2.4.2). Both these kinases are classed as serine / threonine kinases (see Hunter, 1991) and the possible recognition motifs, and their occurrence in α -G_{i-2}, are shown in table 3.1.

Table 3.1

The occurrence of protein kinase recognition motifs in α -G_{i-2}.

PKA = protein kinase A; PKC = protein kinase C; CDPKII = Calmodulin-dependent protein kinase II; CKI = Casein kinase I; CKII = Casein kinase II; PKG = cGMP dependent protein kinase; GSKIII = Glycogen synthase kinase III; GHK = Growth associated histone H1 kinase (MPF, cdc2+/CDC28 protein kinase); S = serine, K = lysine, R = arginine, V = valine, S(P) = phospho-serine, D = aspartic acid, E = glutamic acid, P = proline, x = any amino acid; Ratios refers to the number of phosphorylation sites that fit the motif out of all sites identified to date (Pearson & Kemp, 1991); references: 1 = Pearson & Kemp, 1991; 2 = Kennelly & Krebs, 1991; 3 = Hug & Sarre, 1993; 4 = Azzi *et al.*, 1992

Kinase	Site(s)	Ratio	Serine	Ref
PKA	RxS	21/46	None	1
PKA	RRxS	12/46	None	1
PKA	RxxS	11/46	None	1
PKA	KRxxS	2/46	None	1
PKA	a) RR/KxxS		None	2
PKA	b) RxxS		None	2
PKA	c) RxS		None	2
PKA	RS		16 144 207	2
	(a>b>c)			
PKC	RxxSxR		None	3
PKC	SxK/R		44 207 247	4
PKC	K/RxxS		None	4
PKC	K/RxxSxK/R		None	4
PKC	K/RxS		None	4
PKC	K/RxSxK/R		None	4
PKC	SxK/R	20/37	44 207 247	1
PKC	K/RxxS	13/37	None	1
PKC	K/RxxSxxK/R	7/37	None	1
PKC	K/RxS	10/37	None	1
PKC	K/RxSxK/R	6/37	None	1
PKC	a) R/K ₁₋₃ x ₂₋₀ Sx ₂₋₀ R/K ₁₋₃		16 144 207	2
PKC	b) Sx ₂₋₀ R/K ₁₋₃		16 44 144 207 306	2
PKC	c) R/K ₁₋₃ x ₂₋₀ S		16 47 144 207	2
	(a>b≥c)			
CDPKII	xRxxS	13/20	None	1
CDPKII	xRxxSV	6/20	None	1
CDPKII	RxxS		None	2
CKI	S(P)xxS	5/9	47	1
CKI	a) S(P)x ₁₋₃ S		47 306	2
CKI	b) (D/E ₂₋₄ ,x ₂₋₀)xS		47 62 125 264 302	2
	a>b			
CKII	SxxE	23/30	62 306	1
CKII	SxxD	3/20	6 229	1
CKII	S(D/E/S(P)) ₁₋₃ ,x ₂₋₀		6 62 229 306	2
PKG	R/KxS	9/10	None	1
PKG	R/KxxS	8/10	None	1
PKG	R/KR/KxS	7/10	None	1
PKG	R/KxxxS	5/10	166 247	1
PKG	SxR/K	2/10	44 207 247	1
PKG	R/K ₂₋₃ xS		166 247	2
GSKIII	SxxxS(P)	6/12	302	1
GSKIII	Sx ₃ S(P)		302	2
GHK	SPxK/R	6/15	None	1
GHK	K/RSP	5/15	None	1
GHK	SPK/R	4/15	None	1
GHK	SPxK/R		None	2

3.1.3 Protein structure

Proteins consist of twenty different amino acids which are used to form a poly-peptide chain referred to as the primary structure of the protein. This poly-peptide chain can then undergo spontaneous folding to produce a secondary structure and finally a tertiary structure. The folded protein may also form a subunit in some larger protein giving a final protein that is described as possessing quaternary structure (see Argos, 1989; Chou & Fasman, 1978; Chothia & Finkelstein, 1990).

The folding of the poly-peptide to form the secondary structure only takes into account the poly-peptide backbone of the protein and not the side-chain configurations. The secondary structures typically consists of α -helices, β -sheets and β -turns (see section 3.1.3.2). The tertiary folding of the protein takes into consideration the arrangement of the atoms, the occurrence of disulphide bridges and the interaction of the side chains (see Argos, 1989; Chou & Fasman, 1978).

3.1.3.1 Primary sequence of α -G_{i-2}

The primary sequence of rat α -G_{i-2} was determined by Itoh *et al.* in 1986 and Jones and Reed in 1987 (Itoh *et al.*, 1986; Jones & Reed, 1987). The primary sequence is shown in figure 3.1 and in Appendix 12. The primary sequence consists of 355 amino acids and has a predicted molecular weight of 40,503.

3.1.3.2 Secondary structure of α -G_{i-2}

A protein can possess four classes of secondary structure and these structures can be predicted, albeit with a certain degree of uncertainty, using a range of methods (see Argos, 1989). The four classes of structure are typical protein structures (α -helices, β -sheets, turns; see Argos, 1989; Chou & Fasman, 1978; Garnier, Osguthorpe & Robson, 1978), trans-membrane helices, signal and target structures and antigenic sites (see Argos, 1989). The methods used to carry out such predictions can be divided into three groups, probabilistic (or statistical), physico-chemical, and information theory.

Probabilistic methods rely on the analysis of proteins whose secondary structure is known and the analysis of the amino acid sequence in the secondary structures. From such an analysis the amino acids are assigned a value and these values are then used to predict whether that type of secondary structure is likely to occur in another protein. The analysis of the secondary structure of a new protein is carried out by assigning the amino acid values for the structure of interest (e.g. α -helix) and then averaging the values of the amino acids over a four to eight amino acid stretch. If the mean value for the amino acids is greater than some pre-determined threshold value then the region of protein is reported as

Figure 3.1: The primary sequence of rat α -G_{i-2}

The primary sequence of rat α -G_{i-2} (Itoh *et al.*, 1986).

having a high probability for the occurrence of that type of secondary structure (see Argos, 1989; Chou & Fasman, 1978; Garnier *et al.*, 1978). Examples of this type of method are those of Chou / Fasman (see Chou & Fasman, 1978) and Garnier / Robson (see Garnier *et al.*, 1978) and these methods are used for the prediction of secondary structures such as α -helices, β -sheets and β -turns (see Argos, 1989; Chou & Fasman, 1978; Garnier *et al.*, 1978).

Physico-chemical methods rely on examining the primary sequence of a protein for the occurrence of defined patterns in the distribution of polar and non-polar amino acids. An example of this is if a spatial construction of an α -helix is formed then one side will contain hydrophilic amino acids and the other hydrophobic, therefore examining a primary sequence for regions where such arrangements are possible will give a prediction for the occurrence of α -helices. If the primary sequence is examined and regions are found where alternating polar and non-polar amino acids occur then this may indicate the presence of β -strands (see Argos, 1989).

The information theory approach is similar to the probabilistic approach in that it examines known secondary structures and then analyses their amino acid composition. The information derived from this approach is then used to predict secondary structures in other proteins. The approach can be viewed as examining a known secondary structure and then looking for sequence homology in the new protein that corresponds to that sequence (see Argos, 1989).

The accuracy of the above prediction methods for α -helices, β -sheets and β -turns lies between 50 and 60% (see Argos, 1989) with accuracy approaching 90% (see Chou & Fasman, 1978) with some of the more refined methods available or when a combination of methods is used (see Argos, 1989; Chou & Fasman, 1978). These levels of accuracy compare favourably with the random prediction of the three structures which would only give 33%. A combination of methods maybe used when it is known that one tends to over predict the occurrence of certain structures whilst another under-predicts (see Chou & Fasman, 1978).

The prediction of the occurrence of secondary structures, and a final tertiary structure (see section 3.1.3.3) of α -G_{i-2} has been carried out by Bourne's group (Berlot & Bourne, 1992; Conklin & Bourne, 1993; Masters, Stroud & Bourne, 1986). An information theory approach has been taken where the known sequence and established structure of EF-Tu and p21^{ras}, determined by x-ray crystallography, has been exploited in the prediction of the protein structure of the α -subunit of the heterotrimeric G-proteins. As EF-Tu and p21^{ras} have a shorter primary sequence than α -G_{i-2} then secondary structure prediction methods have been used for the insert and extension regions. By using a combination of the methods of Chou / Fasman (see Chou & Fasman, 1978) and Garnier / Robson (see Garnier *et al.*, 1978) the secondary structures of α -G_{i-2} was predicted and only regions of the protein that possessed the same structure in both prediction methods were

considered as possessing that structure. The results are shown in figures 3.2 and 3.18 and discussed in sections 3.3.5. and 3.4.

3.1.3.3 Tertiary structure of α -G_{i-2}

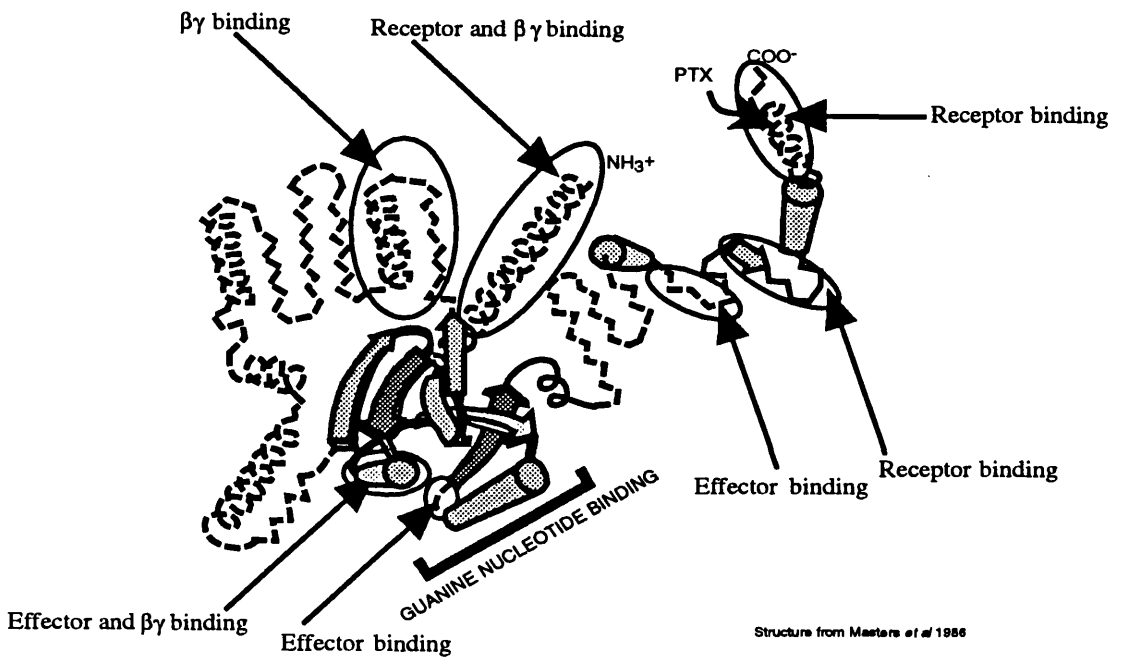
The prediction of the tertiary structure of a protein is complicated and usually relies on the comparison of the sequence of known tertiary structures of proteins with those of the new protein; this process is described as knowledge based modelling (see Sali *et al.*, 1990; Baron, Norman & Campbell, 1991). By the use of this approach it has been possible to model the tertiary structure of α -G_{i-2} (Conklin & Bourne, 1993; Masters *et al.*, 1986).

The structure is based on the known configuration of the GTP binding domain of the proteins EF-Tu (bacterial elongation factor) and p21^{ras} (see section 1.2.2; see figure 3.2; Conklin & Bourne, 1993; Masters *et al.*, 1986). Both EF-Tu and p21^{ras} are considerably shorter polypeptides than any of the α -subunits but it is possible to align the proteins and therefore infer the structure of the G-protein α -subunit (see Berlot & Bourne, 1992; Conklin & Bourne, 1993; Masters *et al.*, 1986). Using this approach EF-Tu and p21^{ras} have been aligned with the G-protein α -subunits and the secondary and tertiary structures predicted. As EF-Tu and p21^{ras} are shorter poly-peptides than the α -subunits this leaves six regions that do not occur in EF-Tu or p21^{ras}. The regions of unknown structure occur at the N and C terminals and also comprise of four insertions within the protein (see figures 3.18 and 3.2; see Berlot & Bourne, 1992; Conklin & Bourne, 1993; Masters *et al.*, 1986). Using these strategies (see Berlot & Bourne, 1992; Conklin & Bourne, 1993; Masters *et al.*, 1986) an approximation for the structure of the heterotrimeric G-protein α -subunit has been proposed. The protein is believed to be arranged with the GTP-binding domain facing the cytoplasm of the cell with the α -subunit anchored to the membrane via the N-terminal. From the N-terminal extension, the peptide chain leads into the first β -sheet which forms part of the GTP-binding domain (see figures 3.2 and 3.18). The protein is then arranged with the first (i1) and third (i3) inserts facing the cytoplasm and inserts two (i2) and four (i4), and the C-terminal extension facing the membrane (see figures 3.18 and 3.2; see Berlot & Bourne, 1992; Conklin & Bourne, 1993; Masters *et al.*, 1986).

The regions of the protein involved in GTP binding have been predicted from both the studies of the structure of EF-Tu and p21^{ras}. The use of antibodies, mutations, chemical cross linking and peptide competition studies has led to the suggestion for the location of some of the other functional domains of the protein (see figures 3.18 and 3.2; Conklin & Bourne, 1993; Masters *et al.*, 1986). Thus it has been found that the receptor interacts with a portion of the N-terminal extension, the C-terminal extension and sections of the tenth turn and sixth β -sheet; the $\beta\gamma$ -subunit binds to part of the N-terminal extension, the second α -helix and a region at the start of the first insertion; and the effector interacts with the second and fourth insertions and part of the second α -helix (see figures 3.2 and 3.18; see Conklin & Bourne, 1993).

Figure 3.2: Tertiary structure of α -G_{i-2}

Tertiary structure of α -G_{i-2} (Berlot & Bourne, 1992; Conklin & Bourne, 1993; Masters *et al.*, 1986). Barrels represent regions of α -helix, arrows β -sheets of EF-Tu and p21^{ras}, and dashed lines extensions and insertions.



3.1.4 *Enzymatic cleavage, prediction of peptides and their movement in two-dimensional chromatography*

The prediction of peptide fragments produced by enzymatic cleavage and estimations of their mass-charge ratios was based on the methods outlined in Boyle *et al.* (1991). Although it is possible to predict the peptides produced by the enzymes, the tertiary and secondary structures of the protein may mask the cleavage sites and the amino acid sequence at the cleavage site may effect the efficiency of the enzyme. Peptides were predicted by following the information as outlines in sections 3.1.4.1, 3.1.4.2 and 3.1.4.3.

If the peptides produced by the enzymes can be predicted then the movement of the peptide in two-dimensional chromatography can be estimated based on the mass-charge ratio of the peptide in the first electrophoretic dimension and its R_f value in the second ascending chromatography dimension. The mass-charge ratio can be calculated from the equation:

$$m_r = keM^{-2/3}$$

Where m_r = mass-charge ratio, k = constant, e = charge on the peptide, and M = molecular weight of the peptide plus the additional phosphate groups (Offord, 1966; see Boyle *et al.*, 1991). The charge of the peptide can be calculated from the sum of the charges at pH1.9 of its constituents where the N-terminal and the amino acids arginine, histidine and lysine have a charge of +1, cysteine a charge of approximately -1 and phospho-serine a charge of -1 (see Boyle *et al.*, 1991). Mass-charge ratios were calculated using a macro written for Excel on the Macintosh (see Appendix 12).

The R_f value of the peptide can be calculated by using the known R_f values of the individual amino acids (see Boyle *et al.*, 1991) and by calculating the sum of the R_f values of the individual amino acids in the peptide and dividing by the number of amino acids present (see Boyle *et al.*, 1991). This method of prediction is not very accurate as the R_f values of the individual amino acids do not take into consideration the loss of charge on the NH_2 and $COOH$ groups when the peptide is formed. As a consequence of this the resulting predicted R_f values for the peptides tends to be lower and closer together than the actual values (see Boyle *et al.*, 1991).

Furthermore, additional information concerning the phosphopeptides can be derived from the final pattern of spots on the autoradiography. Thus, two spots of similar mass-charge ratio that are only separated by ascending chromatography may indicate a peptide that contains more than one phosphorylation site of which only one is phosphorylated at a given time. Such peptides would have the same mass charge ratios and may have different R_f values. Another indication of the identity of the peptide is if the pattern of spots is seen to lie on a diagonal. In such instances, if the diagonal slopes towards the anode then this indicates that the peptide contains multiple phosphorylation sites

with each spot representing a change in the number of phosphate groups and where the peptide furthest from the application origin contains the least number of phosphorylated residues. If the diagonal slopes toward the cathode this indicates that the peptides are partial cleavage products and are related by the addition of a single basic residue (lysine [K], arginine [R] or histidine [H]; see Boyle *et al.*, 1991).

3.1.4.1 Prediction of tryptic cleavage products of α -G₁₋₂

Trypsin catalyses the hydrolysis of the peptide bonds between the COOH of arginine (R) or lysine (K) residues and the NH₂ group of the next amino and the efficiency of the enzyme can be affected by the surrounding amino acids. Trypsin will not cleave at either arginine - proline or lysine - proline and will cleave more slowly if the basic residue (R or K) is adjacent to an acidic residue (aspartic acid [D] or glutamic acid [E]) or cysteine (C). Cleavage can also be affected by the occurrence of multiple arginine or lysine residues, or when arginine or lysine occurs in the following sequence, Arg/Lys - x - P-Ser/P-Thr where P-Ser, P-Thr and x are phospho-serine, phospho-threonine and any amino acid, respectively. Interestingly the occurrence of the phosphorylation site next to the cleavage point does not always affect the hydrolysis (see Boyle *et al.*, 1991; Carrey, 1989; Smyth, 1967).

3.1.4.2 Prediction of V8 cleavage products

V8 is a glutamic acid (E) and aspartic acid (D) specific protease produced by *Staphylococcus aureus*, which under certain incubation conditions has been reported to be specific only for glutamic acid (see Boyle *et al.*, 1991; Carrey, 1989; Drapeau, 1977). The incubation conditions required for glutamic acid specificity are the inclusion of ammonium bicarbonate in the reaction buffer (see Boyle *et al.*, 1991; Carrey, 1989; Drapeau, 1977) but it has been shown that the bicarbonate only inhibits the rate of cleavage at aspartic acid and under prolonged incubation conditions or high enzyme concentration, cleavage at aspartic acid will still occur (Sørensen, Sørensen & Breddam, 1991).

The activity of the enzyme is also affected by modifications near the cleavage site in the protein such as carboxymethylation (Sellinger & Wolfson, 1991) and also shows reduced rates of cleavage at glutamic acid when it occurs in the following sequences; proline - x - glutamic acid; glutamic acid - aspartic acid; glutamic acid - proline; and glutamic acid - x - proline (where x is any amino acid; Breddam & Meldal, 1992).

3.1.4.3 Prediction of α -chymotrypsin cleavage products

α -chymotrypsin is a protease that cleaves at tyrosine (Y), phenylalanine (F) and tryptophan (W; see Boyle *et al.*, 1991; Carrey, 1989; Smyth, 1967) although it has also been reported to cleave at leucine (L), methionine (M) and alanine (A; see Carrey, 1989; Smyth, 1967). Cleavage at the additional sites seems to be dependent on the adjoining

amino acids to the cleavage site and unless incubations conditions are carefully controlled the enzyme can exhibit a broad range of specificities (see Smyth, 1967).

3.2 *Aims*

The phosphorylation of the α -subunits of G-proteins has been reported both *in vitro* and *in vivo* (see section 3.1.1; Carlson *et al.*, 1989; Lounsbury *et al.*, 1991; Lounsbury *et al.*, 1993; Lincoln, 1991) and in rat hepatocytes the phosphorylation of α -G_{i-2}, but not α -G_s or α -G_{i-3}, has been demonstrated (Bushfield *et al.*, 1991; Bushfield *et al.*, 1990b).

The only G-protein that has had the site of phosphorylation identified is α -G_z and this has been found to be serine 27 which is not found in any of the other G-proteins (Lounsbury *et al.*, 1993).

The aim of the work described in this chapter was to identify the phosphorylation sites in rat hepatocyte α -G_{i-2}. This was achieved by raising antisera which would specifically immunoprecipitate α -G_{i-2}, and using the antisera to obtain ³²P labelled α -G_{i-2} from rat hepatocytes which had been incubated with various agents to activate the different cellular signalling systems. The recovered phosphorylated α -G_{i-2} was then digested with TPCCK-trypsin, V8 or α -chymotrypsin and the peptides separated by two-dimensional chromatography. The peptides were recovered and either further digested or subjected to phosphoamino acid analysis. In addition, theoretical studies of possible enzyme cleavage products were carried out and the mass-charge ratio of the peptides determined. This information was then used to predict the phosphorylation sites in rat hepatocyte α -G_{i-2} and to examine their relationship to known or predicted structures and functions of the protein.

3.3 *Results*

3.3.1 *Production and characterisation of polyclonal rabbit anti- α -G_{i-2} antisera*

Antibodies were raised in adult New Zealand white rabbits as described in section 2.2.1. All antisera was subjected to Western blotting (see section 2.2.15) and examined for the ability to immunoprecipitate phosphorylated α -G_{i-2} from rat hepatocytes (see sections 2.2.2 to 2.2.5).

During the course of the study ten different animals were injected with conjugated peptides that would produce anti- α -G_{i-1+2} antibodies, except rabbit 1605 which received a peptide unique to α -G_{i-2} (see table 3.2). The α -G_{i-2} peptide used were KNNLKDCGLF which is the C-terminal decapeptide and CLERIAQSDYI which is from an internal sequence unique to α -G_{i-2} (peptides from Biomac, Department of Biochemistry, Glasgow University except the peptide for rabbit 1607 which was produced on a poly-L-lysine backbone by the Department of Virology, Glasgow University). Antisera 1430 and 1432 were raised and characterised by Dr. Mark Bushfield; antisera 1520 to 1607 were raised and characterised

by myself under the supervision of Dr. Mark Bushfield; antisera 1867 and 1868 were raised and characterised by myself; and antiserum 2394 was produced from peptide samples sent to Eastacres Biologicals, USA with characterisation carried out by myself.

All the pre-immune sera were tested and they all failed to show protein binding. It was found that antisera from immunised rabbits 1430, 1432, 1520, 1867, 1868 and 2394 were able to recognise α -G_{i-2} in Western blots of samples from rat hepatocytes and that antibody binding could be successfully competed out by the inclusion of a small quantity of the peptide used to raise them. Antisera 1521, 1605, 1606 and 1607 all showed poor or non-specific results in Western blotting (results not shown, see table 3.2).

Antisera which showed good Western blotting characteristics were tested for their ability to immunoprecipitate ³²P labelled α -G_{i-2}. Of the antisera tested (1430, 1432, 1520, 1867, 1868 and 2394) only 1867 and 1432 showed good immunoprecipitation characteristics; 1520 and 2394 showed moderate to poor characteristics; and 1430 and 1868 did not immunoprecipitate detectable levels of the phosphorylated protein (see figure 3.3). Titration experiments with antiserum 1867 showed that 50 μ l of serum gave a maximum immunoprecipitation (see figure 3.3).

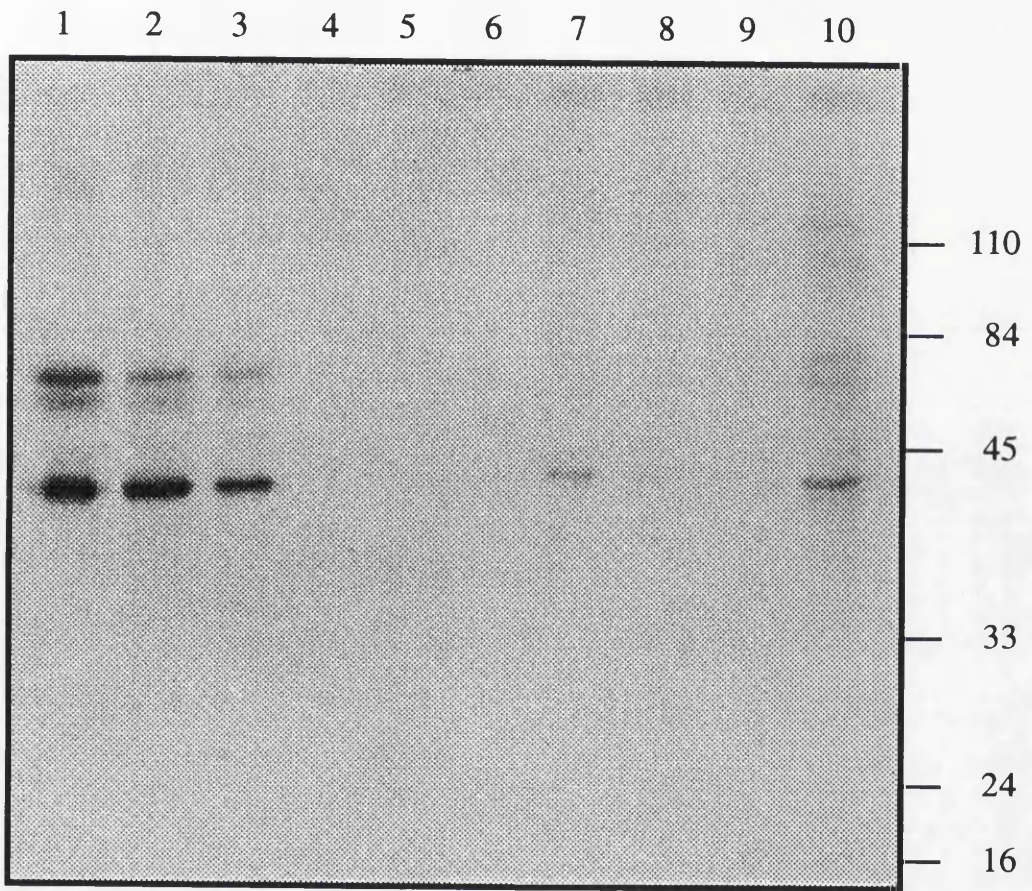
Table 3.2: Antibodies raised for the detection and immunoprecipitation of α -G_{i-2} from rat hepatocytes.

Number	Peptide	G-protein	Coupling	Blotting	Precipitation
1430	KNNLKDCGLF	α_{i1+2}	Glutaraldehyde / KLH	1:500	-
1432	KNNLKDCGLF	α_{i1+2}	Sulfo MBS / KLH	1:500	++
1520	KNNLKDCGLF	α_{i1+2}	Glutaraldehyde / KLH	1:500	+
1521	KNNLKDCGLF	α_{i1+2}	Glutaraldehyde / KLH	NSB	NT
1605	CLERIAQSDYI	α_{i2}	Sulfo MBS / KLH	NSB	NT
1606	KNNLKDCGLF	α_{i1+2}	Glutaraldehyde / KLH	Poor	+
1607	KNNLKDCGLF	α_{i1+2}	Poly-lysine backbone	NSB	NT
1867	KNNLKDCGLF	α_{i1+2}	Glutaraldehyde / KLH	1:5000	+++
1868	KNNLKDCGLF	α_{i1+2}	Glutaraldehyde / KLH	1:500	-
2394	KNNLKDCGLF	α_{i1+2}	Glutaraldehyde / KLH	1:500	+

Number represents the identification number of the antiserum; peptide shows the decapeptide sequence used; G-protein indicates in which α -subunits the sequence occurs; coupling, the coupling procedure used; blotting, the maximum dilution used in Western blotting; and precipitation indicates whether the antiserum were a very strong (+++), strong (++), weak (+), or very poor (-) immunoprecipitator of phosphorylated α -G_{i-2}; NT indicates that the antisera was not tested

Figure 3.3: Immunoprecipitation of ^{32}P labelled $\alpha\text{-G}_{i-2}$ with antisera 1867, 1868, 2394 and 1432

Immunoprecipitation of ^{32}P labelled $\alpha\text{-G}_{i-2}$ with antisera 1867 (lanes 1 [100 μl], 2 [50 μl] and 3 [10 μl]), 1868 (lanes 4 [100 μl], 5 [50 μl] and 6 [10 μl]), and 2394 (lanes 7 [100 μl], 8 [50 μl] and 9 [10 μl]). Lane 10 shows a control lane in which 100 μl of antiserum 1432, which had been characterised as $\alpha\text{-G}_{i-2}$ specific by Dr. Mark Bushfield, was used to immunoprecipitate the phospho-protein from rat hepatocytes. As can be seen 1867 is a strong immunoprecipitater with 50 μl giving a maximum response (lane 2); 1868 does not immunoprecipitate $^{32}\text{P}\text{-}\alpha\text{-G}_{i-2}$; and 2394 gives a poor immunoprecipitate and all immunoprecipitation antisera produced a protein of the same molecular weight (~40 kDa).



The specificity of the immunoprecipitation of antisera 1432 was tested by Dr. Mark Bushfield and it was found that the antibody specifically immunoprecipitated α -G_{i-2} (results not shown). The specificity of 1867 was characterised by comparing the molecular weight of the precipitated protein to that of the protein immunoprecipitated by 1432 and it was found that both antisera immunoprecipitated a protein of approximately 40 kDa which is the correct weight for α -G_{i-2} (see figure 3.3). Peptide competition studies on antiserum 1867 showed that immunoprecipitation of the protein could be inhibited by incubating the antisera overnight with the α -G_{i-2} peptide KNNLKDCGLF but incubation with the equivalent peptide from α -G_{i-3} (KNNLKECGLF) did not effect immunoprecipitation (see figure 3.4). Although the immunoprecipitation experiments also showed that other phospho-proteins were precipitated, notably one at approximately 50 kDa (see figures 3.3 and 3.4), the results shown in figure 3.4 (peptide competition studies) demonstrate that the precipitation of the main band at 40 kDa is α -G_{i-2} antibody specific (see figure 3.4, lanes 2 and 3). The antiserum 1867 can therefore be considered to be α -G_{i-2} specific because it immunoprecipitates a protein of the correct molecular weight and the precipitation can be inhibited by a specific α -G_{i-2} peptides. The antiserum cannot be immunoprecipitating α -G_{i-3} as the equivalent peptide did not inhibit immunoprecipitation (lane 4). Furthermore, it can not be immunoprecipitating α -G_{i-1}, which has the same C-terminal peptide sequence as α -G_{i-2}, as it has been demonstrated that rat hepatocytes do not contain α -G_{i-1} (Griffiths, Knowler & Houslay, 1990; Bushfield *et al.*, 1990b).

3.3.2 *Two-dimensional thin layer analysis of phosphopeptides derived from α -G_{i-2}*

In order to assess whether α -G_{i-2} was subjected to multiple-site phosphorylation, and to determine the phosphorylation site(s), [³²P]-labelled α -G_{i-2} was digested using the enzymes trypsin (see section 3.1.4.1), α -chymotrypsin (see section 3.1.4.3) and V8 (see section 3.1.4.2) and separated by two-dimensional phosphopeptide mapping analysis (see section 2.2.2 to 2.2.9; see Boyle *et al.*, 1991). This was performed using phosphorylated α -G_{i-2} immunoprecipitated from control cells (basal state) and from cells that had been pre-treated with various agents in order to activate PKC (phorbol ester PMA) or PKA (8-bromo-cAMP, non-hydrolysable analogue of cAMP).

3.3.2.1 *Trypsin digestion products*

Two dimensional analysis of the phosphopeptides resulting from trypsin digestion of α -G_{i-2} from control cells identified three major phosphopeptides (labelled C1, C2 and C3; see figures 3.5 and 3.16) all of which were positively charged. Peptides C1, C2 and C3 were resolved by chromatography but only C3 was resolved by electrophoresis at pH1.9 (see figures 3.5, 3.6 and 3.16). These three peptides were consistently identified using cell preparations from twelve different animals.

Figure 3.4 Specificity of the immunoprecipitation of α -G_{i-2} by antisera 1867

Hepatocytes were labelled with ³²P for 65 minutes and then subjected to detergent extraction, immunoprecipitation with antiserum 1867, SDS-PAGE and autoradiography (see sections 2.2.2 - 2.2.5) Lane 1 show control (1867 only), lanes 2 and 3 antiserum 1867 in the presence of two different concentrations of α -G_{i-2} peptide and lane 4 antiserum 1867 pre-incubated with an equivalent α -G_{i-3} peptide. As can be seen only the α -G_{i-2} peptide competes out α -G_{i-2} immunoprecipitation therefore demonstrating the antiserum only precipitates α -G_{i-2}. The molecular weight of the immunoprecipitated phospho-protein was approximately 40 kDa. The results shown are from a typical experiment which was performed three times with similar results.

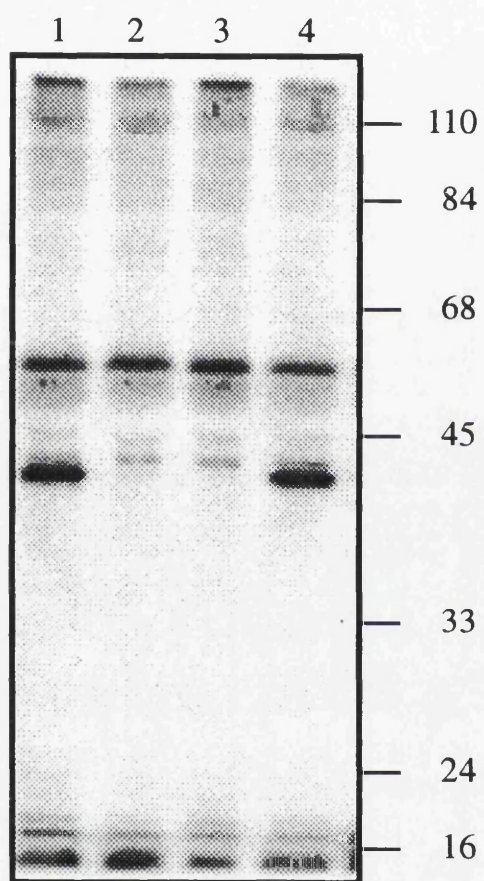
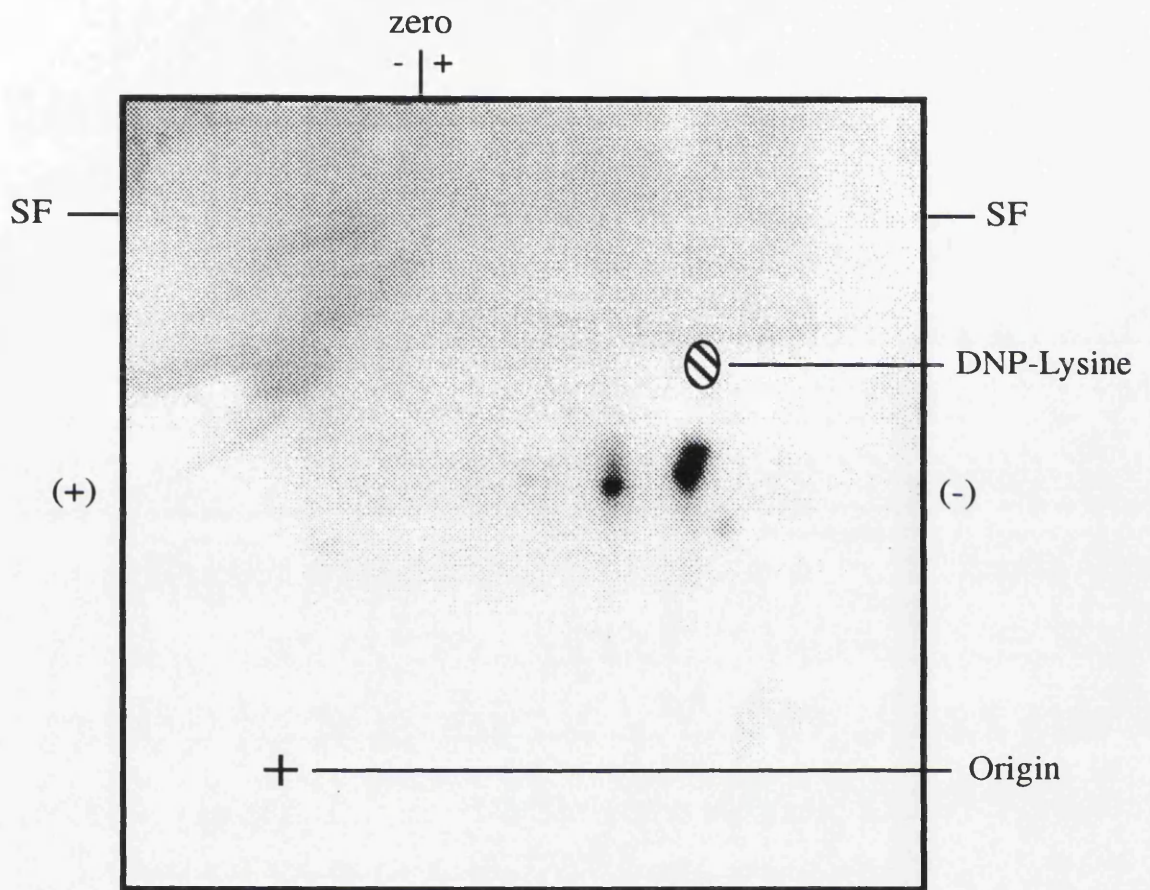


Figure 3.5: Phosphopeptide map of α -G_{i-2} from Sprague Dawley rat hepatocytes incubated with vehicle solution and then digested with trypsin

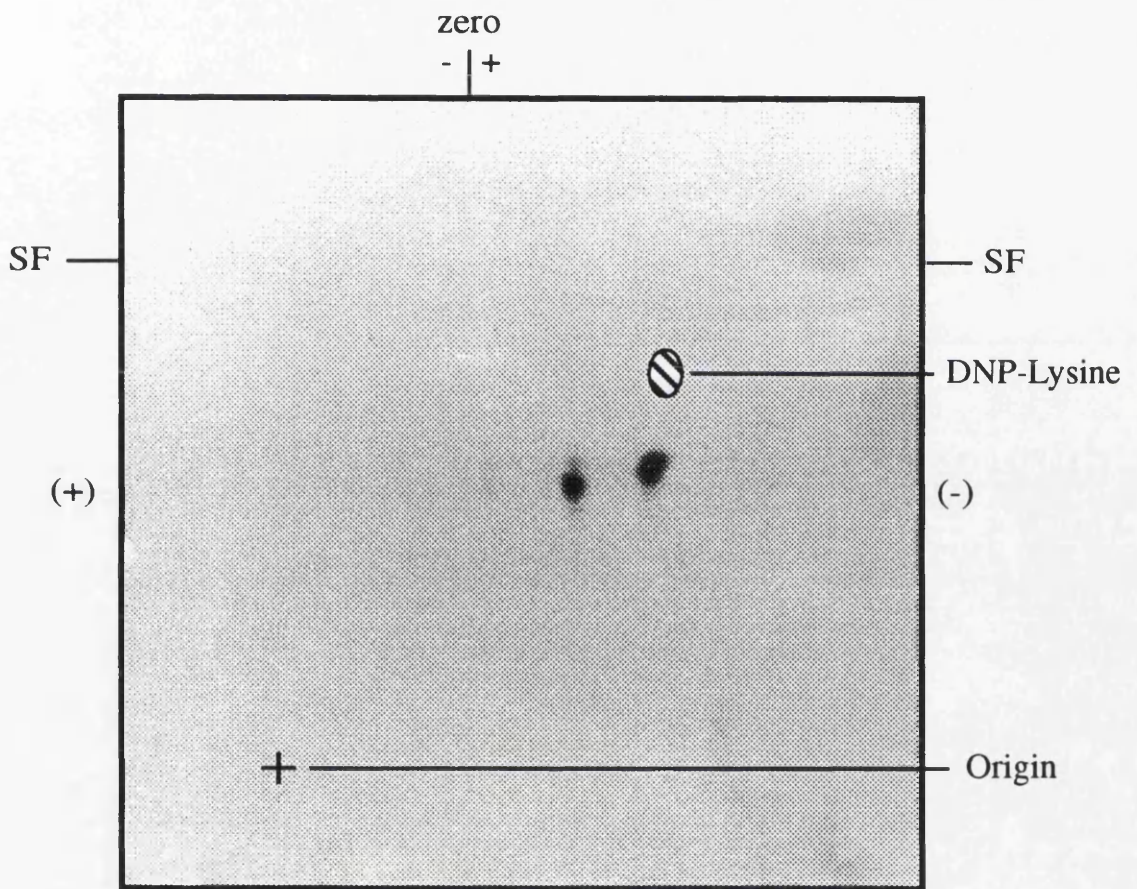
Hepatocytes were labelled with ³²P (see sections 2.2.2 and 2.2.3) and then challenged with vehicle solution. The hepatocytes were harvested and α -G_{i-2} immunoprecipitated with antiserum 1867 before being subjected to SDS-PAGE. The protein was recovered from the gel and digested with TPCCK-treated trypsin as described in experimental procedures (see sections 2.2.4 - 2.2.9). ³²P-labelled tryptic phosphopeptides were then separated on thin-layer cellulose plates by electrophoresis at pH1.9 and ascending chromatography. The final position of DNP-lysine is marked on each plate, SF represents the position of the solvent front, origin is the point of application of the sample, (+) and (-) indicate the orientation of the electric field, and the bar at the top of the plate indicates the separation of the negative, neutral and positive markers. The autoradiograph shows the result from a typical experiment where vehicle produced spots C1, C2, and C3. Diagrammatic representation of the results is shown in figure 3.16. The experiment was performed at least three times with similar results.



Sprague Dawley, control, trypsin

Figure 3.6: Phosphopeptide map of α -G_{i-2} from Sprague Dawley rat hepatocytes incubated with PMA and then digested with trypsin

Hepatocytes were labelled with ³²P (see sections 2.2.2 and 2.2.3) and then challenged with PMA (100 ng/ml) for 15 minutes. The hepatocytes were harvested and α -G_{i-2} immunoprecipitated with antiserum 1867 before being subjected to SDS-PAGE. The protein was recovered from the gel and digested with TPCK-treated trypsin as described in experimental procedures (see sections 2.2.4 - 2.2.9). ³²P-labelled tryptic phosphopeptides were then separated on thin-layer cellulose plates by electrophoresis at pH1.9 and ascending chromatography. The final position of DNP-lysine is marked on each plate, SF represents the position of the solvent front, origin is the point of application of the sample, (+) and (-) indicate the orientation of the electric field, and the bar at the top of the plate indicates the separation of the negative, neutral and positive markers. The autoradiograph shows the result from a typical experiments where PMA produced spots C1, C2, and C3. Diagrammatic representation of the results is shown in figure 3.16. The experiment was performed at least three times with similar results.



Sprague Dawley, PMA, trypsin

Digestion of α -G_{i-2} phosphoprotein from hepatocytes that had been treated with PMA also produced a similar spot pattern to that of control (see figure 3.6 and 3.16) with all three tryptic peptides (C1, C2, and C3) present. Due to the method used to produce the peptide maps it was not possible to establish if PMA treatment caused an increase in the level of phosphorylation of any of the peptides.

The digestion and separation of α -G_{i-2} phosphopeptides from hepatocytes that had been incubated with 8-bromo-cAMP again showed the presence of the phosphopeptides C1, C2 and C3 but also revealed the presence of another phosphopeptide (AN; see figures 3.7 and 3.16). This novel peptide had a greater mass-charge ratio (see section 3.1.4) than C1, C2 or C3 and also exhibited a lower mobility in the second dimension.

Work carried out by Dr. Mark Bushfield (see Morris *et al.*, 1994) showed that trypsin digestion of α -G_{i-2} from control hepatocytes only produced two peptides C1 and C2. Careful examination of Dr. Bushfield's autoradiography also revealed the presence of a very faint spot which was equivalent to C3. Experiments in which reduced digestion times (five hours instead of ten; see section 2.2.8) and lower concentrations of the enzyme were used (half standard concentrations; see section 2.2.8) produced autoradiographs that did not contain the peptide C3 thus confirming the work of Dr. Bushfield (see figure 3.8).

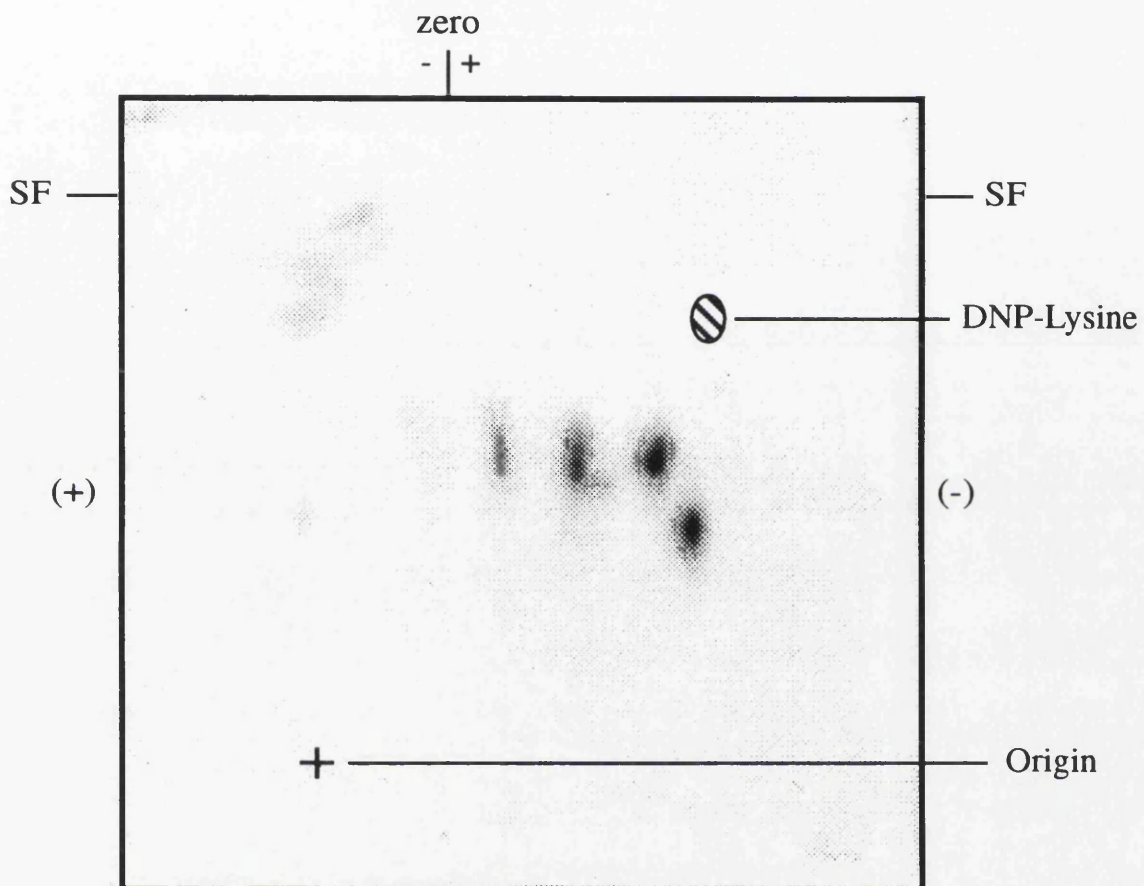
3.3.2.2 V8 digestion of the tryptic peptides

Further digestion of the peptides C1, C2 and C3, pooled from several plates, by V8 showed that all three peptides were susceptible to cleavage (see figures 3.9 and 3.16). Individual cleavage of spots C1, C2 and C3 confirmed that C1 gave C2' (see figures 3.10 and 3.16); C2 produced C2' and C2'' (see figures 3.11 and 3.14); C3 gave C3' (see figures 3.12 and 3.16); and AN gave AN' (see figures 3.13 and 3.16). All of these peptides were positively charged at pH1.9 and all the V8 peptides, except AN', had greater mass-charge ratios than their parent tryptic peptides and also exhibited a decrease in R_f values (see figures 3.9 and 3.16; see section 3.1.4).

Samples of the phosphopeptides C1, C2, C3 and AN when digested with V8 produced peptides C2', C2'', C3' and AN' (see figures 3.14 and 3.16). The rate of cleavage of AN to produce AN' was very slow using the standard method (see section 2.2.8) and early experiments only showed small amounts of AN' being produced. If the standard digestion times and enzyme concentrations were doubled then a stronger signal for AN' could be achieved but again not all of AN was digested (see figure 3.14). Peptide AN' had a mass-charge ratio between that of C3 and C2 and had similar R_f values to C3 and C2 (see figures 3.14 and 3.16).

Figure 3.7: Phosphopeptide map of α -G_{i-2} from Sprague Dawley rat hepatocytes incubated with 8-bromo-cAMP and then digested with trypsin

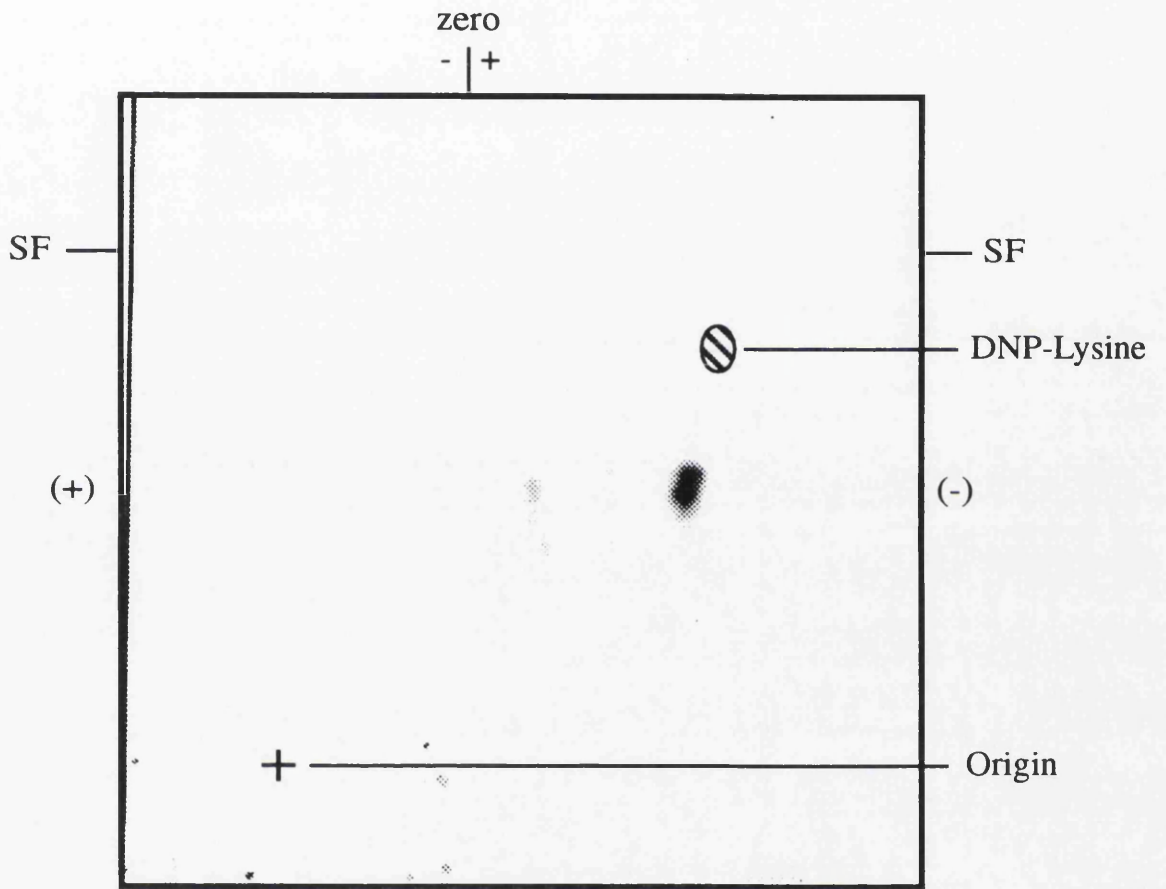
Hepatocytes were labelled with ³²P (see sections 2.2.2 and 2.2.3) and then challenged with 300 μ M 8-bromo-cAMP for 15 minutes. The hepatocytes were harvested and α -G_{i-2} immunoprecipitated with antiserum 1867 before being subjected to SDS-PAGE. The protein was recovered from the gel and digested with TPCCK-treated trypsin as described in experimental procedures (see sections 2.2.4 - 2.2.9). ³²P-labelled tryptic phosphopeptides were then separated on thin-layer cellulose plates by electrophoresis at pH1.9 and ascending chromatography. The final position of DNP-lysine is marked on each plate, SF represents the position of the solvent front, origin is the point of application of the sample, (+) and (-) indicate the orientation of the electric field, and the bar at the top of the plate indicates the separation of the negative, neutral and positive markers. The autoradiograph shows the result from typical experiments where 8-bromo-cAMP produced spots C1, C2, C3 and AN. Diagrammatic representation of the results is shown in figure 3.16. The experiment was performed at least three times with similar results.



Sprague Dawley, 8-bromo-cAMP, trypsin

Figure 3.8: Phosphopeptide map of α -G_{i-2} from Sprague Dawley rat hepatocytes incubated with vehicle solution and then digested with trypsin: shortened digestion period

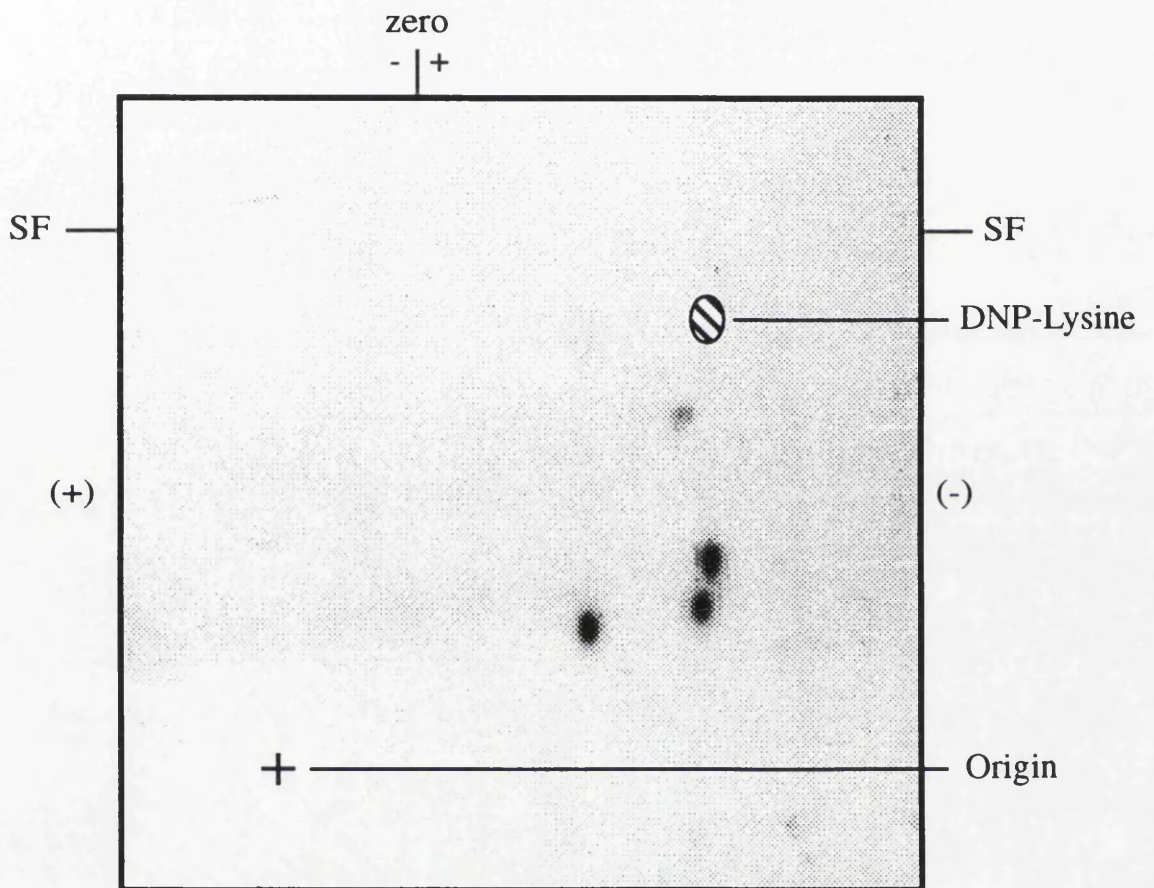
Hepatocytes were labelled with ³²P (see sections 2.2.2 and 2.2.3) and then challenged with vehicle solution. The hepatocytes were harvested and α -G_{i-2} immunoprecipitated with antiserum 1867 before being subjected to SDS-PAGE. The protein was recovered from the gel and digested with TPCK-treated trypsin with an incubation time reduced to 5 hours at 37°C. ³²P-labelled tryptic phosphopeptides were then separated on thin-layer cellulose plates by electrophoresis at pH1.9 and ascending chromatography. The final position of DNP-lysine is marked on each plate, SF represents the position of the solvent front, origin is the point of application of the sample, (+) and (-) indicate the orientation of the electric field, and the bar at the top of the plate indicates the separation of the negative, neutral and positive markers. The autoradiograph shows the result from a typical experiment where vehicle produced spots C1 and C2. Diagrammatic representation of the results is shown in figure 3.16. The experiment was performed at least three times with similar results.



Sprague Dawley, control, trypsin (shortened digestion period)

Figure 3.9: Phosphopeptide map of α -G_{i-2} from Sprague Dawley rat hepatocytes incubated with vehicle solution and then first digested with trypsin followed by V8

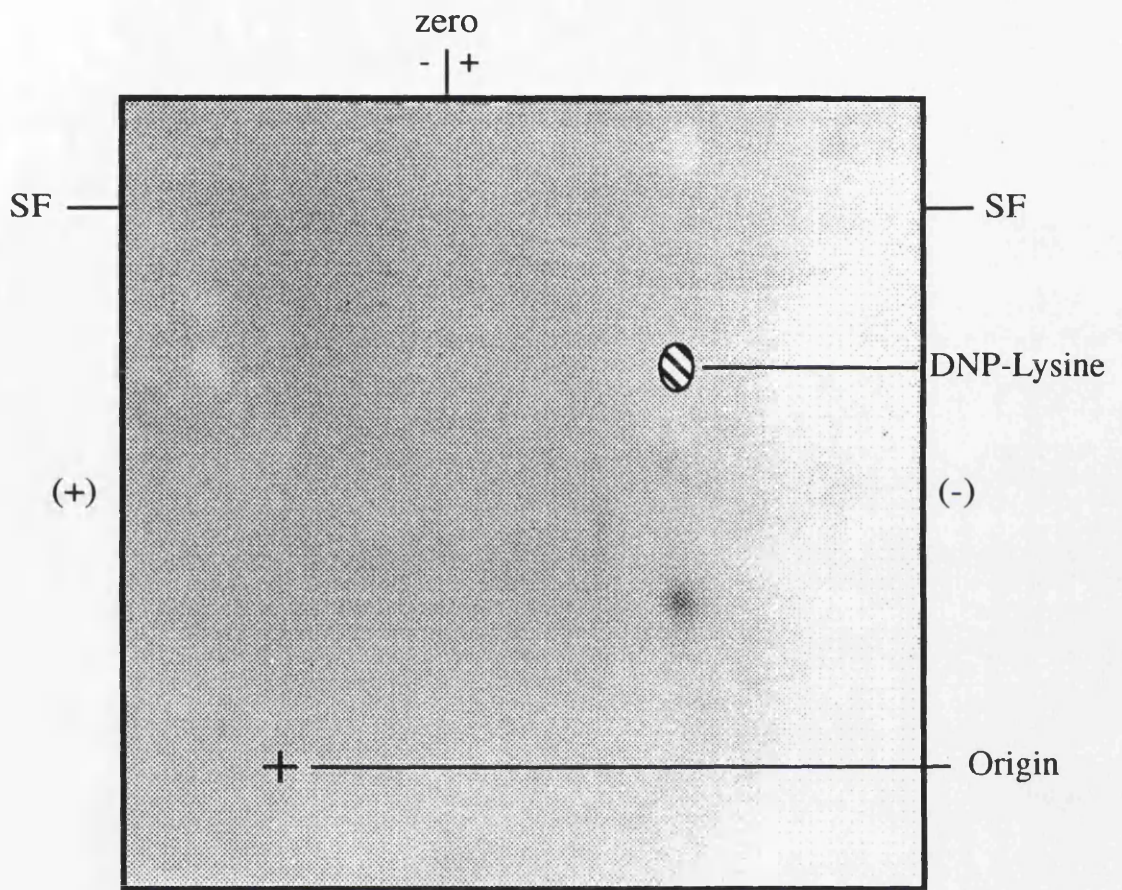
Hepatocytes were labelled with ³²P (see sections 2.2.2 and 2.2.3) and then challenged with vehicle. The hepatocytes were harvested and α -G_{i-2} immunoprecipitated with antiserum 1867 before being subjected to SDS-PAGE. The protein was recovered from the gel and digested with TPCK-treated trypsin (see figure 3.5), the peptides collected (see section 2.2.4 - 2.2.10) and then digested with V8 as described in Chapter 2 (see sections 2.2.8 - 2.2.9). ³²P-labelled tryptic / V8 phosphopeptides were separated on thin-layer cellulose plates by electrophoresis at pH1.9 and ascending chromatography. The final position of DNP-lysine is marked on each plate, SF represents the position of the solvent front, origin is the point of application of the sample, (+) and (-) indicate the orientation of the electric field, and the bar at the top of the plate indicates the separation of the negative, neutral and positive markers. Each condition was performed at least three times with similar results and the autoradiograph shows the result from a typical experiment where vehicle produced spots C2', C2'' and C3' on V8 digestion. Diagrammatic representation in figure 3.16 shows the digestion of α -G_{i-2} by trypsin and V8.



Sprague Dawley, control, trypsin and V8

Figure 3.10: Phosphopeptide map of α -G_{i-2} from Sprague Dawley rat hepatocytes incubated with vehicle solution and digested with trypsin: Digestion of tryptic peptide C1 with V8 to give C2'

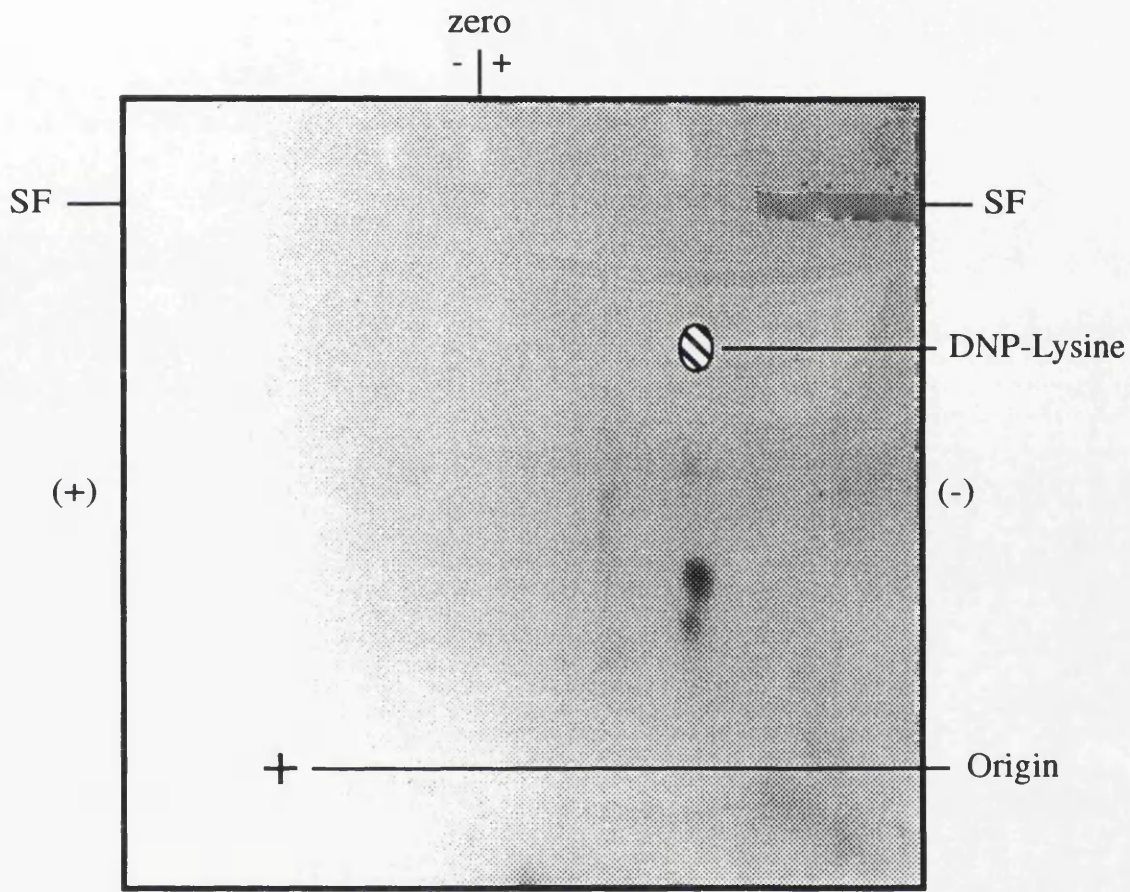
Hepatocytes were labelled with ³²P (see sections 2.2.2 and 2.2.3) and then challenged with vehicle. The hepatocytes were harvested and α -G_{i-2} immunoprecipitated with antiserum 1867 before being subjected to SDS-PAGE. The protein was recovered from the gel and digested with TPCK-trypsin as described in chapter 2 (see sections 2.2.4 - 2.2.9). ³²P-labelled tryptic phosphopeptides were then separated on thin-layer cellulose plates by electrophoresis at pH1.9 and ascending chromatography. The final position of DNP-lysine is marked on each plate, SF represents the position of the solvent front, origin is the point of application of the sample, (+) and (-) indicate the orientation of the electric field, and the bar at the top of the plate indicates the separation of the negative, neutral and positive markers. The autoradiographs showed the typical tryptic peptide pattern (see figure 3.5) and the peptide from spot C1 was recovered (see section 2.2.10), subjected to V8 digestion and analysed by two-dimensional chromatography as described above (see sections 2.2.8 - 2.2.9). The autoradiographs shows the results from a typical experiment where the spot C1 produced spots C2'. Diagrammatic representation in figure 3.16 shows the digestion of α -G_{i-2} by V8. Each condition was performed at least three times with similar results.



Sprague Dawley, C1 to C2", trypsin then V8

Figure 3.11: Phosphopeptide map of α -G_{i-2} from Sprague Dawley rat hepatocytes incubated with vehicle solution and digested with trypsin: Digestion of tryptic peptide C2 with V8 to give C2' and C2"

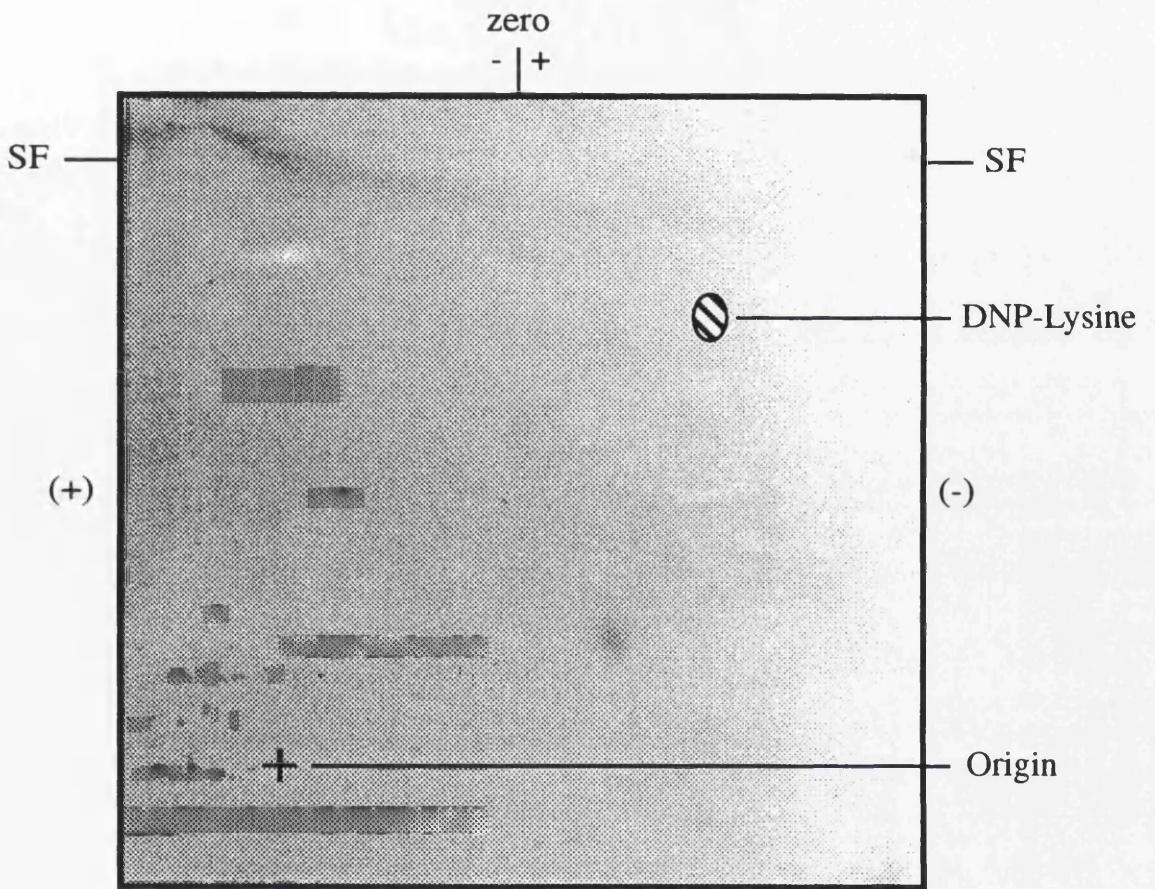
Hepatocytes were labelled with ³²P (see sections 2.2.2 and 2.2.3) and then challenged with vehicle. The hepatocytes were harvested and α -G_{i-2} immunoprecipitated with antiserum 1867 before being subjected to SDS-PAGE. The protein was recovered from the gel and digested with TPCK-trypsin as described in chapter 2 (see sections 2.2.4 - 2.2.9). ³²P-labelled tryptic phosphopeptides were then separated on thin-layer cellulose plates by electrophoresis at pH1.9 and ascending chromatography. The final position of DNP-lysine is marked on each plate, SF represents the position of the solvent front, origin is the point of application of the sample, (+) and (-) indicate the orientation of the electric field, and the bar at the top of the plate indicates the separation of the negative, neutral and positive markers. The autoradiographs showed the typical tryptic peptide pattern (see figure 3.5) and the peptide from spot C2 was recovered (see section 2.2.10), subjected to V8 digestion and analysed by two-dimensional chromatography as described above (see sections 2.2.8 - 2.2.9). The autoradiographs shows the results from a typical experiment where the spot C2 produced spots C2' and C2". Diagrammatic representation in figure 3.16 shows the digestion of α -G_{i-2} by V8. Each condition was performed at least three times with similar results.



Sprague Dawley, C2 to C2' and C2'', trypsin then V8

Figure 3.12: Phosphopeptide map of α -G_{i-2} from Sprague Dawley rat hepatocytes incubated with vehicle solution and digested with trypsin: Digestion of tryptic peptide C3 with V8 to give C3'

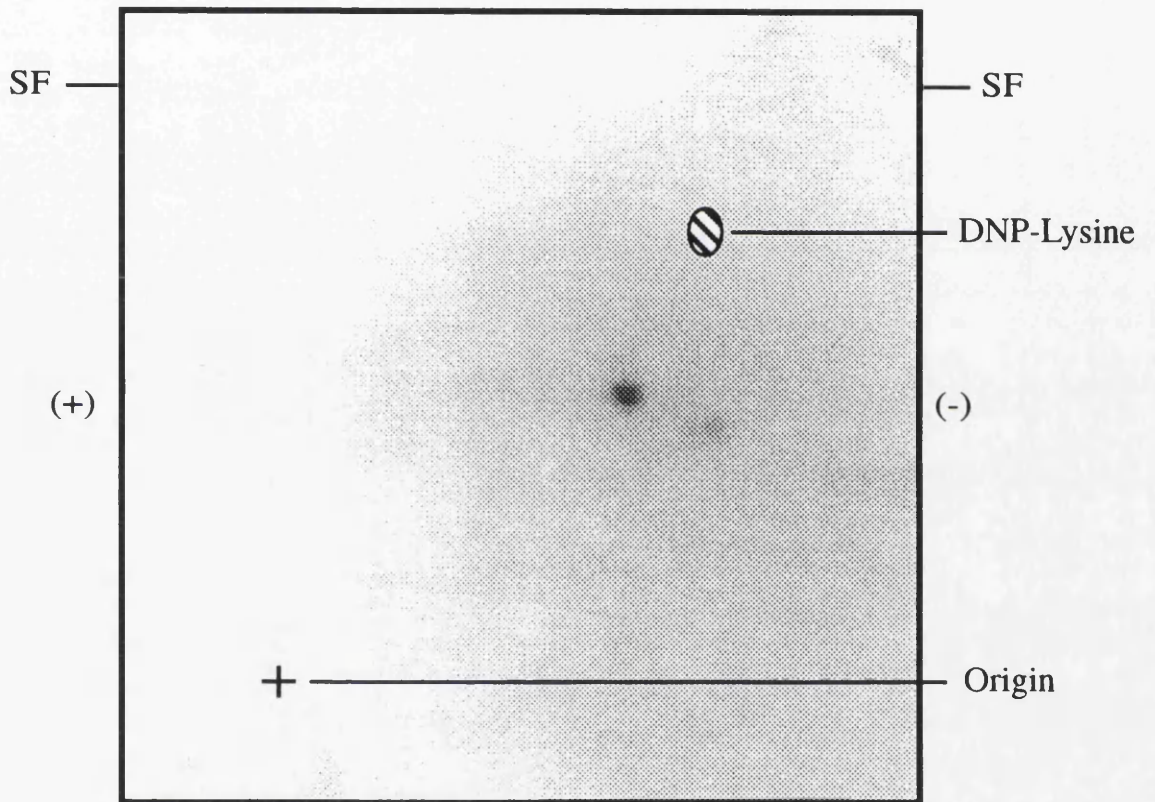
Hepatocytes were labelled with ³²P (see sections 2.2.2 and 2.2.3) and then challenged with vehicle. The hepatocytes were harvested and α -G_{i-2} immunoprecipitated with antiserum 1867 before being subjected to SDS-PAGE. The protein was recovered from the gel and digested with TPCK-trypsin as described in chapter 2 (see sections 2.2.4 - 2.2.9). ³²P-labelled tryptic phosphopeptides were then separated on thin-layer cellulose plates by electrophoresis at pH1.9 and ascending chromatography. The final position of DNP-lysine is marked on each plate, SF represents the position of the solvent front, origin is the point of application of the sample, (+) and (-) indicate the orientation of the electric field, and the bar at the top of the plate indicates the separation of the negative, neutral and positive markers. The autoradiographs showed the typical tryptic peptide pattern (see figure 3.5) and the peptide from spot C3 was recovered (see section 2.2.10), subjected to V8 digestion and analysed by two-dimensional chromatography as described above (see sections 2.2.8 - 2.2.9). The autoradiographs shows the results from a typical experiment where the spot C3 produced spot C3'. Diagrammatic representation in figure 3.16 shows the digestion of α -G_{i-2} by V8. Each condition was performed at least three times with similar results.



Sprague Dawley, peptide C3 to C3', trypsin then V8

Figure 3.13: Phosphopeptide map of α -G_{i-2} from Sprague Dawley rat hepatocytes incubated with 8-bromo-cAMP and digested with trypsin: Digestion of tryptic peptide AN with V8 to give AN'

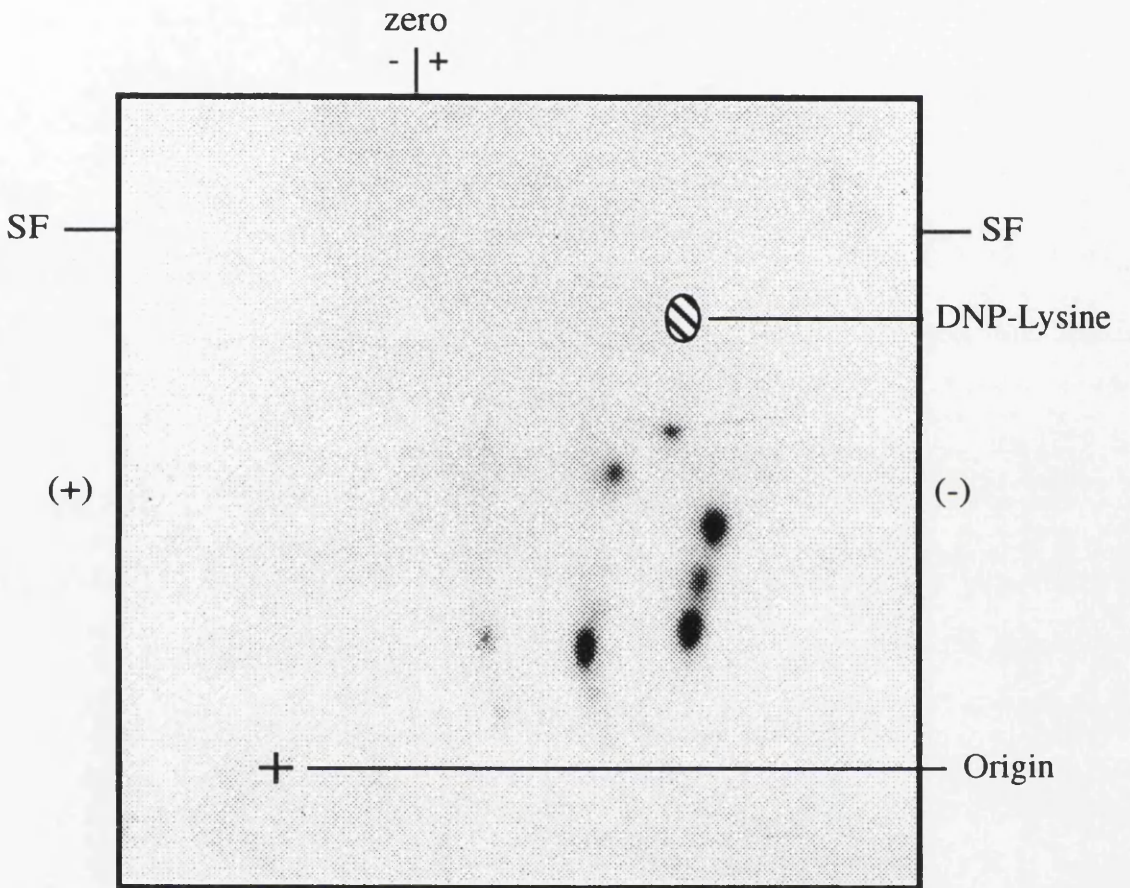
Hepatocytes were labelled with ³²P (see sections 2.2.2 and 2.2.3) and then challenged with 300 μ M 8-bromo-cAMP. The hepatocytes were harvested and α -G_{i-2} immunoprecipitated with antiserum 1867 before being subjected to SDS-PAGE. The protein was recovered from the gel and digested with TPCK-trypsin as described in Chapter 2 (see sections 2.2.4 - 2.2.9). ³²P-labelled tryptic phosphopeptides were then separated on thin-layer cellulose plates by electrophoresis at pH1.9 and ascending chromatography. The final position of DNP-lysine is marked on each plate, SF represents the position of the solvent front, origin is the point of application of the sample, (+) and (-) indicate the orientation of the electric field, and the bar at the top of the plate indicates the separation of the negative, neutral and positive markers. The autoradiographs showed the typical tryptic peptide pattern (see figure 3.5) and the peptide from spot AN was recovered (see section 2.2.10), subjected to V8 digestion and analysed by two-dimensional chromatography as described above (see sections 2.2.8 - 2.2.9). The autoradiographs shows the results from a typical experiment where the spot AN produced spot AN'. Diagrammatic representation in figure 3.16 shows the digestion of α -G_{i-2} by V8. Each condition was performed at least three times with similar results.



Sprague Dawley, tryptic peptide AN digested with V8 to give AN'

Figure 3.14: Phosphopeptide map of α -G_{i-2} from Sprague Dawley rat hepatocytes incubated with 8-bromo-cAMP and digested with trypsin followed by V8

Hepatocytes were labelled with ³²P (see sections 2.2.2 and 2.2.3) and then challenged with 300 μ M 8-bromo-cAMP for 15 minutes. The hepatocytes were harvested and α -G_{i-2} immunoprecipitated with antiserum 1867 before being subjected to SDS-PAGE. The protein was recovered from the gel and digested with TPCK-treated trypsin (see figure 3.5), the peptides collected (see section 2.2.4 - 2.2.10) and then digested with V8 as described in chapter 2 (see sections 2.2.8 - 2.2.9). ³²P-labelled tryptic / V8 phosphopeptides were separated on thin-layer cellulose plates by electrophoresis at pH1.9 and ascending chromatography. The final position of DNP-lysine is marked on each plate, SF represents the position of the solvent front, origin is the point of application of the sample, (+) and (-) indicate the orientation of the electric field, and the bar at the top of the plate indicates the separation of the negative, neutral and positive markers. Each condition was performed at least three times with similar results and the autoradiograph shows the result from a typical experiment where 8-bromo-cAMP produced spots C2', C2'', C3' and AN' on V8 digestion. Diagrammatic representation in figure 3.16 shows the digestion of α -G_{i-2} by trypsin and V8.



Sprague Dawley, 8-bromo-cAMP, trypsin and V8

3.3.2.3 V8 digestion

Phosphorylated α -G_{i-2} from hepatocytes that had been incubated with control (vehicle), PMA and 8-bromo-cAMP were digested with the enzyme V8 using the method outlined in section 2.2.8.

From experiments carried out on at least six separate occasions it was found that only α -G_{i-2} from control or PMA treated hepatocytes could be digested by the enzyme (see figures 3.15 and 3.16) and that samples from cells that had been incubated with 8-bromo-cAMP could not be cleaved.

The phosphopeptides that were produced by V8 cleavage of the protein had the same mass-charge ratios and R_f values as the peptides C2', C2'' and C3' and it was therefore concluded that the peptides were C2', C2'' and C3' (see figures 3.15 and 3.16).

3.3.2.4 α -chymotrypsin digestion

Attempts to produce two-dimensional phospho-peptide maps from α -chymotrypsin cleaved samples of α -G_{i-2} from control, PMA or 8-bromo-cAMP treated hepatocytes were unsuccessful. On the five occasions that this was attempted the resulting autoradiography either contained no discernible phosphopeptides or a series of poorly defined smudges (results not shown).

3.3.3 Phosphoamino acid analysis of peptides C1, C2, C3 and AN

Phosphoamino acid analysis was carried out as outlined in section 2.2.11 with the samples from the acid digestion of phosphopeptides C1, C2, C3 and AN being applied to four separate locations on the t.l.c. plate.

Analysis of the samples showed that all four peptides contained phospho-serine and no other phosphoamino acids were detected (see figure 3.17).

3.3.4 Prediction of enzymatic digestion products of phosphorylated α -G_{i-2} and associated mass-charge ratios

From the results outlined in section 3.3.3 then it is clear that the phosphorylation of α -G_{i-2} only occurs on serine residues and that the phosphoprotein can be digested by both trypsin and V8. Using this information, along with the digestion characteristics of the enzymes outlined in section 3.1.4.1 and 3.1.4.2, a range of possible peptides were predicted and these are shown in Appendix 12.

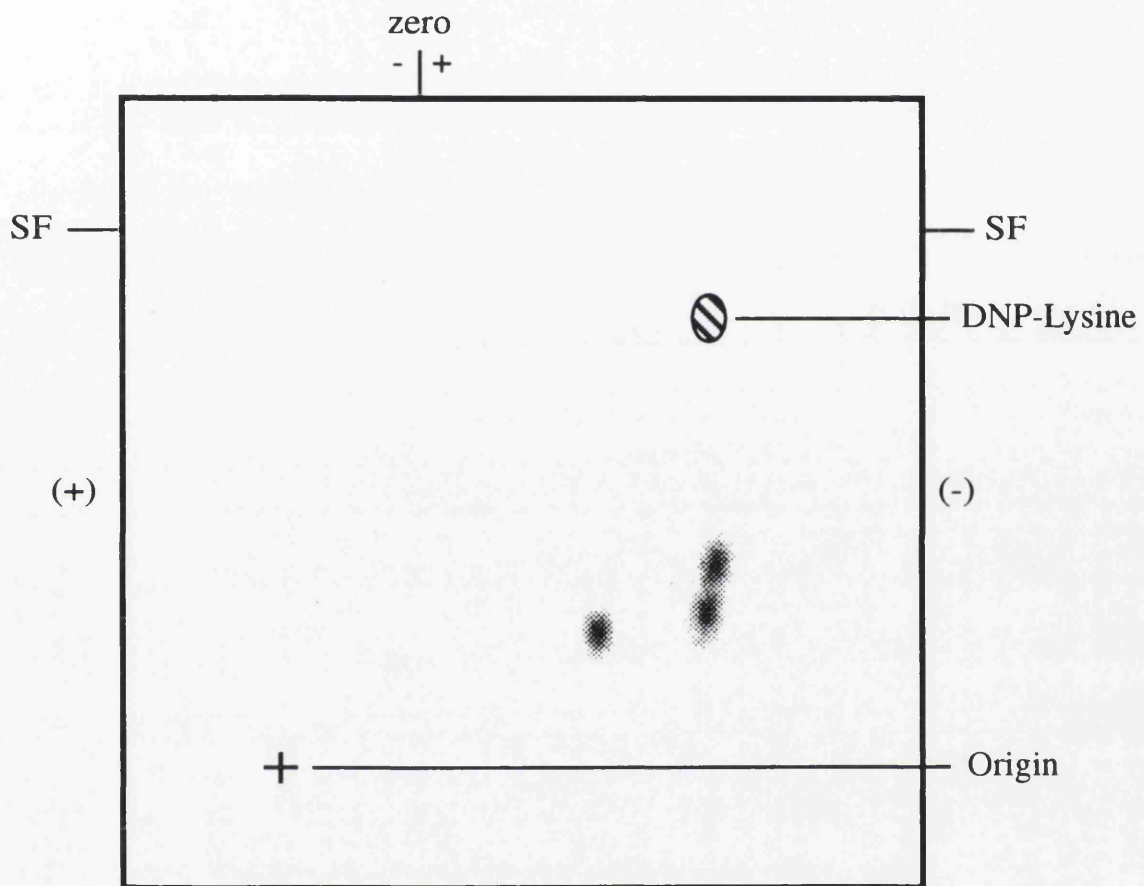
3.3.5 Prediction of the secondary structure of α -G_{i-2}

As discussed in section 3.1.3 and 3.1.3.2, the secondary structure of proteins can be predicted by using a range of methods.

Although the secondary and tertiary structures of heterotrimeric G-protein α -subunits has not been determined, predictions have been made about these based upon the

Figure 3.15: Phosphopeptide map of α -G_{i-2} from Sprague Dawley rat hepatocytes incubated with vehicle solution and digested with V8

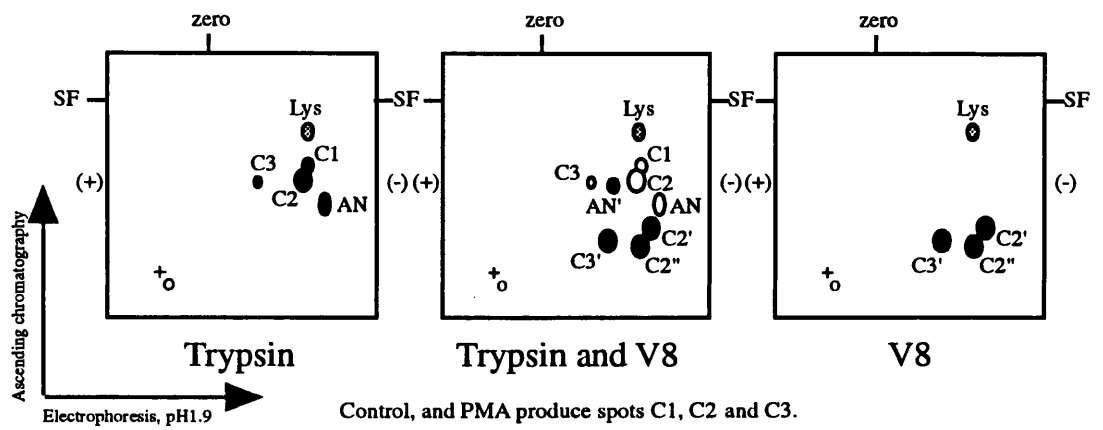
Hepatocytes were labelled with ³²P (see sections 2.2.2 and 2.2.3) and then challenged with vehicle. The hepatocytes were harvested and α -G_{i-2} immunoprecipitated with antiserum 1867 before being subjected to SDS-PAGE. The protein was recovered from the gel and digested with V8 as described in chapter 2 (see sections 2.2.4 - 2.2.9). ³²P-labelled tryptic phosphopeptides were then separated on thin-layer cellulose plates by electrophoresis at pH1.9 and ascending chromatography. The final position of DNP-lysine is marked on each plate, SF represents the position of the solvent front, origin is the point of application of the sample, (+) and (-) indicate the orientation of the electric field, and the bar at the top of the plate indicates the separation of the negative, neutral and positive markers. The autoradiographs show the results from a typical experiments where vehicle produced spots C2', C2'' and C3'. Diagrammatic representation in figure 3.16 shows the digestion of α -G_{i-2} by V8. Each condition was performed at least three times with similar results.



Sprague Dawley, control, V8

Figure 3.16: Diagrammatic representation of the peptide distribution after two-dimensional chromatography

Diagrammatic representation of the peptide distribution after two-dimensional chromatography. Black spots represent peptides present under the conditions stated, clear spots indicate peptides that have been digested by the second enzyme.

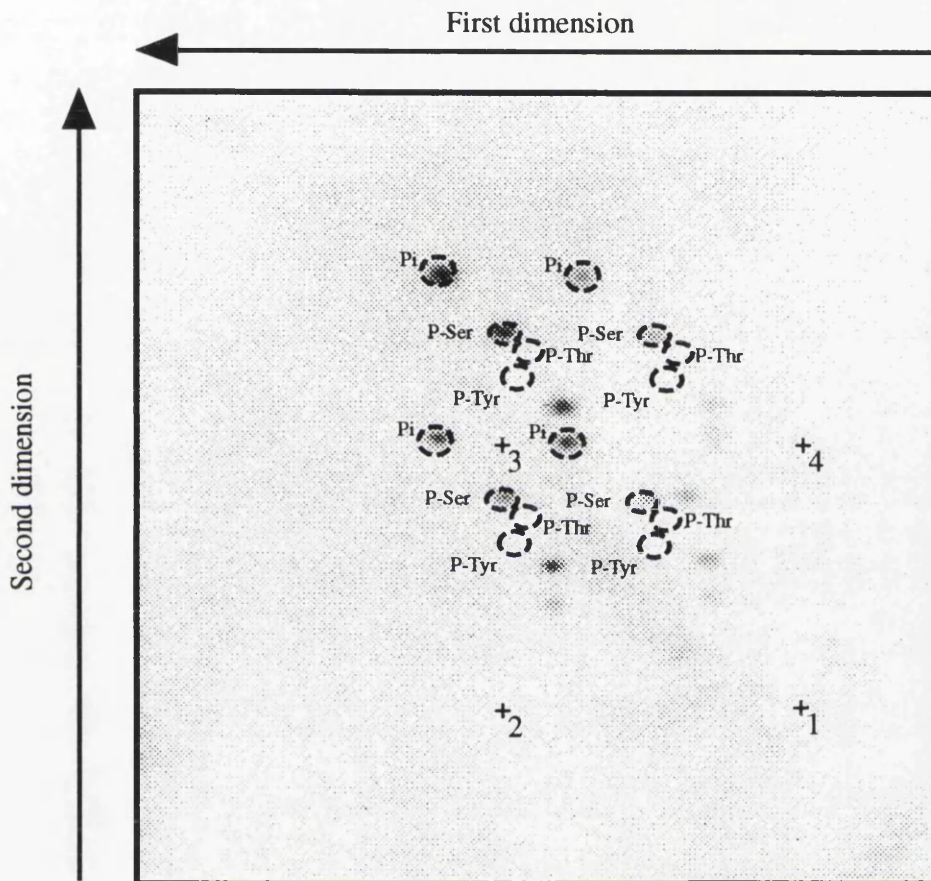


Control, and PMA produce spots C1, C2 and C3.

8BrcAMP produce spot AN

Figure 3.17: Phosphoamino acid analysis of tryptic peptides C1, C2, C3 and AN

Peptides C1, C2, C3 and AN were recovered from t.l.c. plates and subjected to phosphoamino acid analysis as outlined in sections 2.2.10 and 2.2.11). Peptide C1 was applied to position 1, C2 to position 2, C3 to position 3 and AN to position 4. The plate was run at pH1.9 in the first dimension and rotated 90° anti-clockwise before being run in the second dimension. P_i represents phosphate liberated from the peptide as a result of hydrolysis. P-Ser, P-Thr, and P-Tyr represent the final position of the applied standards phosphoserine, phosphothreonine and phosphotyrosine (see section 2.2.11 and figure 2.2). As can be seen all the peptides produced phosphoserine therefore confirming that the phosphorylation sites are serines.



Sprague Dawley, phosphoamino acid analysis

known structures of EF-Tu and p21^{ras} (see section 3.1.3.3). As EF-Tu and p21^{ras} are considerably smaller than any of the heterotrimeric G-protein α -subunits, then novel regions of the heterotrimeric G-proteins, namely inserts 1 to 4 and the N and C-terminal extension, have to be predicted *de novo* (see section 3.1.3.3; see Conklin & Bourne, 1993; Masters *et al.*, 1986). Here this has been attempted using established methods for the prediction of α -helices, β -sheets and turn regions (see section 3.3.1.2; see Argos, 1989; Chou & Fasman, 1978; Garnier *et al.*, 1978); flexible regions (see Karplus & Schulz, 1987; Karplus & Schulz, 1989); and surface probability plot (see Emini *et al.*, 1985) using the computer program DNASTAR (DNASTAR Ltd., UK). In the prediction of α -helices, β -sheets and turn regions, the methods of Chou-Fasman and Garnier-Robson were combined and only regions that were predicted by both methods to contain such secondary structure were taken (see figure 3.18). It is interesting to note that if the probabilistic prediction methods (see section 3.1.3.2) and the information theory method (see sections 3.1.3.2 and 3.1.3.3) based on p21^{ras} and EF-Tu are compared then a degree of correlation is found (see figure 3.18).

3.4 Discussion

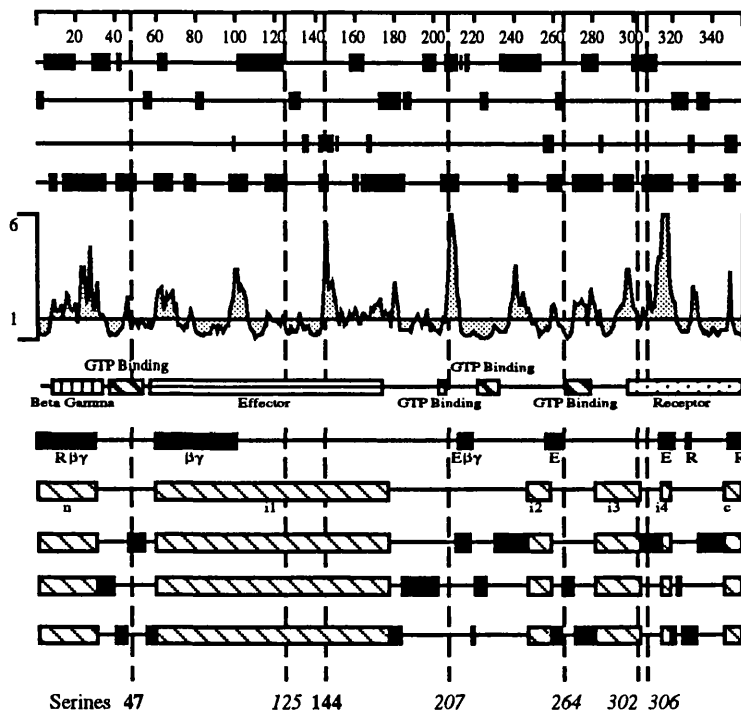
The data presented in section 3.3.1 showed that antiserum 1867 can be considered to be α -G_{i-2} specific because it immunoprecipitates a protein of the correct molecular weight and the precipitation can be inhibited by a specific α -G_{i-2} peptides. The antiserum did not immunoprecipitate α -G_{i-3} as the equivalent decapeptide does not inhibit immunoprecipitation and it can not be immunoprecipitating α -G_{i-1}, which has the same C-terminal peptide sequence as α -G_{i-2}, as it has been demonstrated that rat hepatocytes do not contain α -G_{i-1} (Griffiths *et al.*, 1990; Bushfield *et al.*, 1990b).

In order to gauge whether α -G_{i-2} was subjected to multiple-site phosphorylation phosphopeptides of the protein were produced by enzymatic cleavage with trypsin, α -chymotrypsin and V8 and the peptides separated by two-dimensional phosphopeptide mapping. This was performed using phosphorylated α -G_{i-2} immunoprecipitated from control hepatocytes (basal state) and from hepatocytes that had been pre-treated with various agents in order to activate PKC and/or PKA. Two dimensional analysis of the phosphopeptides resulting from trypsin digestion of α -G_{i-2} from control cells identified three major phosphopeptides (labelled C1, C2 and C3) all of which were positively charged. Peptides C1, C2 and C3 were resolved by chromatography but only C3 was resolved by electrophoresis at pH1.9 (see figures 3.5 and 3.16). These three peptides were consistently identified using cell preparations from twelve different animals.

Previous work by Dr. Mark Bushfield (see Morris *et al.*, 1994) only produced the two peptides C1 and C2, upon trypsin digestion of phosphorylated α -G_{i-2}. The

Figure 3.18: The location of the seven proposed sites of serine phosphorylation shown in conjunction with predicted secondary structure and protein features of α -G_{i-2}

The location of the seven proposed sites (based on mass charge ratio data) of serine phosphorylation are shown in conjunction with predicted secondary structure and protein features of α -G_{i-2}. Serines 125, 207, 264, 302 and 306 are shown in italic print as they have been eliminated as potential sites based on kinase motifs and change of mass charge ratio upon further digestion (see Discussion section 3.4). Serines 47 and 144 are shown in bold type as these are the most likely candidates for PKC phosphorylation sites. Alpha, beta and turn structure predictions were based on the regions of agreement between the prediction methods of Chou / Fasman (see Chou & Fasman, 1978) and Garnier / Robson (see Garnier *et al.*, 1978). Flexible region predictions were by using the method of Karplus / Schulz (see Karplus & Schulz, 1987; Karplus & Schulz, 1989) and the surface probability plot was derived using the method of Emini (see Emini *et al.*, 1985). Structural predictions were performed using the program DNASTAR. Protein features were derived from the information in Masters *et al.*, 1986, Jones & Reed, 1987, Berlot & Bourne, 1992 and Conklin & Bourne, 1993. (R = receptor; E = effector; n = N-terminal extension; c = C-terminal extension; i1 - i4 = inserts 1 to 4)



Alpha, Regions - Chou-Fasman / Garnier-Robson

Beta, Regions - Chou-Fasman / Garnier-Robson

Turn, Regions - Chou-Fasman / Garnier-Robson

Flexible Regions - Karplus-Schulz

Surface Probability Plot - Emini

Protein Features (Masters)

Interaction sites (Conklin)

Inserts (Conklin)

Alpha (Conklin)

beta (Conklin)

turn (Conklin)

Serines 47 125 144 207 264 302 306

increased digestion times of the protein used in this study caused the production of the third peptide C3 from either C1 or C2 (see figure 3.8; see section 3.3.2.1). This showed that the peptide C3 must contain the same phosphorylation site and be a shorter peptide than either C1 or C2.

Further digestion of the peptides C1, C2 and C3 by V8 showed that all three peptides were susceptible to cleavage (see figures 3.9 to 3.12 and 3.16) and individual cleavage of spots C1, C2 and C3 confirmed that C1 gave C2', C2 produced C2' and C2'', C3 gave C3', and AN gave AN' (see figures 3.10 to 3.13) which again were all positively charged. These results showed that the peptides C1 and C2 must contain the same phosphorylation site as both peptides are able to produce a common peptide, C2', upon cleavage with V8. As it has already been determined that peptide C3 is produced from increased digestion of C1 and C2, and hence contains the same phosphorylation site as either C1 or C2, then it would appear that peptides C1, C2 and C3 all contain the same phosphorylation site and are just different products of partial digestions.

Examination of the V8 cleavage data of peptides C1, C2 and C3 revealed that as C1 only gave the peptide C2' and C2 gave C2' and C2'' then it would seem likely that C1 is the shorter of the two peptides. The peptide C3, which is a trypsin cleavage product of C1 and C2, gave the V8 peptide C3'. If C1 and C2 are the parent peptides of C3 then they should also produce the peptide C3' on V8 cleavage. Whilst no clear evidence was obtained to this end, it may be explained in terms of a failure of V8 to digest the peptides C1 and C2 to their smallest components as a result of secondary structure masking of the cleavage site or as a requirement for longer digestion periods. However, secondary digestion of trypsin cleavage products often proved difficult due to the small amounts of labelled material recovered from the t.l.c. plates after the first analysis and so the identification of C3' from C2 or C1 may not have been possible due to the low levels of radioactivity. More strenuous efforts to address this problem were not possible due to the considerable amounts of radioactivity (2 mCi) already used in the experiments.

Digestion of phosphorylated control α -G_{i-2} with V8 produced peptides corresponding to the peptides C2', C2'' and C3' (see figure 3.15). This demonstrates that the peptides C1, C2 and C3 must therefore contain two V8 cleavage points on either side of the phosphorylation site.

Treatment of hepatocytes with the protein kinase C activator PMA resulted in increased labelling of the protein (see Chapter 4; section 4.3.2) with no evidence for the appearance of any other phosphopeptides (see figure 3.6). This demonstrates that as α -G_{i-2} is known to be phosphorylated by PKC *in vitro* (Sauvage *et al.*, 1991) and that phosphorylation *in vivo* does not give additional sites then some of the pool of α -G_{i-2} must undergo PKC mediated phosphorylation in resting / unstimulated cells.

The idea that peptides C1, C2 and C3 are related is further supported by previous stoichiometry data obtained in the laboratory (Bushfield *et al.*, 1990b; see Morris *et al.*,

1994) which showed that PMA incubation of hepatocytes gave a stoichiometry of ~ 1 mol ^{32}P / mol $\alpha\text{-G}_{i-2}$.

In contrast, treatment of hepatocytes with 8-bromo-cAMP resulted in the appearance of a novel labelled phosphopeptide (labelled AN; see figures 3.7 and 3.16). This indicated that the activation of PKA in intact hepatocytes results in the phosphorylation of $\alpha\text{-G}_{i-2}$ at a site within the peptide AN which was not normally phosphorylated under basal conditions. Again this peptide was sensitive to V8 treatment, producing peptide AN' (see figure 3.14), although increased incubation times were required. Attempts to cleave peptide AN with V8, unlike peptides C1, C2 or C3 (see figures 3.10 to 3.12), also required increased enzyme concentrations and incubation times. As it has already been established that peptides C1, C2 and C3 produce the peptides C2', C2'' and C3' then the new peptide produced in figure 3.14 by V8 cleavage of 8-bromo-cAMP samples must be AN'. It is interesting to note that V8 cleavage of AN' required increased digestion times and that even then not all of the AN peptide was digested (see figure 3.14). As peptides AN and AN' were not produced from $\alpha\text{-G}_{i-2}$ in either control or PMA-treated hepatocytes then this demonstrates that $\alpha\text{-G}_{i-2}$ does undergo multi-site phosphorylation. As $\alpha\text{-G}_{i-2}$ has been phosphorylated by PKC but not PKA *in vitro* (Lincoln, 1991; Sauvage *et al.*, 1991) then it appears that the protein undergoes multi-site phosphorylation by at least two kinases, one of which is PKC and the other is unknown.

Examination of the autoradiography does not show the presence of any diagonal spot patterns that may give an indication to the peptides structure (see figure 3.16; see section 3.1.4; see Boyle *et al.*, 1991). The similar mass-charge ratios of C1 and C2 indicate that it may be the same peptide that contains two different phosphorylation sites though this idea does not fit the data for the generation of peptide C3 as longer digestions should produce two additional phospho-peptides and just not the one.

The amino acid sequence of rat $\alpha\text{-G}_{i-2}$ is known (Itoh *et al.*, 1986) and hence it is possible to predict, using the information on enzyme digestion characteristics presented in sections 3.1.4.1 and 3.1.4.2, the peptides that might be produced as a result of enzyme cleavage (see Boyle *et al.*, 1991; Carrey, 1989; Smyth, 1967). In an ideal experiment trypsin cleaves at arginine (R) and lysine (K), but it can also produce partial digestion products as a result of the occurrence of multiple cleavage sites, modifications such as phosphorylations near to the point of cleavage and where the cleavage site is next to glutamic acid or proline (see section 3.1.4.1; see Boyle *et al.*, 1991; Carrey, 1989; Smyth, 1967). Such features can therefore lead to the production of further peptides due to partial digestion. Cleavage of a protein by V8 occurs mainly at glutamic acid (E) but it can also cleave at aspartic acid (D; see section 3.1.4.2; see Boyle *et al.*, 1991; Carrey, 1989; Drapeau, 1977; Sørensen *et al.*, 1991; Sellinger & Wolfson, 1991; Breddam & Meldal, 1992). The primary sequence of $\alpha\text{-G}_{i-2}$ contains 20 serines, 21 threonines and 12 tyrosines, as well as multiple trypsin and V8 cleavage sites, some of which possess

characteristics that may make them less susceptible to cleavage, thus the prediction of the peptides that are produced is, to say the least, somewhat complicated.

To aid the analysis the following deductive approach was made:- It was found that the phospho acceptor was serine (see section 3.3.3 and figure 3.17) and that both under basal conditions, and when PKC was activated, three peptides were produced (C1, C2 and C3; see section 3.3.2.1) that were related and that all contained phospho-serine in a sequence that had a V8 cleavage site on either side. As the phosphorylation was PKC-mediated, the primary sequence of α -G_{i-2} was examined for the occurrence of PKC recognition motifs (see table 3.1; see section 3.1.2 see Azzi *et al.*, 1992; Hug & Sarre, 1993; Kennelly & Krebs, 1991; Pearson & Kemp, 1991). In this respect serines 16, 44, 47, 144, 207, 247, and 306 all occurred in regions that formed a possible PKC recognition motif (see table 3.1). These serines and their associated sequences were then used for the prediction of tryptic peptides (see Appendix 12).

The mass-charge ratios of the predicted tryptic peptides were calculated and as it was known that peptides C1, C2 and C3 had positive mass-charge ratios (see section 3.3.2.1) then any peptides which gave a negative or zero mass-charge ratio were eliminated. The peptides C1, C2 and C3 could produce peptides C2', C2" and C3' on V8 cleavage and these peptides could also be produced by the cleavage of α -G_{i-2} by V8. This indicated that the phospho-serine must have a V8 cleavage site on either side. The sequence of the remaining peptides were then examined to see which peptides possessed such a sequence and any that did not were again eliminated. Using the remaining peptides, the corresponding V8 peptides were predicted and their mass-charge ratios calculated. From the results obtained in section 3.3.2.2 it is known that the V8 peptides C2', C2" and C3' have a positive mass-charge ratio. This means that any predicted V8 peptide that has zero or negative mass-charge ratio cannot be the peptides C2', C2" and C3'. This enabled the elimination of some of the predicted V8 peptides and also their parent tryptic peptides.

By the above approach it was possible to reduce the number of possible serine phosphorylation sites from seven to four. The remaining sites are serines 47, 144, 207 and 306 (see Appendix 12). The results in section 3.3.2.1 show that the trypsin digestion of α -G_{i-2} produces three peptides C1, C2, and C3. If serines 47, 144, 207 and 306 were to produce the tryptic peptides, and as it is predicted that C1, C2 and C3 represent the same phosphorylation site, then each serine should produce at least three predicted tryptic peptides. Serine 47 produced three such peptides and also a range of predicted V8 peptides that could fit the tryptic and V8 digestion patterns. Serine 144 produced at least five tryptic peptides and an associated range of V8 peptides which could also accommodate the experimental data. However serine 207 only produced two tryptic and V8 peptides, enabling this to be eliminated from consideration as the phosphorylation site as also with serine 306 which produced insufficient potential tryptic peptides.

The tertiary structure of α -G_{i-2} has been predicted based on the structural similarities with EF-Tu and p21^{ras} (see section 3.1.3.3; Conklin & Bourne, 1993; Masters *et al.*, 1986). From examination of the predicted structures it was found that serine 47 occurred in a highly conserved region of the G-protein families, the GTP binding domain, and at the start of an α -helix (see figures 3.2 and 3.18; see Conklin & Bourne, 1993; Masters *et al.*, 1986). Although the location of the serine in the GTP binding domain indicated that a phosphorylation at that site could have the potential to affect GTP binding, the location in such a site, coupled with the prediction from a surface probability plot (Emini *et al.*, 1985) that it would not occur on the surface of the protein, indicates that it may not be readily available to interact with protein kinases (see figure 3.18). Serine 144 is found two-thirds of the way through the first insert (see figure 3.18; see Conklin & Bourne, 1993; Masters *et al.*, 1986). This is a region of no known secondary structure or attributable function (see figure 3.18; see Conklin & Bourne, 1993; Masters *et al.*, 1986), although it is thought to occur next to the GTP binding pocket and to be exposed facing into the cytoplasm (see Conklin & Bourne, 1993). Predictions of the secondary structure of this insert suggest that serine 144 has a good probability of being on the surface of the molecule, close to a region turn and in a region of flexibility (see figure 3.18). This makes serine 144 a good potential candidate for kinase action and in a region of the protein where a phosphorylation may have conformational effects. Indeed, serine 144 is only found in α -G_s and members of the α -G_i family, except α -G_{gust} and the rod and cone α -subunits. Interestingly α -G_{gust} and the rod and cone α -subunits belong to a different 'branch' of the G-protein phylogenetic tree from the other members of the α _i family (see figure 1.1; see Birnbaumer, 1992).

In order to try to clarify further whether serine 47 or 144 is the most likely target for PKC-mediated phosphorylation an alternative approach to determine the phosphorylation sites was taken. This involved working through from predicted tryptic and V8 peptides to secondary structure and finally applying kinase motif recognition data. From the predicted peptides resulting from trypsin cleavage all that do not contain serine can be eliminated as it is known that the phosphorylation sites are serine (see section 3.3.3 and figure 3.17). The mass-charge ratio of the remaining tryptic peptides can be calculated and all zero or negatively charged peptides discounted as the peptides that are produced are positively charged (see figure 3.5 and 3.6). As peptides C2', C2" and C3' could be produced from basal / PKC phosphorylated α -G_{i-2} by either trypsin followed by V8, or just by V8, then the peptides C1, C2 and C3 must contain a serine surrounded by two V8 sensitive sites and hence all peptides that do not contain such an arrangement can also be eliminated. Finally, if the tryptic peptide produces a zero or negatively charged V8 peptide then these peptides, and their parent tryptic peptides, can also be discounted as all the V8 peptides produced are positive. By carrying out this process of elimination there are six

potential candidate sites which fit the criteria and these are serines 125, 144, 207, 264, 302 and 306.

Serine 125 is an unlikely phosphorylation site as it does not fit any of the recognised motifs for phosphorylation (see table 3.1; see Azzi *et al.*, 1992; Hug & Sarre, 1993; Kennelly & Krebs, 1991; Pearson & Kemp, 1991), interestingly, is not found in G_s , G_{i-1} or G_{i-3} (see table 3.3). In addition it is in the first insert (see figure 3.18) and appears to be at the end of an α helix and just before the start of a β sheet, but is not likely to be a surface amino acid based on surface probability plots (see figure 3.18).

Serine 144 is a good candidate site as it has a positive charge cluster associated with arginines although the glutamic acid does add a degree of negative charge just after the arginine (see table 3.3). A serine surrounded by two positively charged arginines is typical of PKC and PKA sites ($K/RX_{(0-2)}SX_{(0-2)}K/R$ or $SX_{(0-2)}K/R$ for PKC and $K/RX_{(0-2)}S$ for PKA; see Azzi *et al.*, 1992; Hug & Sarre, 1993; Kennelly & Krebs, 1991; Pearson & Kemp, 1991; see table 3.1). Out of twenty serines in α - G_{i-2} only seven fit the PKC and three fit the PKA motif (see table 3.1; PKA sites are also PKC sites). Serine 144 is found in α - G_s , α - G_{i-1} , α - G_{i-3} and G_0 but in all cases there is a slight difference in the motif (see table 3.3). Based on the mass charge ratio data, that is the change in mass charge of the tryptic peptide following V8 cleavage serine 144 is the most likely site for PKC mediated phosphorylation. The surrounding amino acids of serine 144 give it a high probability of being on the surface of the protein, in a region of flexibility and of turn, and is also hydrophilic (see figure 3.18). With its location on the surface, good kinase motif and in region that could alter the shape and hence the function of the protein, it makes the site a very good point for kinase interaction.

Serine 207 again displays the characteristics of PKC and PKA sites (see table 3.1; see Azzi *et al.*, 1992; Hug & Sarre, 1993; Kennelly & Krebs, 1991; Pearson & Kemp, 1991). It is in a region of the G_i family that is perfectly conserved in the rat for ten amino acids on the N-terminal side and twenty two amino acids on the C-terminal side of the serine. The region also shows a 80% homology with α - G_s but out of only seven amino acids that are different one is the serine. Again using the data derived from the change in the mass charge ratios it indicates that this serine is the PKA site as cleavage of the tryptic peptide by V8 causes a decrease in the mass-charge ratio and the only peptide that decreases is AN. The location characteristics of serine 207 place it just at the start of an α -helix, close to an effector and $\beta\gamma$ binding site, and near the GTP binding site. Again this makes it a likely site for kinase interaction. Serine 207 is found just at the end of the GTP binding region which is an equivalent region to the site of cholera toxin catalysed ADP-ribosylation in α - G_s which has the effect of permanently activating the enzyme (see Birnbaumer *et al.*, 1990; Conklin & Bourne, 1993; Masters *et al.*, 1986). It would therefore seem possible that a phosphorylation at this site may have some effect on the GTPase activity of the protein or on the rate of GDP / GTP exchange. It could be speculated that as this is most

likely the AN site, that such a phosphorylation could cause a decrease in GTPase activity, and hence prolonged activation so suppressing further cAMP production, or it could cause an increase in GTPase activity and so remove the inhibitory effects of the protein on cAMP production, or interfere with GTP binding. Serine 207 can be discounted as a potential PKC site as all the peptides produced under conditions that would activate PKC produce tryptic peptides (C1, C2 and C3) whose mass-charge ratio increases or changes very little upon V8 cleavage (C2', C2'' and C3'). Predictions for tryptic peptides that contain serine 207 and undergo V8 cleavage show a decrease for mass-charge ratio. Although this fits the characteristics of peptide AN to AN' the serine at 207 has to be discounted as a potential phosphorylation site as the method used for predicting the six sites does not work for cAMP mediated phosphorylations as the resulting protein is resistant to V8 cleavage (see section 3.3.2.3).

Serine 264 again is an unlikely phosphorylation site as it does not fit any of the PKC recognition motifs for phosphorylation but it does fit a motif for casein kinase I (see

Table 3.3: Summary of the seven potential phosphorylation sites, associated kinase motifs and occurrence in other G-proteins.

Serine	Kinase							
	PKA	PKC	CKII	GSKIII	α -G _s	α -G _{i-1}	α -G _{i-3}	α -G _o
ESGK ⁴⁷ STIVKQ	-	+	-	-	Yes	Yes	Yes	Yes
PEDL ¹²⁵ SGVIRR	-	-	-	-	No	No	No	No
FGR ¹⁴⁴ SREYQLN	+	+	-	-	Y/N	Y/N	Y/N	Y/N
GGQR ²⁰⁷ SERKKW	+	+	-	-	No	Yes	Yes	Yes
FDTDT ²⁶⁴ SIILFL	-	-	-	-	Y/N	Yes	Yes	Yes
A ³⁰² SYIQ ³⁰⁶ SKFED	-	+(306)	+(306)	+(302)	No	No	No	No

The serines are shown with the surrounding amino acids that would contribute to the kinase recognition site. All known kinase motifs were examined (see table 3.1; Azzi *et al.*, 1992; Hug & Sarre, 1993; Kennelly & Krebs, 1991; Pearson & Kemp, 1991). The serines were examined for their occurrence in α -G_s (Itoh *et al.*, 1986), α -G_{i-1} (Jones & Reed, 1987), α -G_{i-3} (Jones & Reed, 1987; Itoh *et al.*, 1988) or α -G_o (Itoh *et al.*, 1986). 'No' indicates that the serine is not present, 'Y / N' indicates the presence of the serine but there is some change in the surrounding amino acids, 'Yes' shows that the serine is present and the motif is conserved.

table 3.1; see Azzi *et al.*, 1992; Hug & Sarre, 1993; Kennelly & Krebs, 1991; Pearson & Kemp, 1991). The site is found in α -G_{i-1} and α -G_{i-3} and has a certain degree of homology with the equivalent site in α -G_s. Serine 264 appears to be at the start of a β sheet and at the end of a region of turn (see figure 3.18). The surface plot predicts that it is not likely to be associated with the surface of the molecule and hence inaccessible to kinases (see figure 3.18). Serine 264 is found at the start of the GTP binding region and the end of an effector binding region (see figure 3.18; see Birnbaumer *et al.*, 1990; Conklin & Bourne, 1993; Masters *et al.*, 1986). Although this would make it an ideal location for effecting some change in the characteristics of the protein it is in such a position that may not be readily accessible to the kinases.

The final two serines are 302 and 306. Unfortunately these serines are not separated by digestion by either trypsin or V8 but from the mass-charge ratio data it is indicated that only one of the sites can be phosphorylated at any time, but no indication is given as to which site. Neither of the serines fit the PKA motif but 302 does fit the motifs for glycogen synthase kinase III and casein kinase I (GSKIII, SX₃S(phos); and CKI, (D/E₂₋₄,X₂₋₀)XS; see Pearson & Kemp, 1991; Woodgett, 1991; see tables 3.1 and 3.3) although the motif for GSKIII requires the phosphorylation of serine 306 and the motif for CKI is not very good (see Kennelly & Krebs, 1991; see tables 3.1 and 3.2). Serine 306 fits the motifs for PKC, and casein kinases I and II (CKII; SX₂E/D; see Azzi *et al.*, 1992; Hug & Sarre, 1993; Kennelly & Krebs, 1991; Pearson & Kemp, 1991; see tables 3.1 and 3.3). Serine 302 represents the only potential glycogen synthase kinase III site in α -G_{i-2} and one of four casein kinase II sites. Neither of these serines are found in any of the G-protein α -subunits with the exception of transducin (α -G_t; see section 1.2.2.2) which contains an equivalent to serine 306 (see table 3.3). Phosphorylation of serine 302 by GSKIII would require the phosphorylation of serine 306 which possess the motif for CKII and these two kinase have already been reported as acting together in the phosphorylation of proteins (see Woodgett, 1991). The phosphorylation of serine 302 would seem unlikely as it also requires the phosphorylation of serine 306 and the data from mass-charge ratio analysis indicates that only one of the serines can be phosphorylated. Serine 306 occurs in an α -helix and just before an effector interaction region (see Conklin & Bourne, 1993; Masters *et al.*, 1986; see figure 3.18). Serine 306 can be discounted as a site of phosphorylation because as like serine 207 the predicted mass charge ratio decreases when the tryptic peptide is digested with V8.

From the two approaches taken to predict which serine is contained in the tryptic peptides C1, C2 and C3 both methods indicated that the most likely candidate is serine 144 with the first method also predicting serine 47. As stated above serine 144 occurs in the first insert and serine 47 in the GTP binding pocket (see figure 3.18). This indicates that serine 47 is less likely to be accessible to protein kinases than serine 144. In addition, serine 47 occurs in all the known G-protein α -subunits whereas serine 144 is only found in

α -G_s and some members of the α_i family (see table 3.3). Reports on the phosphorylation of G-proteins are confused with different groups finding different phosphorylation events in different cell-types (see section 3.1.1) and the only reported identification of a phosphorylation site is in α -G_z where it occurs on serine 27 which is unique to that α -subunit (Carlson *et al.*, 1989; Lounsbury *et al.*, 1991; Lounsbury *et al.*, 1993) thus, again, favouring serine 144.

The identification of the 8-bromo-cAMP site found within the peptides AN is more complicated than the identification of the serine in peptides C1, C2 and C3. The phosphorylated form of α -G_{i-2} from hepatocytes that have been incubated with 8-bromo-cAMP is more resistant to V8 cleavage than the PKC phosphorylated α -G_{i-2}. This was shown in experiments where V8 either failed to digest the whole protein or where increased incubation times were required to get digestion of the tryptic peptides (see sections 3.3.3.2 and 3.3.3.3; figure 3.14). What the results do show is that when hepatocytes are treated with 8-bromo-cAMP the resulting phosphorylated form of α -G_{i-2} has undergone some degree of conformational change that now makes it V8 resistant. This indicates the importance of this phosphorylation event in the regulation of the protein as it causes such a change.

From the data presented here the unequivocal identification of the AN site is not possible. The only data available to aid the identification of the site is that the tryptic peptide has a mass-charge ratio greater than those of C1, C2 and C3; that the AN peptide is poorly digested by V8, which results in a decrease in mass-charge ratio; the phosphorylation site in peptide AN is a serine; and phosphorylated α -G_{i-2} from hepatocytes treated with 8-bromo-cAMP is not susceptible to V8 cleavage. In addition, although it is known that 8-bromo-cAMP will activate PKA, the phosphorylation of α -G_{i-2} by this kinase *in vitro*, unlike for PKC, has not been demonstrated (see section 3.1.1). This means that, unlike the analysis of the PKC phosphorylation site that produces peptides C1, C2, and C3, no assumption about the kinase responsible for the phosphorylation of the site in the peptide AN can be made and hence no assumption about which serines may be potential phosphorylation sites based on kinase motifs. Without any information on the possible kinase responsible for the phosphorylation then all twenty serines in α -G_{i-2} have to be considered. This produces a table of possible tryptic peptides that is larger than that in Appendix 12. Using the information that the peptide is positively charged at pH1.9 and contains at least one V8 cleavage site some of the tryptic peptides can be eliminated. The mass-charge ratios of the V8 peptides that would be produced from the remaining tryptic peptides can be calculated and any V8 peptides and their parent tryptic peptides which have zero, negative or show an increased mass-charge ratio when compared to the parent peptide, can be eliminated. By carrying out this procedure a large number of potential peptides for AN and AN' still remain and so no prediction could be made as to which of the serines in α -G_{i-2} were phosphorylated in response to the incubation of hepatocytes with 8-bromo-cAMP.

In an attempt to overcome some of these problems α -G_{i-2} from hepatocytes treated with 8-bromo-cAMP was digested with α -chymotrypsin. These experiments also proved unsuccessful as even the PKC phosphorylated form of the protein seemed to have a chymotrypsin resistant 'core' which was not susceptible to cleavage. The use of α -chymotrypsin as a secondary digestion enzyme did not aid identification as the final levels of peptide recovered were too low for analysis.

The inhibitory G-protein α -G_{i-2} appears to play a pivotal role in controlling the functioning of adenylyl cyclase. The GTP-elicited inhibitory action of α -G_{i-2} which is responsible, due to the high intracellular concentrations of GTP, for tonic inhibition of adenylyl cyclase is lost upon phosphorylation by PKC (Bushfield *et al.*, 1990b; Pyne *et al.*, 1989b). Thus, the phosphorylation-dephosphorylation cycle acting at this site may serve to regulate and/or 'fine-tune' the control of adenylyl cyclase functioning through this G-protein.

By use of two dimensional peptide map it has been possible to show that under basal (resting) conditions that the protein can produce three phosphorylated peptides (C1, C2 and C3) and that challenging the cells with 8-bromo-cAMP produces a second site (AN). By analysis of the data, the prediction of the peptides produced by the enzymes and the calculation of their mass-charge ratios, it has been possible to propose one potential phosphorylation site in the protein under basal conditions from a possible twenty sites. This site is serine 144 and has been shown to occur in predicted secondary structure regions of the protein that may have a potential to affect its function. Ideally the site should be confirmed by the use synthesised peptides, *in vitro* mutagenesis or by automated sequencing (see Boyle *et al.*, 1991). The use of synthesised peptides is not possible as the sequence surrounding serine 144 seems to be able to produce a wide range of peptides and hence it has not been possible to assign any one theoretical peptide to the spots C1, C2 or C3; an approach using site directed mutagenesis *in vivo*, as used by Lounsbury *et al.* (Lounsbury *et al.*, 1993) in the determination of the phosphorylation site in α -G_z, is not possible as all cell types seem to express α -G_{i-2} and the lack of material in the experiments (approximately 20 amole per plate after processing, therefore 6 amole per peptide; see Appendix 13) means that the 10 - 100 pmole required for analysis are not available (see Boyle *et al.*, 1991).

Chapter 4

Phosphorylation of α -G_{i-2} in hepatocytes from Sprague Dawley rats:

Effects of insulin, amylin and streptozotocin-induced diabetes

4.1 Introduction

As discussed in Chapter 3, α -G_{i-2} from rat hepatocytes undergoes multi-site phosphorylation by at least two different kinases. One of the kinases was PKC (see section 1.2.4.2) and the other was activated in a cAMP-dependent manner but appears not to be PKA itself (see sections 1.2.4.1 and 3.1.1).

The phosphorylation of α -G_{i-2} in rat hepatocytes has been investigated and it was found that various agents such as vasopressin, angiotensin II, glucagon, PMA, 8-bromo-cAMP and okadaic acid, caused an increase in the phosphorylation of the protein (Bushfield *et al.*, 1990a; Bushfield *et al.*, 1991; Bushfield *et al.*, 1990b; Bushfield, Pyne & Houslay, 1990c; Pyne *et al.*, 1989b). Furthermore, streptozotocin-induced diabetes in rats (see section 4.1.1) caused both a decrease in the expression of α -G_{i-2} and also effectively abolished the angiotensin II-, vasopressin- and PMA-mediated phosphorylation of α -G_{i-2} due to the remaining α -G_{i-2} already being phosphorylated (Bushfield *et al.*, 1990a; Gawler *et al.*, 1987).

One effect of the phosphorylation of α -G_{i-2} in hepatocytes is to cause a loss of the G_i-mediated inhibition of adenyl cyclase (see section 1.2.2.2; Bushfield *et al.*, 1990a; Bushfield *et al.*, 1991; Bushfield *et al.*, 1990b; Bushfield *et al.*, 1990c; Pyne *et al.*, 1989b). If the phosphorylation of α -G_{i-2} is of physiological significance in the control of the signal transduction system then a method for dephosphorylation must also exist. Indeed, Bushfield suggested that α -G_{i-2} might be at the centre of a futile cycle of phosphorylation and dephosphorylation (Bushfield *et al.*, 1991) and hence the loss of control of such a system in hepatocytes, and also the loss of α -G_{i-2} in streptozotocin-induced diabetes, could have profound effects on the insulin signalling system.

4.1.1 Streptozotocin induced diabetes - type I model

Treatment of rats with streptozotocin causes the destruction of the β -cells in the pancreas resulting in a loss of insulin production in the animal hence producing a model of type I diabetes (see section 1.3.1). Such administrations of streptozotocin cause a range of effects in the animal. It has been found, for example, that the treated animals exhibit a degree of insulin resistance; reduced levels of glucose transporters in the muscle and adipose tissues, which is connected to reduced glucose uptake and also increased insulin binding in the muscle, fat, kidneys and liver but not the brain (Sechi *et al.*, 1992).

The increase in insulin binding is accompanied by an increase in insulin receptor numbers but effects such as insulin suppression of hepatic glucose production show no change (see Giorgino, Chen & Smith, 1992; Nishimura *et al.*, 1989; Burant, Treutelaar & Buse, 1986; Kadowaki *et al.*, 1984). The above effects tend to occur when the animals are examined at least one week after the treatment with streptozotocin (Nishimura *et al.*, 1989).

The insulin resistance that was observed in streptozotocin treated rats may be explained by a loss of auto-phosphorylation of the receptor, and hence a loss of tyrosine kinase activity (Giorgino *et al.*, 1992; Kadowaki *et al.*, 1984; Burant *et al.*, 1986). However, as an increased level in the phosphorylation of IRS1 was observed this suggests either an increase in receptor tyrosine kinase activity or a decrease in phosphatase activity (Giorgino *et al.*, 1992; see section 1.4.3.1). Clearly the increased levels of IRS1 phosphorylation and the decrease in insulin receptor activity are contradictory unless phosphatase activity has been reduced. The animals also show an altered form of the insulin receptor β -subunit which exhibits decreased migration rate in SDS-PAGE and this again may explain why even with the increased number of insulin receptor that some insulin-mediated effects may not change (Burant *et al.*, 1986).

Rats that have been treated with streptozotocin and then examined two weeks later have also been shown to have increased levels of PKC (see section 1.2.4.2) activity in the retina, hearts and hepatocytes (Inoguchi *et al.*, 1992; Tang *et al.*, 1993). When the rat hepatocytes were examined for PKC expression it was found that only α , β II, ϵ , and ζ isoforms were detected, whilst β I, γ , δ , and η were not, and that the levels of β II, α and ϵ isoforms increased upon the induction of diabetes with translocation of β II and α from the cytosol to the membrane occurring (Tang *et al.*, 1993). In the rat heart it was found that there was an increased expression of the α and β II isoforms of PKC (ϵ was not examined) and increased levels of diacylglycerol (see section 1.2.3.2; Inoguchi *et al.*, 1992).

Another reported effect of streptozotocin-induced diabetes was a decreased expression of α -G_{i-2} in hepatocytes accompanied by an increased level of phosphorylation of the remaining pool of α -G_{i-2}. The hepatocytes also exhibited a decreased level of ligand induced ³²P phosphorylation of α -G_{i-2} and this has been explained as a consequence of the increased level of cold-phosphorylation of the α -G_{i-2} pool. This idea was further supported by the observation that the rate of turnover of the phosphate groups on α -G_{i-2} in the diabetic animals was not as high as in the non-diabetic animals (Bushfield *et al.*, 1990a). An explanation for the increased levels of phosphorylation seen in the diabetic animals may be the increased levels of PKC expression and its activator, DAG, reported by Inoguchi and Tang (Inoguchi *et al.*, 1992; Tang *et al.*, 1993).

4.1.2 *Glucagon and amylin*

As discussed in Chapter 1 (sections 1.3.1 and 1.4) insulin plays an important role in glucose homeostasis in the body. Other hormones that is involved in the regulation are glucagon and a recently discovered poly-peptide hormone, called amylin.

Glucagon is a pancreatic polypeptide hormone which consists of a single chain of 29 amino acids. The hormone is produced in response to a decrease in blood glucose levels and stimulates the hydrolysis of glycogen and lipids. The challenge of hepatocytes with glucagon causes a rapid rise in cAMP concentrations which is only transient as the hormone also activates a specific high-affinity cAMP-specific phosphodiesterase (see section 1.2.3.1). It has also been shown that the hormone can cause a weak stimulation of inositol phosphate metabolism, a strong stimulation of phosphatidyl choline metabolism and hence is capable of generating DAG (see section 1.2.3.2). Indeed, it is this generation of DAG that may be responsible for the glucagon-mediated activation of PKC reported by Tang and Houslay (see section 1.2.4.2; see Tang & Houslay, 1992).

Amylin is a 37 amino acid poly-peptide which is co-secreted with insulin from the β -cells of the pancreas and is nearly 50% identical to calcitonin gene-related peptide (CGRP). Amylin was initially isolated, purified and characterised as a major component of the amyloid deposits in the pancreatic islets of non-insulin dependent diabetics (type II; see section 1.3.1). The ratio of amylin and insulin secreted from the β -cells is variable and may reflect different control systems for the gene expression and translation of amylin and insulin. The first reported effect of amylin was a reduction in the insulin-stimulated incorporation of glucose into glycogen in the muscle and it also appears to exert some control on glycogen synthesis in the liver. Indeed, experiments with streptozotocin-treated rats (see section 4.1.1) have shown that to return liver glycogen storage levels to normal, both insulin and amylin treatments are required. This in turn has led to the suggestion that amylin may be of use for the treatment of type I diabetics (see section 1.3.1) in that both insulin and amylin should be administered. In type II patients (see section 1.3.1), where increased levels of insulin production may occur, some of the symptoms observed may be caused by increased levels of amylin (see Westermark *et al.*, 1992; Rink *et al.*, 1993). In fact amylin appears to act as a non-competitive or functional antagonist for insulin in the muscle but there is no evidence that it interferes with the binding of insulin to its receptor or with the subsequent activation of the tyrosine kinase. In addition, it has been reported that amylin inhibits insulin secretion from the β -cells (see Westermark *et al.*, 1992; Rink *et al.*, 1993) and it appears that amylin may produce some of its effects by the activation of adenylyl cyclase resulting in a rise in intracellular cAMP (see Bushfield *et al.*, 1993; Rink *et al.*, 1993). However, to date, no distinct receptor for amylin has been identified and it is thought to act via a shared amylin / CGRP receptor (see Bushfield *et al.*, 1993; Rink *et al.*, 1993).

4.2 Aims

It has been established that in rat hepatocytes α -G_{i-2} undergoes multi-site phosphorylation and that certain ligands can cause an increase in the levels of phosphorylation (Bushfield *et al.*, 1990a; Bushfield *et al.*, 1991; Bushfield *et al.*, 1990b; Bushfield *et al.*, 1990c; Pyne *et al.*, 1989b).

The phosphorylation events were examined further with particular emphasis on the effects of insulin and amylin on the levels of phosphorylation and any other associated effects on ligand-induced phosphorylation. To this end, the dose-response and time-courses relationships for insulin and amylin were established, and the effects of streptozotocin-induced diabetes on α -G_{i-2} phosphorylation examined.

4.3 Results

4.3.1 Effects of insulin on α -G_{i-2} phosphorylation - time course and dose response

Hepatocytes were labelled to isotopic equilibrium with ³²P and challenged with insulin. The methods used for hepatocyte preparation and α -G_{i-2} isolation are as detailed in sections 2.2.2 to 2.2.5.

Figure 4.1 shows a typical autoradiograph of a gel from a time course experiment where the cells were exposed to insulin (10 μ M) for 0, 2, 5, 10 and 15 minutes. As can be seen there was phosphorylation of α -G_{i-2} at 0 minutes (control, basal labelling) and that insulin caused a time-dependent decrease in the ³²P labelling of the protein with a maximum effect at around 5 minutes (see table 4.1 and figure 4.2), where upon a new steady state of labelling of α -G_{i-2} was achieved. This state then persisted for a further ten minutes.

Examination of the dose response of insulin induced inhibition of α -G_{i-2} phosphorylation using a concentration range of 10⁻¹² M to 10⁻⁵ M showed that after 15 minutes incubation that concentrations from 10⁻⁹ M to 10⁻⁵ M significantly inhibited the phosphorylation of α -G_{i-2}, when compared to control (0%), with a maximum inhibition occurring at 10⁻⁸ M (see table 4.2 and figures 4.3 and 4.4).

In all subsequent experiments insulin was used at a concentration of 10⁻⁵ M and with a 15 minute incubation.

4.3.2 Examination of ligand mediated phosphorylation of rat hepatocyte α -G_{i-2} and the effect of insulin

Isolated Sprague Dawley rat hepatocytes were incubated with a range of compounds that stimulated or inhibited different aspects of the secondary messenger systems (see section 1.1).

Table 4.1: Time course of percentage insulin (10 μ M) induced phosphorylation of α -G_{i-2} in Sprague Dawley rat hepatocytes.

Time (min)	Mean	SEM	n=	p=	Sig. Diff.
0	0	0	4		N
2	-12	2	4	0.016	Y
5	-21	2	4	0.004	Y
10	-18	4	4	0.032	Y
15	-23	5	4	0.031	Y

Control, 0 minutes, was taken as 0 % phosphorylation; SEM = standard error of mean; n = number of observations; p = significance value returned by single sample Student's *t*-test; Sig. Diff. = Significantly different from control (0%) by single sample Student's *t*-test, Y = significantly different ($p < 0.05$), N = not significantly differently different ($p > 0.05$).

Table 4.2: Induced levels of α -G_{i-2} phosphorylation by insulin in Sprague Dawley rat hepatocytes.

Log Ins Conc (M)	Mean	SEM	n=	p=	Sig. Diff.
-12	-0	4	4	0.972	N
-11	-3	4	4	0.601	N
-10	-4	2	4	0.235	N
-9	-12	4	3	0.050	Y
-8	-14	6	3	0.049	Y
-7	-12	5	4	0.044	Y
-6	-17	6	3	0.032	Y
-5	-17	3	18	0.007	Y

Control, no insulin, was taken as 0 %; Log Ins Conc (M) = logarithm of the concentration of insulin; SEM = Standard error of mean; n = number of observations; p = significance value returned by single sample Student's *t*-test; Sig. Diff. = significant difference by one sample Student's *t*-test, Y = significantly different ($p < 0.05$), N = not significantly different ($p > 0.05$)

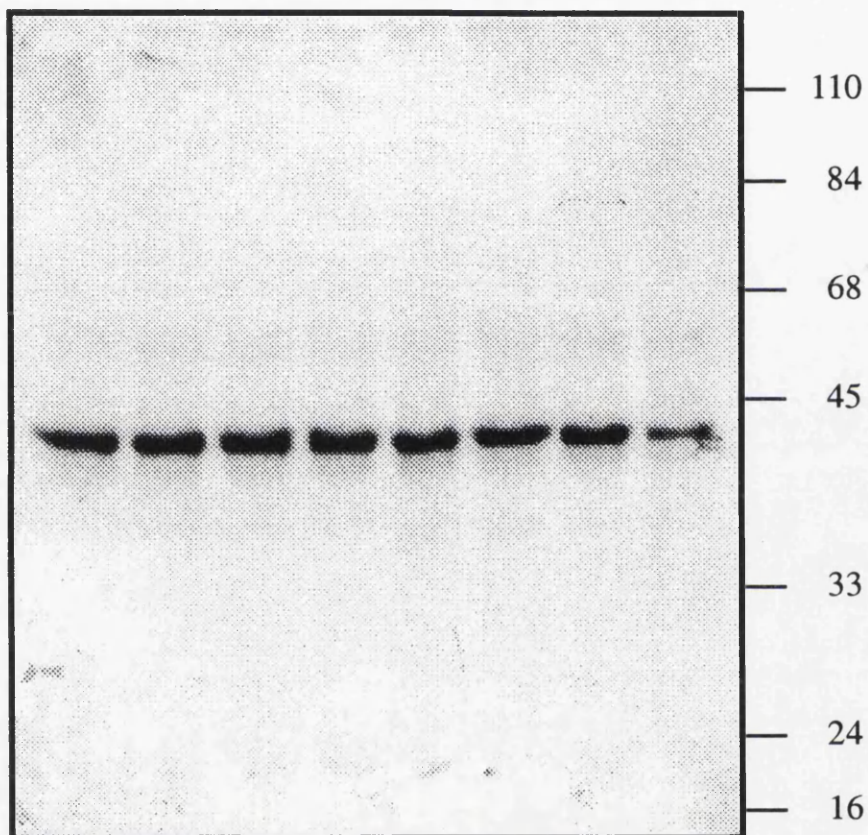
To stimulate cAMP-dependent phosphorylation of α -G_{i-2} both 8-bromo-cAMP (300 μ M), forskolin (100 μ M; see section 1.2.3.1) and glucagon (10 nM; see section 4.1.2) were used. It was found that all the compounds caused a significant increase in the ³²P labelling of α -G_{i-2}, when compared to control (0%; see figures 4.6 and 4.8; see table 4.3).

PKC (see section 1.2.4.2) mediated phosphorylation of α -G_{i-2} was stimulated by the phorbol ester PMA (100 ng/ml; see section 1.2.4.2) and again a significantly increase in the incorporation of ³²P into α -G_{i-2} was observed (see figure 4.6 and table 4.3).

Figure 4.1: Typical insulin time course auto-radiograph

Hepatocytes were labelled with ^{32}P (see sections 2.2.2 and 2.2.3) and then challenged with insulin ($10\ \mu\text{M}$) for 0, 2, 5, 10 and 15 minutes. The hepatocytes were harvested and $\alpha\text{-Gi-2}$ immunoprecipitated with antiserum 1867. The proteins were separated by SDS-PAGE (see sections 2.2.4 and 2.2.5) and the resulting gels dried and put down for autoradiography (see section 2.2.5). The figure shows a typical auto-radiograph from one of four separate experiments. Lanes 1 and 2 are the control (0 minutes) sample; lanes 3 and 4, 2 minutes; lanes 5 and 6, 5 minutes; lane 7, 10 minutes and lane 8, 15 minutes.

1 2 3 4 5 6 7 8



The inclusion of insulin with 8-bromo-cAMP and PMA no longer produced a phosphorylation of α -G_{i-2} that was significantly different from control (0%) although inclusion of glucagon did (see figure 4.6 and table 4.3). Comparison of ligand and ligand plus insulin data, where the ligand-only data were taken as the control, showed insulin only significantly affected glucagon mediated phosphorylation, where it caused an enhancement of the level of phosphorylation (see figure 4.7 and table 4.4).

To examine further cAMP-dependent phosphorylation of α -G_{i-2} hepatocytes were incubated with different combinations of forskolin (see section 1.2.3.1), IBMX (see section 1.2.3.1), and insulin (10 μ M). It was found that the inclusion of forskolin or IBMX in the incubation caused a significant increase in the phosphorylation of rat hepatocyte α -G_{i-2} (see figure 4.8 and table 4.3); the addition of both forskolin and IBMX again caused an increase in the level of phosphorylation but, although it was significantly different from control (0%), it was not significantly different from either the forskolin or IBMX-only stimulations (see figures 4.8 and 4.9, and tables 4.3 and 4.4). The addition of insulin and forskolin or IBMX to the hepatocytes caused an inhibition of the phosphorylation of α -G_{i-2} which was significantly different from the ligand-only values (see figure 4.9 and table 4.4), and the data also showed that insulin had no effect when both forskolin and IBMX stimulated the phosphorylation of α -G_{i-2} (see figure 4.9 and table 4.4).

As the agents 8-bromo-cAMP and forskolin both stimulated the phosphorylation of α -G_{i-2} this suggested that the process maybe either mediated by PKA (see section 1.2.4.1) or by some undefined cAMP-dependent mechanism. In addition, the inhibitory effects of insulin, both on stimulated and basal phosphorylations, indicated that it may be acting by either inhibiting a kinase or stimulating a phosphatase (see section 1.2.4). To examine these effects experiments were carried out using a compound called HA1004 (see section 1.2.4.1) which is known to inhibit PKA. Incubation of ³²P labelled hepatocytes with HA1004 (1 μ M) showed that HA1004 could significantly inhibit basal phosphorylation of α -G_{i-2} but did not significantly affect forskolin stimulated phosphorylation of α -G_{i-2} (see figures 4.10 and 4.11, and tables 4.3 and 4.4). Incubation of hepatocytes with both insulin and HA1004 did not produce an additive effect and left the phosphorylation at basal levels (see figures 4.10 and 4.11, and tables 4.3 and 4.4).

To examine whether insulin inhibition of α -G_{i-2} phosphorylation was by the inhibition of a kinase or the activation of a phosphatase, okadaic acid (1 μ M; see section 1.2.4.3), which is an inhibitor of phosphatases 1 and 2A, was used. It was found that the inclusion of okadaic acid in the incubation caused a significant increase in the phosphorylation of α -G_{i-2} (see figure 4.12 and table 4.3) and that the inclusion of insulin had no effect on this (see figures 4.12 and 4.13; tables 4.3 and 4.4).

The ability of okadaic acid to inhibit phosphatase activity was also used to examine the phorbol ester mediated phosphorylation of rat hepatocyte α -G_{i-2}. PMA (see section 1.2.4.2) and okadaic acid have already been shown to stimulate the phosphorylation

Table 4.3: Percentage stimulation of the phosphorylation of α -G_{i-2} in Sprague Dawley rat hepatocytes.

	Mean	SEM	n=	p=	Sig Diff
Forskolin (100 μ M)	42	9	5	0.010	Y
Insulin (Ins; 10 μ M)	-17	3	18	0.000	Y
IBMX (100 μ M)	46	12	4	0.035	Y
Forskolin (100 μ M) + Insulin (10 μ M)	2	20	5	0.930	N
Forskolin (100 μ M) + IBMX (100 μ M)	34	12	4	0.049	Y
Insulin (10 μ M) + IBMX (100 μ M)	10	5	4	0.210	N
For (100 μ M)+Ins (10 μ M)+IBMX (100 μ M)	39	10	3	0.048	Y
HA1004 (1 μ M)	-16	2	4	0.004	Y
Forskolin (100 μ M) + HA1004 (1 μ M)	-8	22	4	0.772	N
Insulin (10 μ M) + HA1004 (1 μ M)	-42	27	3	0.267	N
PMA (100 ng/ml)	23	4	12	0.000	Y
Okadaic acid (OA; 1 μ M)	112	33	5	0.028	Y
PMA (100 ng/ml) + Insulin (10 μ M)	12	7	10	0.145	N
PMA (100 ng/ml) + Okadaic acid (1 μ M)	85	18	4	0.020	Y
PMA (100 ng/ml) + Ins (10 μ M)+ OA (1 μ M)	97	29	4	0.046	Y
8-bromo-cAMP (8BrcAMP; 300 μ M)	93	12	10	0.000	Y
8BrcAMP (300 μ M) + Insulin (10 μ M)	28	9	3	0.086	N
Okadaic acid (1 μ M) + Insulin (10 μ M)	111	15	4	0.005	Y
Glucagon (Gluc; 10 nM)	37	13	6	0.038	Y
Glucagon (10 nM) + Insulin (10 μ M)	33	3	5	0.001	Y
Amylin (Amy; 1 μ M)	17	4	5	0.011	Y
Amylin (1 μ M) + PMA (100 ng/ml)	29	4	4	0.007	Y
Amylin (1 μ M) + Glucagon (10 nM)	19	8	5	0.090	N
Insulin (10 μ M) + Amylin (1 μ M)	26	5	5	0.007	Y
Amy (1 μ M)+Ins (10 mM)+Gluc (10 nM)	6	16	6	0.709	N

Control was taken as 0 % phosphorylation; SEM = Standard error of mean; n = number of observations; p = significance value returned by single sample Student's *t*-test; Sig Diff = Significantly different by single sample Student's *t*-test from control (0%), Y = significantly different ($p < 0.05$), N = not significantly different ($p > 0.05$); IBMX = 3-isobutyl-1-methylxanthine; For = Forskolin; HA1004 = N - (2'-guanidinoethyl) - 5 - isoquinoline - sulfonamide; Ins = Insulin; PMA = Phorbol 12-myristate 13-acetate; OA = Okadaic acid; 8BrcAMP = 8-bromo-cAMP; Gluc = Glucagon; Amy = Amylin

Figure 4.2: Time course of insulin induced phosphorylation of α -G_{i-2}

Time course of insulin induced phosphorylation of α -G_{i-2} from Sprague Dawley rat hepatocytes labelled with ³²P (see sections 2.2.2 and 2.2.3) and then challenged with 10 μ M insulin for 0, 2, 5, 10 and 15 minutes. The hepatocytes were harvested and α -G_{i-2} immunoprecipitated with antiserum 1867. The proteins were separated by SDS-PAGE (see sections 2.2.4 and 2.2.5) and the resulting gels dried and put down for autoradiography (see section 2.2.5). The level of phosphorylation achieved was determined by Cerenkov counting of gel chips that contained phosphorylated α -G_{i-2}. The results are expressed as mean \pm SEM (n = 4; see table 4.2). All points are significantly different (p<0.05, single sample Student's *t*-test) from control (0 minutes, 0%) although points at 2, 5, 10 and 15 minutes are not significantly different from each other.

Time course of insulin induced phosphorylation of alpha-Gi-2 in Sprague Dawley rat hepatocytes

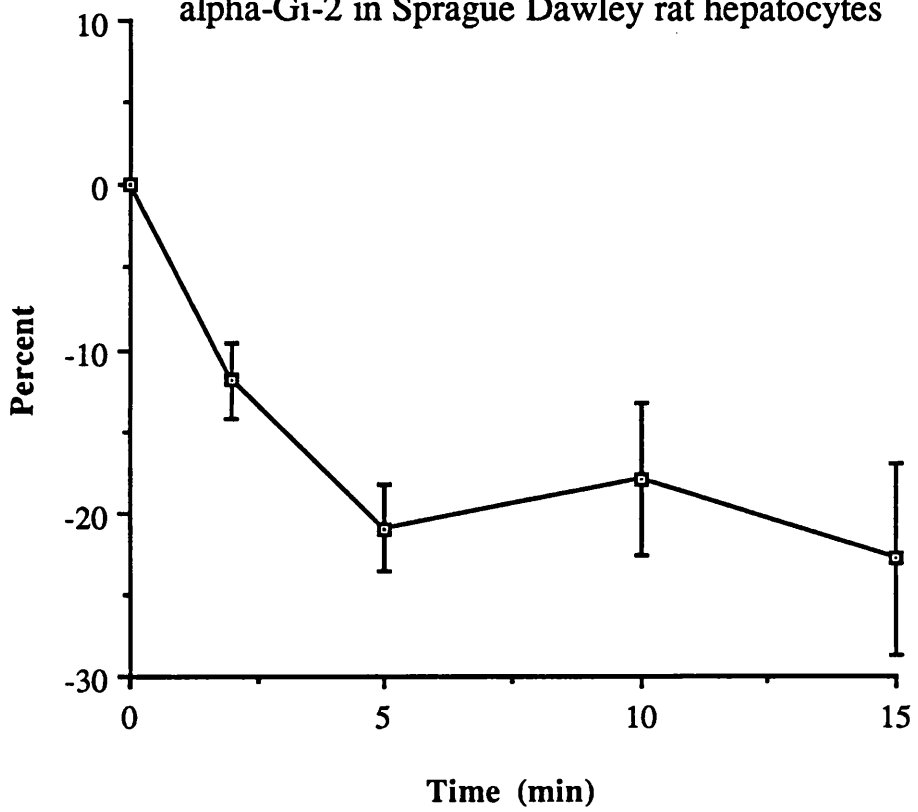


Figure 4.3: Typical insulin dose response curve auto-radiograph

A typical insulin dose response curve auto-radiograph. Sprague Dawley rat hepatocytes were labelled with ^{32}P (see sections 2.2.2 and 2.2.3) and were challenged with insulin (10^{-12} to 10^{-5} M) for 15 minutes. The hepatocytes were harvested and $\alpha\text{-G}_{i-2}$ immunoprecipitated with antiserum 1867. The proteins were separated by SDS-PAGE (see sections 2.2.4 and 2.2.5) and the resulting gels dried and put down for autoradiography (see section 2.2.5). Lane 1 contains the control sample (no insulin); lane 2, insulin 10^{-12} M; lane 3, insulin 10^{-11} M; lane 4, insulin 10^{-10} M; lane 5, insulin 10^{-9} M; lane 6, insulin 10^{-8} M; lane 7, insulin 10^{-7} M; lane 8, insulin 10^{-6} M; lane 9, insulin 10^{-5} M; and lane 10, another control (no insulin).

Figure 4.4: Dose response curve for the insulin induced phosphorylation of α -G_{i-2} in Sprague Dawley rat hepatocytes

Dose response curve for the insulin induced phosphorylation of α -G_{i-2} in Sprague Dawley rat hepatocytes labelled with ³²P (see sections 2.2.2 and 2.2.3) and then challenged with insulin (10⁻¹² to 10⁻⁵ M) for 15 minutes. The hepatocytes were harvested and α -G_{i-2} immunoprecipitated with antiserum 1867. The proteins were separated by SDS-PAGE (see sections 2.2.4 and 2.2.5) and the resulting gels dried and put down for autoradiography (see section 2.2.5). The level of phosphorylation achieved was determined by Cerenkov counting of gel chips that contained phosphorylated α -G_{i-2}. The data are expressed as mean \pm SEM (n \geq 4; see table 4.2) where * indicates that the data are significantly different (p<0.05) from control (0%) with data tested using a single sample Student's *t*-test.

Dose response curve for insulin induced phosphorylation of alpha-Gi-2 in Sprague Dawley rat hepatocytes

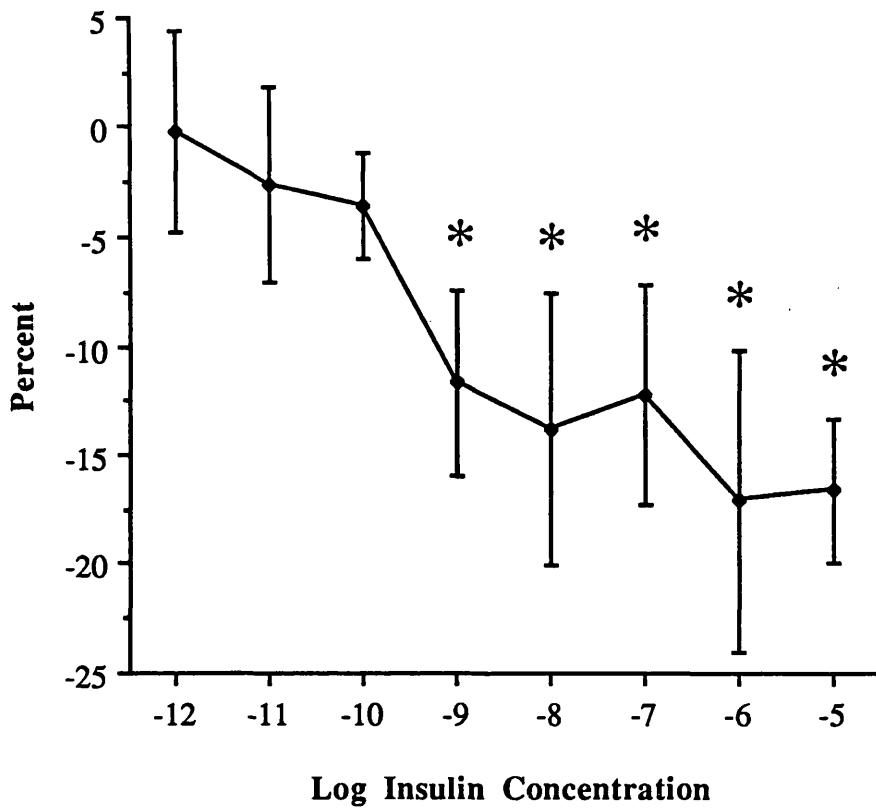


Figure 4.5: A typical auto-radiograph of ^{32}P phosphorylated $\alpha\text{-G}_{i-2}$ from Sprague Dawley rat hepatocytes that have been challenged with vehicle solution, 8-bromo-cAMP, PMA, glucagon, insulin, 8-bromo-cAMP and insulin, glucagon and insulin, PMA and insulin, and vehicle solution

A typical auto-radiograph of an SDS-PAGE gel containing $\alpha\text{-G}_{i-2}$ immunoprecipitated from rat hepatocytes that had been labelled with ^{32}P (see sections 2.2.2 and 2.2.3) and then challenged with vehicle solution (lane 1), 8-bromo-cAMP (lane 2; 300 μM), PMA (lane 3; 100 ng/ml), glucagon (lane 4; 10 nM), insulin (lane 5; 10 μM), 8-bromo-cAMP and insulin (lane 6), glucagon and insulin (lane 7), PMA and insulin (lane 8), and vehicle solution (lane 9) for 15 minutes. Where the hepatocytes were challenged with a ligand and insulin, the insulin was added first followed immediately by the ligand.

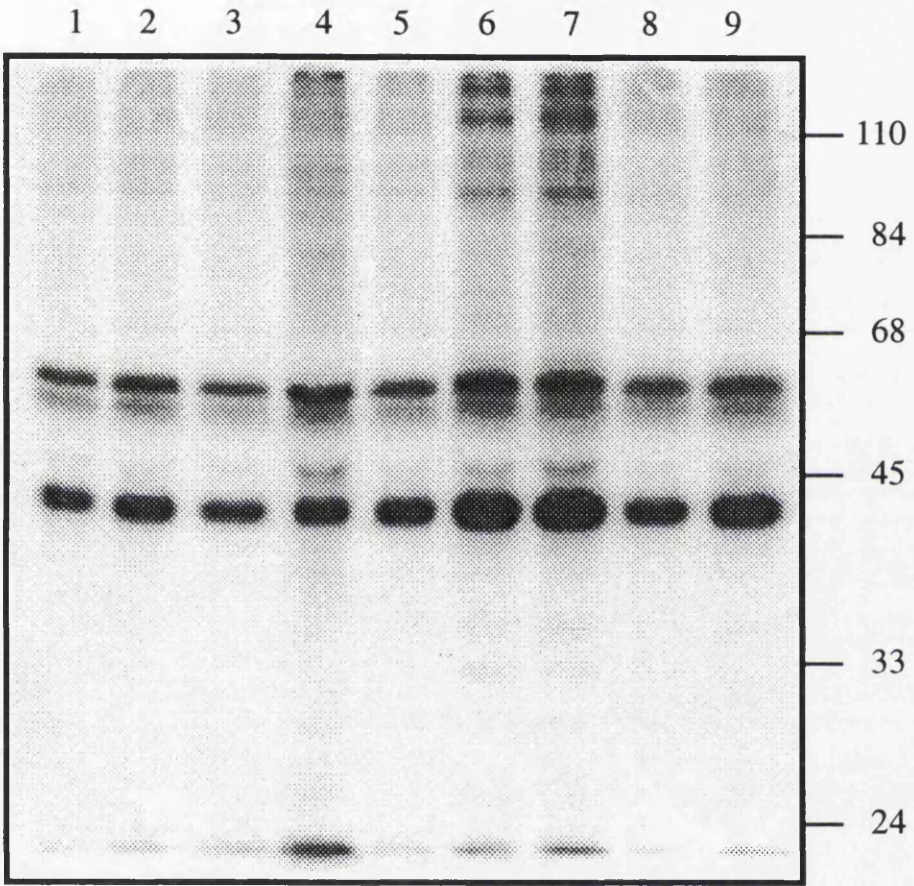


Figure 4.6: Percentage phosphorylation of α -G_{i-2} in Sprague Dawley rat hepatocytes: Effects of 8-bromo-cAMP, PMA, glucagon, and insulin

Stimulation of α -G_{i-2} phosphorylation in Sprague Dawley rat hepatocytes labelled with ³²P (see sections 2.2.2 and 2.2.3) and then challenged with 8-bromo-cAMP (8BrcAMP; 300 μ M), PMA (100 ng/ml), glucagon (Gluc; 10 nM), and insulin (Ins; 10 μ M) for 15 minutes. Where the hepatocytes were challenged with a ligand and insulin, the insulin was added first followed immediately by the ligand. The hepatocytes were harvested and α -G_{i-2} immunoprecipitated with antiserum 1867. The proteins were separated by SDS-PAGE (see sections 2.2.4 and 2.2.5) and the resulting gels dried and put down for autoradiography (see section 2.2.5). The level of phosphorylation achieved was determined by Cerenkov counting of gel chips that contained phosphorylated α -G_{i-2}. The data are expressed as mean \pm SEM (n \geq 4; see table 4.3) where * indicates that the data are significantly different (p<0.05) from control (0%) with data tested using a single sample Student's *t*-test.

Figure 4.7: Percentage inhibition of ligand induced α -G_{i-2} phosphorylation in Sprague Dawley rat hepatocytes: Effects of insulin on 8-bromo-cAMP, PMA and glucagon induced phosphorylations

Insulin induced inhibition of ligand induced α -G_{i-2} phosphorylation in Sprague Dawley rat hepatocytes labelled with ³²P (see sections 2.2.2 and 2.2.3). The hepatocytes were challenged with 8-bromo-cAMP (8Br; 300 μ M), PMA (100 ng/ml), glucagon (Gluc; 10 nM), insulin (Ins; 10 μ M) for 15 minutes in the presence and absence of insulin (Ins; 10 μ M). The hepatocytes were harvested and α -G_{i-2} immunoprecipitated with antiserum 1867. The proteins were separated by SDS-PAGE (see sections 2.2.4 and 2.2.5) and the resulting gels dried and put down for autoradiography (see section 2.2.5). The level of phosphorylation achieved was determined by Cerenkov counting of gel chips that contained phosphorylated α -G_{i-2}. The data are expressed as mean \pm SEM (n \geq 4; see table 4.4) where * indicates that the data are significantly different (p<0.05) from control (ligand in the absence of insulin, 0%) with data tested using a single sample Student's *t*-test.

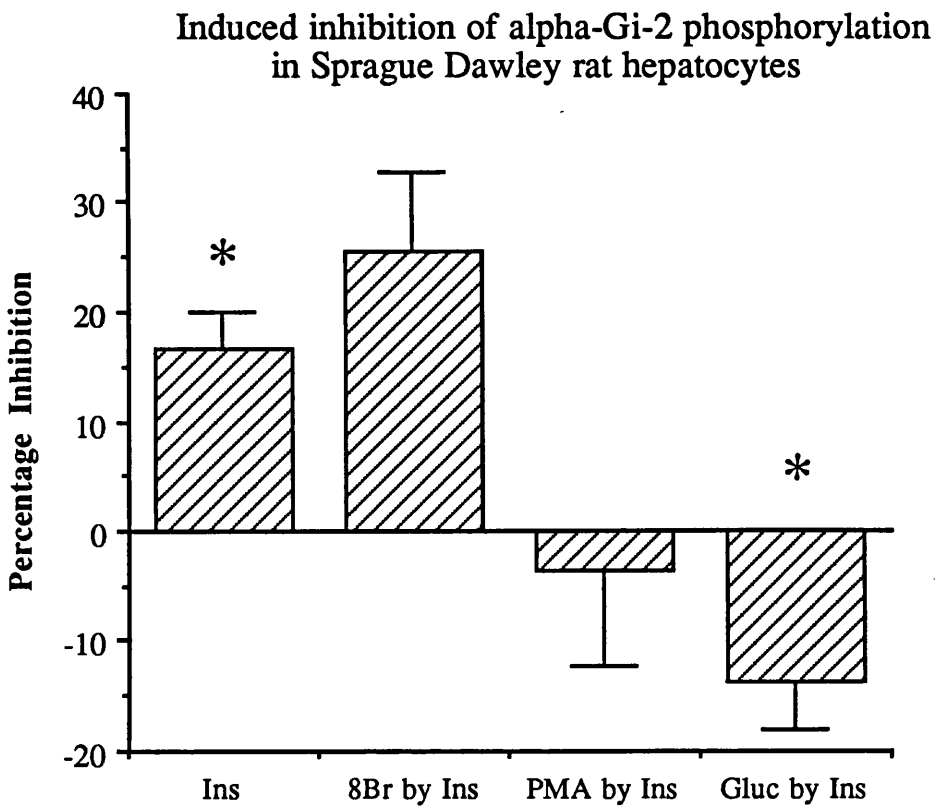
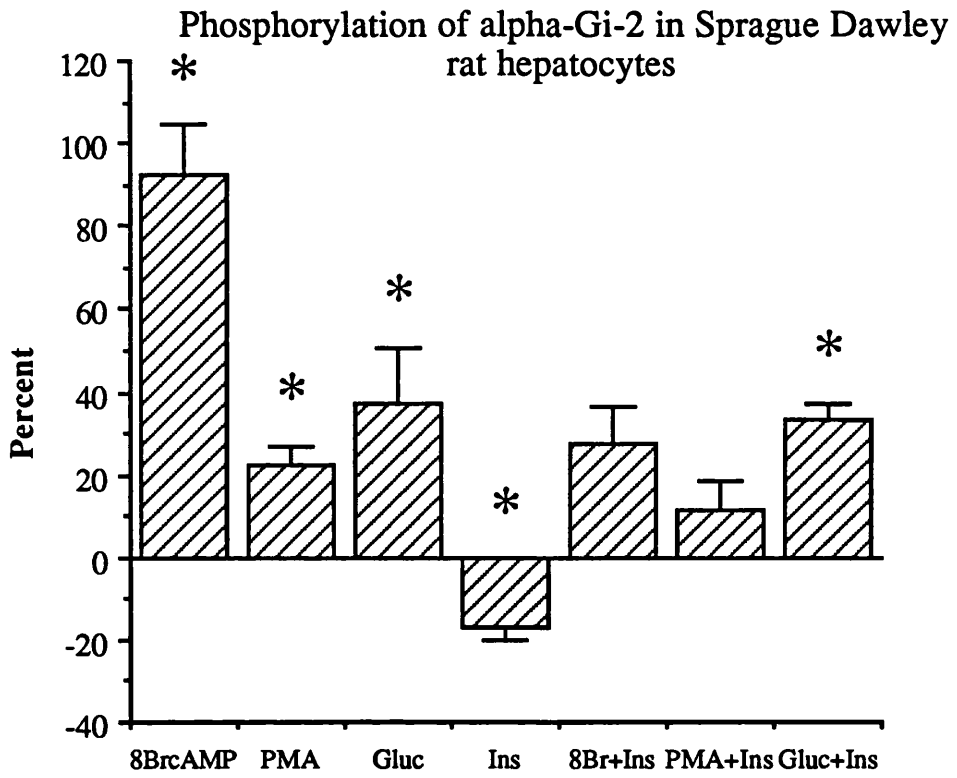


Figure 4.8: Percentage phosphorylation of α -G_{i-2} in Sprague Dawley rat hepatocytes: Effects of forskolin, IBMX, and insulin

Stimulation of α -G_{i-2} phosphorylation in Sprague Dawley rat hepatocytes labelled with ³²P (see sections 2.2.2 and 2.2.3) and then challenged with forskolin (For; 100 μ M), IBMX (100 μ M), and insulin (Ins; 10 μ M) for 15 minutes. Where the hepatocytes were challenged with two or more ligands the ligands were added at the same time. The hepatocytes were harvested and α -G_{i-2} immunoprecipitated with antiserum 1867. The proteins were separated by SDS-PAGE (see sections 2.2.4 and 2.2.5) and the resulting gels dried and put down for autoradiography (see section 2.2.5). The level of phosphorylation achieved was determined by Cerenkov counting of gel chips that contained phosphorylated α -G_{i-2}. The data are expressed as mean \pm SEM (n \geq 4; see table 4.3) where * indicates that the data are significantly different (p<0.05) from control (0%) with data tested using a single sample Student's *t*-test.

Figure 4.9: Percentage inhibition of ligand induced α -G_{i-2} phosphorylation in Sprague Dawley rat hepatocytes: Effects of insulin or IBMX on forskolin, and IBMX induced phosphorylations

Insulin induced inhibition of ligand induced α -G_{i-2} phosphorylation in Sprague Dawley rat hepatocytes labelled with ³²P (see sections 2.2.2 and 2.2.3). The hepatocytes were challenged with forskolin (For; 100 μ M), IBMX (100 μ M), and insulin (Ins; 10 μ M) for 15 minutes. Where the hepatocytes were challenged with two or more ligands the ligands were added at the same time. The hepatocytes were harvested and α -G_{i-2} immunoprecipitated with antiserum 1867. The proteins were separated by SDS-PAGE (see sections 2.2.4 and 2.2.5) and the resulting gels dried and put down for autoradiography (see section 2.2.5). The level of phosphorylation achieved was determined by Cerenkov counting of gel chips that contained phosphorylated α -G_{i-2}. The data are expressed as mean \pm SEM (n \geq 4; see table 4.4) where * indicates that the data are significantly different (p<0.05) from control (ligand only, 0%) with data tested using a single sample Student's *t*-test.

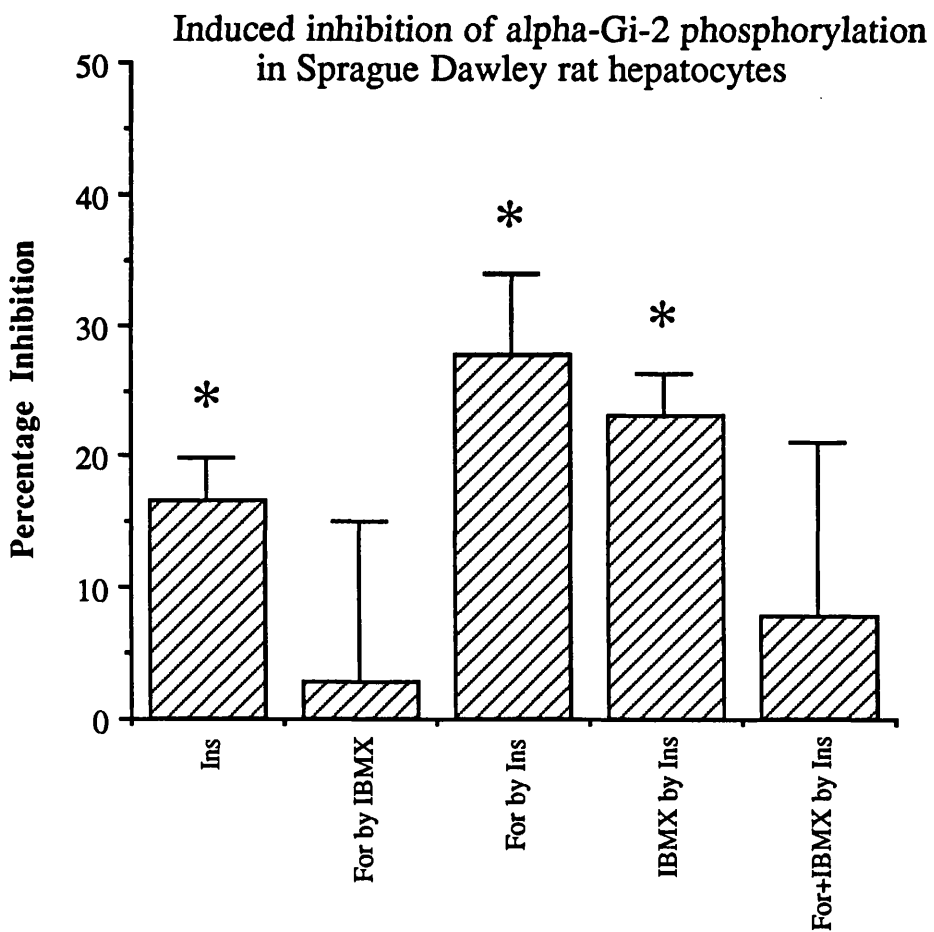
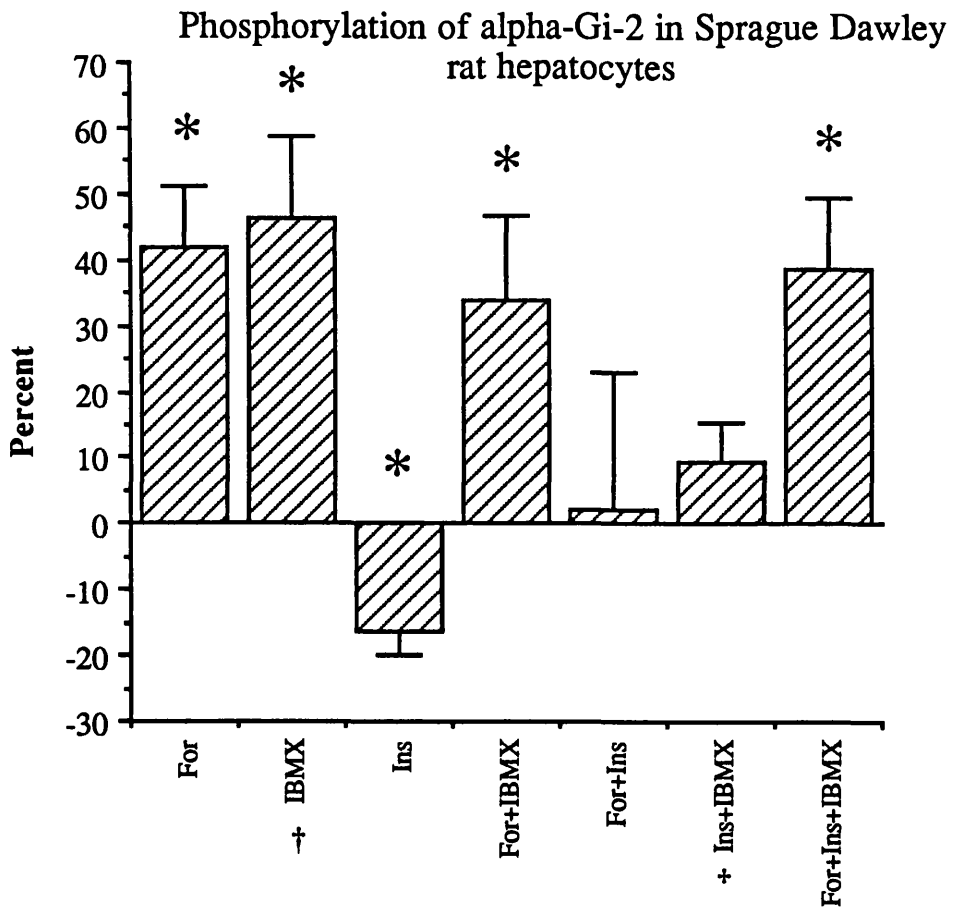


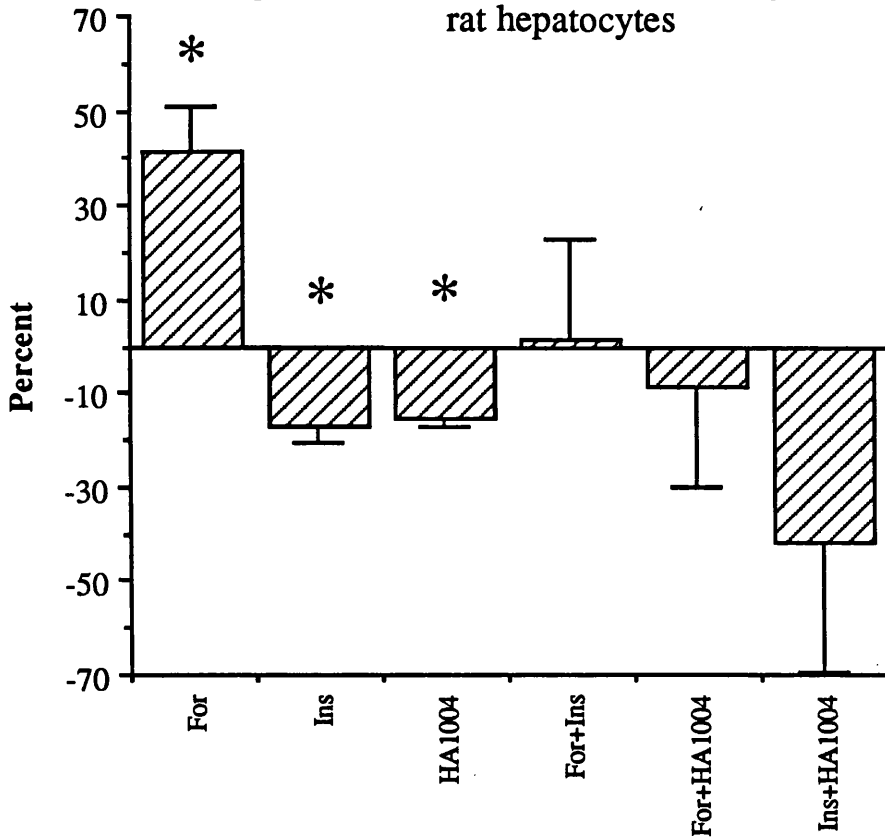
Figure 4.10: Percentage phosphorylation of α -G_{i-2} in Sprague Dawley rat hepatocytes: Effects of forskolin, HA1004, and insulin

Stimulation of α -G_{i-2} phosphorylation in Sprague Dawley rat hepatocytes labelled with ³²P (see sections 2.2.2 and 2.2.3) and then challenged with forskolin (For; 100 μ M), insulin (Ins; 10 μ M) and HA1004 (1 μ M) for 15 minutes. Where the hepatocytes were challenged with two or more ligands the ligands were added at the same time. The hepatocytes were harvested and α -G_{i-2} immunoprecipitated with antiserum 1867. The proteins were separated by SDS-PAGE (see sections 2.2.4 and 2.2.5) and the resulting gels dried and put down for autoradiography (see section 2.2.5). The level of phosphorylation achieved was determined by Cerenkov counting of gel chips that contained phosphorylated α -G_{i-2}. The data are expressed as mean \pm SEM (n \geq 4; see table 4.3) where * indicates that the data are significantly different (p<0.05) from control (0%) with data tested using a single sample Student's *t*-test.

Figure 4.11: Percentage inhibition of ligand induced α -G_{i-2} phosphorylation in Sprague Dawley rat hepatocytes: Effects of insulin or HA1004, on forskolin and HA1004 induced phosphorylations

Insulin induced inhibition of ligand induced α -G_{i-2} phosphorylation in Sprague Dawley rat hepatocytes labelled with ³²P (see sections 2.2.2 and 2.2.3). The hepatocytes were challenged with forskolin (For; 100 μ M), insulin (Ins; 10 μ M) and HA1004 (1 μ M) for 15 minutes. Where the hepatocytes were challenged with two or more ligands the ligands were added at the same time. The hepatocytes were harvested and α -G_{i-2} immunoprecipitated with antiserum 1867. The proteins were separated by SDS-PAGE (see sections 2.2.4 and 2.2.5) and the resulting gels dried and put down for autoradiography (see section 2.2.5). The level of phosphorylation achieved was determined by Cerenkov counting of gel chips that contained phosphorylated α -G_{i-2}. The data are expressed as mean \pm SEM (n \geq 4; see table 4.4) where * indicates that the data are significantly different (p<0.05) from control (ligand only, 0%) with data tested using a single sample Student's *t*-test.

Phosphorylation of alpha-Gi-2 in Sprague Dawley rat hepatocytes



Induced inhibition of alpha-Gi-2 phosphorylation in Sprague Dawley rat hepatocytes

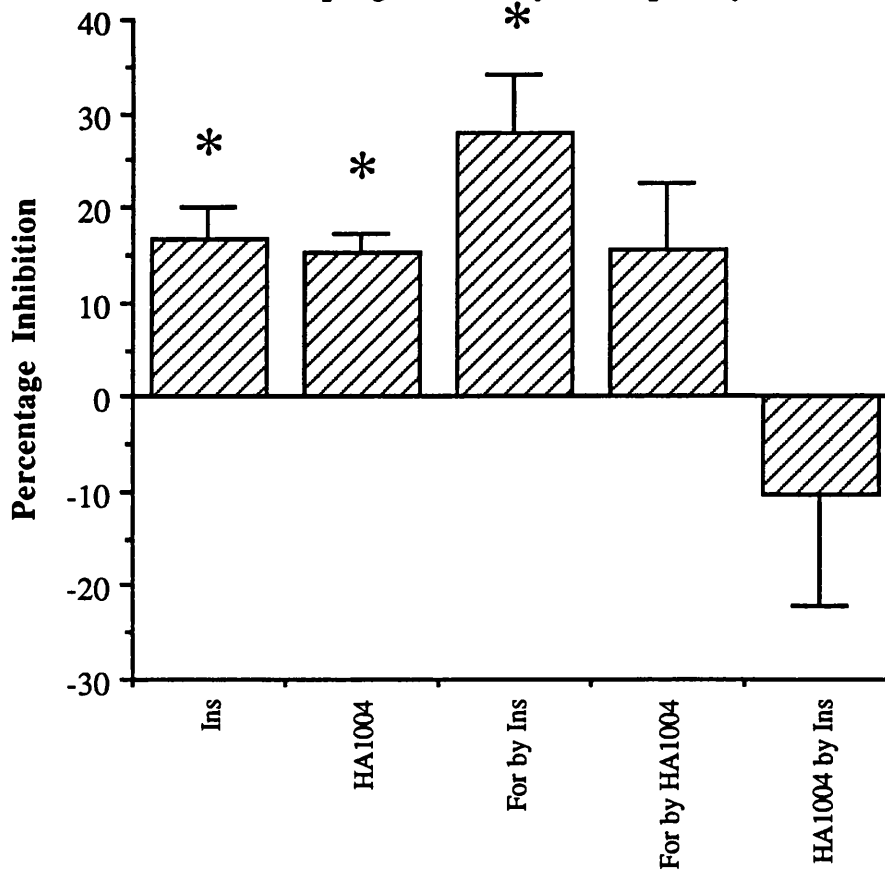


Figure 4.12: Percentage phosphorylation of α -G_{i-2} in Sprague Dawley rat hepatocytes: Effects of okadaic acid, HA1004, and insulin

Stimulation of α -G_{i-2} phosphorylation in Sprague Dawley rat hepatocytes labelled with ³²P (see sections 2.2.2 and 2.2.3) and then challenged with insulin (Ins; 10 μ M), okadaic acid (OA; 1 μ M) and HA1004 (1 μ M) for 15 minutes. Where the hepatocytes were challenged with two or more ligands the ligands were added at the same time. The hepatocytes were harvested and α -G_{i-2} immunoprecipitated with antiserum 1867. The proteins were separated by SDS-PAGE (see sections 2.2.4 and 2.2.5) and the resulting gels dried and put down for autoradiography (see section 2.2.5). The level of phosphorylation achieved was determined by Cerenkov counting of gel chips that contained phosphorylated α -G_{i-2}. The data are expressed as mean \pm SEM (n \geq 4; see table 4.3) where * indicates that the data are significantly different (p<0.05) from control (0%) with data tested using a single sample Student's *t*-test.

Figure 4.13: Percentage inhibition of ligand induced α -G_{i-2} phosphorylation in Sprague Dawley rat hepatocytes: Effects of insulin, on okadaic acid and HA1004 induced phosphorylations

Insulin induced inhibition of ligand induced α -G_{i-2} phosphorylation in Sprague Dawley rat hepatocytes labelled with ³²P (see sections 2.2.2 and 2.2.3). The hepatocytes were challenged with insulin (Ins; 10 μ M), okadaic acid (OA; 1 μ M) and HA1004 (1 μ M) for 15 minutes. Where the hepatocytes were challenged with two or more ligands the ligands were added at the same time. The hepatocytes were harvested and α -G_{i-2} immunoprecipitated with antiserum 1867. The proteins were separated by SDS-PAGE (see sections 2.2.4 and 2.2.5) and the resulting gels dried and put down for autoradiography (see section 2.2.5). The level of phosphorylation achieved was determined by Cerenkov counting of gel chips that contained phosphorylated α -G_{i-2}. The data are expressed as mean \pm SEM (n \geq 4; see table 4.4) where * indicates that the data are significantly different (p<0.05) from control (ligand only, 0%) with data tested using a single sample Student's *t*-test.

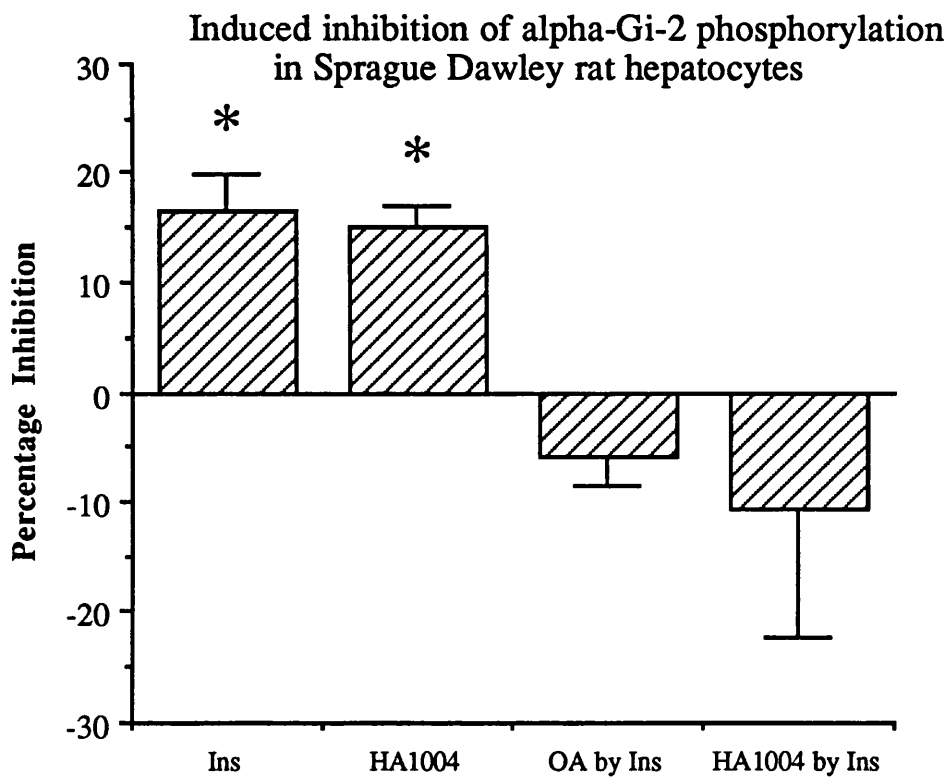
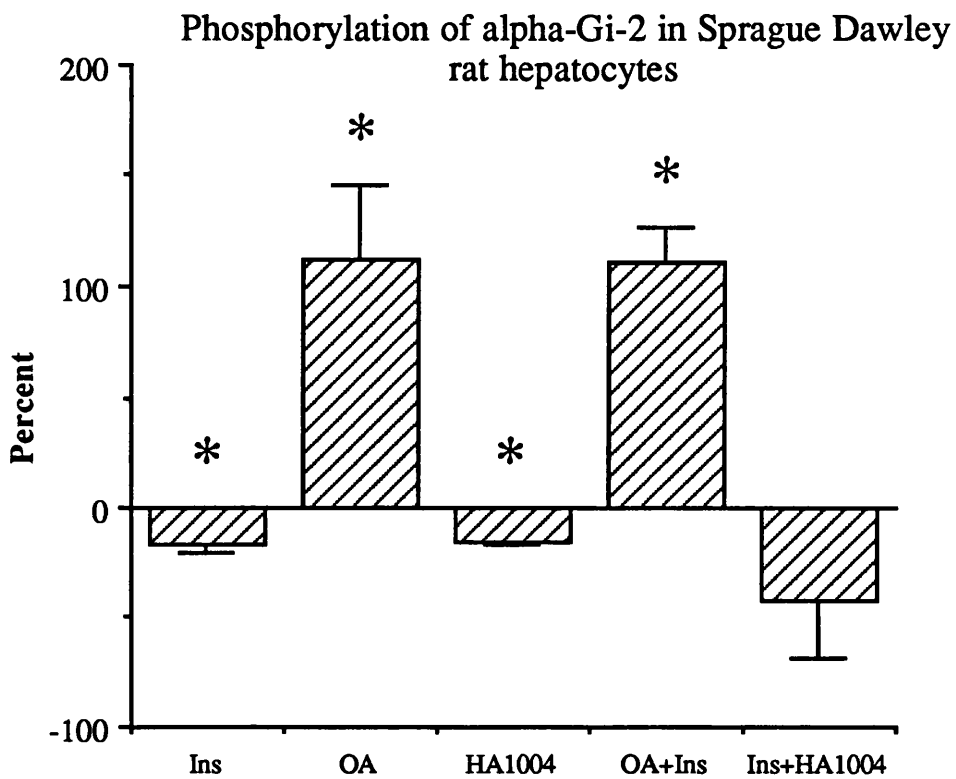


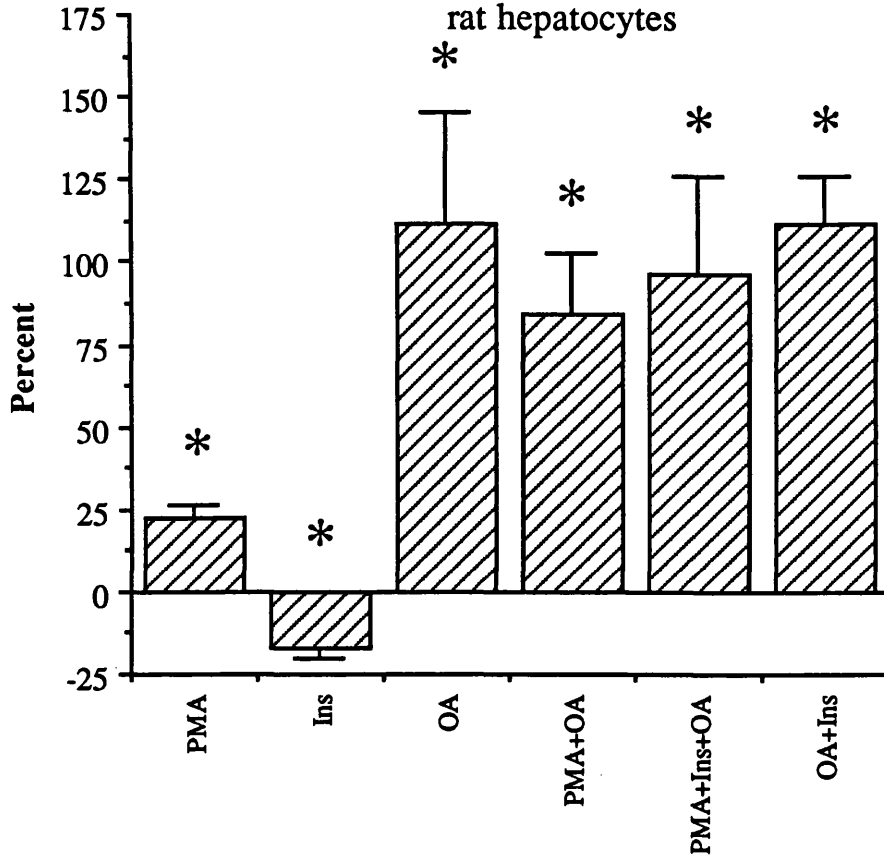
Figure 4.14: Percentage phosphorylation of α -G_{i-2} in Sprague Dawley rat hepatocytes: Effects of okadaic acid, PMA, and insulin

Stimulation of α -G_{i-2} phosphorylation in Sprague Dawley rat hepatocytes labelled with ³²P (see sections 2.2.2 and 2.2.3) and then challenged with PMA (100 ng/ml), insulin (Ins; 10 μ M), and okadaic acid (OA; 1 μ M) for 15 minutes. Where the hepatocytes were challenged with two or more ligands the ligands were added at the same time. The hepatocytes were harvested and α -G_{i-2} immunoprecipitated with antiserum 1867. The proteins were separated by SDS-PAGE (see sections 2.2.4 and 2.2.5) and the resulting gels dried and put down for autoradiography (see section 2.2.5). The level of phosphorylation achieved was determined by Cerenkov counting of gel chips that contained phosphorylated α -G_{i-2}. The data are expressed as mean \pm SEM (n \geq 4; see table 4.3) where * indicates that the data are significantly different (p<0.05) from control (0%) with data tested using a single sample Student's *t*-test.

Figure 4.15: Percentage inhibition of ligand induced α -G_{i-2} phosphorylation in Sprague Dawley rat hepatocytes: Effects of insulin or okadaic acid, on okadaic acid and PMA induced phosphorylations

Insulin induced inhibition of ligand induced α -G_{i-2} phosphorylation in Sprague Dawley rat hepatocytes labelled with ³²P (see sections 2.2.2 and 2.2.3). The hepatocytes were challenged with PMA (100 ng/ml), insulin (Ins; 10 μ M), and okadaic acid (OA; 1 μ M) for 15 minutes. Where the hepatocytes were challenged with two or more ligands the ligands were added at the same time. The hepatocytes were harvested and α -G_{i-2} immunoprecipitated with antiserum 1867. The proteins were separated by SDS-PAGE (see sections 2.2.4 and 2.2.5) and the resulting gels dried and put down for autoradiography (see section 2.2.5). The level of phosphorylation achieved was determined by Cerenkov counting of gel chips that contained phosphorylated α -G_{i-2}. The data are expressed as mean \pm SEM (n \geq 4; see table 4.4) where * indicates that the data are significantly different (p<0.05) from control (ligand only, 0%) with data tested using a single sample Student's *t*-test.

Phosphorylation of alpha-Gi-2 in Sprague Dawley rat hepatocytes



Induced inhibition of alpha-Gi-2 phosphorylation in Sprague Dawley rat hepatocytes

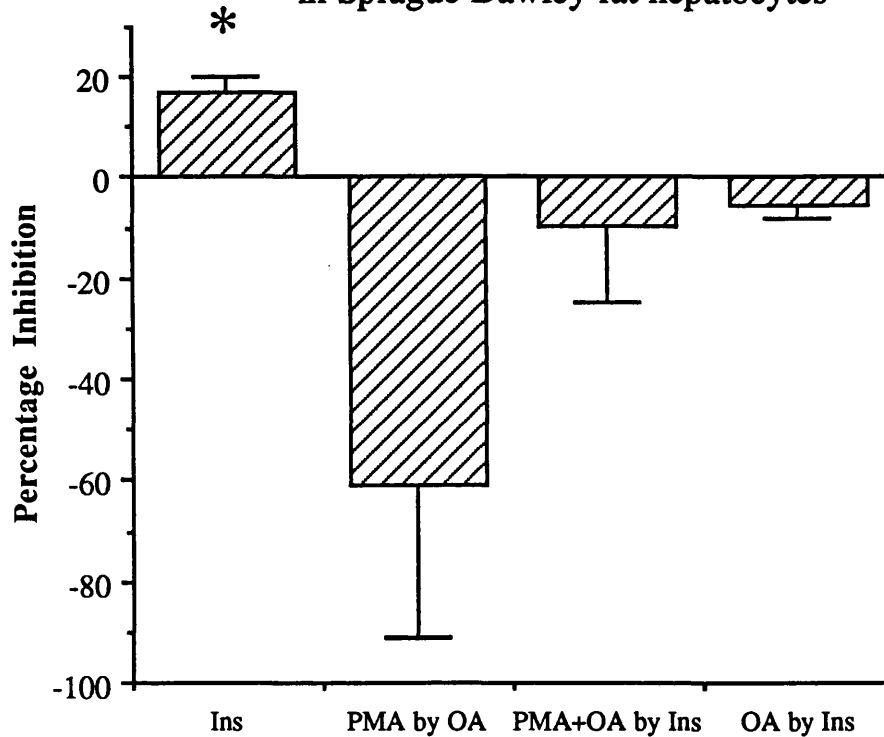


Figure 4.16: A typical auto-radiograph of immunoprecipitated α -G_{i-2} from hepatocytes from Sprague Dawley rats: Dose response for amylin, 10^{-12} to 10^{-6} M

A typical auto-radiograph of an SDS-PAGE gel containing immunoprecipitated α -G_{i-2} from hepatocytes labelled with ^{32}P (see sections 2.2.2 and 2.2.3) and then challenged with vehicle (lane 1), amylin 10^{-11} M (lane 2), amylin 10^{-10} M (lane 3), amylin 10^{-9} M (lane 4), amylin 10^{-8} M (lane 5), amylin 10^{-7} M (lane 6), amylin 10^{-6} M (lane 7), and vehicle (lane 8) for 15 minutes. The hepatocytes were harvested and α -G_{i-2} immunoprecipitated with antiserum 1867. The proteins were separated by SDS-PAGE (see sections 2.2.4 and 2.2.5) and the resulting gels dried and put down for autoradiography (see section 2.2.5).

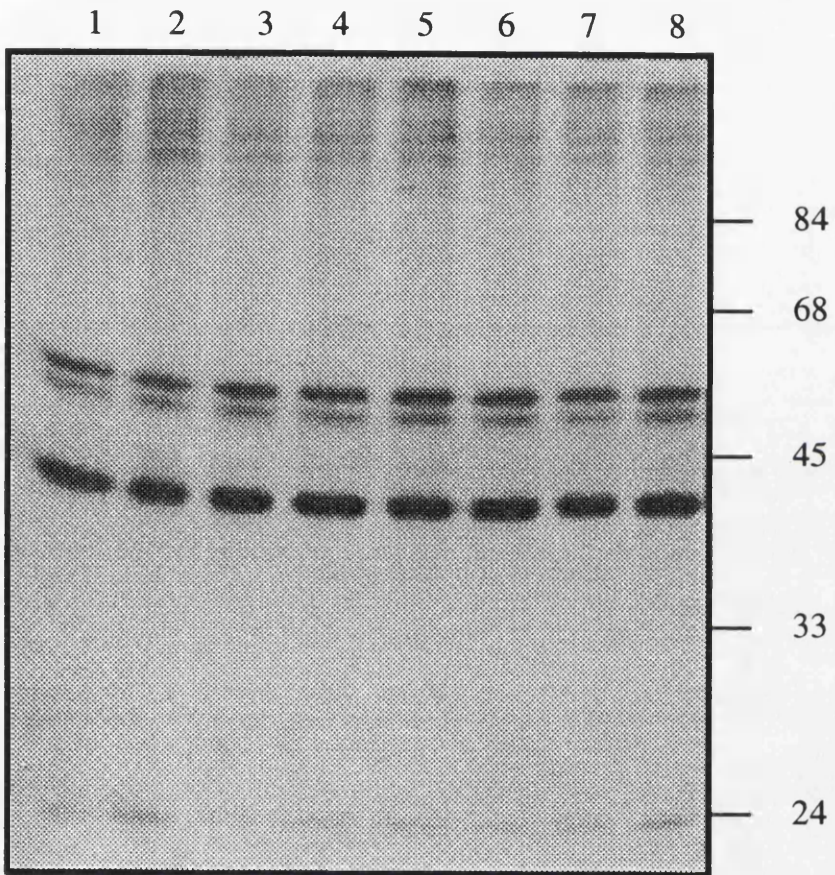
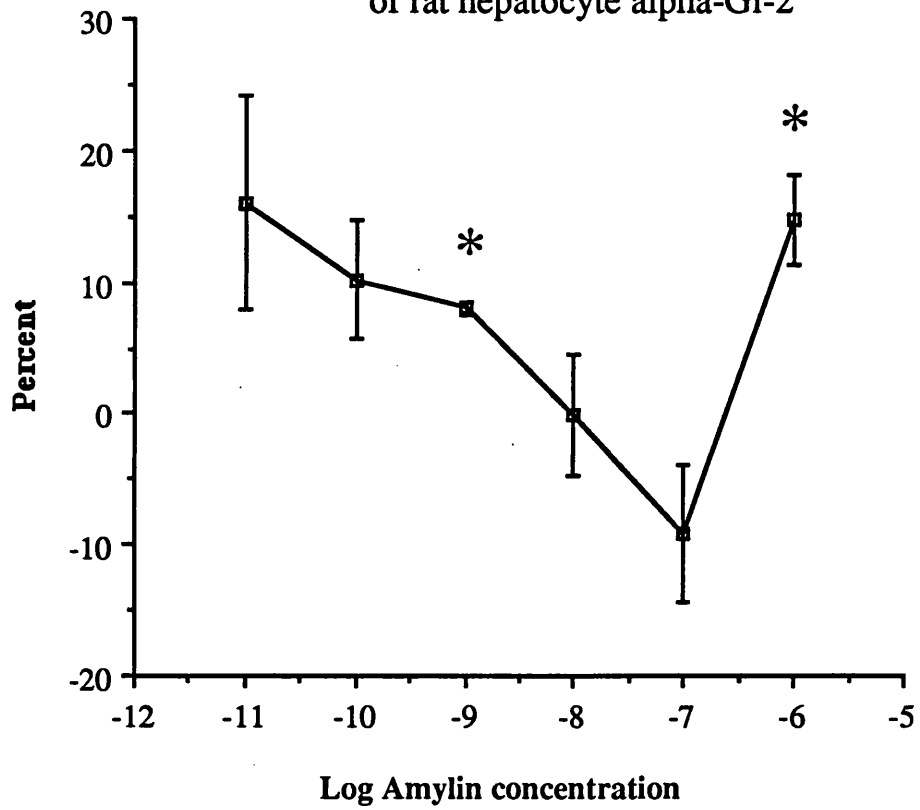


Figure 4.17: Dose response curve for the amylin induced phosphorylation of α -G_{i-2} in Sprague Dawley rat hepatocytes

Dose response curve for the amylin induced phosphorylation of α -G_{i-2} in Sprague Dawley rat hepatocytes labelled with ³²P (see sections 2.2.2 and 2.2.3) and then challenged with amylin (10⁻¹¹ to 10⁻⁶ M) for 15 minutes. The hepatocytes were harvested and α -G_{i-2} immunoprecipitated with antiserum 1867. The proteins were separated by SDS-PAGE (see sections 2.2.4 and 2.2.5) and the resulting gels dried and put down for autoradiography (see section 2.2.5). The level of phosphorylation achieved was determined by Cerenkov counting of gel chips that contained phosphorylated α -G_{i-2}. The data are expressed as mean \pm SEM (n \geq 4; see table 4.2) where * indicates that the data are significantly different (p<0.05) from control (0%) with data tested using a single sample Student's *t*-test.

Dose response curve for amylin induced phosphorylation of rat hepatocyte alpha-Gi-2



At a concentration of 1 μM amylin caused a significant increase in the level of phosphorylation of $\alpha\text{-G}_{i-2}$ when compared to control (0%; see figure 4.18). As amylin is considered to be a 'partner' of insulin, and may play a role in the insulin / glucagon control over blood glucose levels and glycogen storage (see sections 1.3.1 and 4.1.2), then the action of amylin on glucagon and insulin mediated phosphorylation events was examined.

Glucagon (10 nM) and PMA (100 ng/ml) caused an increase in the level of phosphorylation of $\alpha\text{-G}_{i-2}$, whilst insulin (10 μM) inhibited the basal and some ligand mediated phosphorylations (see section 4.3.2; figures 4.6 and 4.18, and table 4.3). The inclusion of amylin with PMA and glucagon had no significant effect (see figure 4.19 and table 4.4) but the effect of insulin on amylin induced phosphorylation of $\alpha\text{-G}_{i-2}$ was to significantly enhance it, that is amylin reversed the insulin inhibition of basal phosphorylation (see figure 4.19 and table 4.4)

4.3.4 *Effects of streptozotocin induced diabetes on the phosphorylation of $\alpha\text{-G}_{i-2}$ in Sprague Dawley rat hepatocytes*

Male Sprague Dawley rats were injected with streptozotocin (see Appendix 2) to induce a model of type I diabetes and hepatocytes were prepared as described in section 2.2.2. Experiments were then carried out to examine the effect of streptozotocin induced diabetes on the phosphorylation of $\alpha\text{-G}_{i-2}$.

It was found that in hepatocytes from diabetic animals the levels of phosphorylation induced by 8-bromo-cAMP (300 μM), PMA (100 ng/ml), glucagon (10 nM) and insulin (10 μM) were not significantly different from control (0%; see figure 4.20 and table 4.6) and the reduced levels of 8-bromo-cAMP-, PMA- and glucagon-mediated phosphorylation were significantly different from those found in non-diabetic

Table 4.5: Effects of different concentration of amylin on the phosphorylation of $\alpha\text{-G}_{i-2}$ in Sprague Dawley rat hepatocytes.

Log Amy Conc (M)	Mean	SEM	n=	p=	Sig Diff
-11	16	8	3	0.187	N
-10	10	4	3	0.154	N
-9	8	1	3	0.003	Y
-8	0	5	4	0.971	N
-7	-9	5	4	0.176	N
-6	15	3	7	0.011	Y

Control, no amylin, was taken as 0 % phosphorylation; Log Amy Conc (M) = Logarithm of the concentration of amylin; SEM = standard error of mean; p = significance value returned by single sample Student's *t*-test; n = number of observations; Sig Diff = Significance difference test, single sample Student's *t*-test, against control (0%), Y = significantly different ($p < 0.05$), N = not significantly different ($p > 0.05$)

animals (see figure 4.20 and table 4.6).

Examination of insulin-induced inhibition of ligand-mediated phosphorylation of α -G_{i-2} showed that insulin was only able to significantly inhibit 8-bromo-cAMP induced phosphorylation (see figure 4.21 and table 4.7). When these results were compared with those from non-diabetic animals (see figure 4.21 and table 4.7) it was found that, even though there had been a loss of the significant effect of insulin on glucagon-mediated phosphorylation, the change that occurred was not significant.

Table 4.6: Ligand induced percentage stimulation of the phosphorylation of α -G_{i-2} in 'normal' and 'type I' diabetic Sprague Dawley rat hepatocytes.

NORMAL							
	Mean	SEM	n=	p=	Sig Dif		
8BrcAMP	92	12	10	0.000	Y		
PMA	22	4	12	0.000	Y		
Gluc	37	13	6	0.038	Y		
Ins	-17	3	18	0.000	Y		
8Br+Ins	28	9	3	0.086	N		
PMA+Ins	12	7	10	0.145	N		
Gluc+Ins	33	4	5	0.001	Y		
TYPE I							
	Mean	SEM	n=	p=	Sig Dif	p=	Sig Dif N / T I
8BrcAMP	22	7	4	0.054	Y	0.050	Y
PMA	6	2	3	0.076	Y	0.086	Y
Gluc	-15	6	4	0.076	Y	0.015	Y
Ins	-14	6	3	0.125	Y	0.770	N
8Br+Ins	8	6	4	0.296	N	0.106	N
PMA+Ins	-8	9	4	0.122	N	0.152	N
Gluc+Ins	-2	8	4	0.826	N	0.003	N

Control was taken as 0 % phosphorylation; SEM = Standard error of mean; n = number of observations; p = significance value returned by single sample Student's *t*-test; Sig Dif = significant difference by one sample Student's *t*-test from control (0%), Y = significantly different (p<0.05), N = not significantly different (p>0.05); Sig Dif N / T I = Comparison of the significant difference by two-sample Student's *t*-test between phosphorylation events in 'normal' and 'type I' diabetic Sprague Dawley rat hepatocytes, Y = significantly different (p<0.05), N = not significantly different (p>0.05); 8Br = 8BrcAMP = 8-bromo-cAMP, 300 μ M; PMA = Phorbol 12-myristate 13-acetate, 100 ng/ml; Gluc = Glucagon, 10 nM; Ins = Insulin, 10 μ M.

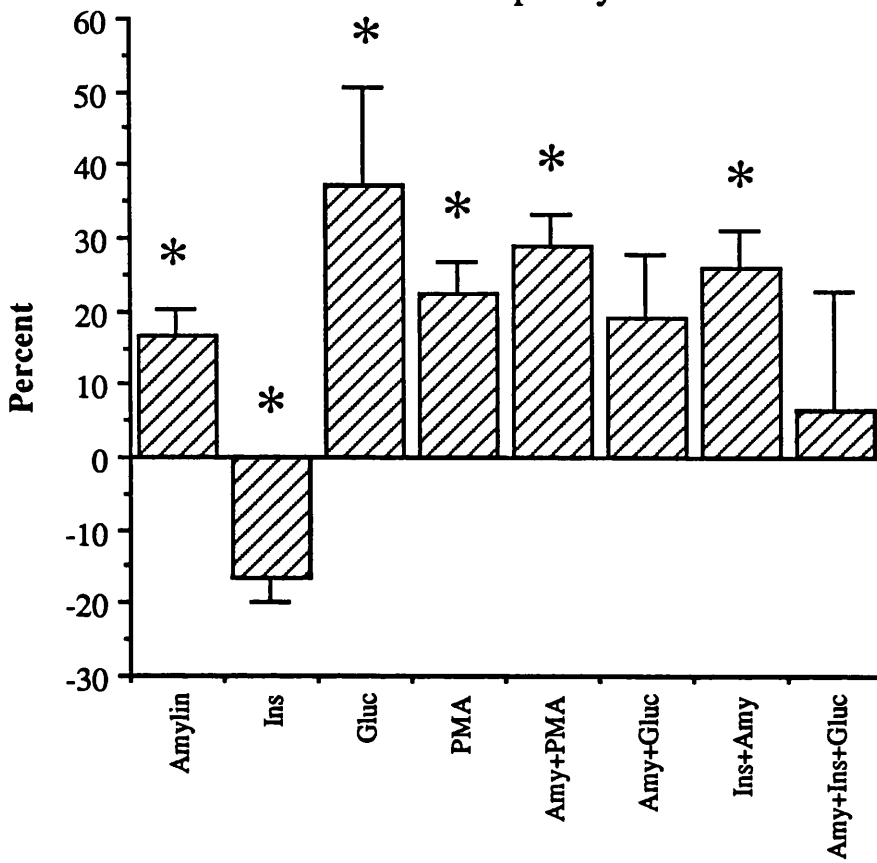
Figure 4.18: Percentage phosphorylation of α -G_{i-2} in Sprague Dawley rat hepatocytes: Effects of amylin, PMA, glucagon, and insulin

Stimulation of α -G_{i-2} phosphorylation in Sprague Dawley rat hepatocytes labelled with ³²P (see sections 2.2.2 and 2.2.3) and then challenged with amylin (Amy; 1 μ M), insulin (Ins; 10 μ M), glucagon (Gluc; 10 nM), and PMA (100 ng/ml) for 15 minutes. Where the hepatocytes were challenged with two or more ligands the ligands were added at the same time. The hepatocytes were harvested and α -G_{i-2} immunoprecipitated with antiserum 1867. The proteins were separated by SDS-PAGE (see sections 2.2.4 and 2.2.5) and the resulting gels dried and put down for autoradiography (see section 2.2.5). The level of phosphorylation achieved was determined by Cerenkov counting of gel chips that contained phosphorylated α -G_{i-2}. The data are expressed as mean \pm SEM (n \geq 4; see table 4.3) where * indicates that the data are significantly different (p<0.05) from control (0%) with data tested using a single sample Student's *t*-test.

Figure 4.19: Percentage inhibition of ligand induced α -G_{i-2} phosphorylation in Sprague Dawley rat hepatocytes: Effects of amylin or insulin on amylin, PMA and glucagon induced phosphorylations

Insulin induced inhibition of ligand induced α -G_{i-2} phosphorylation in Sprague Dawley rat hepatocytes labelled with ³²P (see sections 2.2.2 and 2.2.3). The hepatocytes were challenged with amylin (Amy; 1 μ M), insulin (Ins; 10 μ M), glucagon (Gluc; 10 nM), and PMA (100 ng/ml) for 15 minutes. Where the hepatocytes were challenged with two or more ligands the ligands were added at the same time. The hepatocytes were harvested and α -G_{i-2} immunoprecipitated with antiserum 1867. The proteins were separated by SDS-PAGE (see sections 2.2.4 and 2.2.5) and the resulting gels dried and put down for autoradiography (see section 2.2.5). The level of phosphorylation achieved was determined by Cerenkov counting of gel chips that contained phosphorylated α -G_{i-2}. The data are expressed as mean \pm SEM (n \geq 4; see table 4.4) where * indicates that the data are significantly different (p<0.05) from control (ligand only, 0%) with data tested using a single sample Student's *t*-test.

Phosphorylation of alpha-Gi-2 in Sprague Dawley rat hepatocytes



Induced inhibition of alpha-Gi-2 phosphorylation in Sprague Dawley rat hepatocytes

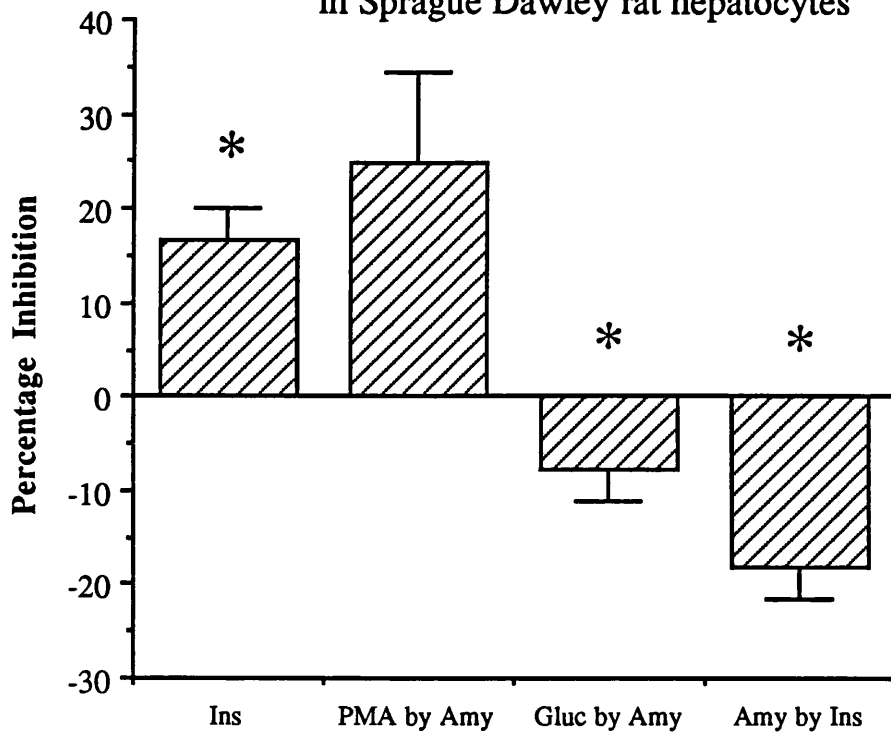


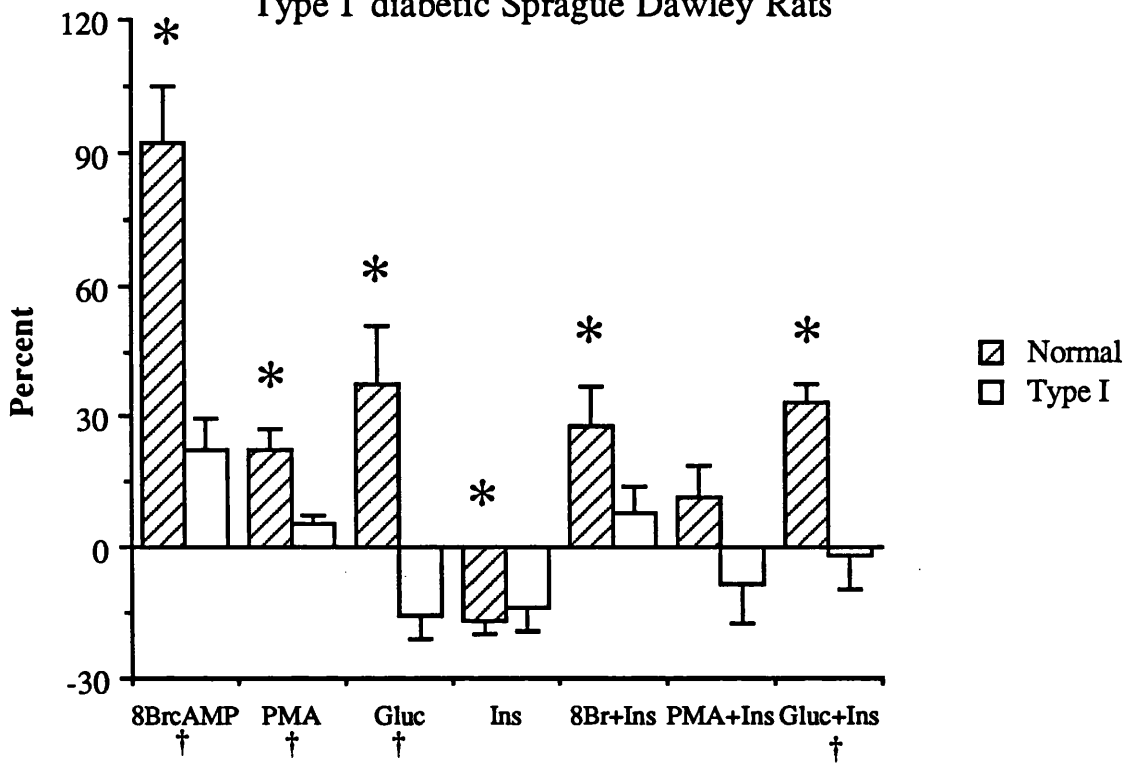
Figure 4.20: Percentage phosphorylation of α -G_{i-2} in hepatocytes from 'normal' and streptozotocin treated Sprague Dawley rats: Effects of 8-bromo-cAMP, PMA, glucagon, and insulin

Stimulation of α -G_{i-2} phosphorylation in 'normal' and 'type I' diabetic Sprague Dawley rat hepatocytes labelled with ³²P (see sections 2.2.2 and 2.2.3) and then challenged with 8-bromo-cAMP (8Br or 8BrcAMP; 300 μ M), PMA (100 ng/ml), glucagon (Gluc; 10 nM), and insulin (Ins; 10 μ M) for 15 minutes. Where the hepatocytes were challenged with a ligand and insulin the insulin was added first followed immediately by the ligand. The hepatocytes were harvested and α -G_{i-2} immunoprecipitated with antiserum 1867. The proteins were separated by SDS-PAGE (see sections 2.2.4 and 2.2.5) and the resulting gels dried and put down for autoradiography (see section 2.2.5). The level of phosphorylation achieved was determined by Cerenkov counting of gel chips that contained phosphorylated α -G_{i-2}. Normal refers to animals that were not injected with streptozotocin whilst Type I refers to animals that were treated. The data are expressed as mean \pm SEM (n \geq 4; see table 4.5) where * indicates that the data are significantly different (p<0.05) from control (0%) with data tested using a single sample Student's *t*-test and † indicates a significant difference, by a two-sample Student's *t*-test, between streptozotocin treated and untreated animals.

Figure 4.21: Percentage inhibition of ligand induced α -G_{i-2} phosphorylation in hepatocytes from 'normal' and streptozotocin treated Sprague Dawley rats: Effects of insulin or inulin on 8-bromo-cAMP, PMA and glucagon induced phosphorylations

Insulin induced inhibition of ligand induced α -G_{i-2} phosphorylation in 'normal' and 'type I' diabetic Sprague Dawley rat hepatocytes labelled with ³²P (see sections 2.2.2 and 2.2.3). The hepatocytes were challenged with 8-bromo-cAMP (8Br; 300 μ M), PMA (100 ng/ml), glucagon (Gluc; 10 nM), insulin (Ins; 10 μ M) for 15 minutes in the presence and absence of insulin (10 μ M). The hepatocytes were harvested and α -G_{i-2} immunoprecipitated with antiserum 1867. The proteins were separated by SDS-PAGE (see sections 2.2.4 and 2.2.5) and the resulting gels dried and put down for autoradiography (see section 2.2.5). The level of phosphorylation achieved was determined by Cerenkov counting of gel chips that contained phosphorylated α -G_{i-2}. Normal refers to animals that were not injected with streptozotocin whilst Type I refers to animals that were treated. The data are expressed as mean \pm SEM (n \geq 4; see table 4.6) where * indicates that the data are significantly different (p<0.05) from control (ligand in the absence of insulin, 0%) with data tested using a single sample Student's *t*-test.

Phosphorylation of alpha-Gi-2 in 'normal' and 'Type I' diabetic Sprague Dawley Rats



Percentage inhibition by insulin of drug mediated phosphorylation of alpha-Gi-2 in hepatocytes from 'normal' and 'Type I' Sprague Dawley Rats

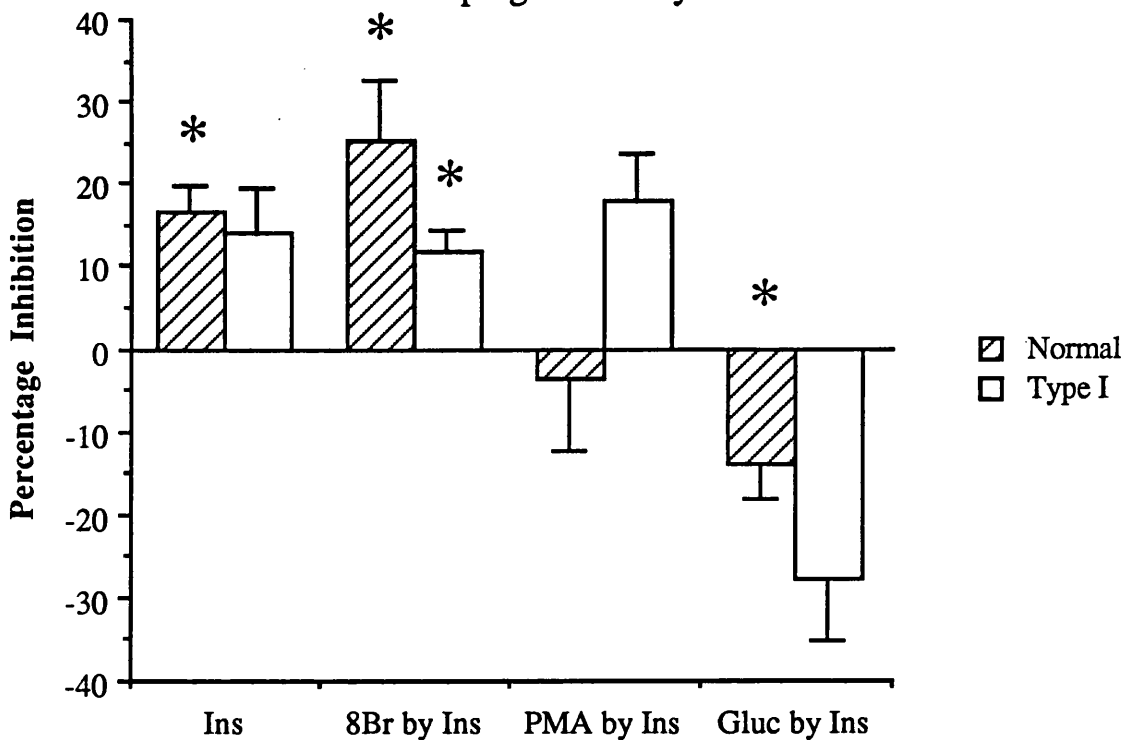


Table 4.7: Percentage inhibition by insulin of ligand induced phosphorylation of α -G_{i-2} in 'normal and 'type I' diabetic Sprague Dawley rat hepatocytes.

NORMAL							
	Mean	SEM	n=	p=	Sig Dif		
8Br by Ins	25	7	3	0.074	N		
PMA by Ins	-4	9	12	0.681	N		
Gluc by Ins	-14	4	5	0.036	Y		
TYPE I							
	Mean	SEM	n=	p=	Sig Dif	p=	Sig Dif N / T I
8Br by Ins	12	3	4	0.023	Y	0.105	N
PMA by Ins	18	6	3	0.068	N	0.252	N
Gluc by Ins	-28	7	3	0.062	N	0.124	N

Control was taken as 0% phosphorylation; SEM = Standard error of mean; n = number of observations; p = significance value returned by single sample Student's *t*-test; Sig Dif = significant difference by one sample Student's *t*-test, Y = significantly different ($p < 0.05$), N = not significantly different ($p > 0.05$); Sig Dif N / T I = Comparison of the significant difference by two-sample Student's *t*-test between phosphorylation events in 'normal' and 'type I' diabetic Sprague Dawley rat hepatocytes, Y = significantly different ($p < 0.05$), N = not significantly different ($p > 0.05$); 8Br = 8-bromo-cAMP, 300 μ M; PMA = Phorbol 12-myristate 13-acetate, 100 ng/ml; Gluc = Glucagon, 10 nM; Ins = Insulin, 10 μ M.

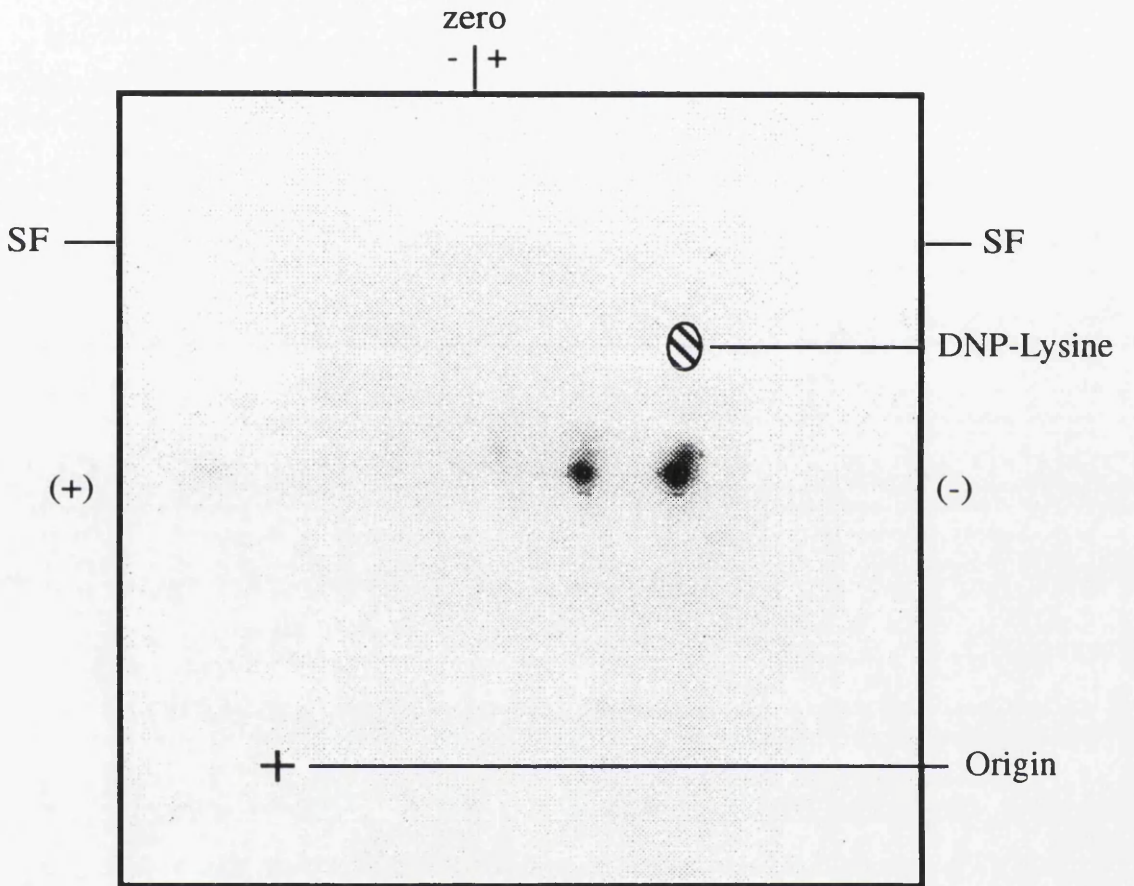
4.3.5 *Two-dimensional phosphopeptide mapping of tryptic peptide of α -G_{i-2} from ligand treated hepatocytes from 'normal' and streptozotocin treated Sprague Dawley rats*

Samples of phosphorylated α -G_{i-2} from non-diabetic Sprague Dawley rat hepatocytes were digested with trypsin and subjected to two-dimensional peptide mapping using the methods described in section 2.2.6 to 2.2.9. The analysis and results for PMA and 8-bromo-cAMP treated samples were as outlined in sections 3.3.2 to 3.3.2.1 and 3.4 (see section 3.3.2.1, and figures 3.6 and 3.7, respectively). PMA-treated samples produced three peptides C1, C2 and C3 (see section 3.3.2.1 and figures 3.6 and 3.16) whilst 8-bromo-cAMP treated cells produced peptides C1, C2, C3 and AN (see section 3.3.2.1 and figures 3.7 and 3.16).

The results obtained for the two-dimensional phosphopeptides maps of phosphorylated α -G_{i-2} from non-diabetic rat hepatocytes that had been exposed to various ligands, and various combination of ligands, could be divided into two distinct groups. It was found that the compounds either produced the 'three-spot' pattern, that is C1, C2 and

Figure 4.22: Phosphopeptide map of α -G_{i-2} from Sprague Dawley rat hepatocytes incubated with insulin and then digested with trypsin

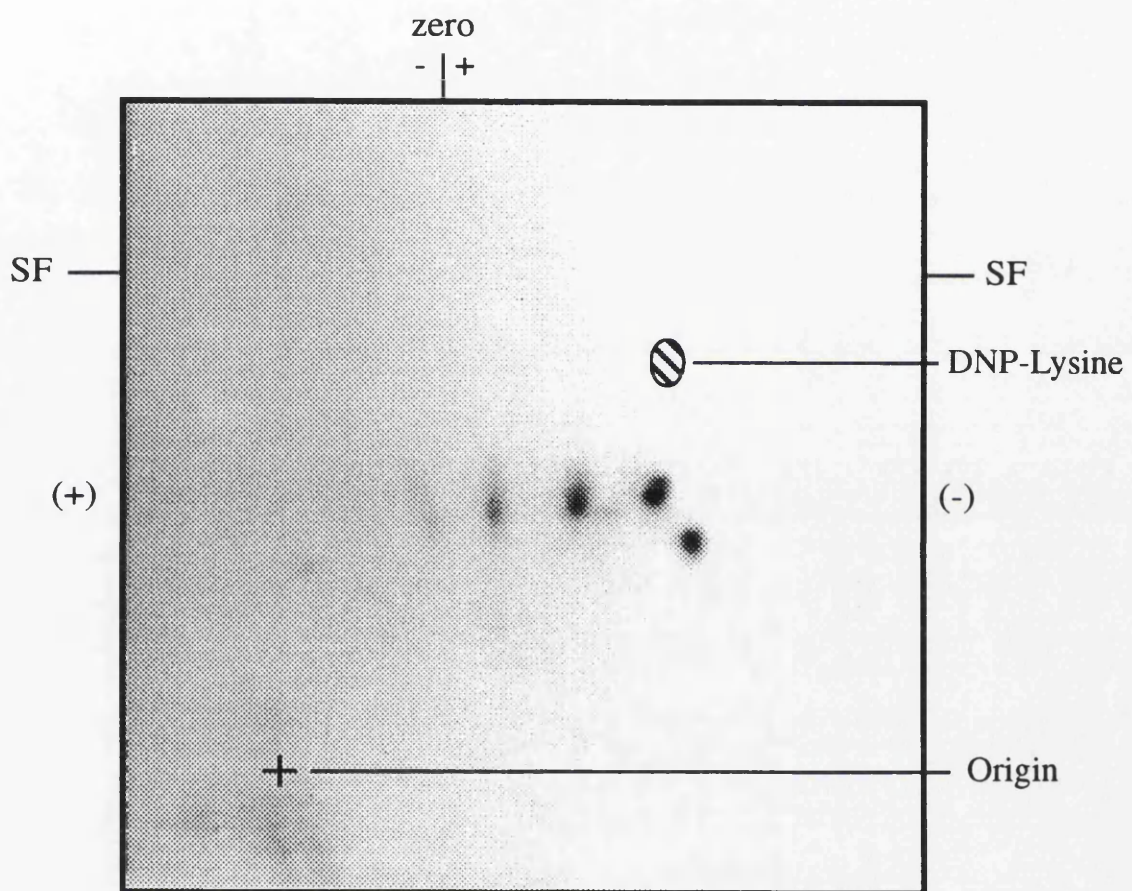
Hepatocytes were labelled with ³²P (see sections 2.2.2 and 2.2.3) and then challenged with insulin (10 μ M). The hepatocytes were harvested and α -G_{i-2} immunoprecipitated with antiserum 1867 before being subjected to SDS-PAGE. The protein was recovered from the gel and digested with TPCCK-treated trypsin as described in experimental procedures (see sections 2.2.4 - 2.2.9). ³²P-labelled tryptic phosphopeptides were then separated on thin-layer cellulose plates by electrophoresis at pH1.9 and ascending chromatography. The final position of DNP-lysine is marked on each plate, SF represents the position of the solvent front, origin is the point of application of the sample, (+) and (-) indicate the orientation of the electric field, and the bar at the top of the plate indicates the separation of the negative, neutral and positive markers. The autoradiograph shows the result from a typical experiment where insulin produced spots C1, C2, and C3. Diagrammatic representation of the results is shown in figure 3.16. The experiment was performed at least three times with similar results.



Sprague Dawley, Insulin, trypsin

Figure 4.23: Phosphopeptide map of α -G_{i-2} from Sprague Dawley rat hepatocytes incubated with glucagon and then digested with trypsin

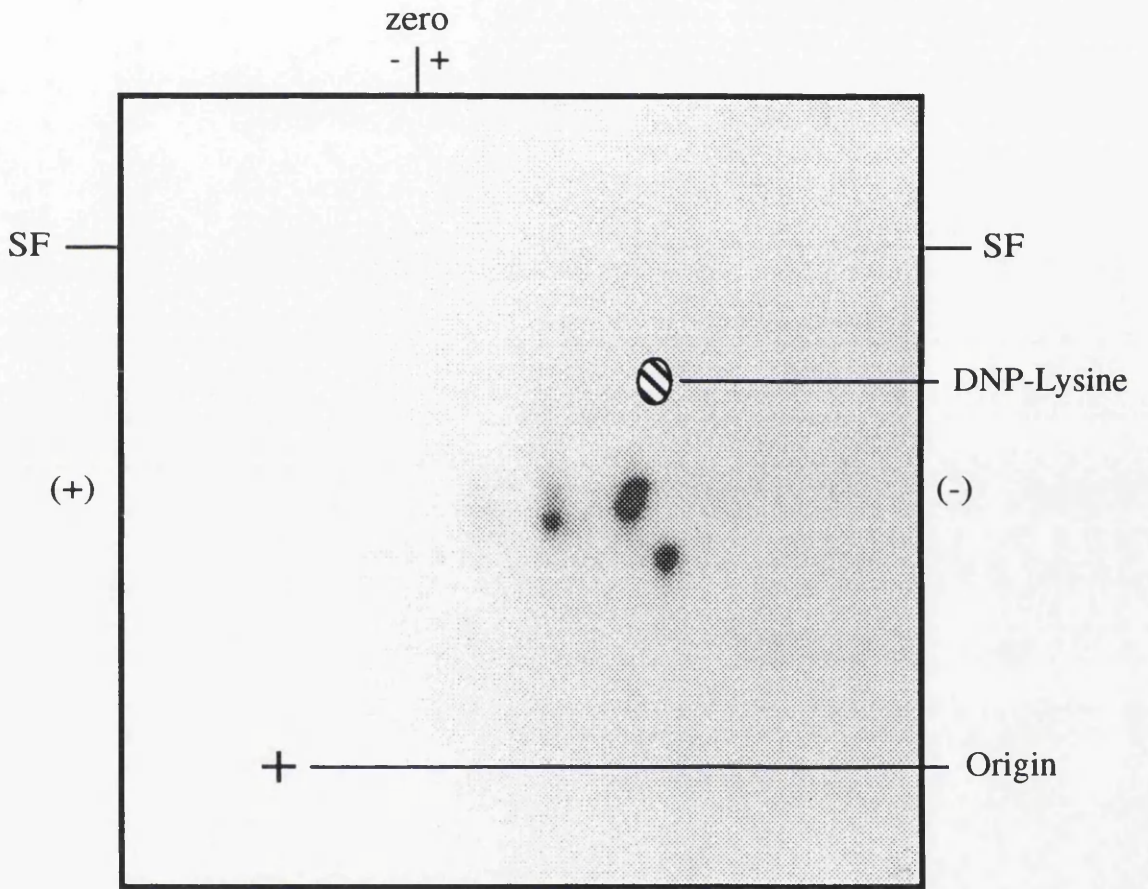
Hepatocytes were labelled with ³²P (see sections 2.2.2 and 2.2.3) and then challenged with glucagon (10 nM). The hepatocytes were harvested and α -G_{i-2} immunoprecipitated with antiserum 1867 before being subjected to SDS-PAGE. The protein was recovered from the gel and digested with TPCK-treated trypsin as described in experimental procedures (see sections 2.2.4 - 2.2.9). ³²P-labelled tryptic phosphopeptides were then separated on thin-layer cellulose plates by electrophoresis at pH1.9 and ascending chromatography. The final position of DNP-lysine is marked on each plate, SF represents the position of the solvent front, origin is the point of application of the sample, (+) and (-) indicate the orientation of the electric field, and the bar at the top of the plate indicates the separation of the negative, neutral and positive markers. The autoradiograph shows the result from a typical experiment where glucagon produced spots C1, C2, C3 and AN. Diagrammatic representation of the results is shown in figure 3.16. The experiment was performed at least three times with similar results.



Sprague Dawley, glucagon, trypsin

Figure 4.24: Phosphopeptide map of α -G_{i-2} from Sprague Dawley rat hepatocytes incubated with 8-bromo-cAMP and insulin and then digested with trypsin

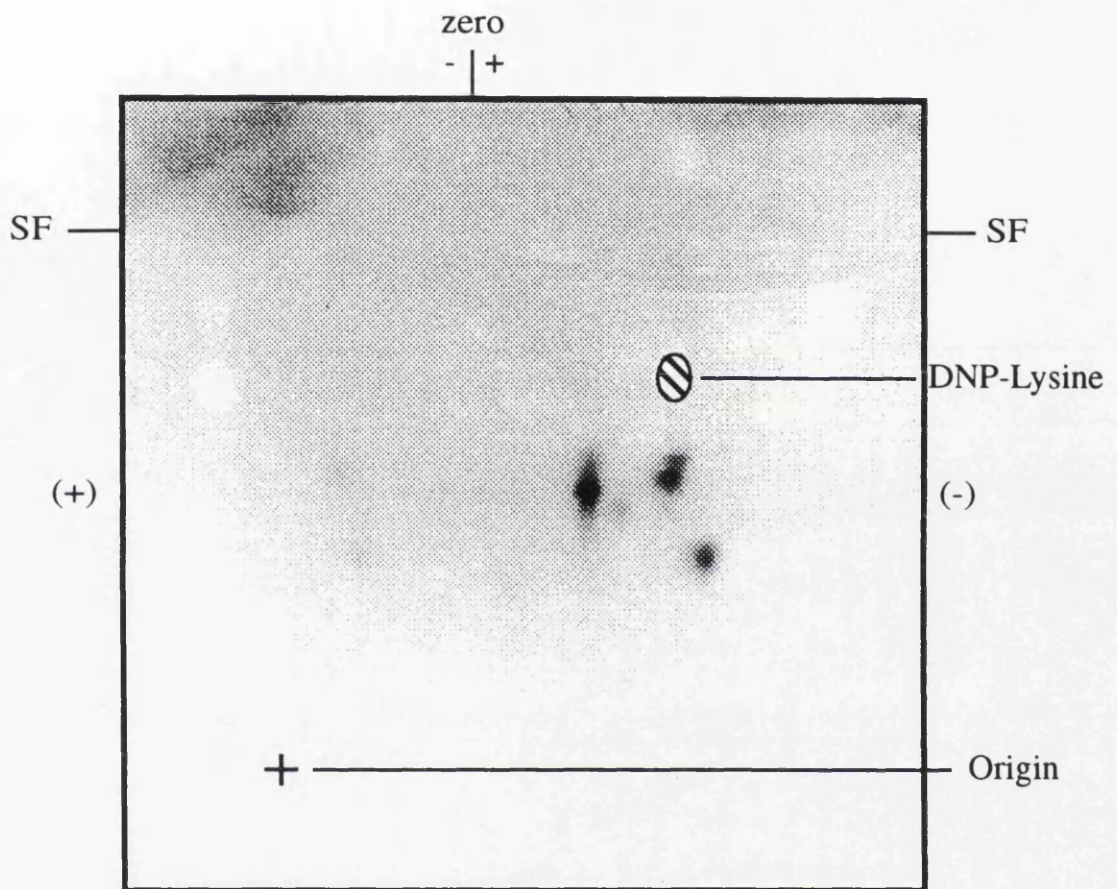
Hepatocytes were labelled with ³²P (see sections 2.2.2 and 2.2.3) and then challenged with 8-bromo-cAMP (300 μ M) and insulin (10 μ M). The hepatocytes were harvested and α -G_{i-2} immunoprecipitated with antiserum 1867 before being subjected to SDS-PAGE. The protein was recovered from the gel and digested with TPCCK-treated trypsin as described in experimental procedures (see sections 2.2.4 - 2.2.9). ³²P-labelled tryptic phosphopeptides were then separated on thin-layer cellulose plates by electrophoresis at pH1.9 and ascending chromatography. The final position of DNP-lysine is marked on each plate, SF represents the position of the solvent front, origin is the point of application of the sample, (+) and (-) indicate the orientation of the electric field, and the bar at the top of the plate indicates the separation of the negative, neutral and positive markers. The autoradiograph shows the result from a typical experiment where 8-bromo-cAMP and insulin produced spots C1, C2, C3 and AN. Diagrammatic representation of the results is shown in figure 3.16. The experiment was performed at least three times with similar results.



Sprague Dawley, 8-bromo-cAMP and insulin, trypsin

Figure 4.25: Phosphopeptide map of α -G_{i-2} from Sprague Dawley rat hepatocytes incubated with glucagon and insulin and then digested with trypsin

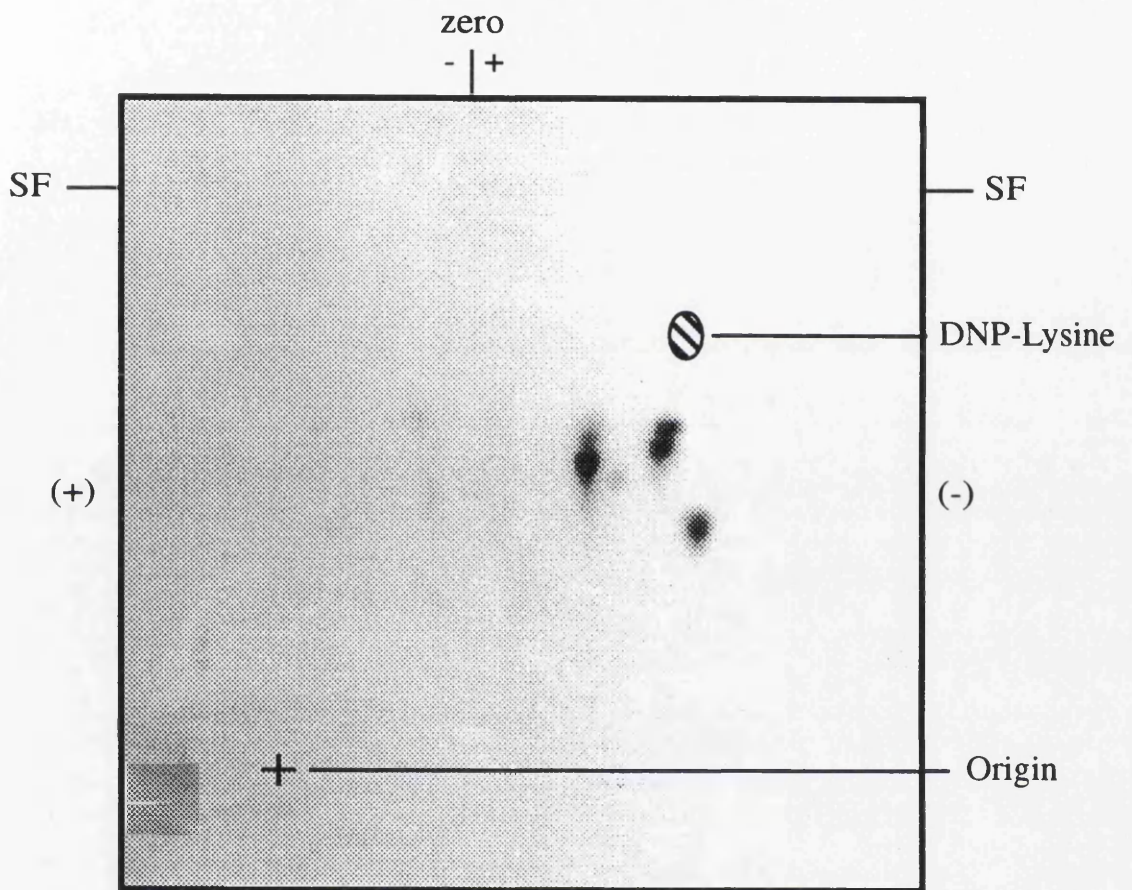
Hepatocytes were labelled with ³²P (see sections 2.2.2 and 2.2.3) and then challenged with glucagon (10 nM) and insulin (10 μ M). The hepatocytes were harvested and α -G_{i-2} immunoprecipitated with antiserum 1867 before being subjected to SDS-PAGE. The protein was recovered from the gel and digested with TPCK-treated trypsin as described in experimental procedures (see sections 2.2.4 - 2.2.9). ³²P-labelled tryptic phosphopeptides were then separated on thin-layer cellulose plates by electrophoresis at pH1.9 and ascending chromatography. The final position of DNP-lysine is marked on each plate, SF represents the position of the solvent front, origin is the point of application of the sample, (+) and (-) indicate the orientation of the electric field, and the bar at the top of the plate indicates the separation of the negative, neutral and positive markers. The autoradiograph shows the result from a typical experiment where glucagon and insulin produced spots C1, C2, C3 and AN. Diagrammatic representation of the results is shown in figure 3.16. The experiment was performed at least three times with similar results.



Sprague Dawley, glucagon and insulin, trypsin

Figure 4.26: Phosphopeptide map of α -G_{i-2} from Sprague Dawley rat hepatocytes incubated with forskolin and then digested with trypsin

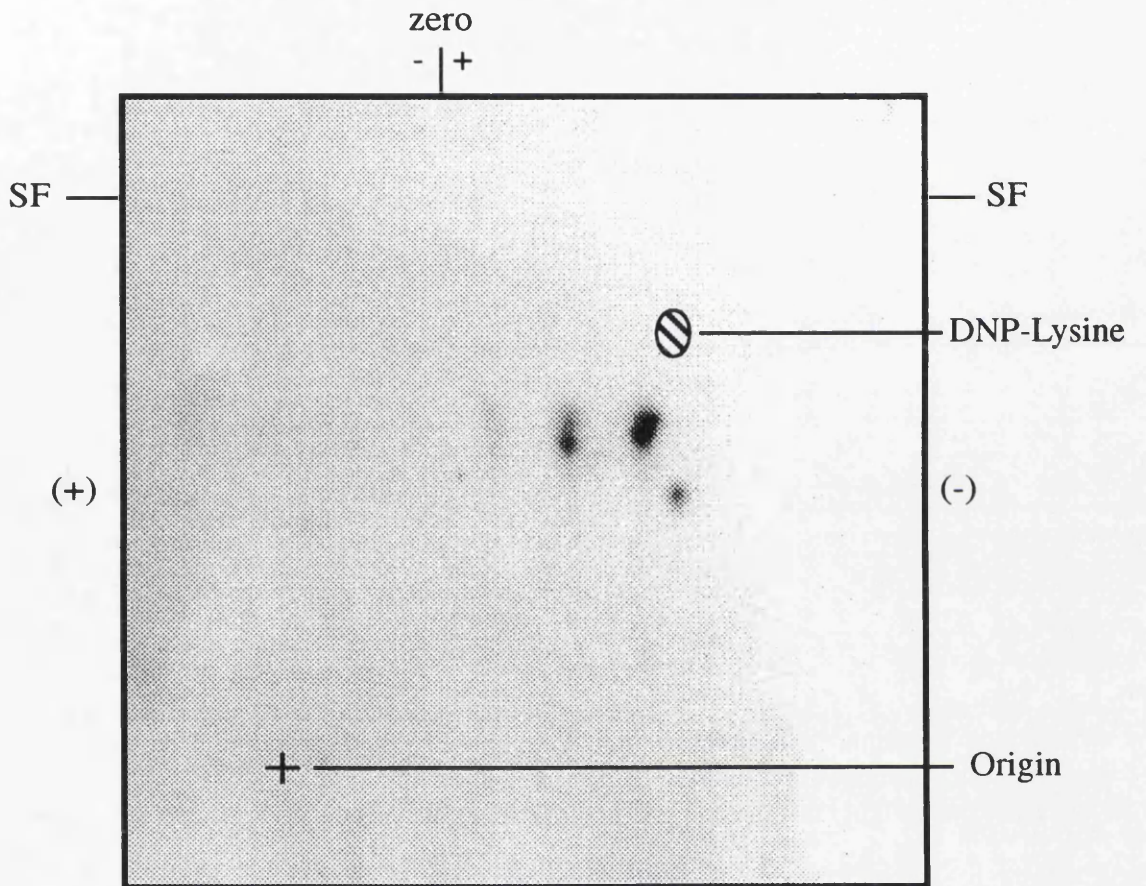
Hepatocytes were labelled with ^{32}P (see sections 2.2.2 and 2.2.3) and then challenged with forskolin (100 μM). The hepatocytes were harvested and α -G_{i-2} immunoprecipitated with antiserum 1867 before being subjected to SDS-PAGE. The protein was recovered from the gel and digested with TPCK-treated trypsin as described in experimental procedures (see sections 2.2.4 - 2.2.9). ^{32}P -labelled tryptic phosphopeptides were then separated on thin-layer cellulose plates by electrophoresis at pH1.9 and ascending chromatography. The final position of DNP-lysine is marked on each plate, SF represents the position of the solvent front, origin is the point of application of the sample, (+) and (-) indicate the orientation of the electric field, and the bar at the top of the plate indicates the separation of the negative, neutral and positive markers. The autoradiograph shows the result from a typical experiment where forskolin produced spots C1, C2, C3 and AN. Diagrammatic representation of the results is shown in figure 3.16. The experiment was performed at least three times with similar results.



Sprague Dawley, forskolin, trypsin

Figure 4.27: Phosphopeptide map of α -G_{i-2} from Sprague Dawley rat hepatocytes incubated with IBMX and then digested with trypsin

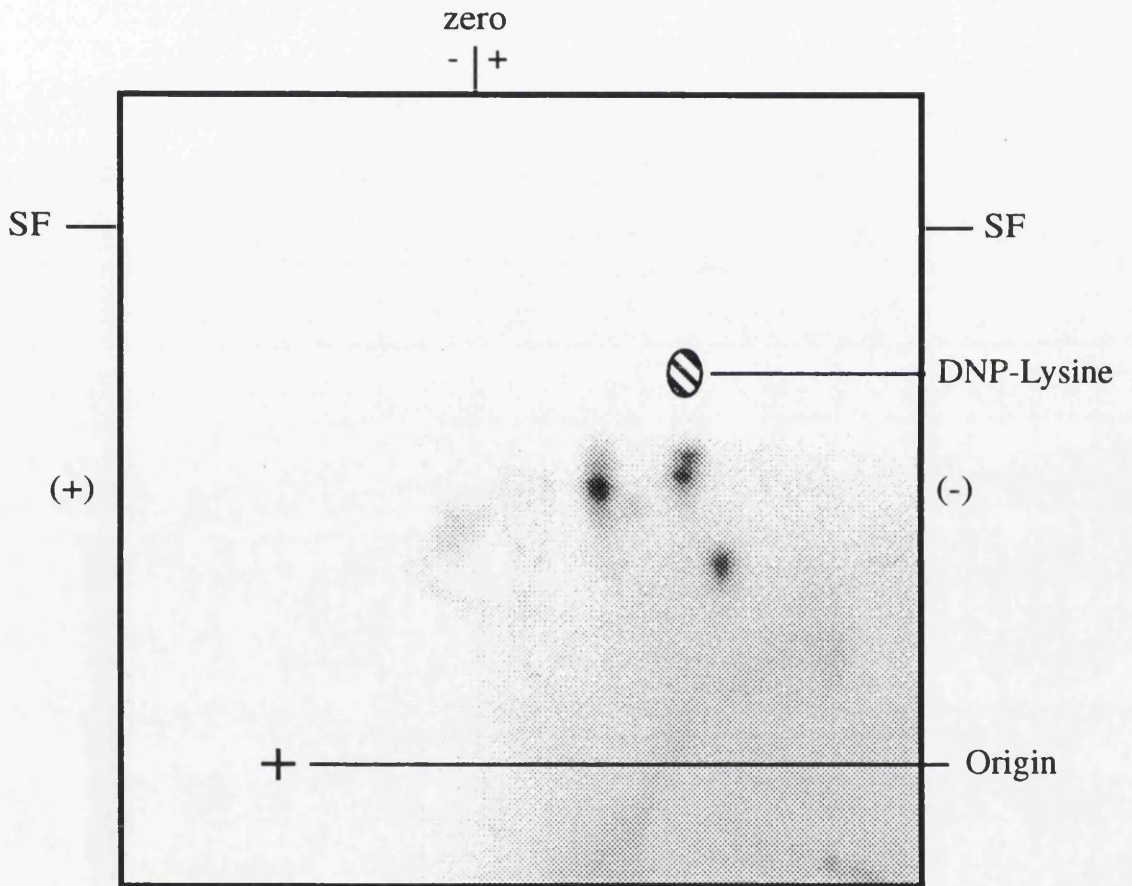
Hepatocytes were labelled with ³²P (see sections 2.2.2 and 2.2.3) and then challenged with IBMX (100 μ M). The hepatocytes were harvested and α -G_{i-2} immunoprecipitated with antiserum 1867 before being subjected to SDS-PAGE. The protein was recovered from the gel and digested with TPCK-treated trypsin as described in experimental procedures (see sections 2.2.4 - 2.2.9). ³²P-labelled tryptic phosphopeptides were then separated on thin-layer cellulose plates by electrophoresis at pH1.9 and ascending chromatography. The final position of DNP-lysine is marked on each plate, SF represents the position of the solvent front, origin is the point of application of the sample, (+) and (-) indicate the orientation of the electric field, and the bar at the top of the plate indicates the separation of the negative, neutral and positive markers. The autoradiograph shows the result from a typical experiment where IBMX produced spots C1, C2, C3 and AN. Diagrammatic representation of the results is shown in figure 3.16. The experiment was performed at least three times with similar results.



Sprague Dawley, IBMX, trypsin

Figure 4.28: Phosphopeptide map of α -G_{i-2} from Sprague Dawley rat hepatocytes incubated with forskolin and IBMX and then digested with trypsin

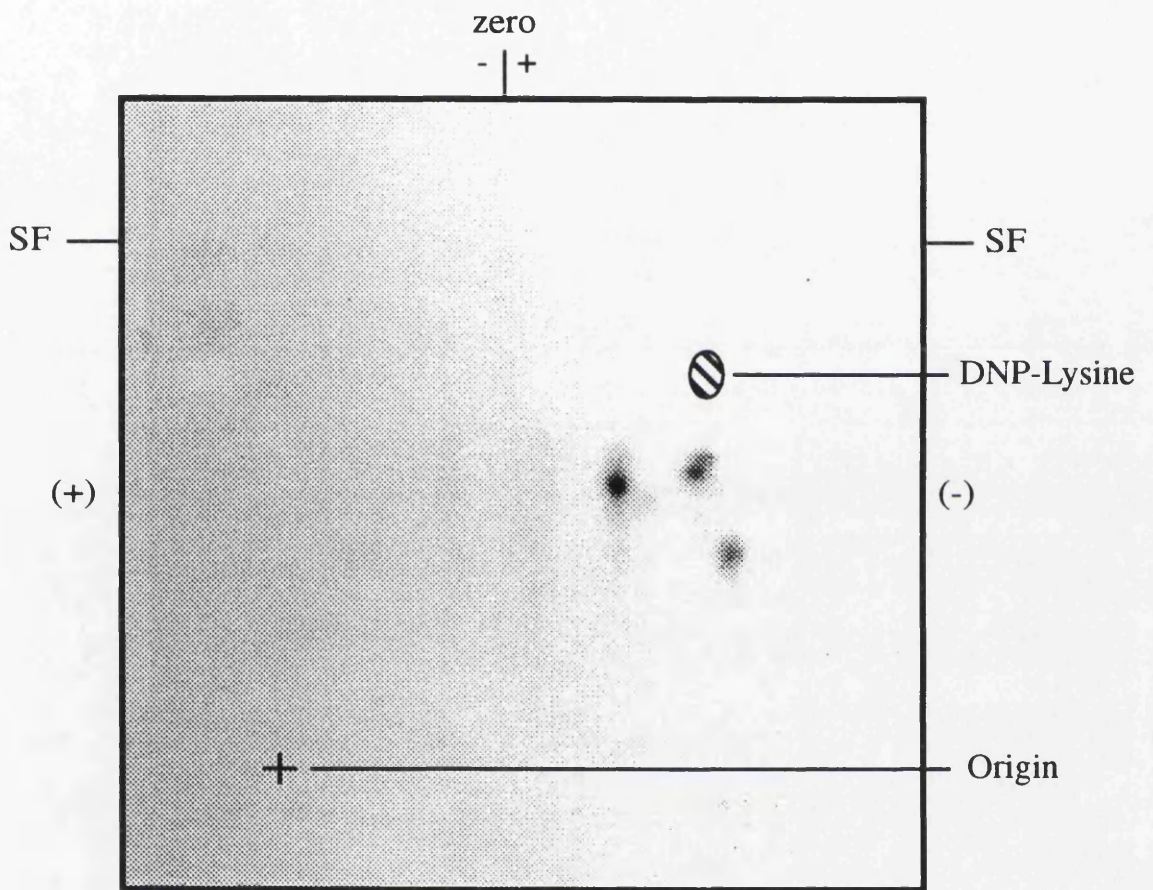
Hepatocytes were labelled with ^{32}P (see sections 2.2.2 and 2.2.3) and then challenged with forskolin (100 μM) and IBMX (100 μM). The hepatocytes were harvested and α -G_{i-2} immunoprecipitated with antiserum 1867 before being subjected to SDS-PAGE. The protein was recovered from the gel and digested with TPCK-treated trypsin as described in experimental procedures (see sections 2.2.4 - 2.2.9). ^{32}P -labelled tryptic phosphopeptides were then separated on thin-layer cellulose plates by electrophoresis at pH1.9 and ascending chromatography. The final position of DNP-lysine is marked on each plate, SF represents the position of the solvent front, origin is the point of application of the sample, (+) and (-) indicate the orientation of the electric field, and the bar at the top of the plate indicates the separation of the negative, neutral and positive markers. The autoradiograph shows the result from a typical experiment where forskolin and IBMX produced spots C1, C2, C3 and AN. Diagrammatic representation of the results is shown in figure 3.16. The experiment was performed at least three times with similar results.



Sprague Dawley, forskolin and IBMX, trypsin

Figure 4.29: Phosphopeptide map of α -G_{i-2} from Sprague Dawley rat hepatocytes incubated with forskolin and insulin and then digested with trypsin

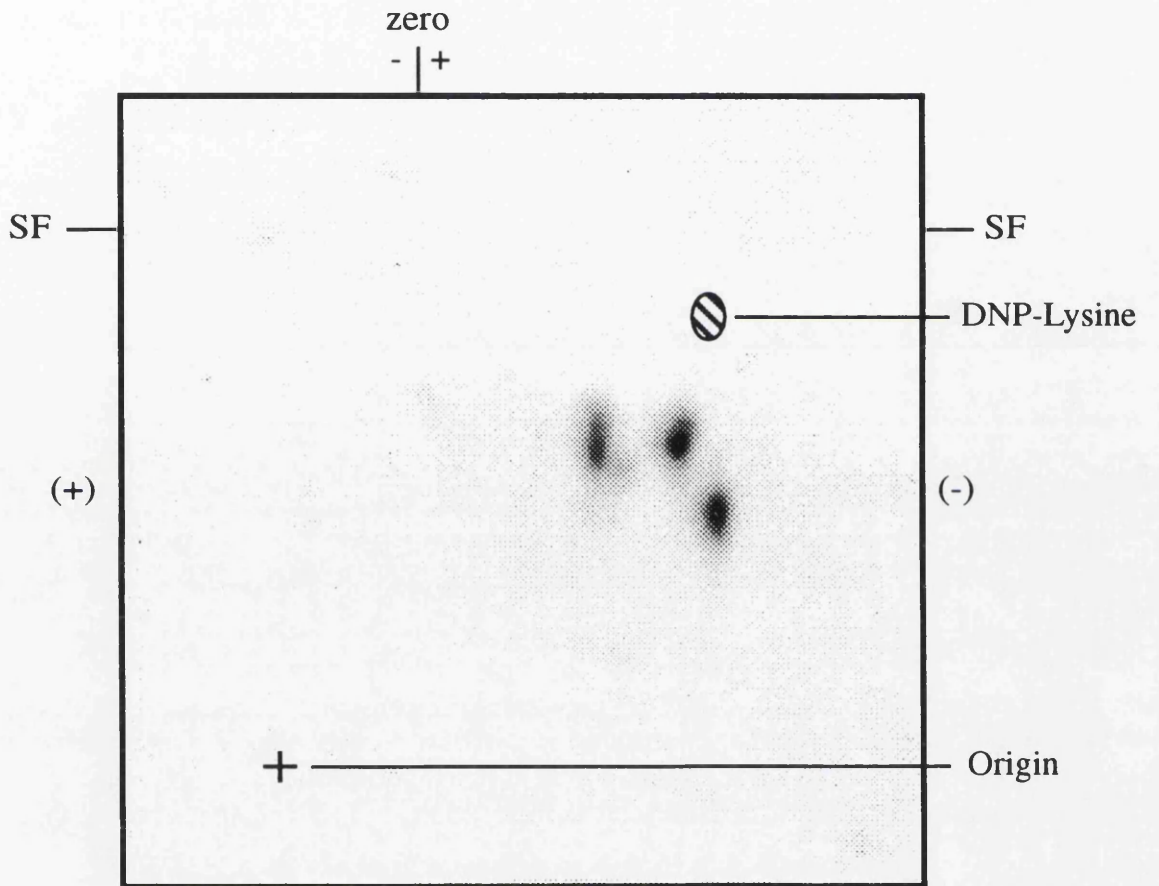
Hepatocytes were labelled with ³²P (see sections 2.2.2 and 2.2.3) and then challenged with forskolin (100 μ M) and insulin (10 μ M). The hepatocytes were harvested and α -G_{i-2} immunoprecipitated with antiserum 1867 before being subjected to SDS-PAGE. The protein was recovered from the gel and digested with TPCK-treated trypsin as described in experimental procedures (see sections 2.2.4 - 2.2.9). ³²P-labelled tryptic phosphopeptides were then separated on thin-layer cellulose plates by electrophoresis at pH1.9 and ascending chromatography. The final position of DNP-lysine is marked on each plate, SF represents the position of the solvent front, origin is the point of application of the sample, (+) and (-) indicate the orientation of the electric field, and the bar at the top of the plate indicates the separation of the negative, neutral and positive markers. The autoradiograph shows the result from a typical experiment where forskolin and insulin produced spots C1, C2, C3 and AN. Diagrammatic representation of the results is shown in figure 3.16. The experiment was performed at least three times with similar results.



Sprague Dawley, forskolin and insulin, trypsin

Figure 4.30: Phosphopeptide map of α -G_{i-2} from Sprague Dawley rat hepatocytes incubated with okadaic acid and then digested with trypsin

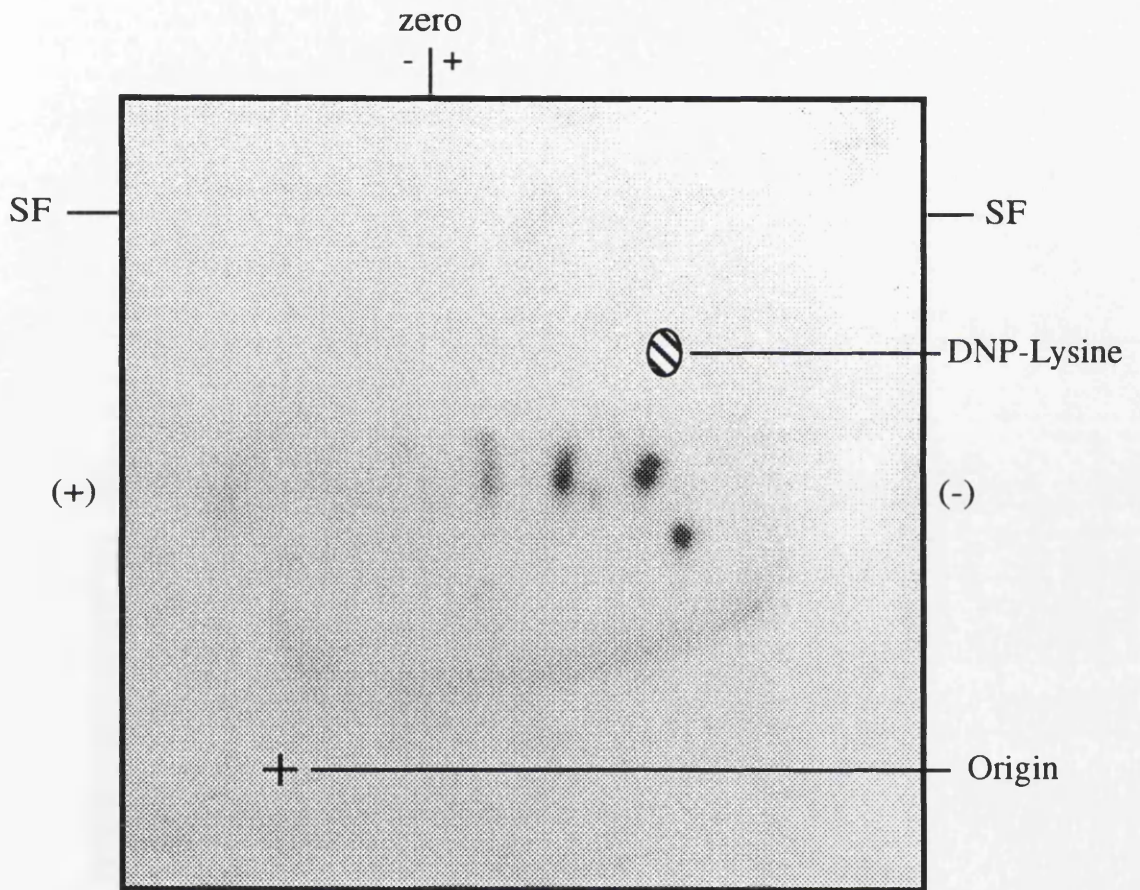
Hepatocytes were labelled with ³²P (see sections 2.2.2 and 2.2.3) and then challenged with okadaic acid (1 μ M). The hepatocytes were harvested and α -G_{i-2} immunoprecipitated with antiserum 1867 before being subjected to SDS-PAGE. The protein was recovered from the gel and digested with TPCCK-treated trypsin as described in experimental procedures (see sections 2.2.4 - 2.2.9). ³²P-labelled tryptic phosphopeptides were then separated on thin-layer cellulose plates by electrophoresis at pH1.9 and ascending chromatography. The final position of DNP-lysine is marked on each plate, SF represents the position of the solvent front, origin is the point of application of the sample, (+) and (-) indicate the orientation of the electric field, and the bar at the top of the plate indicates the separation of the negative, neutral and positive markers. The autoradiograph shows the result from a typical experiment where okadaic acid produced spots C1, C2, C3, and AN. Diagrammatic representation of the results is shown in figure 3.16. The experiment was performed at least three times with similar results.



Sprague Dawley, okadaic acid, trypsin

Figure 4.31: Phosphopeptide map of α -G_{i-2} from Sprague Dawley rat hepatocytes incubated with amylin (1 μ M) and then digested with trypsin

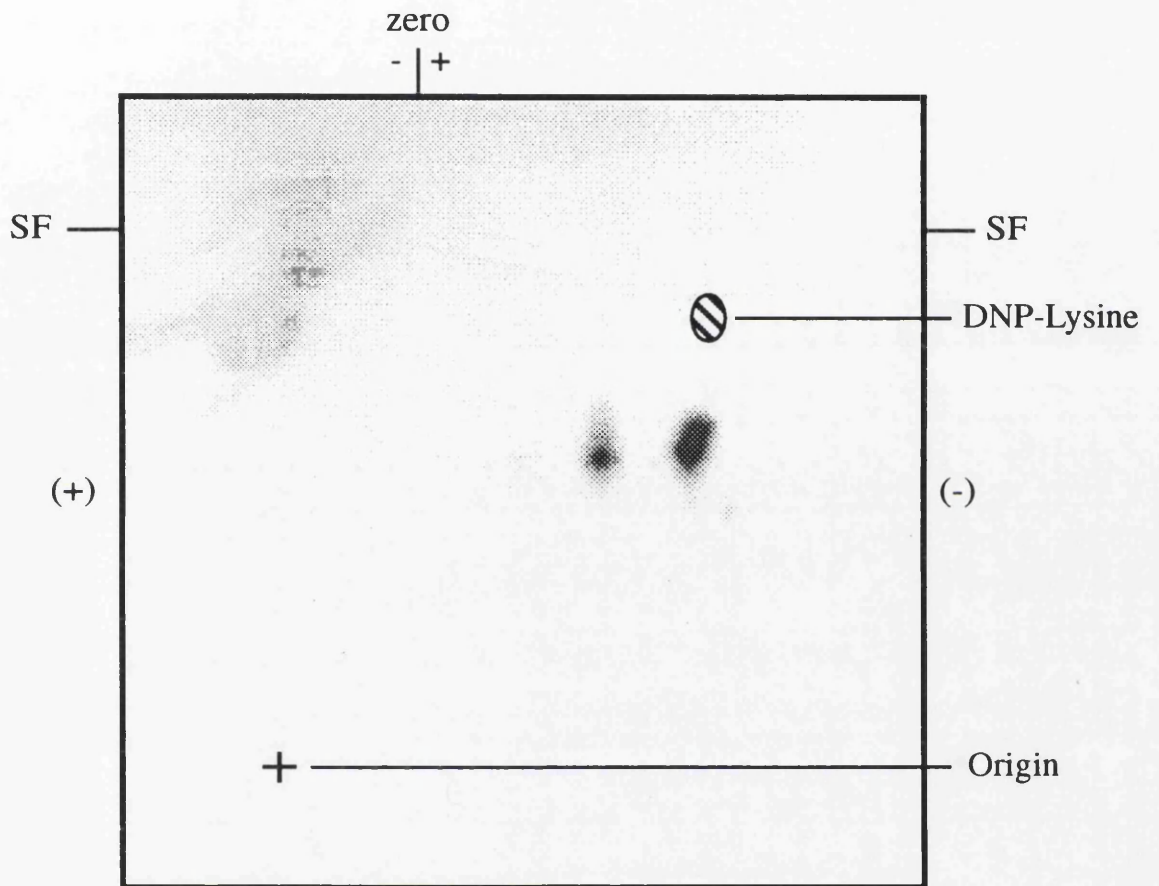
Hepatocytes were labelled with ³²P (see sections 2.2.2 and 2.2.3) and then challenged with amylin (1 μ M). The hepatocytes were harvested and α -G_{i-2} immunoprecipitated with antiserum 1867 before being subjected to SDS-PAGE. The protein was recovered from the gel and digested with TPCK-treated trypsin as described in experimental procedures (see sections 2.2.4 - 2.2.9). ³²P-labelled tryptic phosphopeptides were then separated on thin-layer cellulose plates by electrophoresis at pH1.9 and ascending chromatography. The final position of DNP-lysine is marked on each plate, SF represents the position of the solvent front, origin is the point of application of the sample, (+) and (-) indicate the orientation of the electric field, and the bar at the top of the plate indicates the separation of the negative, neutral and positive markers. The autoradiograph shows the result from a typical experiment where amylin produced spots C1, C2, C3 and AN. Diagrammatic representation of the results is shown in figure 3.16. The experiment was performed at least three times with similar results.



Sprague Dawley, amylin, trypsin

Figure 4.32: Phosphopeptide map of α -G_{i-2} from Sprague Dawley rat hepatocytes incubated with amylin (0.1 pM) and then digested with trypsin

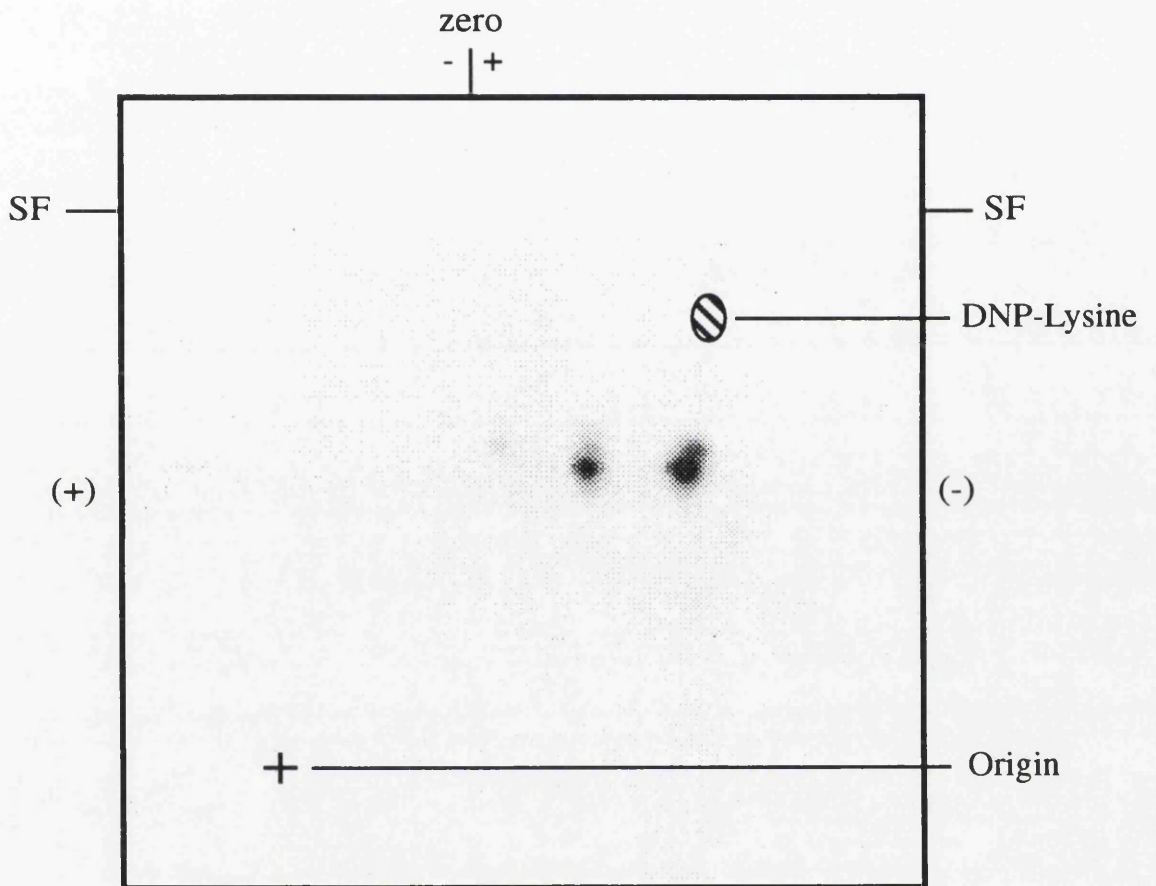
Hepatocytes were labelled with ³²P (see sections 2.2.2 and 2.2.3) and then challenged with amylin (0.1 pM). The hepatocytes were harvested and α -G_{i-2} immunoprecipitated with antiserum 1867 before being subjected to SDS-PAGE. The protein was recovered from the gel and digested with TPCK-treated trypsin as described in experimental procedures (see sections 2.2.4 - 2.2.9). ³²P-labelled tryptic phosphopeptides were then separated on thin-layer cellulose plates by electrophoresis at pH1.9 and ascending chromatography. The final position of DNP-lysine is marked on each plate, SF represents the position of the solvent front, origin is the point of application of the sample, (+) and (-) indicate the orientation of the electric field, and the bar at the top of the plate indicates the separation of the negative, neutral and positive markers. The autoradiograph shows the result from a typical experiment where amylin produced spots C1, C2, and C3. Diagrammatic representation of the results is shown in figure 3.16. The experiment was performed at least three times with similar results.



Sprague Dawley, amylin (0.1 pM), trypsin

Figure 4.33: Phosphopeptide map of α -G_{i-2} from streptozotocin treated Sprague Dawley rat hepatocytes incubated with vehicle solution and then digested with trypsin

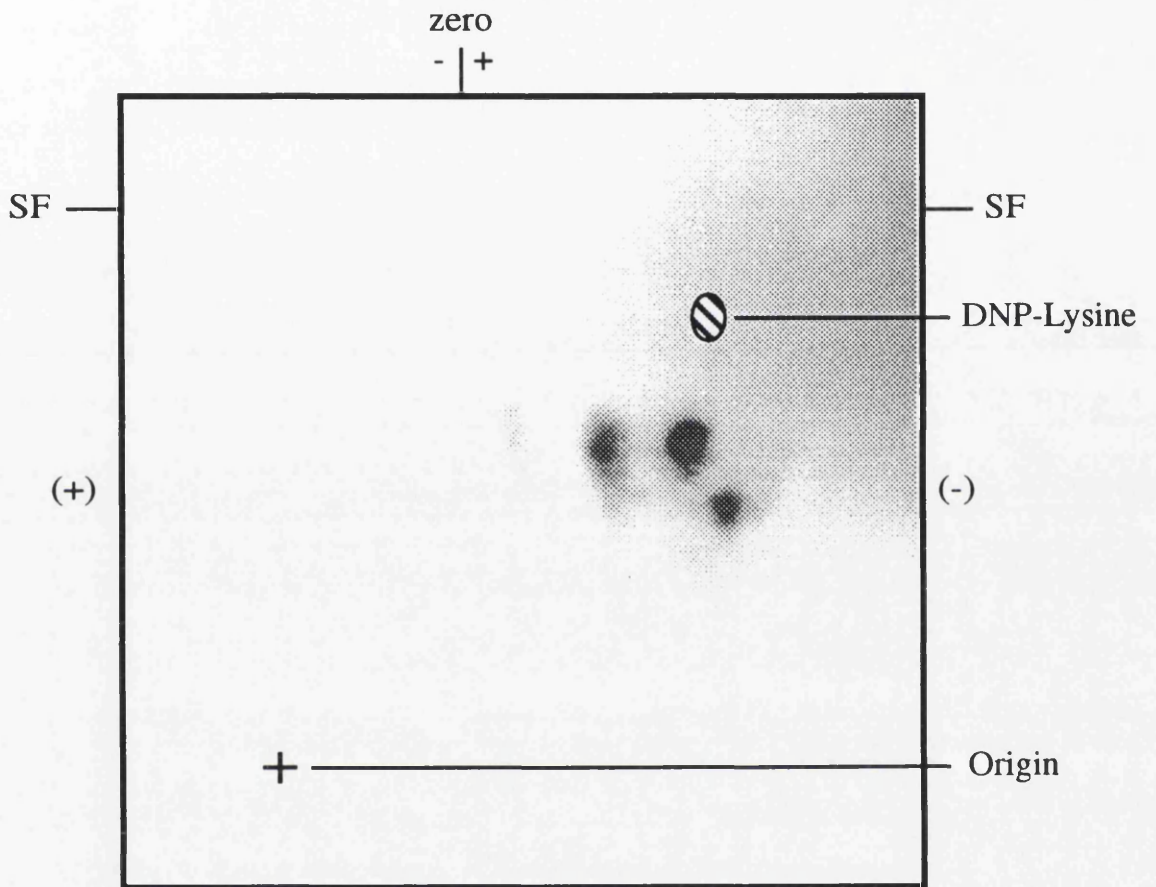
Hepatocytes from streptozotocin treated ('type I' diabetic) Sprague Dawley rats were labelled with ³²P (see sections 2.2.2 and 2.2.3) and then challenged with vehicle solution. The hepatocytes were harvested and α -G_{i-2} immunoprecipitated with antiserum 1867 before being subjected to SDS-PAGE. The protein was recovered from the gel and digested with TPCK-treated trypsin as described in experimental procedures (see sections 2.2.4 - 2.2.9). ³²P-labelled tryptic phosphopeptides were then separated on thin-layer cellulose plates by electrophoresis at pH1.9 and ascending chromatography. The final position of DNP-lysine is marked on each plate, SF represents the position of the solvent front, origin is the point of application of the sample, (+) and (-) indicate the orientation of the electric field, and the bar at the top of the plate indicates the separation of the negative, neutral and positive markers. The autoradiograph shows the result from a typical experiment where vehicle produced spots C1, C2, and C3. Diagrammatic representation of the results is shown in figure 3.16. The experiment was performed at least three times with similar results.



Sprague Dawley, diabetic, control, trypsin

Figure 4.34: Phosphopeptide map of α -G_{i-2} from streptozotocin treated Sprague Dawley rat hepatocytes incubated with 8-bromo-cAMP and then digested with trypsin

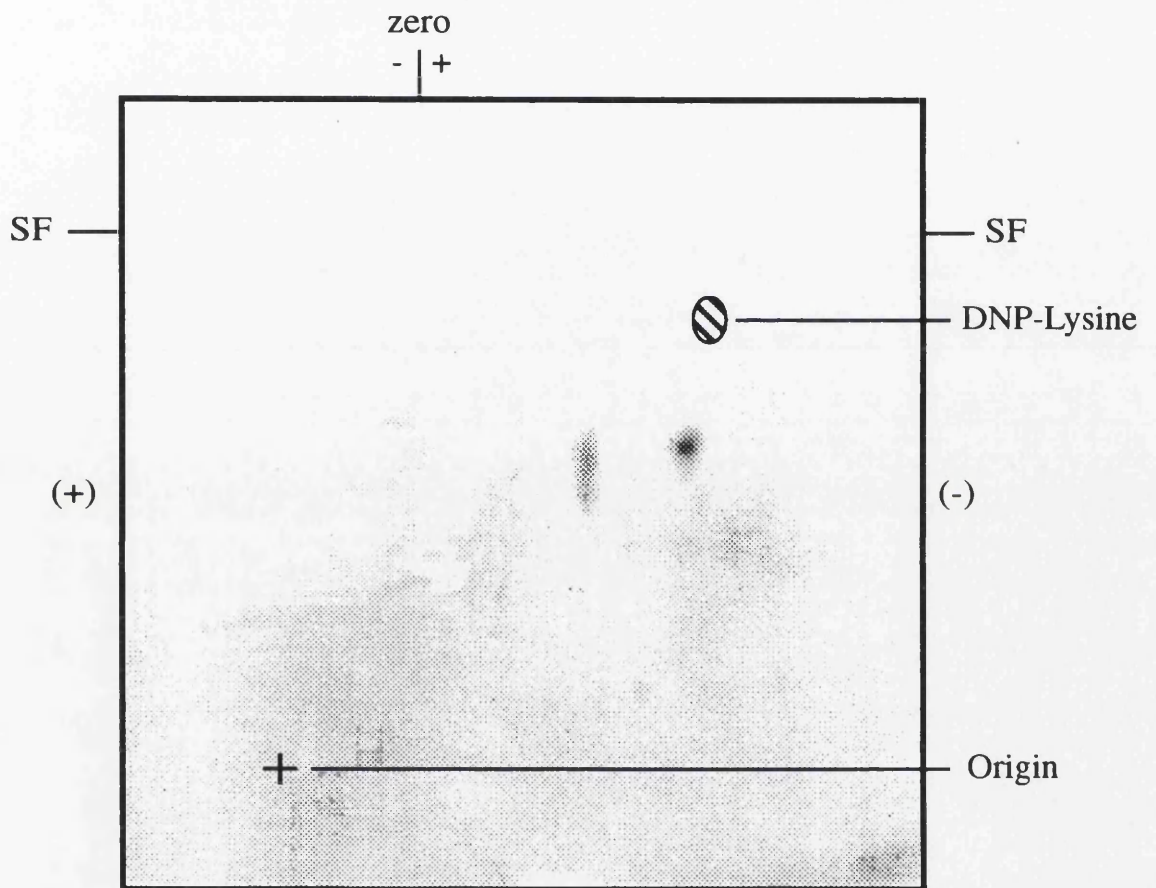
Hepatocytes from streptozotocin treated ('type I' diabetic) Sprague Dawley rats were labelled with ³²P (see sections 2.2.2 and 2.2.3) and then challenged with 8-bromo-cAMP (300 μ M). The hepatocytes were harvested and α -G_{i-2} immunoprecipitated with antiserum 1867 before being subjected to SDS-PAGE. The protein was recovered from the gel and digested with TPCK-treated trypsin as described in experimental procedures (see sections 2.2.4 - 2.2.9). ³²P-labelled tryptic phosphopeptides were then separated on thin-layer cellulose plates by electrophoresis at pH1.9 and ascending chromatography. The final position of DNP-lysine is marked on each plate, SF represents the position of the solvent front, origin is the point of application of the sample, (+) and (-) indicate the orientation of the electric field, and the bar at the top of the plate indicates the separation of the negative, neutral and positive markers. The autoradiograph shows the result from a typical experiment where 8-bromo-cAMP produced spots C1, C2, C3 and AN. Diagrammatic representation of the results is shown in figure 3.16. The experiment was performed at least three times with similar results.



Sprague Dawley diabetic, 8-bromo-cAMP, trypsin

Figure 4.35: Phosphopeptide map of α -G_{i-2} from streptozotocin treated Sprague Dawley rat hepatocytes incubated with PMA and then digested with trypsin

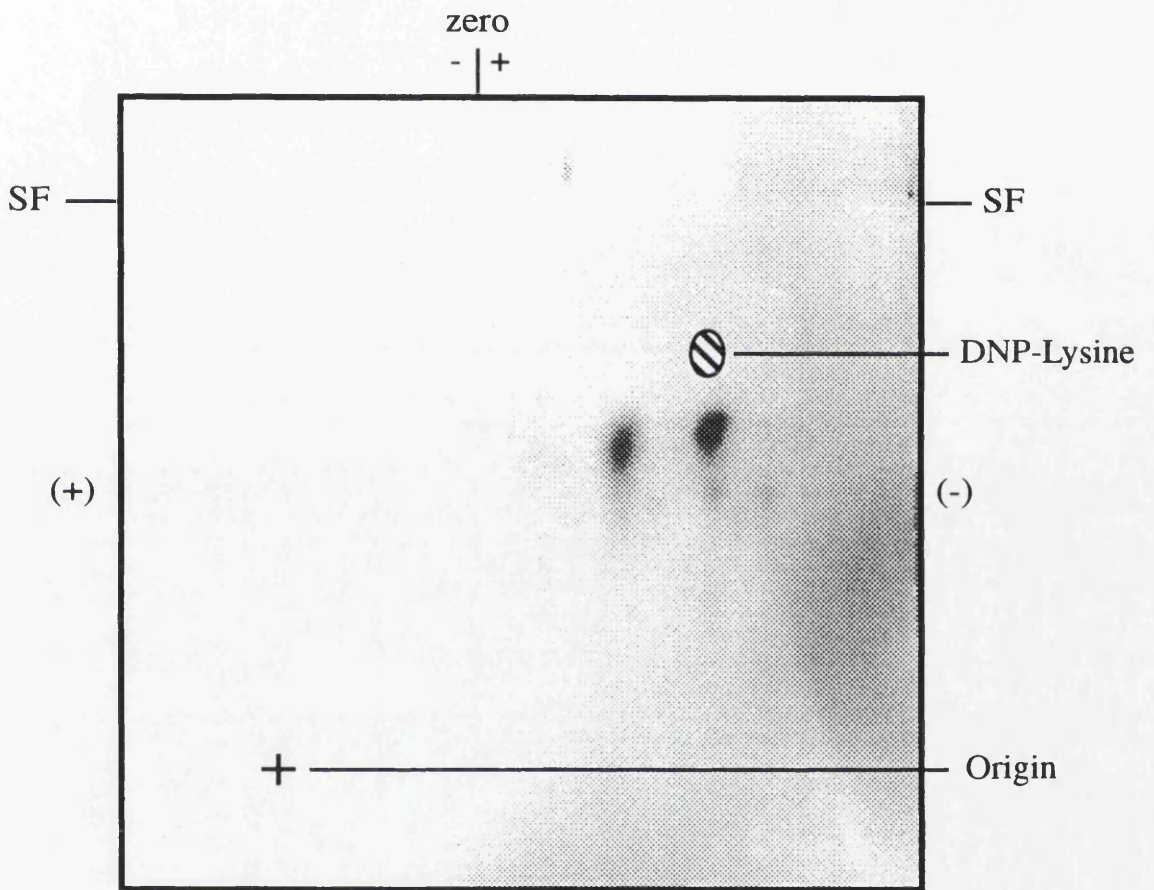
Hepatocytes were labelled with ³²P (see sections 2.2.2 and 2.2.3) and then challenged with PMA (100 ng/ml). The hepatocytes were harvested and α -G_{i-2} immunoprecipitated with antiserum 1867 before being subjected to SDS-PAGE. The protein was recovered from the gel and digested with TPCK-treated trypsin as described in experimental procedures (see sections 2.2.4 - 2.2.9). ³²P-labelled tryptic phosphopeptides were then separated on thin-layer cellulose plates by electrophoresis at pH1.9 and ascending chromatography. The final position of DNP-lysine is marked on each plate, SF represents the position of the solvent front, origin is the point of application of the sample, (+) and (-) indicate the orientation of the electric field, and the bar at the top of the plate indicates the separation of the negative, neutral and positive markers. The autoradiograph shows the result from a typical experiment where PMA produced spots C1, C2, and C3. Diagrammatic representation of the results is shown in figure 3.16. The experiment was performed at least three times with similar results.



Sprague Dawley, 'type I', PMA

Figure 4.36: Phosphopeptide map of α -G_{i-2} from streptozotocin treated Sprague Dawley rat hepatocytes incubated with glucagon and then digested with trypsin

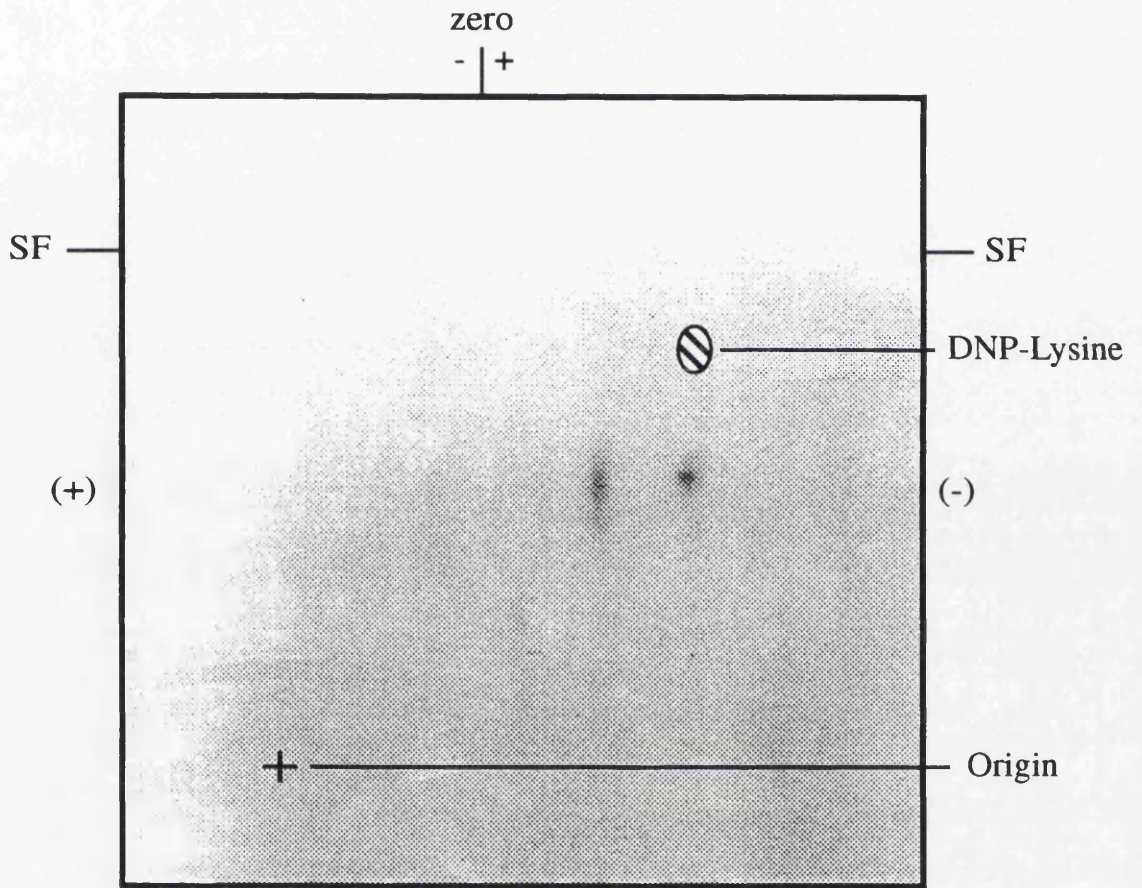
Hepatocytes from streptozotocin treated ('type I' diabetic) Sprague Dawley rats were labelled with ³²P (see sections 2.2.2 and 2.2.3) and then challenged with glucagon (10 nM). The hepatocytes were harvested and α -G_{i-2} immunoprecipitated with antiserum 1867 before being subjected to SDS-PAGE. The protein was recovered from the gel and digested with TPCK-treated trypsin as described in experimental procedures (see sections 2.2.4 - 2.2.9). ³²P-labelled tryptic phosphopeptides were then separated on thin-layer cellulose plates by electrophoresis at pH1.9 and ascending chromatography. The final position of DNP-lysine is marked on each plate, SF represents the position of the solvent front, origin is the point of application of the sample, (+) and (-) indicate the orientation of the electric field, and the bar at the top of the plate indicates the separation of the negative, neutral and positive markers. The autoradiograph shows the result from a typical experiment where glucagon produced spots C1, C2, C3 and AN. Diagrammatic representation of the results is shown in figure 3.16. The experiment was performed at least three times with similar results.



Sprague Dawley, 'type I', glucagon, trypsin

Figure 4.37: Phosphopeptide map of α -G_{i-2} from streptozotocin treated Sprague Dawley rat hepatocytes incubated with insulin and then digested with trypsin

Hepatocytes from streptozotocin treated ('type I' diabetic) Sprague Dawley rats were labelled with ³²P (see sections 2.2.2 and 2.2.3) and then challenged with insulin (10 μ M). The hepatocytes were harvested and α -G_{i-2} immunoprecipitated with antiserum 1867 before being subjected to SDS-PAGE. The protein was recovered from the gel and digested with TPCK-treated trypsin as described in experimental procedures (see sections 2.2.4 - 2.2.9). ³²P-labelled tryptic phosphopeptides were then separated on thin-layer cellulose plates by electrophoresis at pH1.9 and ascending chromatography. The final position of DNP-lysine is marked on each plate, SF represents the position of the solvent front, origin is the point of application of the sample, (+) and (-) indicate the orientation of the electric field, and the bar at the top of the plate indicates the separation of the negative, neutral and positive markers. The autoradiograph shows the result from a typical experiment where insulin produced spots C1, C2, and C3. Diagrammatic representation of the results is shown in figure 3.16. The experiment was performed at least three times with similar results.



Sprague Dawley, diabetic, insulin, trypsin

C3, or produced the 'four-spot' pattern of C1, C2, C3 and AN. The only compounds, other than control or PMA, that produced a three-spot pattern were insulin (see figure 4.22) and amylin (0.1 pM; see figure 4.32). Glucagon (see figure 4.23), 8-bromo-cAMP plus insulin (see figure 4.24), glucagon plus insulin (see figure 4.25), forskolin (see figure 4.26), IBMX (see figure 4.27), forskolin plus IBMX (see figure 4.28), forskolin plus insulin (see figure 4.29), okadaic acid (see figure 4.30), and amylin (1 μ M; see figure 4.31) all produced the four spot pattern of C1, C2, C3 and AN.

Samples of phosphorylated α -G_{i-2} from hepatocytes of animals that had been injected with streptozotocin were also examined by trypsin digestion and two-dimensional phospho-peptide mapping. Samples from control (see figure 4.33) and hepatocytes that had been incubated with 8-bromo-cAMP (see figure 4.34), PMA (see figure 4.35), glucagon (see figure 4.36) and insulin (see figure 4.37) were tested and it was found that control, PMA and insulin treated hepatocytes gave peptides C1, C2 and C3 whilst glucagon and 8-bromo-cAMP samples gave peptides C1, C2, C3 and AN.

4.4 Discussion

It has been established that α -G_{i-2} from Sprague Dawley rat hepatocytes undergoes multi-site phosphorylation (see Chapter 3; Morris *et al.*, 1994) and that the level of phosphorylation can be increased by agents such as vasopressin, angiotensin II, glucagon, PMA, 8-bromo-cAMP and okadaic acid (Bushfield *et al.*, 1990a; Bushfield *et al.*, 1991; Bushfield *et al.*, 1990b; Bushfield *et al.*, 1990c; Pyne *et al.*, 1989b) yet no attempt had been made to examine the effects of insulin or amylin on the phosphorylation events in 'normal' or streptozotocin treated rats.

In the papers by Bushfield and Pyne (Bushfield *et al.*, 1990a; Bushfield *et al.*, 1991; Bushfield *et al.*, 1990b; Bushfield *et al.*, 1990c; Pyne *et al.*, 1989b) the hepatocytes exhibited a basal level of phosphorylation and this again was shown to occur in the hepatocytes used in these studies. Indeed, Bushfield (Bushfield *et al.*, 1991) demonstrated by the use of the phosphatase inhibitor okadaic acid, that α -G_{i-2} was at the centre of a futile cycle of phosphorylation and dephosphorylation and again this futile cycle effect was also demonstrated with okadaic acid in these studies (see section 4.3.2, table 4.3 and figure 4.12). Interestingly, two-dimensional phospho-peptide analysis of trypsin digestion products of the okadaic acid-induced phosphorylated α -G_{i-2} showed that four phosphopeptides were produced which corresponded to peptides C1, C2, C3, and AN (see figure 4.30; see Chapter 3, sections 3.3.2.1 and 3.4, figure 3.16). This indicated that, even under basal conditions, phosphorylation was occurring at two different sites in the protein with the AN site possibly experiencing the greater turn-over in phosphorylation as it is not normally detected in unstimulated cells.

The incubation of ³²P labelled hepatocytes with insulin caused both a time and dose-dependent inhibition on the phosphorylation of α -G_{i-2} with the maximum effect being

achieved at about 5 minutes and an effective concentration of 10^{-9} M (see figures 4.2 and 4.4, tables 4.1 and 4.2; section 4.3.1). As it is known that α -G_{i-2} exerts a tonic inhibitory effect on adenylyl cyclase, and that the phosphorylation of α -G_{i-2} caused a loss of this inhibitory effect, then the effect of insulin mediated dephosphorylation of α -G_{i-2} may be to cause an increase in the tonic inhibition of cyclase, and hence a desensitisation of the cAMP system.

For insulin to decrease the phosphorylation of α -G_{i-2} it could act in one of two ways. As resting (basal, control) cells appear to be involved in a futile cycle of phosphorylation and dephosphorylation as part of the control of α -G_{i-2} activity, then insulin may act by either inhibiting a kinase or by stimulating the activity of a phosphatase.

The effect of insulin on the activation of two of the kinases believed to be involved in the futile cycle, PKC and PKA, was explored by the use of ligands that had either a direct stimulatory effect on the kinases (e.g. PMA or 8-bromo-cAMP), or activated a kinase by stimulating the production of a secondary messenger (e.g. forskolin stimulated cAMP production). Alternatively, the kinase activity was examined by using inhibitors that prevented the degradation of the kinase-activating secondary messengers (e.g. IBMX inhibition of phosphodiesterases), or by using kinase inhibitors such as HA1004 (see section 1.2.4.1). The role of the phosphatase in the cycle was examined by the use of phosphatase inhibitor okadaic acid (see sections 1.2.4.1 and 1.2.4.3) which, in hepatocytes, has been shown to produce its half maximal effect on protein dephosphorylation at 200 nM, with maximal effect at 1 μ M resulting in the stimulation of gluconeogenesis and glucose output (Haystead *et al.*, 1989; see Hardie *et al.*, 1991).

To examine how insulin exerted its effects on the PKC-mediated phosphorylation of α -G_{i-2} the phorbol ester PMA was used. It was shown that PMA could stimulate the phosphorylation of α -G_{i-2} and that this occurred, as discussed in Chapter 3, at the same site as in unstimulated cells, that is serine 144 (see section 3.3.2.1 and figures 3.5 and 3.6). When cells were incubated with both PMA and insulin it was found that even though insulin inhibited basal phosphorylation, no change in the phosphorylation occurred (see section 4.3.2 and figures 4.6 and 4.7). This indicated that insulin did not significantly inhibit the activity of PKC, or activate a phosphatase that was specific for the removal of the phosphate group on serine 144. It is possible that as PMA-stimulated phosphorylation is only an increase of $22 \pm 4\%$ (n=12) above control (0%), then the insulin effect is not detectable. Alternatively, as PMA stimulates the activity of most of the members of the PKC family, other than ζ and possibly θ (see table 1.2), and insulin may only affect one isoform then any effect may be masked by the gross activation of the PKCs.

The other kinase that has been implicated in the phosphorylation of α -G_{i-2} is PKA, although it has been argued that it does not directly phosphorylate the protein as this has not been demonstrated *in vitro* (see section 3.4; Lincoln, 1991). The involvement of

PKA at some stage in the phosphorylation of α -G_{i-2} is indicated by the fact that both 8-bromo-cAMP, which will activate PKA, and forskolin, which will raise intracellular cAMP levels and therefore activate PKA, caused a significant increase in the phosphorylation of the protein (see section 4.3.2, table 4.3 and figures 4.6 and 4.8). However, as the increased cAMP levels will also cause an increase in Ca²⁺ influx then these ligands will also indirectly activate PKC (see Houslay, 1991a; see section 1.2.4.2). Phosphopeptide mapping of tryptic peptides of α -G_{i-2} from cells that were treated with 8-bromo-cAMP, forskolin or IBMX, produced maps that contained four phosphopeptides, C1, C2, C3 and AN (see figures 3.5, 3.6 and 3.7; and 4.26, 4.27, and 4.28) and, although the presence of peptide AN showed an obvious increase in the incorporation of ³²P into α -G_{i-2}, any changes in the labelling of PKC-site represented by peptides C1, C2 or C3, could not be detected due to the unquantifiable nature of the phosphopeptide mapping method.

The inclusion of the kinase inhibitor, HA1004, together with forskolin did not significantly inhibit the phosphorylation of α -G_{i-2} (see section 4.3.2, table 4.3 and figures 4.10 and 4.11). At the concentration the inhibitor was used, 1 μ M, it is considered to be specific for PKA and PKG (see section 1.2.4.1), and its inability to inhibit forskolin-stimulated phosphorylation may indicate that it was either failing to enter the cells, although this was discounted by the observation that it could affect basal phosphorylation levels (see figure 4.11 and table 4.3), or that the inhibitor was effective against PKA-mediated phosphorylation but was unable to inhibit any increased PKC activity. The inhibition of basal phosphorylation levels by HA1004, besides indicating that the inhibitor could enter the cells, suggested that either PKA was actively phosphorylating α -G_{i-2} under basal conditions, although PKA-mediated phosphorylation, that is peptide AN, was not detected in two-dimensional phosphopeptide maps from unstimulated cells unless okadaic acid was present; or at the concentration used, HA1004 was still able to inhibit PKC-mediated phosphorylation which is known to occur as part of the futile cycle.

These studies were complemented by the use of the phosphodiesterase inhibitor IBMX which elicited a significant phosphorylation of α -G_{i-2} in cells where no agonist of the cAMP system was added. The increased level of phosphorylation was determined to be cAMP-dependent as phosphopeptide mapping revealed the presence of the tryptic peptide AN which was only found when cAMP levels were raised (see figure 4.27). However, when IBMX was added in conjunction with a stimulator of the cAMP system, such as forskolin, it did not cause a significant increase in phosphorylation (see figures 4.8 and 4.9). The fact that IBMX could not enhance forskolin stimulated phosphorylation indicates that, at the concentration of forskolin used (100 μ M), the level of cAMP produced was sufficient to fully activate PKA and so cause the phosphorylation of α -G_{i-2}.

As IBMX was also able to increase the level of α -G_{i-2} phosphorylation (see figure 4.8), and produce the four spot pattern (see figure 4.27), then this shows that even

under basal, unstimulated, conditions that cAMP is being produced and that only the inhibition of phosphodiesterase activity by IBMX is required to produce an increase in the phosphorylation of the protein. This may indicate how easily phosphorylation in the futile phosphorylation / dephosphorylation cycle can be activated as although IBMX is able to increase intracellular cAMP levels in hepatocytes, the levels achieved would not be sufficient to activate PKA. IBMX may be able to activate PKA if the components of the system are compartmentalised. That is, the effects of IBMX were localised, where cAMP concentrations could become sufficiently high to activate PKA.

Work by Bushfield *et al.* (Bushfield *et al.*, 1990b) has shown that the phosphorylation of α -G_{i-2} caused an inactivation of the protein and the loss of inhibition of adenylyl cyclase. As IBMX produced such a phosphorylation then the tonic inhibition of adenylyl cyclase would be lost and more cAMP produced, and hence further phosphorylation of α -G_{i-2}. This may demonstrate that the phosphorylation of α -G_{i-2} has to be tightly controlled otherwise positive feedback could start. The fact that HA1004 also inhibited the phosphorylation of α -G_{i-2} in hepatocytes again demonstrates that the protein is undergoing a futile cycle of phosphorylation and dephosphorylation. In this case the inclusion of HA1004 would inhibit PKA, and possibly PKC, which would result in a decrease in the phosphorylation of α -G_{i-2} and hence an increase in the tonic inhibition of adenylyl cyclase which in turn could produce a decrease in basal cAMP levels and a reduction in the activity of PKA or PKC.

The inclusion of insulin with 8-bromo-cAMP, although producing a decrease in the level of phosphorylation of α -G_{i-2}, did not produce a significant inhibition (see figure 4.6 and 4.7; tables 4.3 and 4.4), but insulin was able to inhibit significantly the forskolin stimulated phosphorylation of α -G_{i-2} (see section 4.3.2, tables 4.3 and 4.4, and figures 4.6, 4.7, 4.8, and 4.9). As 8-bromo-cAMP directly activates PKA and also causes the activation of PKC, then the failure of insulin to inhibit the phosphorylation indicates that its point of action must be before the kinase was activated, and hence was also unlikely to be by the activation of a phosphatase. As insulin was able to inhibit the forskolin-stimulated phosphorylation of α -G_{i-2} this suggested that the inhibition may have occurred before the activation of the kinase, at the kinase itself or by the stimulation of phosphatase activity, but as the 8-bromo-cAMP result indicated that it was before the activation of the kinase, then insulin may have produced its effects by inhibiting the production of cAMP by adenylyl cyclase, or by increasing the rate of cAMP degradation by the activation of a phosphodiesterase. Indeed, the insulin-dependent activation of phosphodiesterases has already been reported (see sections 1.2.3.1 and 1.4.3.2; Kilgour *et al.*, 1989; see Houslay, 1990) as has the inhibition of adenylyl cyclase (see section 1.4.3.2; see Häring, 1991).

When hepatocytes were incubated with forskolin and IBMX (see table 4.3 and figure 4.8) it was found that both compounds did not significantly increase the phosphorylation of α -G_{i-2} when compared to the compounds on their own, thus indicating

that PKA may be maximally activated. The inclusion of insulin with forskolin or IBMX produced a significant inhibition of phosphorylation (see table 4.3 and figure 4.9) but inclusion with forskolin and IBMX did not. This again supported the idea that the inhibition occurs before the activation of the kinase and not at the kinase itself because, if insulin inhibited the kinase activity, then it would be able to affect PKA activity even when the kinase was fully activated.

If insulin were producing the inhibition of forskolin-stimulated phosphorylation of α -G_{i-2} solely by the activation of a phosphodiesterase then insulin should not be able to effect the phosphorylation of α -G_{i-2} induced by IBMX, but as it did (see figures 4.8 and 4.9; tables 4.3 and 4.4) then insulin may have produced its effect by the inhibition of adenylyl cyclase activity and therefore suppressing cAMP production. It would appear that, as insulin was able to inhibit α -G_{i-2} phosphorylation in unstimulated cells, then this would produce increased tonic inhibition of adenylyl cyclase activity. This in turn would lead to a decrease in cAMP levels and possibly the inhibition of kinase activity. This in effect would produce a feedback resulting in the further loss of α -G_{i-2} phosphorylation and hence a further decrease in adenylyl cyclase activity. Hence it seems likely that insulin may be exerting its effects at more than one point in the futile α -G_{i-2} phosphorylation cycle, or that other cellular control mechanisms are operating to prevent such a feedback occurring in unstimulated cells. The failure to detect cAMP-dependent phosphorylation of α -G_{i-2} in unstimulated cells also suggests that the inhibitory effect of insulin must be operating by some other mechanism than just the interaction with some components of the cAMP signalling system.

The idea that the phosphorylation of α -G_{i-2} was connected to the loss of inhibition of adenylyl cyclase was proposed by Bushfield *et al.* (Bushfield *et al.*, 1990b) who argued that as the time course of ligand-induced phosphorylation of α -G_{i-2} matched the time course for the loss of α -G_i inhibition of adenylyl cyclase then the two were connected. Other work has shown that the inhibition of adenylyl cyclase by insulin may not be mediated by G_i but caused either by the action of an unique G-protein or possibly by the phosphorylation of adenylyl cyclase itself (see Häring, 1991). The direct involvement of G_i in the attenuation of adenylyl cyclase has been discounted in experiments which show that in diabetic animals, which exhibit G_i depleted hepatocyte plasma membranes and show a loss of cAMP attenuation, the attenuation can be restored by a drug, metformin, which does not affect G_i levels (see Houslay, 1990). This therefore might explain why a feedback of the insulin-dependent suppression of adenylyl cyclase activity on α -G_{i-2} phosphorylation, which then further inhibits adenylyl cyclase, does not occur as α -G_{i-2} is not inhibiting adenylyl cyclase but has some other function.

Although the insulin-induced inhibition of ligand-mediated α -G_{i-2} phosphorylation by a phosphatase has been discounted by insulin's inability to inhibit

8-bromo-cAMP-mediated phosphorylation of α -G_{i-2} the possible role of phosphatases was still investigated by the use of the phosphatase inhibitor okadaic acid (see section 1.2.4.3).

It was found that exposure of ³²P-labelled hepatocytes to okadaic acid significantly increased the phosphorylation of α -G_{i-2} (see table 4.3 and figure 4.12) and the addition of insulin had no effect (see table 4.4 and figure 4.13). As okadaic acid only inhibits phosphatases PP1 and PP2A, and not phosphatases PP2B and PP2C (see sections 1.2.4.3; see Cohen, 1991; Hardie *et al.*, 1991; Haystead *et al.*, 1989), this suggested that insulin was producing its inhibitory effect by the activation of either phosphatases PP1 or PP2A, although this can be discounted by the 8-bromo-cAMP- and PKC-induced phosphorylation where insulin had no effect.

Finally, the effects of glucagon on the phosphorylation of α -G_{i-2} were examined. It has already been reported (Bushfield *et al.*, 1990b) that glucagon caused an increase in the phosphorylation of α -G_{i-2} and that this was accompanied by a loss of the ability of α -G_{i-2} to inhibit adenylyl cyclase. In these studies it was found that glucagon did cause a phosphorylation of α -G_{i-2} (see section 4.3.2, table 4.3 and figure 4.6), that the phosphorylated protein, when digested with trypsin, produced phospho-peptides C1, C2, C3, and AN, and that insulin enhanced the level of glucagon mediated phosphorylation (see section 4.3.2, table 4.4. and figure 4.7). Glucagon has been shown in isolated hepatocytes to raise intracellular cAMP levels, and so activate PKA, and also to activate PKC (Tang & Houslay, 1992).

What these results showed was that even though insulin was potentially increasing the tonic inhibition of adenylyl cyclase by the dephosphorylation of α -G_{i-2}, that the effect of glucagon, by what ever method, not only increased the phosphorylation α -G_{i-2}, and thus removed insulin's inhibitory effect on adenylyl cyclase, but the presence of insulin enhanced the level of phosphorylation, hence decreasing the inhibition of adenylyl cyclase. This may be another indication of the level of control exerted by insulin and glucagon on the metabolism, and hence the blood levels, of glucose. That is, if insulin is suppressing the release of glucose from the liver, then the situation can be rapidly reversed, and the reversal enhanced, upon exposure of the liver to glucagon by an enhanced level of α -G_{i-2} phosphorylation and therefore the suppression of its inhibition of adenylyl cyclase. In effect insulin may be sensitising the liver to glucagon. As this seems unlikely it may indicate that α -G_{i-2} is not involved in the insulin-induced inhibition of adenylyl cyclase activity, something that has already been suggested from studies in streptozotocin treated rats (see section 1.4.3.2; see Houslay, 1990).

The approach that was taken to try and understand the method by which insulin inhibited the phosphorylation of α -G_{i-2} was limited by only being able to focus on one section of the phosphorylation / dephosphorylation mechanism. When attempts were made to examine more than one section the results became confused. What the results did show was that insulin was possibly affecting the phosphorylation of α -G_{i-2} by more than one

method in hepatocytes and this may be viewed as typical of insulin's actions as it has already been demonstrated that the activated insulin receptor is able to effect a number of different secondary messenger systems (see section 1.4.3.2).

Amylin is a recently discovered polypeptide which is co-secreted with insulin, activates adenylyl cyclase and appears, in some ways, to antagonise the effects of insulin (see section 4.1.2). It was found that amylin did stimulate the phosphorylation of α -G_{i-2} but that a concentration of 10^{-6} M was required (see section 4.3.3, table 4.5 and figure 4.17). Two-dimensional phospho-peptide mapping of α -G_{i-2} from hepatocytes that had been treated with amylin showed that at 0.1 pM only three phospho-peptides (C1, C2 and C3) were produced upon trypsin digestion, whilst amylin at 1 μ M produced a four-spot pattern (C1, C2, C3 and AN; see figures 4.31 and 4.32). This finding fits the data for the dose response curve for the activation of adenylyl cyclase by amylin in Bushfield *et al.* (Bushfield *et al.*, 1993) where it was shown that amylin only activates adenylyl cyclase at concentrations greater than 10^{-8} M, hence 1 μ M amylin gave the four-spot pattern typical of a cAMP / PKA-dependent phosphorylation, whilst amylin at 0.1 pM only produced the three spot pattern of unstimulated cells.

When the effect of amylin (1 μ M) on ligand-stimulated phosphorylation of α -G_{i-2} in hepatocytes was examined it was found that the only effect was a reversal of insulin's inhibition of basal phosphorylation (see tables 4.3 and 4.4 and figures 4.18 and 4.19) thus adding further weight to the argument that amylin acts as an antagonist to insulin, although if this was truly the case then an inhibition of glucagon-stimulated phosphorylation might be expected but this was not found. In addition, as amylin has been shown to stimulate cAMP production, although this was only detected in the presence of a phosphodiesterase inhibitor (Bushfield *et al.*, 1993), and at 1 μ M produces a four spot phosphopeptide map typical of an agonist that activates the cAMP system (see figure 4.31), this again suggested that the components of the signalling system maybe compartmentalised so that small localised changes in secondary messenger concentrations are sufficient to activate the kinases present. This may explain the lack of effect of amylin on glucagon induced phosphorylation, that is the non-additive effect of cAMP production, in terms of a maximised localised phosphorylation which amylin cannot enhance. The greater, although not significantly greater, phosphorylation achieved by the gross activators of PKA, such as 8-bromo-cAMP, may represent the phosphorylation of total cellular α -G_{i-2}, whilst glucagon, amylin and insulin effects maybe localised.

The effects of streptozotocin-induced diabetes in Sprague Dawley rats was examined. It has already been reported that the induction of the diabetes caused changes in the expression and levels of phosphorylation of α -G_{i-2} (see section 4.1.1; Bushfield *et al.*, 1990a). Examination of the tryptic digest products of α -G_{i-2} from hepatocytes that had been incubated with vehicle (control; see section 4.3.5 and figure 4.33), 8-bromo-cAMP (300 μ M; see section 4.3.5 and figure 4.33), PMA (100 ng/ml; see section 4.3.5 and figure

4.35), glucagon (10 nM; see section 4.3.5 and figure 4.36) and insulin (10 μ M; see section 4.3.5 and figure 4.37) showed that the induction of diabetes by streptozotocin did not effect the phosphorylation sites of the protein.

Examination of the levels of ligand induced phosphorylation of α -G_{i-2} showed that 8-bromo-cAMP-, PMA- and glucagon-mediated phosphorylation was significantly decreased when compared to control animals that had not been treated with streptozotocin (see section 4.3.4, table 4.6 and figure 4.20). These finding agree with those of Bushfield *et al.* (Bushfield *et al.*, 1990a) and most probably indicate a higher level of cold-phosphorylation of α -G_{i-2} under basal conditions. It does not represent any decrease in α -G_{i-2} found in streptozotocin-induced diabetes (Bushfield *et al.*, 1990a) as ligand-induced phosphorylated samples were compared to control diabetic animals which would have also shown any changes in α -G_{i-2} expression.

When the effects of insulin on the phosphorylation of α -G_{i-2} in streptozotocin treated rats was examined it was found that although some of the effects were now no longer significantly different from control the change that had occurred were not significant (see section 4.3.4, table 4.7 and figure 4.21).

Treatment of rats with streptozotocin not only destroys the β -cells of the pancreas but it also produces a degree of insulin resistance (see section 4.1.1). From the phosphorylation study results it would appear that insulin resistance may be occurring as some of the insulin effects had lost their significance when compared to control.

Chapter 5

Phosphorylation of α -G_{i-2} in hepatocytes from lean (Fa/+) and obese (Fa/Fa) Zucker rats:

Effects of various agents, insulin and BRL 49653

5.1 Introduction

As discussed in Chapters 3 and 4, α -G_{i-2} from Sprague Dawley rat hepatocytes undergoes multi-site phosphorylation by at least two different kinases. Such phosphorylation events can be induced by a number of different compounds but are basically propagated by the activation of PKC and PKA. It has also been shown that insulin caused a dose- and time-dependent inhibition of the phosphorylation of α -G_{i-2}. From such studies it was concluded that insulin may be acting by the simultaneous activation of an unidentified kinase and a phosphatase. Furthermore, the induction of diabetes in a 'type I' model by streptozotocin, in the Sprague Dawley rat significantly increased the basal phosphorylation of α -G_{i-2} but did not effect the insulin-mediated inhibition of basal phosphorylation (see Chapter 4).

To complement such studies, the role of insulin in the phosphorylation of α -G_{i-2} was examined in insulin-resistant obese (Fa/Fa) Zucker rats which are routinely used as a model of the insulin-resistance seen in type II diabetes (see section 5.1.1). Some phosphorylation events relating to α -G_{i-2} in lean (Fa/+) and obese (Fa/Fa) Zucker rat hepatocytes have already been examined. Such studies showed that vasopressin, angiotensin II, and PMA caused an increase in the phosphorylation of α -G_{i-2} in the lean but not in the obese animals. Associated with this was the loss of the inhibitory function of α -G_{i-2} in the lean animals and, as the G_i-inhibition of adenylyl cyclase (see section 1.2.2.2) could not be detected in hepatocytes from obese Zucker rats, this and the inability to phosphorylate α -G_{i-2} from obese Zuckers was taken as evidence of increased basal levels of phosphorylation of α -G_{i-2} (Bushfield *et al.*, 1990c; Houslay *et al.*, 1989). The loss of G_i function has been disputed by Young *et al.* (1991) who have demonstrated that the effect may be dependent on the plasma membrane preparation method used in the assessment of G_i function.

The expression of G-proteins in obese (Fa/Fa) Zucker rat hepatocytes has been examined and it has been reported that there was no change in the level of α -G_i and a decrease in the level of α -G_s (Houslay *et al.*, 1989). The antisera used in the study and the pertussis toxin α -G_i quantification method detected all isoforms of α -G_i present and hence the data may not show any changes in the levels of the particular isoforms present. In contrast, experiments carried out using cardiomyocytes from obese Zucker rats, which also showed a loss of α -G_i-mediated adenylyl cyclase inhibition, did not show a change in the

expression of three species of α -G_s but did identify a decrease in the expression of α -G_{i-1} and α -G_{i-2} (Eckel, Herberg & Wichelhaus, 1993).

If the phosphorylation of α -G_{i-2} is physiologically significant in the control of the signalling system then the increased level of basal phosphorylation of α -G_{i-2} reported in the obese Zucker rat may indicate a dysfunction that occurs in the 'type II' diabetes (see Bushfield *et al.*, 1990c). As Bushfield *et al.* showed that α -G_{i-2} is at the centre of a futile cycle of phosphorylation and de-phosphorylation in Sprague Dawley rats (Bushfield *et al.*, 1991) then the dysfunction in the Zucker rats may indicate that the fault is either as a result of the activation of a kinase or the deactivation of a phosphatase. Thus it may provide a useful point for target ligands in the treatment of 'type II' diabetes.

Considerable interest has been expressed by the pharmaceutical industry in developing a drug strategy for the treatment of type II diabetes. Type II diabetes represents a heterogeneous disease in that the development of the disease may result from different initiators but resulting in the appearance of a similar set of clinical symptoms (see section 1.3.1). The treatment of the disease can be divided into two main approaches: the achievement of near normal glucose metabolism, that is the abolition of elevated fasting glucose levels and the restoration of glucose tolerance; or the prevention of long term complications (see section 1.3.1). As the dysfunction that occurs in the insulin signalling system is unknown, and as insulin produces a wide range of cellular events by the interaction with a number of different signal transduction systems (see table 1.3 and section 1.4), then there is no clear target point for drug intervention. As a result, most attention has been focused on the treatment of the secondary complications and not the correction of glucose metabolism.

To date the main drug treatment for type II diabetes has involved the use of sulphonylureas and a compound called metformin. The sulphonylureas work by stimulating the production of insulin by the pancreas and this may result in several complications occurring. First, the increased levels of insulin production only adds to the problems already created by the high levels of insulin present and can lead to hypoglycaemia, coma and sometimes death; second, the strain on the pancreas is increased, as a result of the increased insulin production and this may hasten the failure of the organ so that type II diabetes becomes type I as the disease progresses. The method of action of metformin is unknown but it may affect glucose absorption and hepatic gluconeogenesis.

A better approach to the treatment of type II diabetes may therefore be to improve tissue insulin sensitivity. This would have the benefits of avoiding the risk of hypoglycaemia, reducing the strain of excessive insulin production on the pancreas, reducing complications resulting from hyperinsulinaemia and hyperglycaemia, and possibly restoring amylin secretion to normal physiological levels as the level of hyperinsulinaemia decreases (see section 4.1.2). To this end a group of ligands called thiazolidinediones may prove beneficial in the treatment of type II diabetes as it has been shown that they can

increase insulin sensitivity, and decrease hyperinsulinaemia and hyperglycemia (see section 5.1.2).

5.1.1 *The Zucker rat model of 'type II' diabetes*

The Zucker rats (*Rattus norvegicus*) are a strain of rats which resulted from a spontaneous mutation when two strains of laboratory rat were mated, and as a result have a genetic disposition to obesity, although the exact genetic defect is unknown (see Kasiske, O'Donnell & Keane, 1992). The rats were first described in 1961 by Zucker and Zucker (Zucker & Zucker, 1961; see also Bray, 1977) and are now well established as a rodent model for the insulin resistance as seen in type II diabetes (see Ionescu, Sauter & Jeanrenaud, 1985).

The obese (Fa/Fa) Zucker rat displays some of the characteristics associated with 'type II' diabetes (see section 1.3.1) and it has been found that they are hyperinsulinaemic (see Kasiske *et al.*, 1992; Bray, 1977; Stern *et al.*, 1975; Zucker & Antoniadis, 1972) but are not normally hyperglycaemic (see Ionescu *et al.*, 1985; Bray, 1977; Zucker & Antoniadis, 1972), although instances have been reported (McCaleb & Sredy, 1992; Triscari *et al.*, 1979); they are glucose tolerant when it is administered intravenously, but not orally (see Ionescu *et al.*, 1985); are hypoglucagonaemic (see Bray, 1977) and are insulin-resistant (see Kasiske *et al.*, 1992; King *et al.*, 1992; Sherman *et al.*, 1988; Stern *et al.*, 1975).

The lack of hyperglycemia may be explained by increased rates of insulin-independent glucose uptake and incorporation into lipids in the liver of obese (Fa/Fa) rats (Carbó, Lopéz-Soriano & Argilés, 1991). The degree to which hyperinsulinaemia and insulin-resistance develops can be dictated by the diet the rats are fed. It has been found that animals that have diets low in carbohydrates but high in fat exhibit hyperinsulinaemia, insulin resistance in the muscle, and reduced levels of lipogenesis in the adipocytes. In contrast, animals on a high carbohydrate diet exhibit a higher level of hyperinsulinaemia, increased levels of lipogenesis and are insulin-sensitive in the muscles (Stern *et al.*, 1975). In fasting obese (Fa/Fa) rats the insulin levels observed are generally ten-times higher than in lean (Fa/+) animals with postprandial levels rising even higher (Kasiske *et al.*, 1992).

The insulin resistance reported in the muscle is believed to represent an impairment of the glucose transport process (Sherman *et al.*, 1988) such as a failure of the transporter to translocate to the plasma-membrane (King *et al.*, 1992). However, a decrease in the auto-phosphorylation of the insulin receptor in the muscle, but not the liver, has also been reported (Slieker *et al.*, 1990). Interestingly, streptozotocin-treatment of obese rats, which effectively eliminates the hyperinsulinaemia (see section 4.1.1), appears to correct the receptor phosphorylation defect (see Kasiske *et al.*, 1992). In addition, a PKC component of the insulin resistance has been reported as it was found that in lean (Fa/?) Zucker rat hearts and hepatocytes that the phorbol ester, PMA, could stimulate the transport of glucose

and inhibit the insulin effects on transportation, yet in obese (Fa/Fa) rats this effect was abolished. PKC has also been implicated in the alteration in the hormonal responsiveness of hepatocytes from lean (Fa/+) and obese (Fa/Fa) Zucker rats where it was found that the obese animals showed a decreased responsiveness to PMA treatments and also reduced activity of PKC has been found in the heart and liver samples from the obese animals (García-Sánchez *et al.*, 1992; Van der Werve *et al.*, 1987)

5.1.2 The thiazolidinediones and BRL 49653

A number of pharmaceutical companies are developing compounds that could be used in the treatment of type II diabetes. These compounds are based on analogues of thiazolidinedione (see Colca & Morton, 1990; Weinstein *et al.*, 1993).

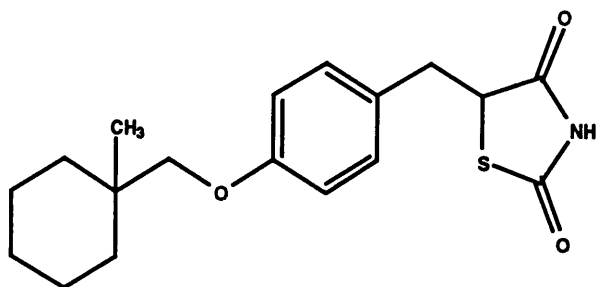
One of the earliest developed compounds was called ciglitazone (5-[4-(1-methylcyclohexyl-methoxy)benzyl]thiazolidine-2,4-dione, developed by Takeda Chemical Industries, Japan; see figure 5.1). Although originally developed for another purpose, it was found that at the high concentrations used during toxicological testing it was able to suppress blood glucose levels. Further examination showed that the compound seemed to produce its effects by improving insulin sensitivity, and hence possessed hypoglycaemic properties. Development of the compound was finally stopped when toxicological complications became apparent (see Colca & Morton, 1990).

Using ciglitazone (see figure 5.1) as a starting compound chemical modifications have been made to reduce the toxic properties and to improve its biological activity in increasing insulin sensitivity (see Colca & Morton, 1990). Examples of the compounds that have been produced and have been shown to have hypoglycaemic effects are pioglitazone (5-[4-[2-(5-ethyl-2-pyridinyl)ethoxy]benzyl]thiazolidine-2,4-dione; Takeda Chemical Industries, Japan; see figure 5.1), CS-045 ((±)-5-[4-(6-hydroxy-2,5,7,8-tetramethylchroman-2-yl-methoxy)benzyl]-2,4-thiazolidinedione; Sankyo Company Ltd., Japan; see figure 5.1); englitazone (also called CP 68,722; (±)-5-[(3,4-dihydro-2-phenylmethyl-2H-1-benzopyran-6-yl)methyl]-thiazolidine-2,4-dione; Pfizer, US; see figure 5.1); and BRL 49653 (5-(4-[2-(N-methyl-N-(2-pyridyl)amino)ethoxy]benzyl)-thiazolidine-2,4-dione; SmithKline Beecham; see figure 5.1). All of these compounds possess the ability to reduce hyperinsulinaemia and hyperglycemia, and improve insulin sensitivity in animal models, but are only effective after chronic daily dosing over a period of days or weeks.

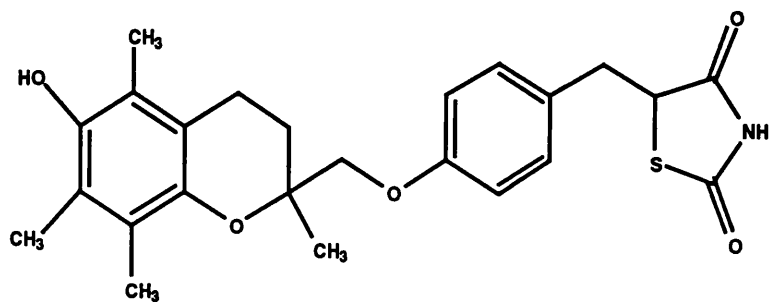
Pioglitazone (see figure 5.1) has been shown to increase insulin sensitivity in obese Wistar rats and obese mice (Kobayashi *et al.*, 1992; see Hofmann *et al.*, 1992; Colca & Morton, 1990). In the obese mice it has been found that the liver's sensitivity to insulin was increased and this therefore helped to reduce the levels of hepatic glucose output and therefore reduce fasting hyperglycemia, and reduce hyperinsulinaemia (Iwanishi &

Figure 5.1: Chemical structures of ciglitazone, CS-045, pioglitazone, englitazone (CP 68722) and BRL 49653

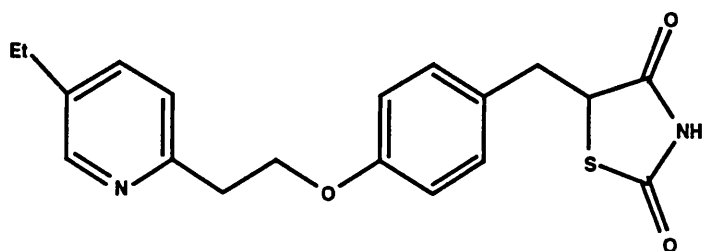
Chemical structures of ciglitazone (5-[4-(1-methylcyclohexyl-methoxy)benzyl]thiazolidine-2,4-dione), CS-045 ((±)-5-[4-(6-hydroxy-2,5,7,8-tetramethyl-chroman-2-yl-methoxy)-benzyl]-2,4-thiazolidinedione), pioglitazone (5-{4-[2-(5-ethyl-2-pyridinyl)ethoxy]benzyl}-thiazolidine-2,4-dione), englitazone (CP 68722; (±)-5-[(3,4-dihydro-2-phenylmethyl-2H-1-benzopyran-6-yl)methyl]-thiazolidine-2,4-dione) and BRL 49653 (5-(4-[2-(N-methyl-N-(2-pyridyl)amino)ethoxy]benzyl)-thiazolidine-2,4-dione).



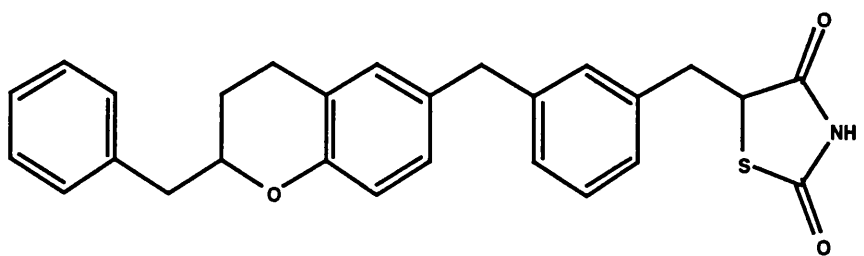
Ciglitazone



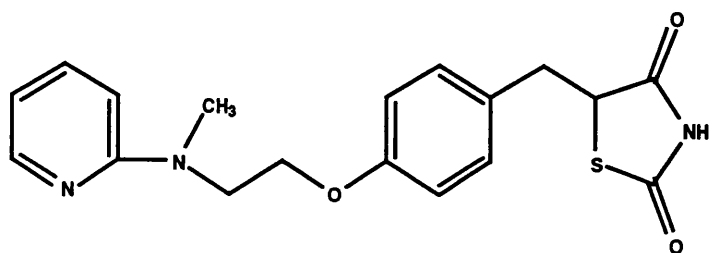
CS-045



Pioglitazone



Englitazone
(CP 68722)



BRL 49653

Kobayashi, 1993; Hofmann *et al.*, 1992; Hofmann, Lorenz & Colca, 1991; Ikeda *et al.*, 1990). It has been demonstrated that the compound can correct the reduction in glucose transporter (GLUT4) expression seen in the fat and muscle of diabetic obese mice, but the method by which it increases the liver's sensitivity to insulin is unknown. However, it has been shown not to involve changes in the expression of the liver glucose transporter GLUT2 which do not change in the diabetic state (Hofmann *et al.*, 1992; Hofmann *et al.*, 1991). Studies in cultured 3T3-F442A cells have demonstrated that pioglitazone may be increasing the expression of GLUT4 in fat cells by stabilising and increasing the half-life of its mRNA (Sandouk, Reda & Hofmann, 1993). Information on its mode of action has also come from studies on the muscle of obese Wistar rats and rats on a high-fat diet where it has been shown that the compound does not effect insulin binding to its receptor but increases the tyrosine kinase activity of the receptor when insulin is present (Iwanishi & Kobayashi, 1993; Kobayashi *et al.*, 1992). Additional evidence from cell culture studies of brown adipose tissue and observation in diabetic rodents, indicate that it may operate by enhancing the growth and differentiation of the tissue (Foellmi, Wyse & Kletzien, 1993).

Englitazone (also called CP 68722; see figure 5.1) was developed by Pfizer and, like all the thiazolidinediones, has the effect of reducing hyperinsulinaemia and hyperglycemia in animal models of type II diabetes (Bowen *et al.*, 1991; Stevenson *et al.*, 1990; see Kreutter *et al.*, 1990). Studies on 3T3-L1 adipocytes have shown that unlike some of the other compounds it is able to stimulate glucose uptake by the cultured cells in the absence of added insulin and that this increase in glucose uptake could be inhibited by the inclusion of a protein synthesis inhibitor. This suggests that the compound may produce its effects by the stimulation of the synthesis of glucose transporters which were able to translocate to the cell membrane (Kreutter *et al.*, 1990). The insulin-independent effect of englitazone has also been reported in isolated rat hepatocytes where it was found that the compound could produce insulin-like effects on glycogenesis, glucose oxidation and glycolysis, but without affecting the auto-phosphorylation of the insulin receptor or the phosphorylation IRS1 (see section 1.4.3.1). In addition, the same study showed that englitazone also antagonised glucagon responses (McPherson *et al.*, 1993).

CS-045 (see figure 5.1) has again been shown to reduce hyperinsulinaemia and hyperglycaemia in animal models of type II diabetes (Fujiwara *et al.*, 1988; see Colca & Morton, 1990) and has also proved successful in studies with diabetic humans (Kaneko *et al.*, 1993; Suter *et al.*, 1992) although some mild side effects have been reported (Kaneko *et al.*, 1993). Again the compound is thought to work by increasing insulin binding in the adipocytes and improving the sensitivity to insulin (Fujiwara *et al.*, 1988).

The antihyperglycaemic properties of BRL 49653 (see figure 5.1) have been assessed in a number of animal models of diabetes and has been shown to be sixty-times more potent than pioglitazone and 100-200 times more potent than CS-045 (Cawthorne *et al.*, 1993). It has been shown that for the compound to produce any effect that the dosage

has to be chronic and the application of a single dose has no effect. In the type II diabetes models used, diabetic mice (ob/ob and db/db) and obese (Fa/Fa) Zucker rats, it was found that the compound reduced hyperinsulinaemia and hyperglycemia and improved glucose tolerance. In addition, in none of the animals studied was it found that excessively high doses of BRL 49653 caused hypoglycaemia (Cawthorne *et al.*, 1993; Young *et al.*, 1993). Studies were also carried out using normal Sprague Dawley rats and Sprague Dawley rats that had 'type-I' diabetes induced by the use of alloxan or streptozotocin (see section 4.1.1). In all cases it was found that the compound had no effect, although increased insulin sensitivity could be observed upon dosing with insulin. This demonstrated that it could not affect non-insulin resistant animals and required the presence of insulin to be active.

Examination of the effect of insulin on adipocytes derived from obese mice that had been treated with BRL 49653 showed that, when compared to animals that had not been treated, the compound increased the number of insulin receptors, improved insulin responsiveness, increased GLUT4 expression and translocation to the membrane and did not effect glucose uptake in the absence of insulin (Cawthorne *et al.*, 1993; Young *et al.*, 1993).

In the obese (Fa/Fa) Zucker rat it was found that treatment of the animal for 21 days with BRL 49653 increased insulin sensitivity as measured by a hyperinsulinaemic-euglycaemic clamp (Cawthorne *et al.*, 1993; Smith *et al.*, 1993). The clamp is performed by an intravenous infusion of insulin to elevate the low basal insulin concentration. This results in a suppression of glucose production by the liver and an increased uptake of glucose by peripheral tissue such as the muscle. To maintain the blood glucose level at the pre-insulin-infusion concentration glucose has to be variably administered. In obese Zucker rats that had not been treated with BRL 49653 it was found that the infusion of insulin did affect blood glucose levels by suppression of glucose output by the liver, and therefore additional glucose was required. Animals that had been treated with BRL 49653 also required additional glucose to maintain the blood glucose level but the level of glucose required was significantly higher hence indicating insulin sensitivity had been restored. In obese Zucker rats it was also found that chronic treatment of the animals with BRL 49653 did not effect the number of insulin receptors present per hepatocyte and did not alter the tyrosine kinase activity of the receptor. These observations suggest that the point of action of BRL 49653 in the Zucker rat hepatocytes is not at the insulin receptor but at some point post-receptor (Smith *et al.*, 1993).

The method by which BRL 49653 produces its effects is unknown although it has been established that it does not bind to any of a wide range of cell surface receptors. Additional information has come from a study on insulin-resistant (high-fat-fed) rats where it was shown that the compound reduced basal insulin levels in the control and insulin resistant rats and reversed insulin resistance in the liver and the muscle. It was proposed that the correction of insulin resistance resulted from the reduced basal levels and therefore

removing any desensitisation effects resulting from hyperinsulinaemia (Kraegen *et al.*, 1993).

5.2 *Aims*

It has been established that α -G_{i-2} undergoes ligand dependent multi-site phosphorylation in Sprague Dawley rat hepatocytes, that insulin affects the basal level of phosphorylation and some changes occur when Sprague Dawley rats are made diabetic by the use of streptozotocin (see Chapters 3 and 4).

To examine further the effects of diabetes on the expression and phosphorylation of α -G_{i-2} in more detail it is proposed to carry out a series of experiments on hepatocytes from lean (Fa/+) and the insulin resistant obese (Fa/Fa) Zucker rat.

The compound BRL 49653 has been shown to be beneficial in restoring insulin-sensitivity and therefore reducing hyperinsulinaemia and hyperglycemia in the obese Zucker rat (see section 5.1.2). Animals that have been dosed with this compound were also examined to see if it affected the phosphorylation characteristics of α -G_{i-2}.

Finally, hepatocytes from lean and obese Zucker rats, which were and were not chronically dosed with BRL 49653, were examined to assess the levels of α -G_{i-2} and PKC isoforms expression and the distribution of the proteins between the cytosol and membrane fractions.

5.3 *Results*

5.3.1 *Treatment of Zucker rats with BRL 49653*

From previous work carried out at SmithKline Beecham (see Cawthorne *et al.*, 1993; Smith *et al.*, 1993; Young *et al.*, 1993) it has been established that Zucker rats require 21 days of oral dosing with BRL 49653 at 3 μ mole per kilogram for the compound to be effective. BRL 49653 was prepared for dosing by dissolving it in a few drops of 1 M NaOH and almost making it up to the required volume to which HCl was added until the compound started to precipitate. Finally, one drop of 1 M NaOH was added and the solution checked for precipitation of the compound. As a result of the previous studies and the nature of the diabetic state in obese Zucker rats, it was decided that animals should be fasted for 5 hours prior to experiments.

It is known that the diet fed to obese Zucker rats can affect their diabetic condition (Stern *et al.*, 1975) and thus the animals used in these studies had free access to standard laboratory rat food (Oxoid rat and mouse breeders diet; H.C. Styles, Bewdley, Worcs. UK; see Young *et al.*, 1991) and water.

5.3.2 *Phosphorylation of α -G_{i-2} in lean (Fa/+) and obese (Fa/Fa) Zucker rat hepatocytes*

Hepatocytes were prepared from lean (Fa/+) and obese (Fa/Fa) Zucker rats as described in section 2.2.2 with the changes noted in section 5.3.1. The hepatocytes were then labelled with ³²P and the phosphorylation experiments carried out as described in sections 2.2.3 to 2.2.5.

Two typical autoradiographs of immunoprecipitated α -G_{i-2} from hepatocytes of lean and obese Zucker rats are shown in figures 5.2 and 5.3. Further analysis of the data by Cerenkov counting of the gel chips containing the phosphorylated α -G_{i-2} revealed that in the lean animals 8-bromo-cAMP (300 μ M), PMA (100 ng/ml) and glucagon (10 nM; see section 4.1.2) all caused a significant increase in the level of phosphorylation of α -G_{i-2} whilst in the obese animals only 8-bromo-cAMP was effective (see figure 5.4 and table 5.1). The inclusion of insulin (10 μ M) in the incubation mixture did not result in a significant phosphorylation of α -G_{i-2} in the lean or the obese animals (see figure 5.4 and table 5.1).

However, when insulin was added in conjunction with various ligands it was found that insulin significantly inhibited PMA and glucagon stimulation of α -G_{i-2} phosphorylation in the lean animals but not 8-bromo-cAMP stimulated, and inhibited 8-bromo-cAMP and glucagon stimulated α -G_{i-2} phosphorylation in the obese animals but did not affect the actions of PMA (see figures 5.5 and table 5.2).

5.3.3 *Effects of chronic dosing of lean (Fa/+) and obese (Fa/Fa) Zucker rats with BRL 49653 on the phosphorylation of α -G_{i-2} in hepatocytes*

Lean and obese Zucker rats were dosed with BRL 49653 as described in section 5.3.1. Hepatocytes were then prepared from lean (Fa/+) and obese (Fa/Fa) Zucker rats as described in section 2.2.2 with the changes noted in section 5.3.1. The hepatocytes were labelled with ³²P and the phosphorylation experiments carried out as described in sections 2.2.3 to 2.2.5.

Two typical autoradiographs of immunoprecipitated α -G_{i-2} from hepatocytes of dosed-lean and dosed-obese Zucker rats are shown in figures 5.6 and 5.7. Further analysis of the data by Cerenkov counting of the gel chips containing the phosphorylated α -G_{i-2} revealed that in the dosed-lean animals, 8-bromo-cAMP (300 μ M), and PMA (100 ng/ml; see section 4.1.2) both caused a significant increase in the level of phosphorylation of α -G_{i-2} (see figure 5.8 and table 5.1), whereas glucagon (10 nM; see section 4.1.2) and insulin did not have any effect (see figure 5.8 and table 5.1). When these data were compared with lean animals that had not been dosed with BRL 49653 it was found that the loss of glucagon stimulated phosphorylations of α -G_{i-2} was significantly different (see figure 5.8).

Figure 5.2: A typical auto-radiograph of ^{32}P phosphorylated $\alpha\text{-G}_{i-2}$ from lean (Fa/+) Zucker rat hepatocytes that have been challenged with vehicle solution, 8-bromo-cAMP, PMA, glucagon, insulin, 8-bromo-cAMP and insulin, glucagon and insulin, PMA and insulin, and vehicle solution

A typical auto-radiograph of an SDS-PAGE gel containing $\alpha\text{-G}_{i-2}$ immunoprecipitated from lean (Fa/+) Zucker rat hepatocytes that had been labelled with ^{32}P (see sections 2.2.2 and 2.2.3) and then challenged with vehicle solution (lane 1), 8-bromo-cAMP (lane 2; 300 μM), PMA (lane 3; 100 ng/ml), glucagon (lane 4; 10 nM), insulin (lane 5; 10 μM), 8-bromo-cAMP and insulin (lane 6), glucagon and insulin (lane 7), PMA and insulin (lane 8), and vehicle solution (lane 9) for 15 minutes. Where the hepatocytes were challenged with a drug and insulin the insulin was added first followed immediately by the drug.

1 2 3 4 5 6 7 8 9

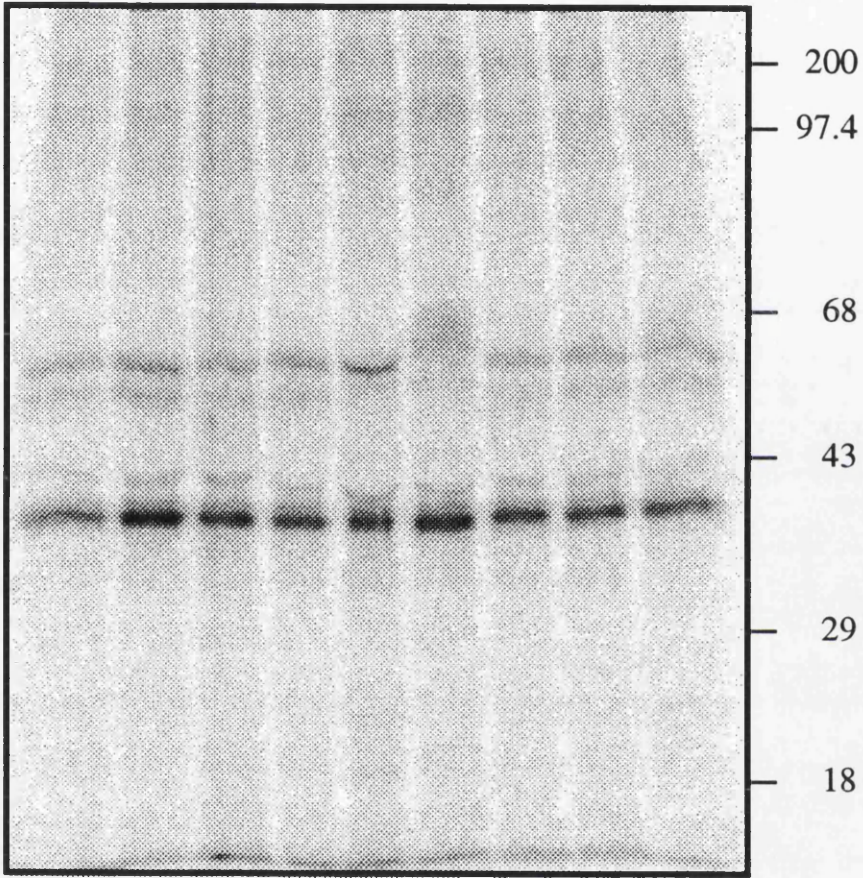


Figure 5.3: A typical auto-radiograph of ^{32}P phosphorylated $\alpha\text{-G}_{i-2}$ from obese (Fa/Fa) Zucker rat hepatocytes that have been challenged with vehicle solution, 8-bromo-cAMP, PMA, glucagon, insulin, 8-bromo-cAMP and insulin, glucagon and insulin, PMA and insulin, and vehicle solution

A typical auto-radiograph of an SDS-PAGE gel containing $\alpha\text{-G}_{i-2}$ immunoprecipitated from obese (Fa/Fa) Zucker rat hepatocytes that had been labelled with ^{32}P (see sections 2.2.2 and 2.2.3) and then challenged with vehicle solution (lane 1), 8-bromo-cAMP (lane 2; 300 μM), PMA (lane 3; 100 ng/ml), glucagon (lane 4; 10 nM), insulin (lane 5; 10 μM), 8-bromo-cAMP and insulin (lane 6), glucagon and insulin (lane 7), PMA and insulin (lane 8), and vehicle solution (lane 9) for 15 minutes. Where the hepatocytes were challenged with a drug and insulin the insulin was added first followed immediately by the drug.

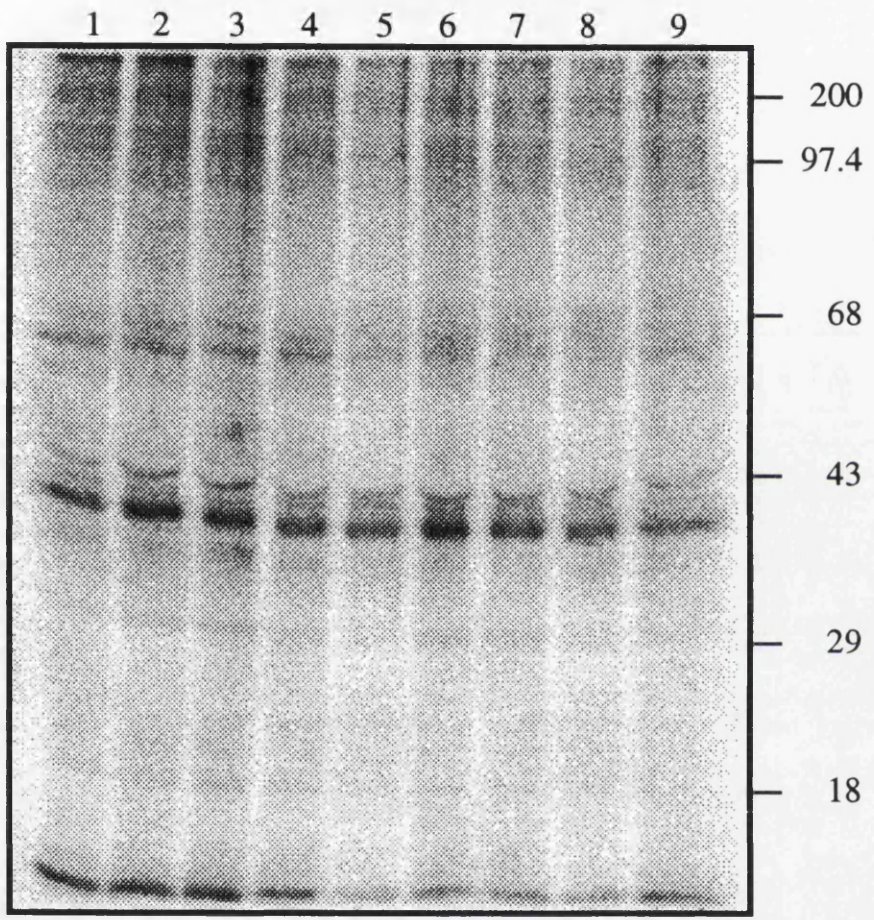


Figure 5.4: Percentage phosphorylation of α -G_{i-2} in lean (Fa/+) and obese (Fa/Fa) Zucker rat hepatocytes: Effects of 8-bromo-cAMP, PMA, glucagon, and insulin

Stimulation of α -G_{i-2} phosphorylation in lean (Fa/+) and obese (Fa/Fa) Zucker rat hepatocytes labelled with ³²P (see sections 2.2.2 and 2.2.3) and then challenged with 8-bromo-cAMP (8Br; 8BrcAMP; 300 μ M), PMA (100 ng/ml), glucagon (Gluc; 10 nM), and insulin (Ins; 10 μ M) for 15 minutes. Where the hepatocytes were challenged with a ligand and insulin the insulin was added first followed immediately by the ligand. The hepatocytes were harvested and α -G_{i-2} immunoprecipitated with antiserum 1867. The proteins were separated by SDS-PAGE (see sections 2.2.4 and 2.2.5) and the resulting gels dried and put down for autoradiography (see section 2.2.5). The level of phosphorylation achieved was determined by Cerenkov counting of gel chips that contained phosphorylated α -G_{i-2}. The data is expressed as mean \pm SEM ($n \geq 4$; see table 5.1) where * indicates that the data are significantly different ($p < 0.05$) from control (0%) with data tested using a single sample Student's *t*-test and † indicates a significant difference between phosphorylations in hepatocytes from Fa/+ and Fa/Fa (two sample Student's *t*-test where $p < 0.05$ was taken as significantly different).

Figure 5.5: Percentage inhibition of ligand induced α -G_{i-2} phosphorylation in lean (Fa/+) and obese (Fa/Fa) Zucker rat hepatocytes: Effects of insulin on 8 bromo-cAMP, PMA and glucagon induced phosphorylations

Insulin induced inhibition of ligand induced α -G_{i-2} phosphorylation in lean (Fa/+) and obese (Fa/Fa) Zucker rat hepatocytes labelled with ³²P (see sections 2.2.2 and 2.2.3). The hepatocytes were challenged with 8-bromo-cAMP (8BrcAMP; 300 μ M), PMA (100 ng/ml), glucagon (Gluc; 10 nM) for 15 minutes in the presence and absence of insulin (Ins; 10 μ M). The hepatocytes were harvested and α -G_{i-2} immunoprecipitated with antiserum 1867. The proteins were separated by SDS-PAGE (see sections 2.2.4 and 2.2.5) and the resulting gels dried and put down for autoradiography (see section 2.2.5). The level of phosphorylation achieved was determined by Cerenkov counting of gel chips that contained phosphorylated α -G_{i-2}. The data are expressed as mean \pm SEM ($n \geq 4$; see table 5.2) where * indicates that the data are significantly different ($p < 0.05$) from control (ligand in the absence of insulin, 0%) with data tested using a single sample Student's *t*-test.

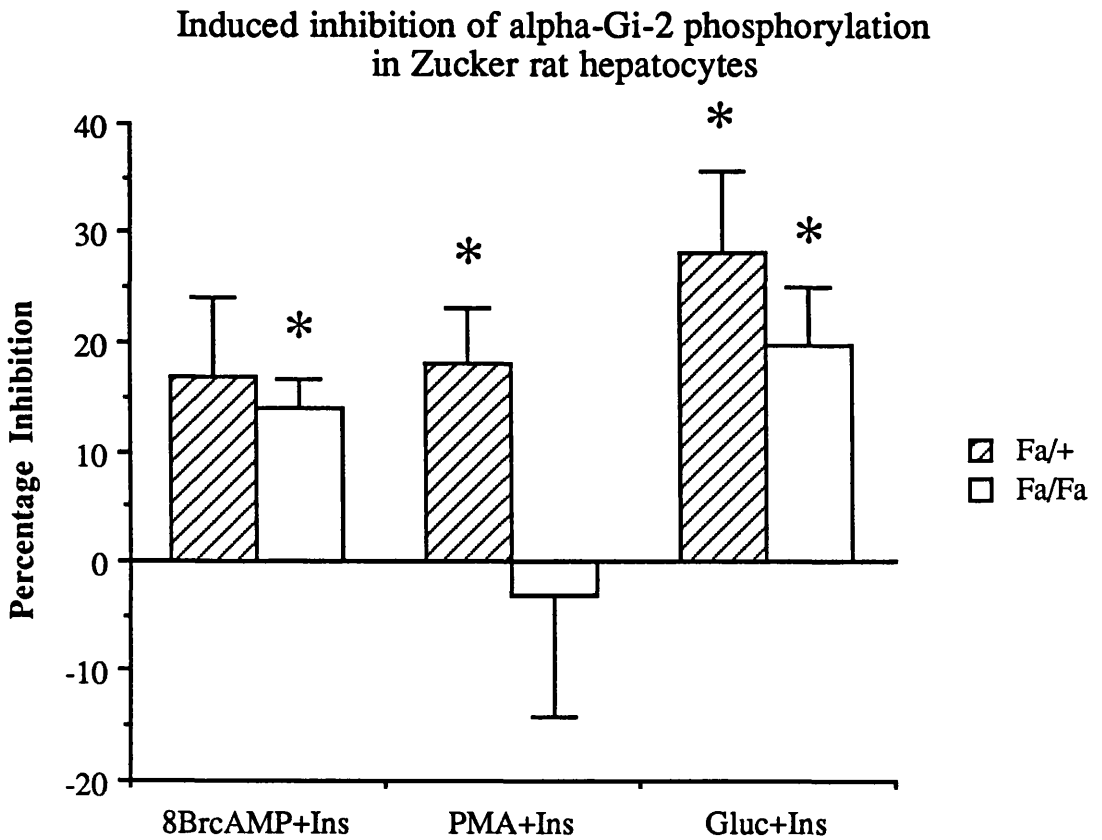
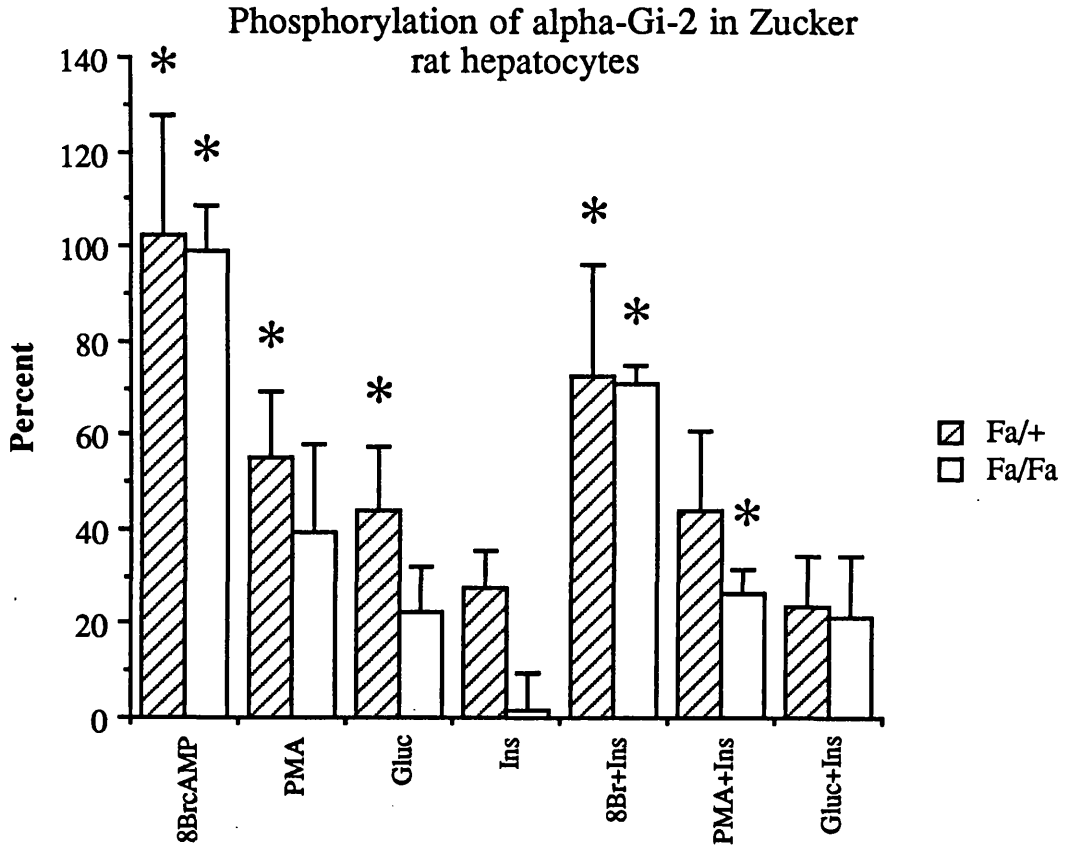


Figure 5.6: A typical auto-radiograph of ^{32}P phosphorylated $\alpha\text{-G}_{i-2}$ from hepatocytes from BRL 49653 dosed lean (Fa/+) Zucker rats that have been challenged with vehicle solution, 8-bromo-cAMP, PMA, glucagon, insulin, 8-bromo-cAMP and insulin, glucagon and insulin, PMA and insulin, and vehicle solution

A typical auto-radiograph of an SDS-PAGE gel containing $\alpha\text{-G}_{i-2}$ immunoprecipitated hepatocytes from lean (Fa/+) Zucker rat that had been dosed with BRL 49653. The hepatocytes were labelled with ^{32}P (see sections 2.2.2 and 2.2.3) and then challenged with vehicle solution (lane 1), 8-bromo-cAMP (lane 2; 300 μM), PMA (lane 3; 100 ng/ml), glucagon (lane 4; 10 nM), insulin (lane 5; 10 μM), 8-bromo-cAMP and insulin (lane 6), glucagon and insulin (lane 7), PMA and insulin (lane 8), and vehicle solution (lane 9) for 15 minutes. Where the hepatocytes were challenged with a drug and insulin, the insulin was added first followed immediately by the drug.

1 2 3 4 5 6 7 8 9

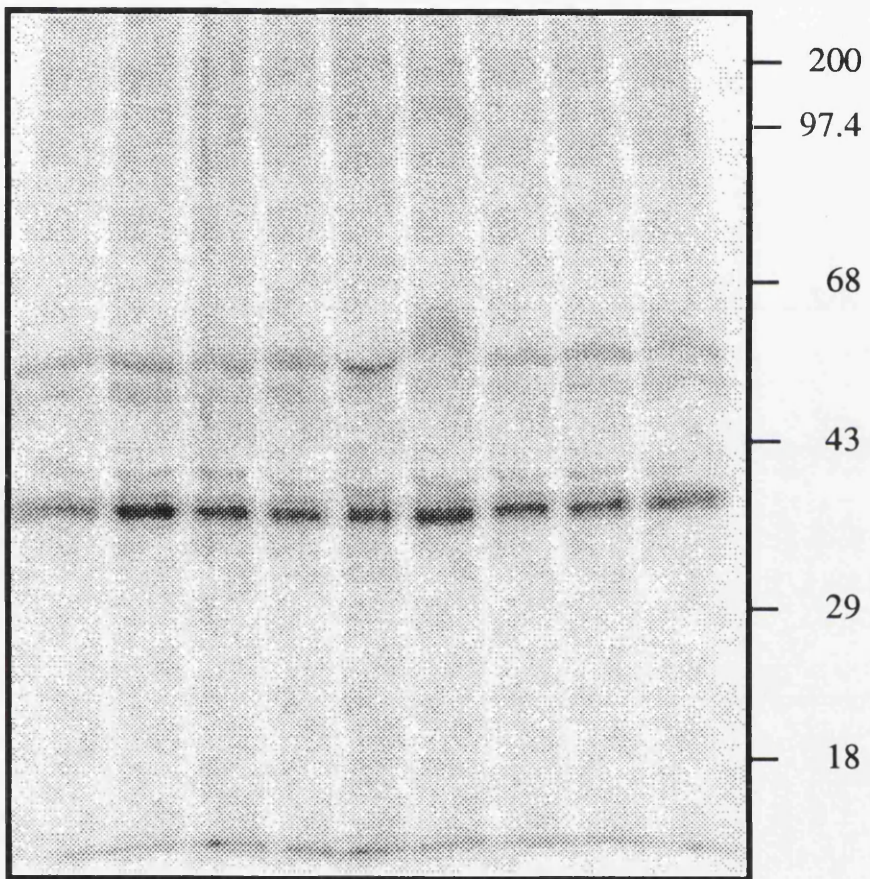


Figure 5.7: A typical auto-radiograph of ^{32}P phosphorylated $\alpha\text{-G}_{i-2}$ from hepatocytes from BRL 49653 dosed obese (Fa/Fa) Zucker rats that have been challenged with vehicle solution, 8-bromo-cAMP, PMA, glucagon, insulin, 8-bromo-cAMP and insulin, glucagon and insulin, PMA and insulin, and vehicle solution

A typical auto-radiograph of an SDS-PAGE gel containing $\alpha\text{-G}_{i-2}$ immunoprecipitated hepatocytes from obese (Fa/Fa) Zucker rat that had been dosed with BRL 49653. The hepatocytes were labelled with ^{32}P (see sections 2.2.2 and 2.2.3) and then challenged with vehicle solution (lane 1), 8-bromo-cAMP (lane 2; 300 μM), PMA (lane 3; 100 ng/ml), glucagon (lane 4; 10 nM), insulin (lane 5; 10 μM), 8-bromo-cAMP and insulin (lane 6), glucagon and insulin (lane 7), PMA and insulin (lane 8), and vehicle solution (lane 9) for 15 minutes. Where the hepatocytes were challenged with a drug and insulin, the insulin was added first followed immediately by the drug.

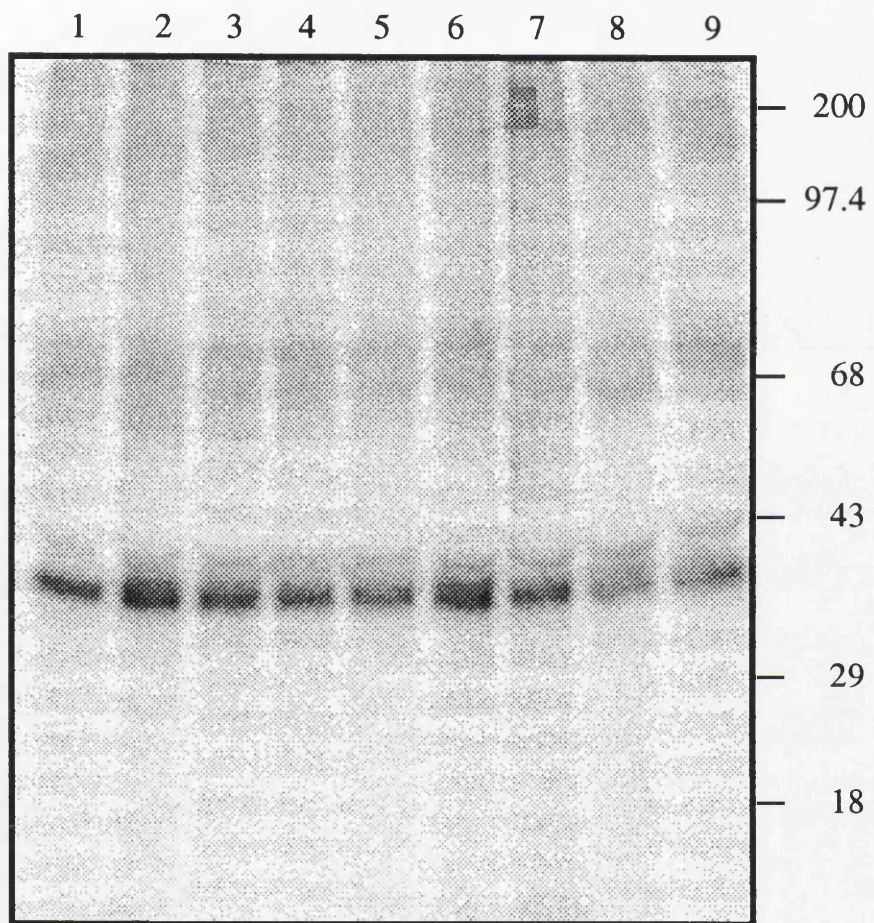


Table 5.1: Percentage stimulation of the phosphorylation of α -G_{i-2} in lean (Fa/+) and obese (Fa/Fa) Zucker rat hepatocytes and the effects of BRL 49653.

	Fa/+					Fa/Fa				
	Mean	SEM	n=	p=	T	Mean	SEM	n=	p=	T
8BrcAMP	103	25	5	0.016	Y	100	9	5	0.000	Y
PMA	56	14	5	0.017	Y	30	17	5	0.169	N
Gluc	40	16	5	0.034	Y	-2	25	5	0.945	N
Ins	40	21	5	0.065	N	2	7	5	0.835	N
8Br + Ins	73	23	5	0.037	Y	71	3	5	0.000	Y
PMA + Ins	44	16	5	0.056	N	27	4	5	0.005	Y
Gluc + Ins	24	10	5	0.090	N	22	12	5	0.167	N

	Fa/+ Dosed					Fa/Fa Dosed				
	Mean	SEM	n=	p=	T	Mean	SEM	n=	p=	T
8BrcAMP	104	19	5	0.006	Y	95	17	4	0.013	Y
PMA	28	8	6	0.021	Y	39	14	5	0.062	N
Gluc	8	9	6	0.445	N	27	12	4	0.127	N
Ins	3	6	6	0.620	N	8	8	5	0.406	N
8Br + Ins	75	15	6	0.005	Y	82	18	5	0.012	Y
PMA + Ins	15	18	5	0.466	N	27	5	5	0.011	Y
Gluc + Ins	15	8	6	0.114	N	12	4	5	0.051	N

Control was taken as 0% phosphorylation of α -G_{i-2}. Fa/+ = lean animals; Fa/Fa = obese animals; Fa/+ Dosed = Fa/+ animals that had been dosed with BRL 49653; Fa/Fa Dosed = Fa/Fa animals that had been dosed with BRL 49653; SEM = standard error of mean; n = number of observations; p = significance value returned by single sample Student's *t*-test; T = result of a single sample Student's *t*-test where Y = phosphorylation was significantly different from control (0%; $p < 0.05$) and N = phosphorylation was not significantly different from control (0%; $p > 0.05$); 8Br = 8BrcAMP = 8-bromo-cAMP (300 μ M); PMA = Phorbol 12-myristate 13-acetate (100 ng/ml); Gluc = Glucagon (10 nM); Ins = Insulin (10 μ M).

When the inhibitory effects of insulin on ligand induced phosphorylation of α -G_{i-2} was examined it was found that insulin (10 μ M) had no effect on the levels of phosphorylation induced by 8-bromo-cAMP (300 μ M), PMA (100 ng/ml) or glucagon (10 nM; see figures 5.9 and table 5.2). Although these data showed some change from that observed in the non-dosed lean the changes that occurred were not significant.

Examination of the data of phosphorylated α -G_{i-2} from dosed-obese animals showed that 8-bromo-cAMP (300 μ M), and PMA (100 ng/ml) caused a significant increase in the level of phosphorylation of α -G_{i-2} (see figure 5.10 and table 5.1) whereas glucagon

(10 nM; see section 4.1.2) and insulin did not (see figure 5.10 and table 5.1). When these data were compared with obese animals that had not been dosed with BRL 49653 it was found that there was no significant change in the levels of phosphorylation (see figure 5.10).

When the inhibitory effects of insulin on ligand induced phosphorylation of α -G_{i-2} in hepatocytes from dosed-obese animals was examined it was found that insulin (10 μ M) no longer significantly inhibited any ligand induced phosphorylations, and although this was a change from the results seen in non-dosed obese animals the change was not significant (see figure 5.11 and table 5.2).

5.3.4 *Two-dimensional phosphopeptide mapping of tryptic peptides of α -G_{i-2} from lean (Fa/+) and obese (Fa/Fa) Zucker rats*

Hepatocytes from lean and obese Zucker rats were labelled with ³²P and incubated with either vehicle, PMA (100 ng/ml) or 8-bromo-cAMP (300 μ M). The phosphorylated α -G_{i-2} was then collected and treated as outlined in sections 2.2.2 to 2.2.9.

Table 5.2: Percentage inhibition of ligand induced phosphorylation of α -G_{i-2} in lean (Fa/+) and obese (Fa/Fa) Zucker rat hepatocytes by insulin and the effects of BRL 49653 on the inhibition.

	Fa/+					Fa/Fa				
	Mean	SEM	n=	p=	T	Mean	SEM	n=	p=	T
8Br + Ins	17	7	4	0.109	N	14	2	5	0.006	Y
PMA + Ins	18	5	5	0.026	Y	-3	10	5	0.780	N
Gluc + Ins	26	6	5	0.013	Y	20	5	3	0.049	Y

	Fa/+ Dosed					Fa/Fa Dosed				
	Mean	SEM	n=	p=	T	Mean	SEM	n=	p=	T
8Br + Ins	17	6	5	0.074	N	0	10	4	0.993	N
PMA + Ins	12	12	5	0.401	N	5	7	5	0.534	N
Gluc + Ins	-10	8	6	0.305	N	10	9	4	0.338	N

Fa/+ = lean animals; Fa/Fa = obese animals; Fa/+ Dosed = Fa/+ animals that had been dosed with BRL 49653; Fa/Fa Dosed = Fa/Fa animals that had been dosed with BRL 49653; SEM = standard error of mean; n = number of observations; p = significance value returned by single sample Student's *t*-test; T = result of a single sample Student's *t*-test where Y = phosphorylation was significantly different from control (0%; p<0.05) and N = phosphorylation was not significantly different from control (0%; p>0.05); 8Br = 8Br-cAMP = 8-bromo-cAMP (300 μ M); PMA = Phorbol 12-myristate 13-acetate (100 ng/ml); Gluc = Glucagon (10 nM); Ins = Insulin (10 μ M).

Figure 5.8: Percentage phosphorylation of α -G_{i-2} in lean (Fa/+) and BRL 49653 dosed lean (Fa/+) Zucker rat hepatocytes: Effects of 8-bromo-cAMP, PMA, glucagon, and insulin

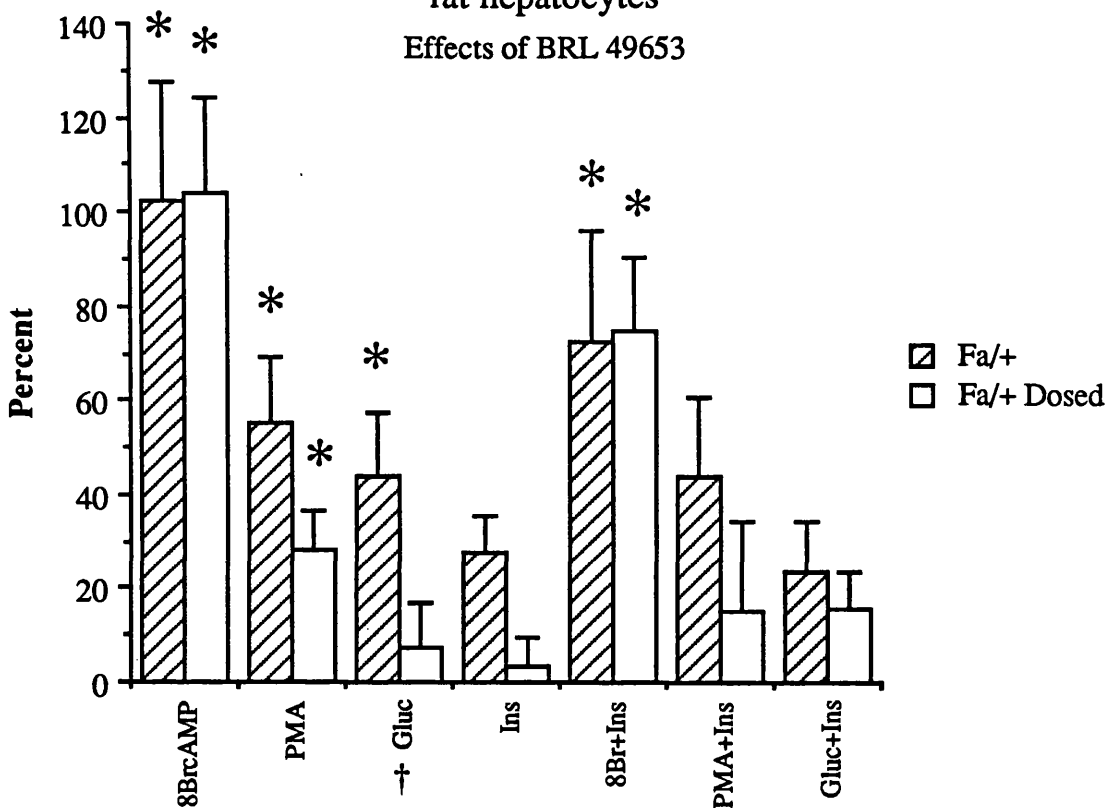
Stimulation of α -G_{i-2} phosphorylation in ³²P labelled hepatocytes (see sections 2.2.2 and 2.2.3) from lean (Fa/+) Zucker rats and lean (Fa/+) Zucker rats that were dosed with BRL 49653. The hepatocytes were challenged with 8-bromo-cAMP (8Br; 8BrcAMP; 300 μ M), PMA (100 ng/ml), glucagon (Gluc; 10 nM), and insulin (Ins; 10 μ M) for 15 minutes. Where the hepatocytes were challenged with a ligand and insulin the insulin was added first followed immediately by the ligand. The hepatocytes were harvested and α -G_{i-2} immunoprecipitated with antiserum 1867. The proteins were separated by SDS-PAGE (see sections 2.2.4 and 2.2.5) and the resulting gels dried and put down for autoradiography (see section 2.2.5). The level of phosphorylation achieved was determined by Cerenkov counting of gel chips that contained phosphorylated α -G_{i-2}. The data are expressed as mean \pm SEM (n \geq 4; see table 5.1) where * indicates that the data are significantly different (p<0.05) from control (0%) with data tested using a single sample Student's *t*-test and † indicates a significant difference between phosphorylations in hepatocytes from Fa/+ and Fa/+ drug rats (two sample Student's *t*-test where p<0.05 was taken as significantly different).

Figure 5.9 Percentage inhibition of ligand induced α -G_{i-2} phosphorylation in lean (Fa/+) and BRL 49653 dosed lean (Fa/+) Zucker rat hepatocytes: Effects of insulin on 8-bromo-cAMP, PMA and glucagon induced phosphorylations

Insulin induced inhibition of ligand induced α -G_{i-2} phosphorylation in ³²P labelled hepatocytes (see sections 2.2.2 and 2.2.3) from lean (Fa/+) Zucker rats and lean (Fa/+) Zucker rats that were dosed with BRL 49653. The hepatocytes were challenged with 8-bromo-cAMP (8BrcAMP; 300 μ M), PMA (100 ng/ml), glucagon (Gluc; 10 nM) for 15 minutes in the presence and absence of insulin (Ins; 10 μ M). The hepatocytes were harvested and α -G_{i-2} immunoprecipitated with antiserum 1867. The proteins were separated by SDS-PAGE (see sections 2.2.4 and 2.2.5) and the resulting gels dried and put down for autoradiography (see section 2.2.5). The level of phosphorylation achieved was determined by Cerenkov counting of gel chips that contained phosphorylated α -G_{i-2}. The data are expressed as mean \pm SEM (n \geq 4; see table 5.2) where * indicates that the data are significantly different (p<0.05) from control (ligand in the absence of insulin, 0%) with data tested using a single sample Student's *t*-test and † indicates a significant difference between phosphorylations in hepatocytes from Fa/+ and Fa/+ drug rats.

Phosphorylation of alpha-Gi-2 in Zucker rat hepatocytes

Effects of BRL 49653



Induced inhibition of alpha-Gi-2 phosphorylation in Zucker rat hepatocytes

Effects of BRL 49653

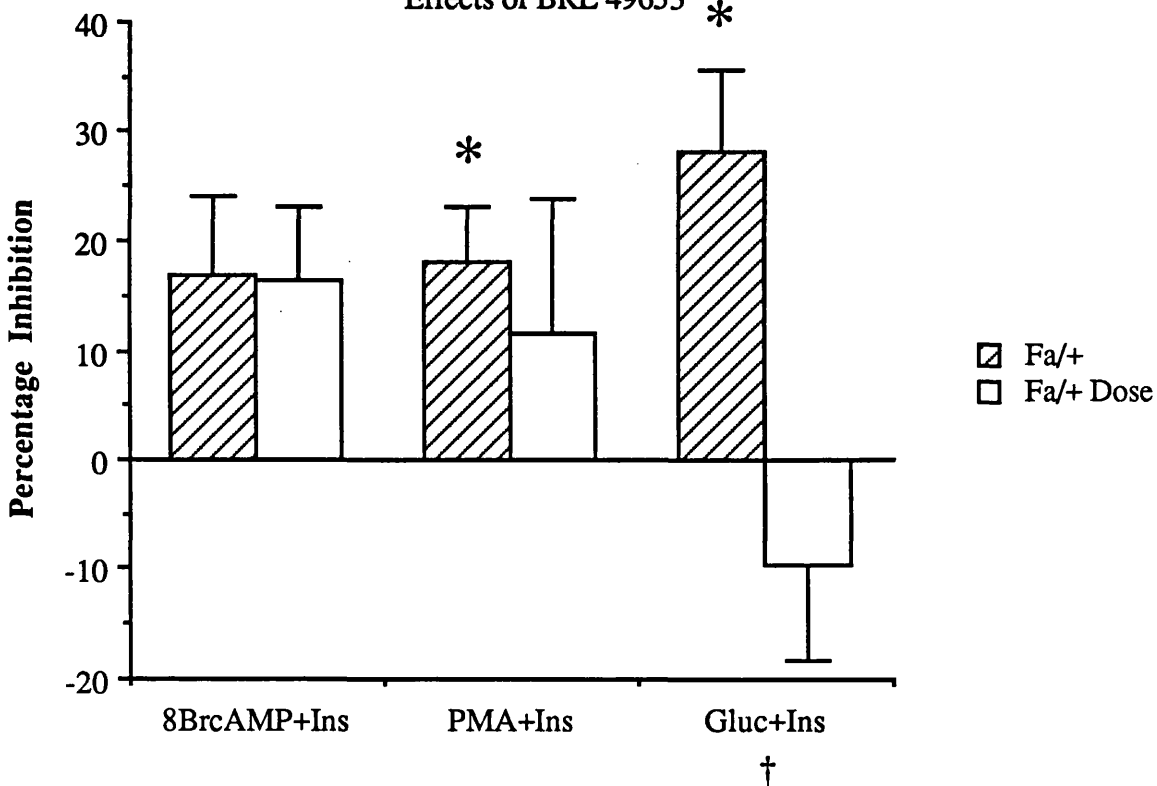


Figure 5.10: Percentage phosphorylation of α -G_{i-2} in obese (Fa/Fa) and BRL 49653 dosed obese (Fa/Fa) Zucker rat hepatocytes: Effects of 8-bromo-cAMP, PMA, glucagon, and insulin

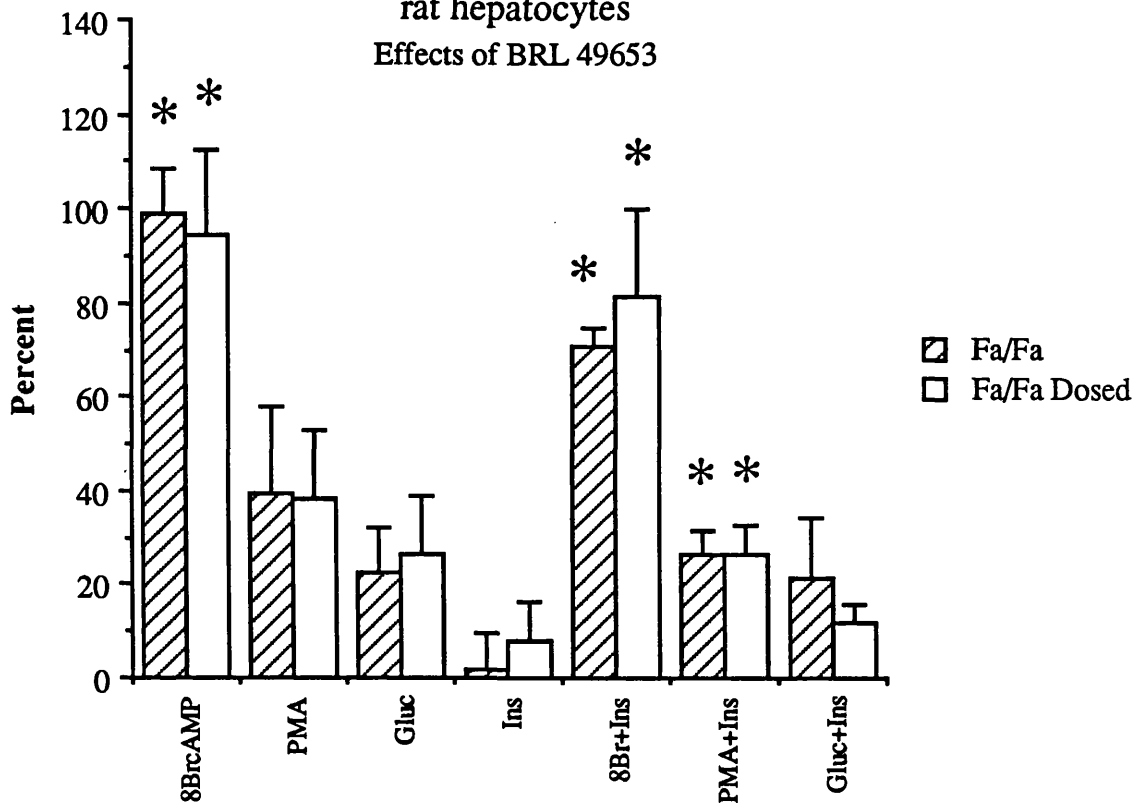
Stimulation of α -G_{i-2} phosphorylation in ³²P labelled hepatocytes (see sections 2.2.2 and 2.2.3) from obese (Fa/Fa) Zucker rats and obese (Fa/Fa) Zucker rats that were dosed with BRL 49653. The hepatocytes were challenged with 8-bromo-cAMP (8Br; 8BrcAMP; 300 μ M), PMA (100 ng/ml), glucagon (Gluc; 10 nM), and insulin (Ins; 10 μ M) for 15 minutes. Where the hepatocytes were challenged with a ligand and insulin the insulin was added first followed immediately by the ligand. The hepatocytes were harvested and α -G_{i-2} immunoprecipitated with antiserum 1867. The proteins were separated by SDS-PAGE (see sections 2.2.4 and 2.2.5) and the resulting gels dried and put down for autoradiography (see section 2.2.5). The level of phosphorylation achieved was determined by Cerenkov counting of gel chips that contained phosphorylated α -G_{i-2}. The data are expressed as mean \pm SEM (n \geq 4; see table 5.1) where * indicates that the data are significantly different (p<0.05) from control (0%) with data tested using a single sample Student's *t*-test and † indicates a significant difference between phosphorylations in hepatocytes from Fa/Fa and Fa/Fa drug rats (two sample Student's *t*-test where p<0.05 was taken as significantly different).

Figure 5.11 Percentage inhibition of ligand induced α -G_{i-2} phosphorylation in obese (Fa/Fa) and BRL 49653 dosed obese (Fa/Fa) Zucker rat hepatocytes: Effects of insulin on 8-bromo-cAMP, PMA and glucagon induced phosphorylation

Insulin induced inhibition of ligand induced α -G_{i-2} phosphorylation in ³²P labelled hepatocytes (see sections 2.2.2 and 2.2.3) from obese (Fa/Fa) Zucker rats and obese (Fa/Fa) Zucker rats that were dosed with BRL 49653. The hepatocytes were challenged with 8-bromo-cAMP (8BrcAMP; 300 μ M), PMA (100 ng/ml), glucagon (Gluc; 10 nM) for 15 minutes in the presence and absence of insulin (Ins; 10 μ M). The hepatocytes were harvested and α -G_{i-2} immunoprecipitated with antiserum 1867. The proteins were separated by SDS-PAGE (see sections 2.2.4 and 2.2.5) and the resulting gels dried and put down for autoradiography (see section 2.2.5). The level of phosphorylation achieved was determined by Cerenkov counting of gel chips that contained phosphorylated α -G_{i-2}. The data are expressed as mean \pm SEM (n \geq 4; see table 5.2) where * indicates that the data are significantly different (p<0.05) from control (ligand in the absence of insulin, 0%) with data tested using a single sample Student's *t*-test and † indicates a significant difference between phosphorylations in hepatocytes from Fa/Fa and Fa/Fa drug rats.

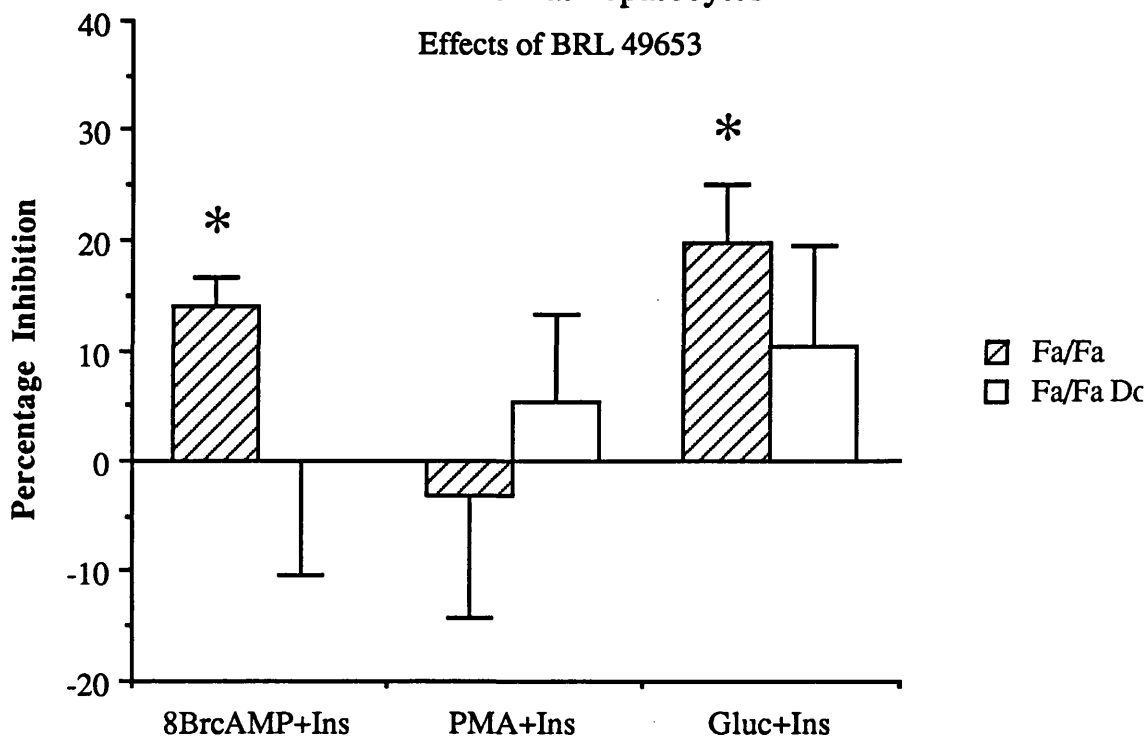
Phosphorylation of alpha-Gi-2 in Zucker rat hepatocytes

Effects of BRL 49653



Induced inhibition of alpha-Gi-2 phosphorylation in Zucker rat hepatocytes

Effects of BRL 49653



It was found that the trypsin digest of α -G_{i-2} derived from hepatocytes from lean and obese animals that had been incubated with vehicle or PMA produced phosphopeptides that gave a three-spot pattern upon separation (see figures 5.12, 5.13, 5.15 and 5.16). The phosphopeptides were identified as C1, C2 and C3 (see Chapter 3; see figure 3.16). Hepatocytes from lean and obese animals that had been incubated with 8-bromo-cAMP gave a four-spot pattern (see figures 5.14 and 5.17) with the phosphopeptides identified as C1, C2, C3 and AN (see Chapter 3; see figure 3.16).

5.3.5 *Phosphoamino acid analysis of ligand stimulated phosphorylation of α -G_{i-2} in hepatocytes from lean (Fa/+) Zucker rats*

When the hepatocytes were treated with one of 8-bromo-cAMP (300 μ M), PMA (100 ng/ml), or insulin (10 μ M) the phosphorylation occurred exclusively on serine residues (see figure 5.18).

5.3.6 *Examination of the levels of α -G_{i-2} expression in lean (Fa/+) and obese (Fa/Fa) Zucker rat hepatocytes, membrane cytosol distribution and the effects of BRL 49653*

Hepatocytes from lean and obese Zucker rats were examined by ELISA (see section 2.2.16) for the level of α -G_{i-2} expression and the distribution of the protein between membrane and cytosol fractions (see section 2.2.13). Samples from lean and obese Zucker rats that had been dosed with BRL 49653 (see section 5.3.1) were also examined.

It was found that the level of expression of α -G_{i-2} per milligram of protein was significantly reduced in the obese (Fa/Fa) animals when compared to the non-diabetic lean (Fa/+) controls (see table 5.3 and figure 5.19). The effect of BRL 49653 was to decrease the level of expression of α -G_{i-2} per milligram of protein in the lean animals but did not effect the levels in the obese animals (see figure 5.19 and table 5.3).

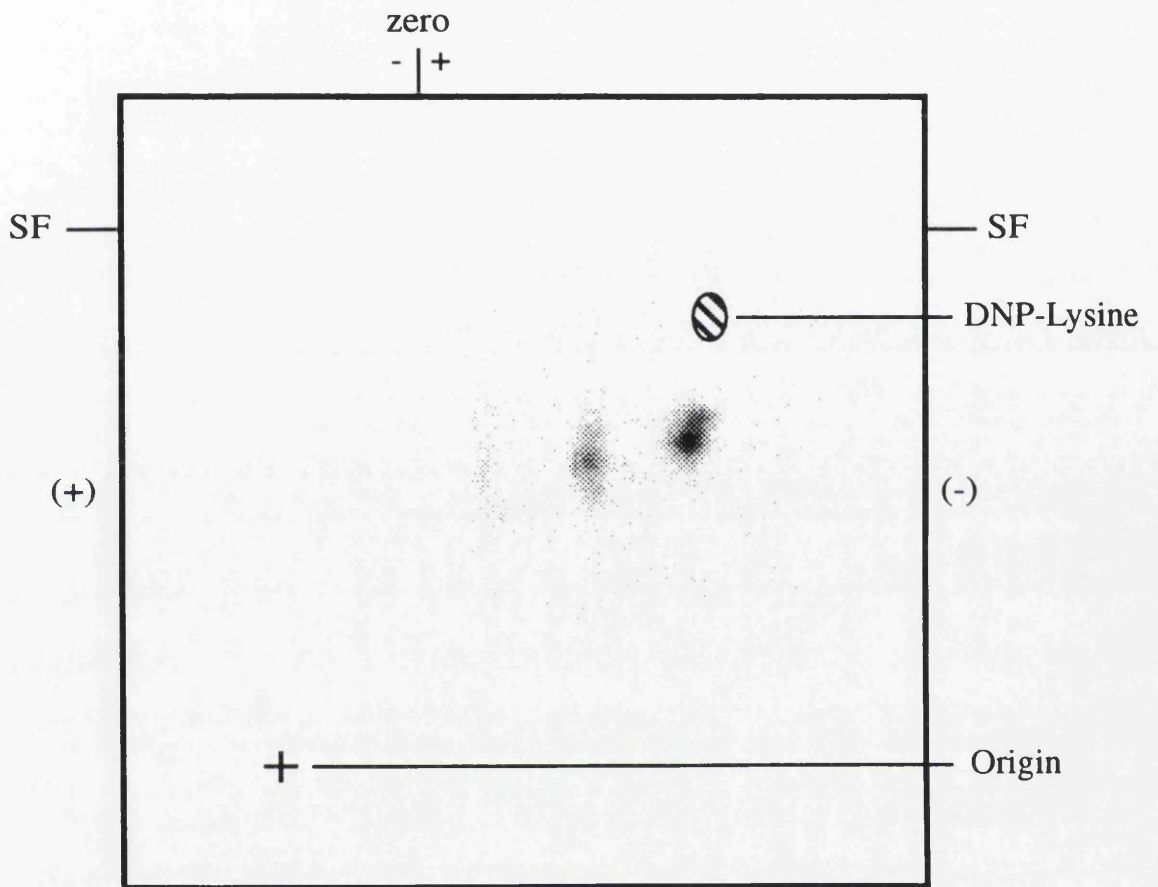
When the distribution of α -G_{i-2} between the membrane and cytosol fractions was examined it was found that there was no significant difference in the distribution except in the obese animals where significantly more was detected in the membrane (see figure 5.20 and table 5.4). BRL 49653 had no effect on the distribution of the protein other than to abolish the significant distribution in the obese (Fa/Fa) animals but the resulting distribution was not significantly different from the non-dosed obese animals.

5.3.7 *Examination of the levels of PKC-isoform expression in lean (Fa/+) and obese (Fa/Fa) Zucker rat hepatocytes, membrane cytosol distribution and the effects of BRL 49653*

Hepatocytes from lean and obese Zucker rats were examined by ELISA (see section 2.2.16) for the level of expression of the PKC-isoforms α , β , δ , ϵ , γ , and ζ . The distribution of the proteins between membrane and cytosol fractions (see section 2.2.13),

Figure 5.12: Phosphopeptide map of α -G_{i-2} from lean (Fa/+) Zucker rat hepatocytes incubated with vehicle solution and then digested with trypsin

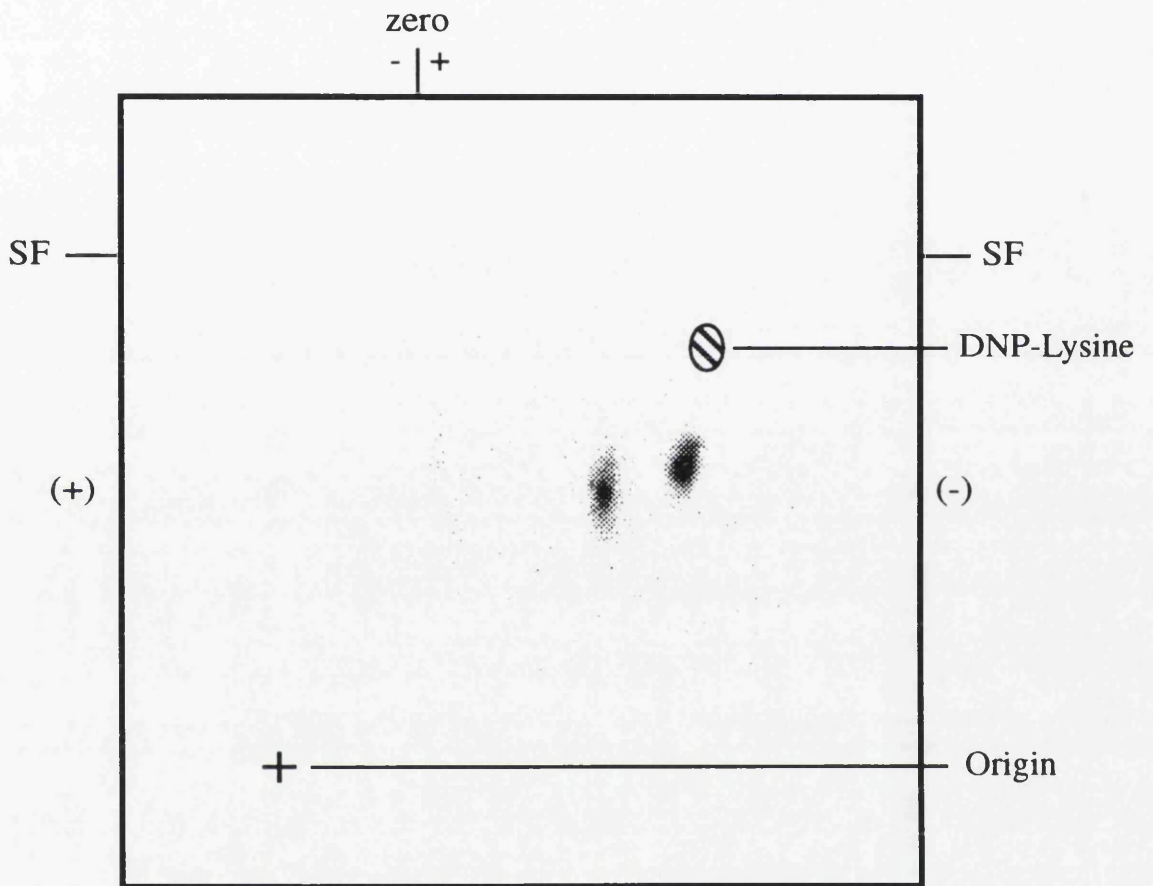
Hepatocytes from lean (Fa/+) Zucker rats were labelled with ³²P (see sections 2.2.2 and 2.2.3) and then challenged with vehicle solution. The hepatocytes were harvested and α -G_{i-2} immunoprecipitated with antiserum 1867 before being subjected to SDS-PAGE. The protein was recovered from the gel and digested with TPCk-treated trypsin as described in experimental procedures (see sections 2.2.4 - 2.2.9). ³²P-labelled tryptic phosphopeptides were then separated on thin-layer cellulose plates by electrophoresis at pH1.9 and ascending chromatography. The final position of DNP-lysine is marked on each plate, SF represents the position of the solvent front, origin is the point of application of the sample, (+) and (-) indicate the orientation of the electric field, and the bar at the top of the plate indicates the separation of the negative, neutral and positive markers. The autoradiograph shows the result from a typical experiment where vehicle produced spots C1, C2, and C3. Diagrammatic representation of the results is shown in figure 3.16. The experiment was performed at least three times with similar results.



Zucker Fa/+, control, trypsin

Figure 5.13: Phosphopeptide map of α -G_{i-2} from lean (Fa/+) Zucker rat hepatocytes incubated with PMA and then digested with trypsin

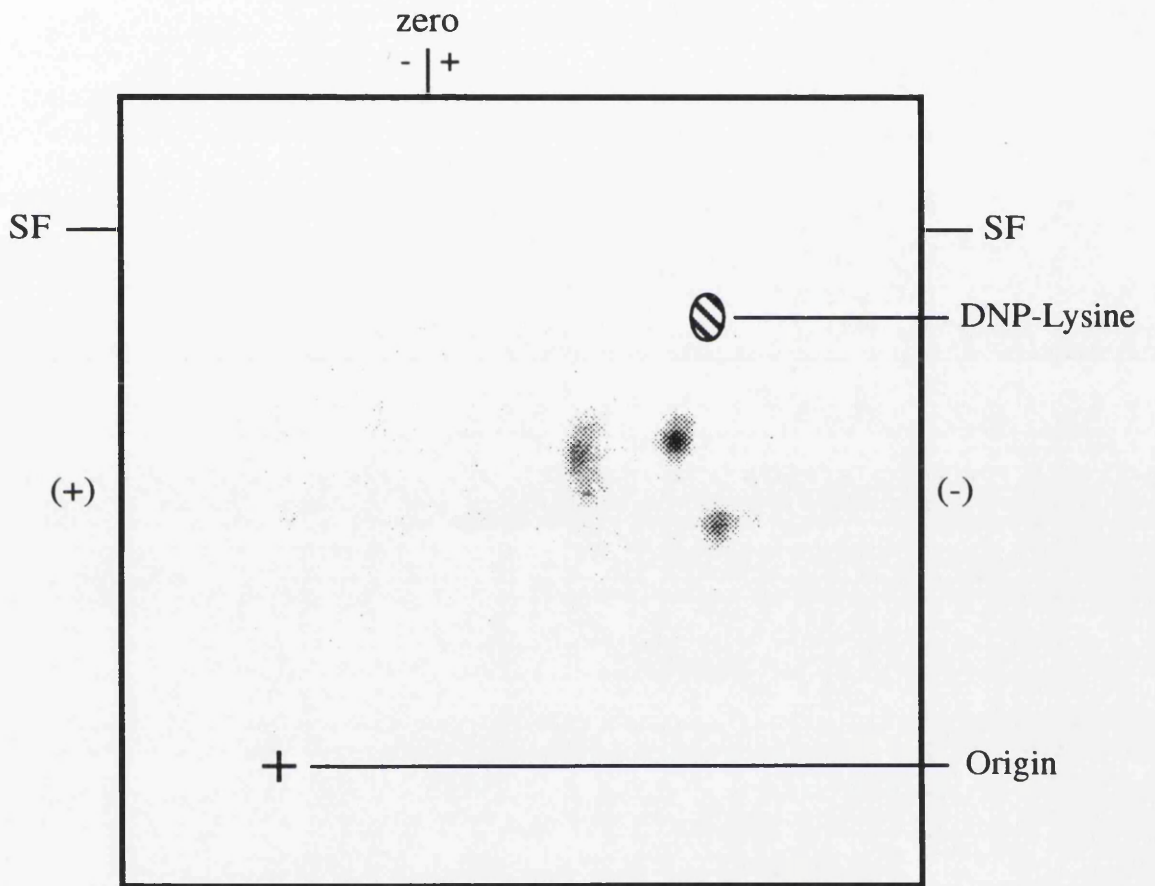
Hepatocytes from lean (Fa/+) Zucker rats were labelled with ³²P (see sections 2.2.2 and 2.2.3) and then challenged with PMA (100 ng/ml) for 15 minutes. The hepatocytes were harvested and α -G_{i-2} immunoprecipitated with antiserum 1867 before being subjected to SDS-PAGE. The protein was recovered from the gel and digested with TPCK-treated trypsin as described in experimental procedures (see sections 2.2.4 - 2.2.9). ³²P-labelled tryptic phosphopeptides were then separated on thin-layer cellulose plates by electrophoresis at pH1.9 and ascending chromatography. The final position of DNP-lysine is marked on each plate, SF represents the position of the solvent front, origin is the point of application of the sample, (+) and (-) indicate the orientation of the electric field, and the bar at the top of the plate indicates the separation of the negative, neutral and positive markers. The autoradiograph shows the result from a typical experiments where PMA produced spots C1, C2, and C3. Diagrammatic representation of the results is shown in figure 3.16. The experiment was performed at least three times with similar results.



Zucker Fa/+, PMA, trypsin

Figure 5.14: Phosphopeptide map of α -G_{i-2} from lean (Fa/+) Zucker rat hepatocytes incubated with 8-bromo-cAMP and then digested with trypsin

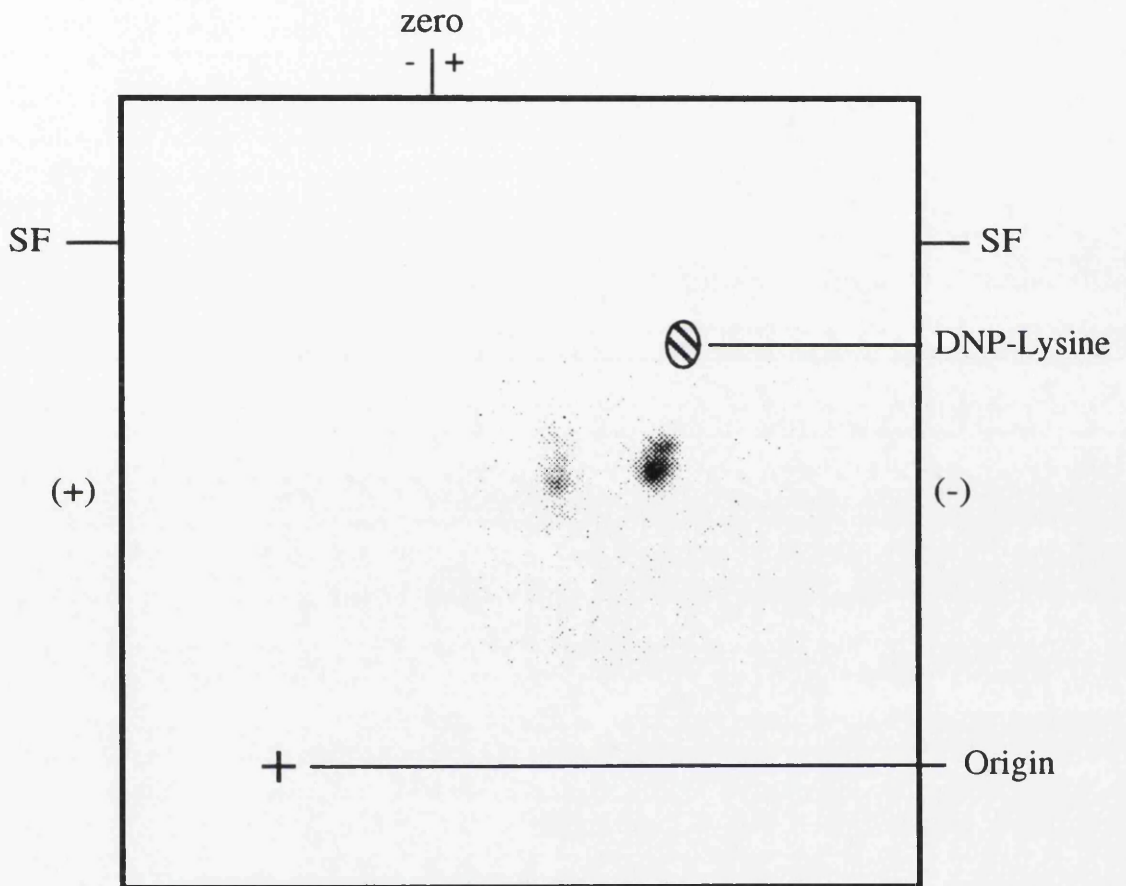
Hepatocytes from lean (Fa/+) Zucker rats were labelled with ³²P (see sections 2.2.2 and 2.2.3) and then challenged with 300 μ M 8-bromo-cAMP for 15 minutes. The hepatocytes were harvested and α -G_{i-2} immunoprecipitated with antiserum 1867 before being subjected to SDS-PAGE. The protein was recovered from the gel and digested with TPCK-treated trypsin as described in experimental procedures (see sections 2.2.4 - 2.2.9). ³²P-labelled tryptic phosphopeptides were then separated on thin-layer cellulose plates by electrophoresis at pH1.9 and ascending chromatography. The final position of DNP-lysine is marked on each plate, SF represents the position of the solvent front, origin is the point of application of the sample, (+) and (-) indicate the orientation of the electric field, and the bar at the top of the plate indicates the separation of the negative, neutral and positive markers. The autoradiograph shows the result from typical experiments where 8-bromo-cAMP produced spots C1, C2, C3 and AN. Diagrammatic representation of the results is shown in figure 3.16. The experiment was performed at least three times with similar results.



Zucker Fa/+, 8-bromo-cAMP, trypsin

Figure 5.15: Phosphopeptide map of α -G_{i-2} from obese (Fa/Fa) Zucker rat hepatocytes incubated with vehicle solution and then digested with trypsin

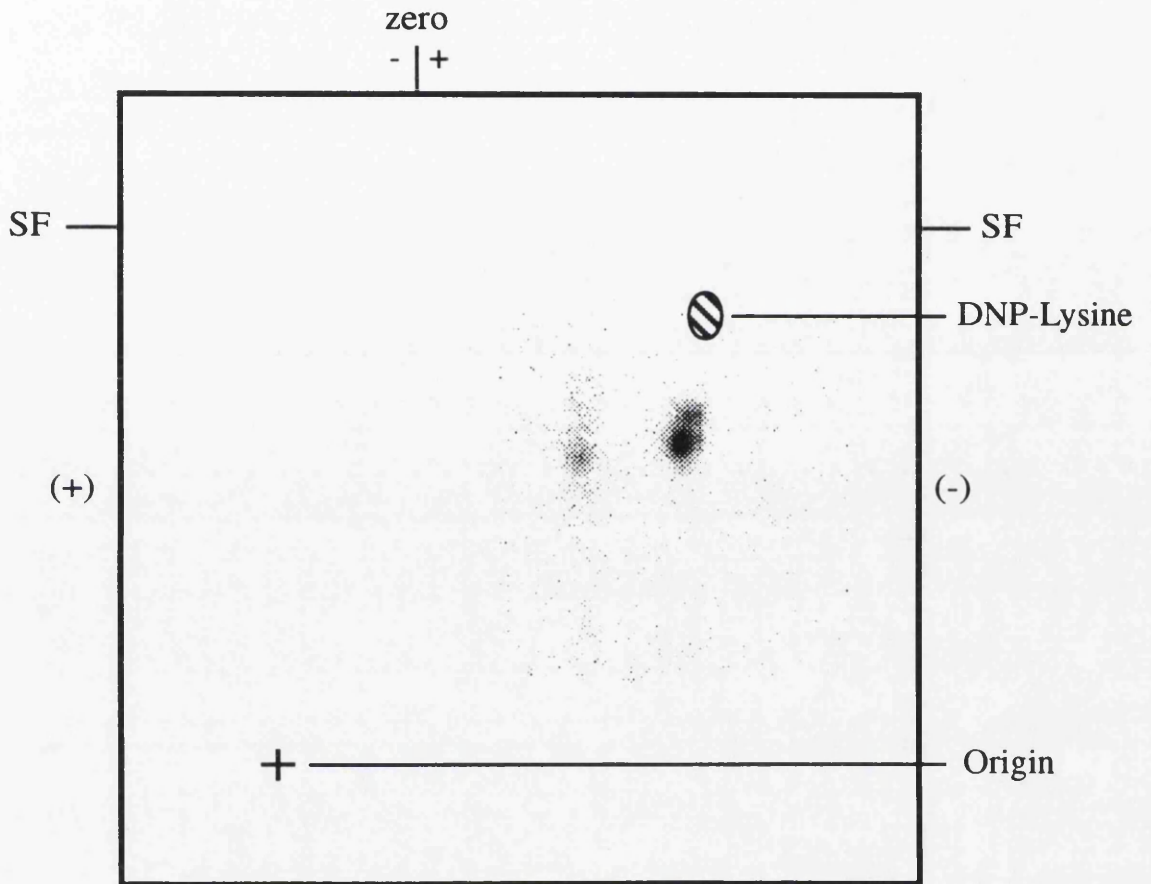
Hepatocytes from obese (Fa/Fa) Zucker rats were labelled with ³²P (see sections 2.2.2 and 2.2.3) and then challenged with vehicle solution. The hepatocytes were harvested and α -G_{i-2} immunoprecipitated with antiserum 1867 before being subjected to SDS-PAGE. The protein was recovered from the gel and digested with TPCCK-treated trypsin as described in experimental procedures (see sections 2.2.4 - 2.2.9). ³²P-labelled tryptic phosphopeptides were then separated on thin-layer cellulose plates by electrophoresis at pH1.9 and ascending chromatography. The final position of DNP-lysine is marked on each plate, SF represents the position of the solvent front, origin is the point of application of the sample, (+) and (-) indicate the orientation of the electric field, and the bar at the top of the plate indicates the separation of the negative, neutral and positive markers. The autoradiograph shows the result from a typical experiment where vehicle produced spots C1, C2, and C3. Diagrammatic representation of the results is shown in figure 3.16. The experiment was performed at least three times with similar results.



Zucker Fa/Fa, control, trypsin

Figure 5.16: Phosphopeptide map of α -G_{i-2} from obese (Fa/Fa) Zucker rat hepatocytes incubated with PMA and then digested with trypsin

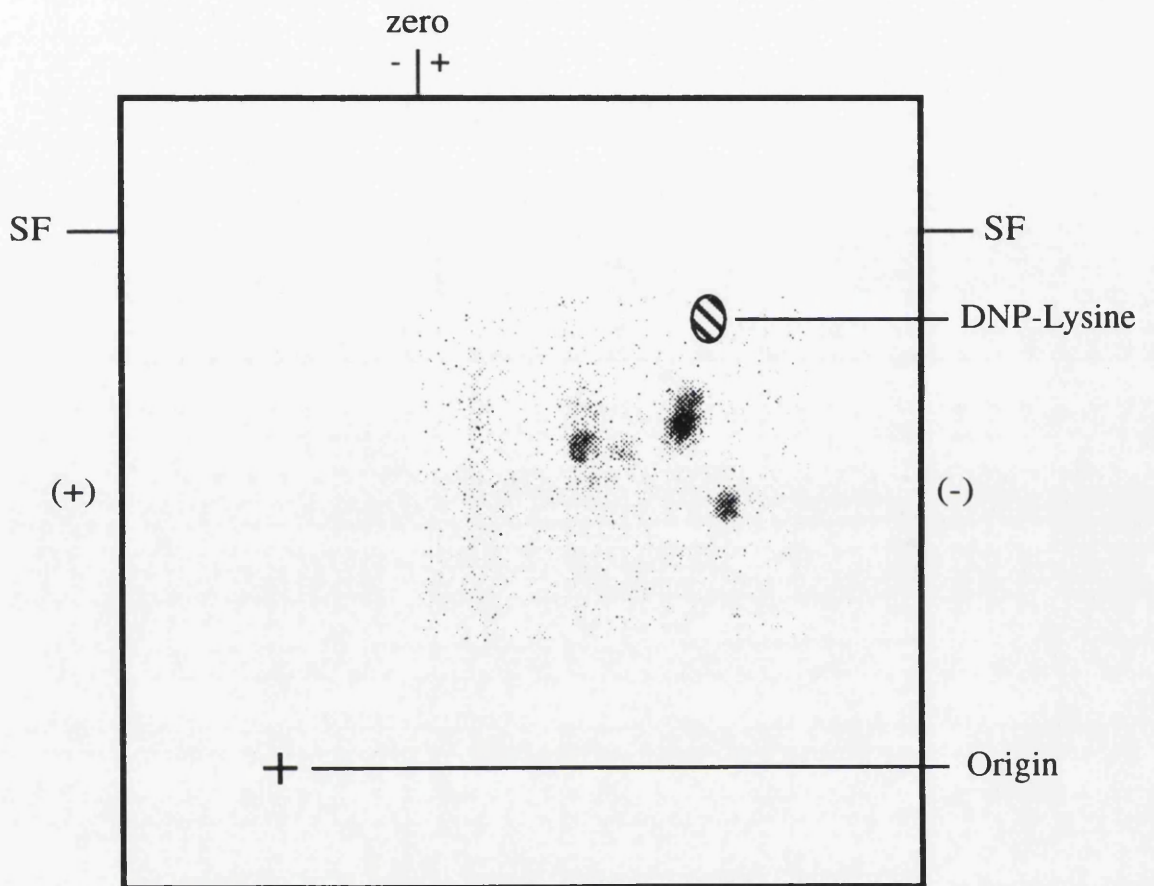
Hepatocytes from obese (Fa/Fa) Zucker rats were labelled with ³²P (see sections 2.2.2 and 2.2.3) and then challenged with PMA (100 ng/ml) for 15 minutes. The hepatocytes were harvested and α -G_{i-2} immunoprecipitated with antiserum 1867 before being subjected to SDS-PAGE. The protein was recovered from the gel and digested with TPCCK-treated trypsin as described in experimental procedures (see sections 2.2.4 - 2.2.9). ³²P-labelled tryptic phosphopeptides were then separated on thin-layer cellulose plates by electrophoresis at pH1.9 and ascending chromatography. The final position of DNP-lysine is marked on each plate, SF represents the position of the solvent front, origin is the point of application of the sample, (+) and (-) indicate the orientation of the electric field, and the bar at the top of the plate indicates the separation of the negative, neutral and positive markers. The autoradiograph shows the result from a typical experiments where PMA produced spots C1, C2, and C3. Diagrammatic representation of the results is shown in figure 3.16. The experiment was performed at least three times with similar results.



Zucker Fa/Fa, PMA, trypsin

Figure 5.17: Phosphopeptide map of α -G_{i-2} from obese (Fa/Fa) Zucker rat hepatocytes incubated with 8-bromo-cAMP and then digested with trypsin

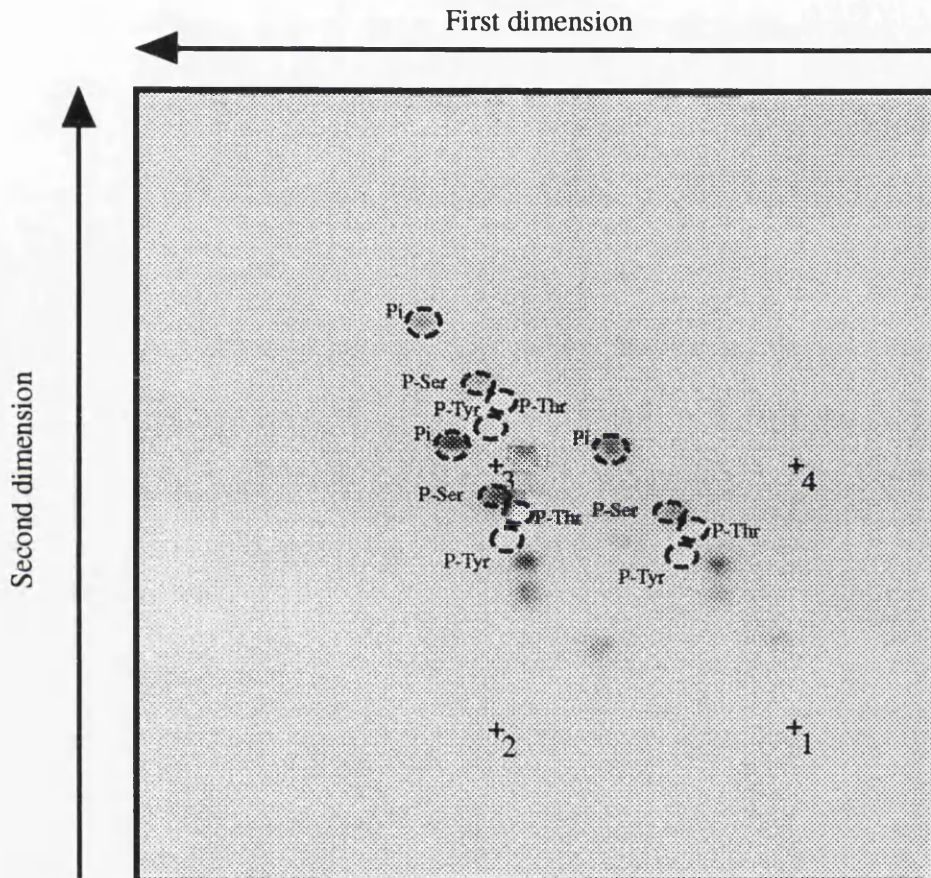
Hepatocytes from obese (Fa/Fa) Zucker rats were labelled with ³²P (see sections 2.2.2 and 2.2.3) and then challenged with 300 μ M 8-bromo-cAMP for 15 minutes. The hepatocytes were harvested and α -G_{i-2} immunoprecipitated with antiserum 1867 before being subjected to SDS-PAGE. The protein was recovered from the gel and digested with TPCK-treated trypsin as described in experimental procedures (see sections 2.2.4 - 2.2.9). ³²P-labelled tryptic phosphopeptides were then separated on thin-layer cellulose plates by electrophoresis at pH1.9 and ascending chromatography. The final position of DNP-lysine is marked on each plate, SF represents the position of the solvent front, origin is the point of application of the sample, (+) and (-) indicate the orientation of the electric field, and the bar at the top of the plate indicates the separation of the negative, neutral and positive markers. The autoradiograph shows the result from typical experiments where 8-bromo-cAMP produced spots C1, C2, C3 and AN. Diagrammatic representation of the results is shown in figure 3.16. The experiment was performed at least three times with similar results.



Zucker Fa/Fa, 8-bromo-cAMP, trypsin

Figure 5.18: Phosphoamino acid analysis of phosphorylated α -G_{i-2} from lean (Fa/+) Zucker rat hepatocytes incubated with 8-bromo-cAMP, PMA and insulin

Hepatocytes from lean (Fa/+) Zucker rats were labelled with ³²P (see sections 2.2.2 and 2.2.3) and then challenged with 8-bromo-cAMP (300 μ M), PMA (100 ng/ml) and insulin (10 μ M) for 15 minutes. The hepatocytes were harvested and α -G_{i-2} immunoprecipitated with antiserum 1867 before being subjected to SDS-PAGE. The protein was recovered from the gel and α -G_{i-2} from hepatocytes that had been incubated with 8-bromo-cAMP, PMA, glucagon and insulin were used for phospho-amino acid analysis as outlined in section 2.2.11). The 8-bromo-cAMP sample was applied to position 1, PMA sample to position 2, and insulin sample to position 3. The plate was run at pH1.9 in the first dimension and rotated 90° anti-clockwise before being run in the second dimension. P_i represents phosphate liberated from the peptide as a result of hydrolysis. P-Ser, P-Thr, and P-Tyr represent the final position of the applied standards phosphoserine, phosphothreonine and phosphotyrosine (see section 2.2.11 and figure 2.2). As can be seen all the samples produced phosphoserine therefore confirming that the phosphorylation sites are serines.



Zucker Fa/+, phosphoamino acid analysis

Figure 5.19: Level of α -G_{i-2} present in hepatocytes from lean (Fa/+) and obese (Fa/Fa) Zucker rat hepatocytes

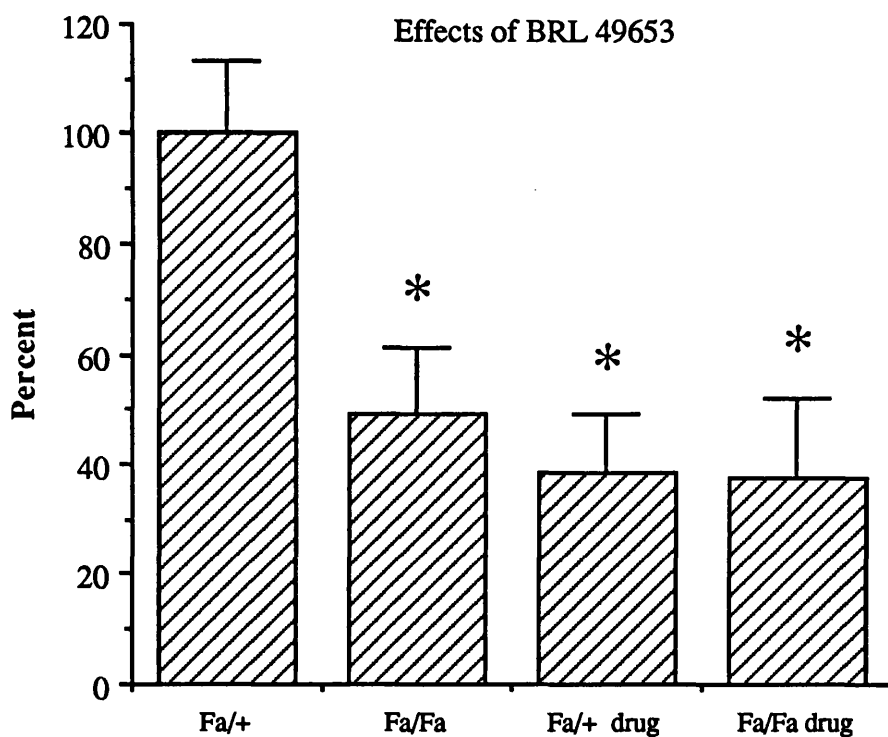
Samples from lean (Fa/+) and obese (Fa/Fa) Zucker rat hepatocytes were examined for the levels of α -G_{i-2} in whole cells. The experiments were also carried out on hepatocytes from Zucker rats that had been given BRL 49653 (Fa/+ drug, Fa/Fa drug). The detection procedure used was an ELISA with constant protein loading per well, and antiserum 1867 used as the primary antibody (see section 2.2.16). All experiments were carried out in quadruplicate with hepatocytes derived from a minimum of three different animals. Results are expressed as mean \pm SEM. * denotes significant difference (two sample Student's *t*-test; $p < 0.05$) between the sample and control (Fa/+).

Figure 5.20: Membrane and cytosol distribution of α -G_{i-2} in Zucker rat hepatocytes

Samples from lean (Fa/+) and obese (Fa/Fa) Zucker rat hepatocytes were examined for the distribution of α -G_{i-2} between the membrane and the cytosol fractions (see section 2.2.13). The experiments were also carried out on membrane and cytosol samples from Zucker rats that had been given BRL 49653 (Fa/+ drug and Fa/Fa drug). The detection procedure used was an ELISA with constant protein loading per well, and antiserum 1867 used as the primary antibody (see section 2.2.16). All experiments were carried out in quadruplicate with hepatocytes derived from a minimum of three different animals and the results are expressed as percentage distribution between the two pools. Results are shown as mean \pm SEM. * denotes significant difference (two sample Student's *t*-test; $p < 0.05$) between cytosol and membrane samples.

Levels of alpha Gi-2 present in hepatocytes from Fa/+ and Fa/Fa Zucker rats

Effects of BRL 49653



Membrane / cytosol distribution of alpha-Gi-2 in Zucker rat hepatocytes

Effects of BRL 49653

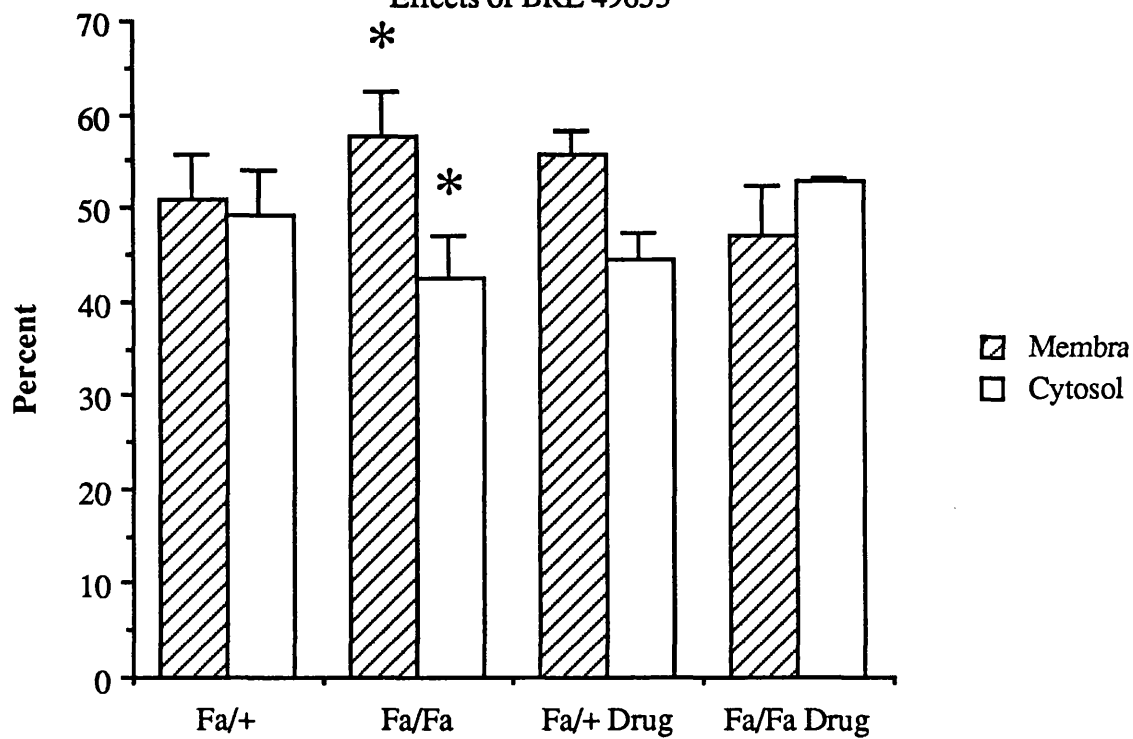


Table 5.3: Summary of ELISA results for the detection of α -Gi-2 and PKC-isoforms in whole cell preparations of hepatocytes from lean (Fa/+) and obese (Fa/Fa) Zucker rats, and the effects of BRL 49653.

	Fa/+	Fa/Fa	Fa/+ drug	Fa/Fa drug
α -Gi-2	-	↓	↓	-*
α -PKC	NSB	NSB	NSB	NSB
β -PKC	NSB	NSB	NSB	NSB
δ -PKC	-	-	↑	↑
ϵ -PKC	-	-	↑	-
γ -PKC	-	-	↑	↑
ζ -PKC	-	-	-	-

Fa/+ = lean Zucker rats; Fa/Fa = obese Zucker rats; Fa/+ drug = Fa/+ Zucker rats that have been dosed with BRL 49653; Fa/Fa drug = Fa/Fa Zucker rats that have been dosed with BRL 49653; - = no change, or for Fa/+ control levels of the protein; "↓" = a significant decrease in expression of the protein (Fa/Fa compared with Fa/+ and drugged samples compared with equivalent non-drugged by two sample Student's *t*-test where $p < 0.05$ was taken as significantly different); NSB = non-specific binding; "↑" = increase in protein expression over respective control (Fa/Fa compared to Fa/+; Fa/+ drug to Fa/+; and Fa/Fa drug to Fa/Fa by two sample Student's *t*-test where $p < 0.05$ was taken as significantly different) * although sample, Fa/Fa drug, is not significantly different from its control (Fa/Fa) the level of α -Gi-2 is still significantly different from Fa/+.

and samples from lean and obese Zucker rats that had been dosed with BRL 49653 (see section 5.3.1), were also examined.

The antisera used in the study were raised at the laboratory by Gary Sweeney and had proved specific for their respective PKC-isoforms in peptide competition studies in Western blotting. It was found that the antisera used for the detection of the PKC-isoforms α and β gave high levels of non-specific binding in ELISAs and so no results were achieved for these isoforms. All the other antisera used gave specific responses.

It was found that the level of expression of δ -PKC per milligram of protein was the same in lean (Fa/+) and obese (Fa/Fa) animals (see table 5.3 and figure 5.21) and that BRL 49653 significantly increased the level of expression of δ -PKC per milligram of protein in the lean and obese animals (see figure 5.21 and table 5.3).

When the distribution of δ -PKC between the membrane and cytosol fractions was examined it was found that there was a significant difference with more being found in the membranes of lean and obese animals, although obesity did not significantly effect the distribution (see table 5.4 and figure 5.22). BRL 49653 had no effect on the distribution of the protein in the obese (Fa/Fa) animals but did make the distribution in the lean animals no

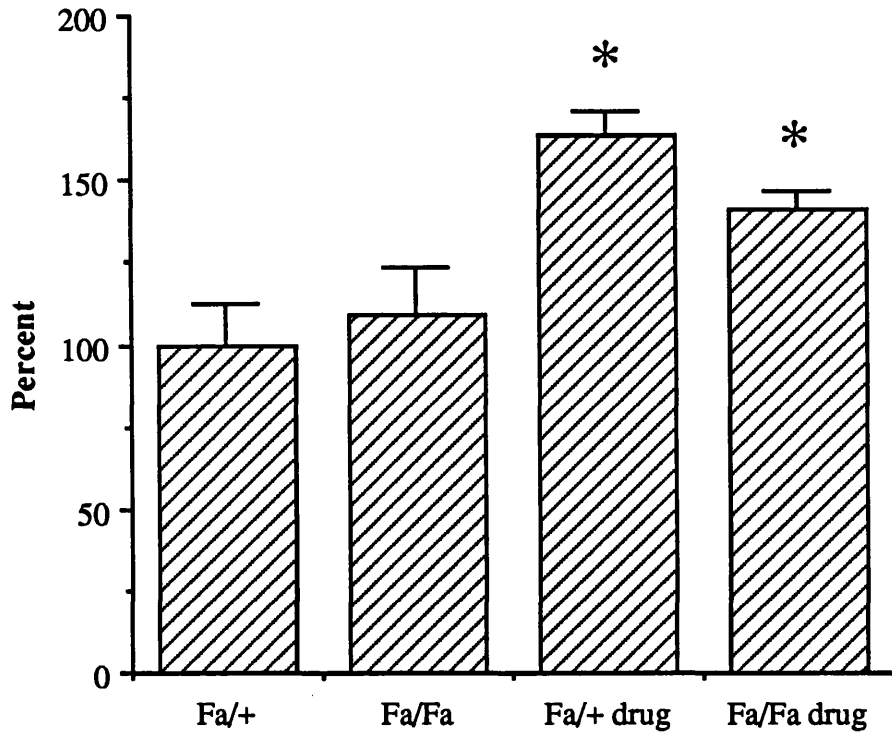
Figure 5.21: Level of δ -PKC present in hepatocytes from lean (Fa/+) and obese (Fa/Fa) Zucker rat hepatocytes

Samples from lean (Fa/+) and obese (Fa/Fa) Zucker rat hepatocytes were examined for the levels of δ -PKC in whole cells. The experiments were also carried out on hepatocytes from Zucker rats that had been given BRL 49653 (Fa/+ drug, Fa/Fa drug). The detection procedure used was an ELISA with constant protein loading per well, and an antiserum specific for δ -PKC which was produced in the laboratory (see section 2.2.16). All experiments were carried out in quadruplicate with hepatocytes derived from a minimum of three different animals. Results are expressed as mean \pm SEM. * denotes significant difference (two sample Student's *t*-test; $p < 0.05$) between the sample and control (Fa/+).

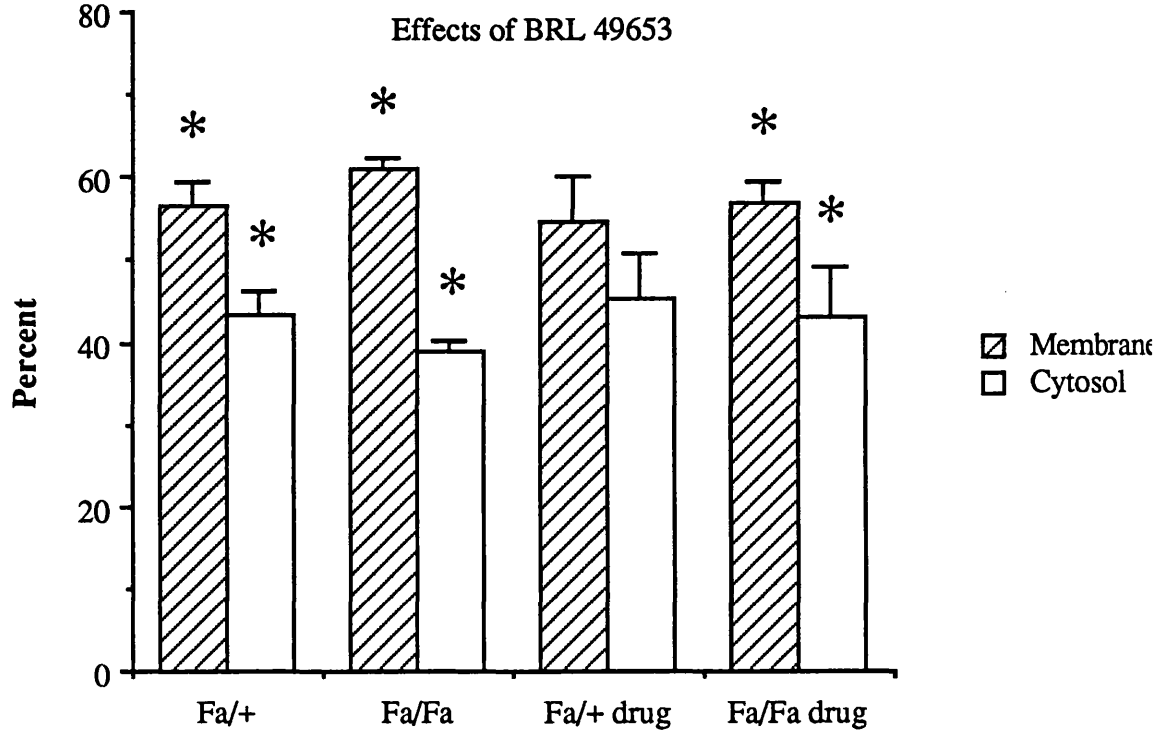
Figure 5.22: Membrane and cytosol distribution of δ -PKC in Zucker rat hepatocytes

Samples from lean (Fa/+) and obese (Fa/Fa) Zucker rat hepatocytes were examined for the distribution of δ -PKC between the membrane and the cytosol fractions (see section 2.2.13). The experiments were also carried out on membrane and cytosol samples from Zucker rats that had been given BRL 49653 (Fa/+ drug and Fa/Fa drug). The detection procedure used was an ELISA with constant protein loading per well, and an antiserum specific for δ -PKC which was produced in the laboratory (see section 2.2.16). All experiments were carried out in quadruplicate with hepatocytes derived from a minimum of three different animals and the results are expressed as percentage distribution between the two pools. Results are shown as mean \pm SEM. * denotes significant difference (two sample Student's *t*-test; $p < 0.05$) between cytosol and membrane samples.

Levels of delta PKC in Zucker rat hepatocytes
Effects of BRL 49653



Percentage membrane cytosol distribution
of delta PKC



longer significantly different, although the resulting change was not significantly different when compared to the non-dosed animals.

The level of expression of ϵ -PKC per milligram of protein was the same in lean (Fa/+) and obese (Fa/Fa) animals (see table 5.3 and figure 5.23) and BRL 49653 significantly increased the level of expression of ϵ -PKC per milligram of protein in the lean but not the obese animals (see figure 5.23 and table 5.3).

When the distribution of ϵ -PKC between the membrane and cytosol fractions was examined it was found that there was a significant difference with more being found in the membranes of lean and obese animals than the cytosol and that obesity significantly affected this distribution (see table 5.4 and figure 5.24). BRL 49653 abolished the significantly different distributions in both the lean and the obese animals, although the resulting change was not significantly different when compared to the non-dosed animals (see table 5.4 and figure 5.24).

Table 5.4: Cellular distribution of α -G_{i-2} and PKC-isoforms in lean (Fa/+) and obese (Fa/Fa) Zucker rat hepatocytes and the effects of BRL 49653.

	Fa/+		Fa/Fa		Fa/+ drug		Fa/Fa drug	
	Mem	Cyto	Mem	Cyto	Mem	Cyto	Mem	Cyto
α -G _{i-2}	=	=	=	=	=	=	=	=
α -PKC	NSB	NSB	NSB	NSB	NSB	NSB	NSB	NSB
β -PKC	NSB	NSB	NSB	NSB	NSB	NSB	NSB	NSB
δ -PKC	+	-	+	-	=†	=†	+	-
ϵ -PKC	+*	-*	+*	-*	=†	=†	=†	=†
γ -PKC	=	=	=	=	=	=	-†	+†
ζ -PKC	+	-	+	-	+	-	+	-

Fa/+ = lean Zucker rats; Fa/Fa = obese Zucker rats; Fa/+ drug = Fa/+ Zucker rats that have been dosed with BRL 49653; Fa/Fa drug = Fa/Fa Zucker rats that have been dosed with BRL 49653; Mem = membrane samples; Cyto = cytosol samples; "=" = equivalent levels of expression in membrane and cytosol samples; + and - show significant distribution of the protein between membrane and cytosol (two sample Student's *t*-test, significantly different if $p < 0.05$); +* and -* indicates that there is a significant difference between membrane and cytosol levels of the protein and that there is also a significant difference in the levels detected between Fa/+ and Fa/Fa samples (two sample Student's *t*-test, significantly different if $p < 0.05$); † = although there has been a change it is not significantly different from the levels found in the control (two sample Student's *t*-test, significantly different if $p < 0.05$); NSB = non-specific binding.

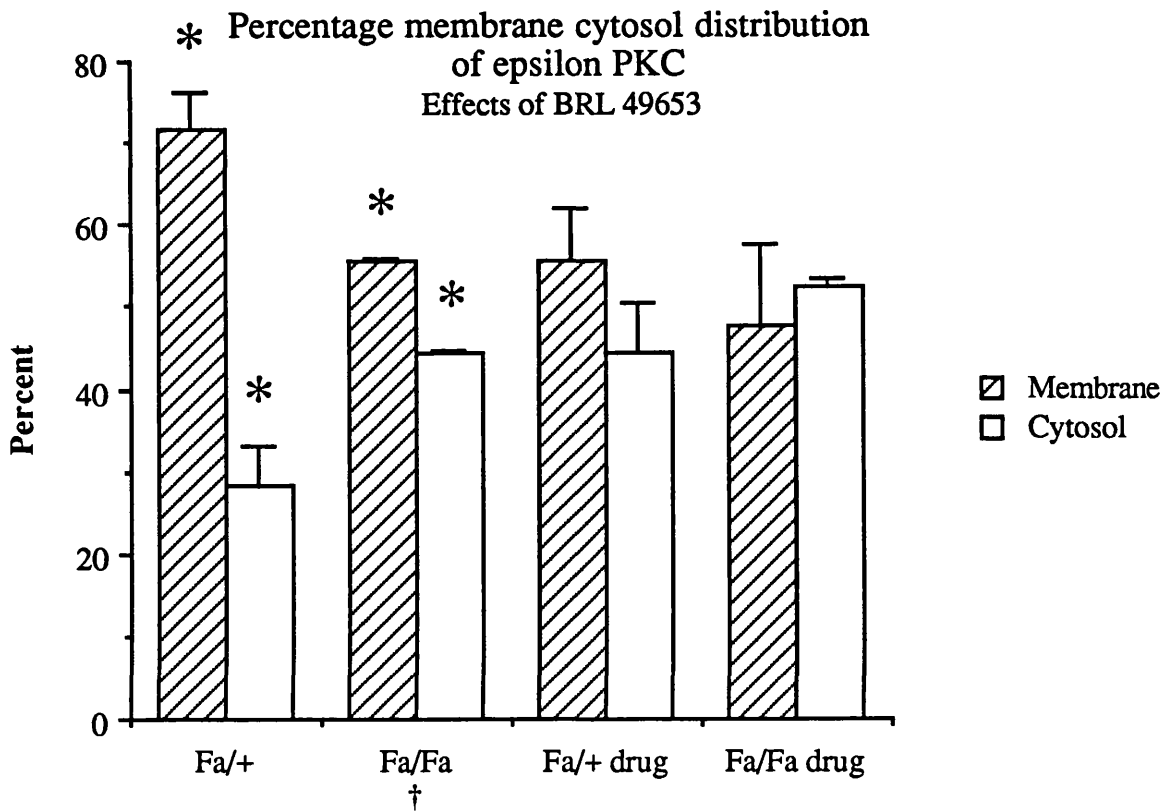
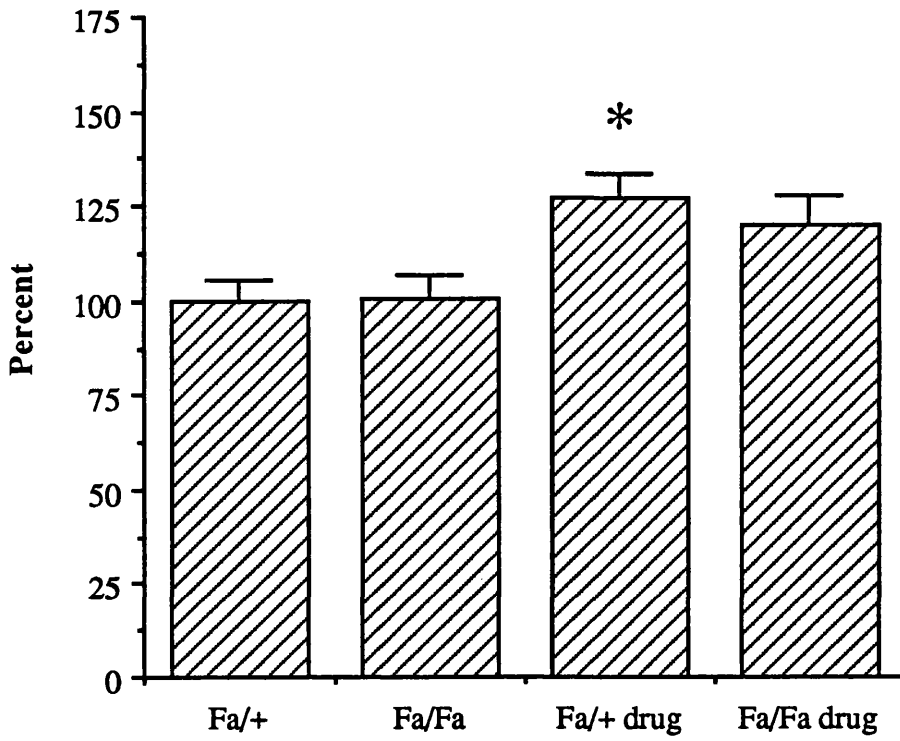
Figure 5.23: Level of ϵ -PKC present in hepatocytes from lean (Fa/+) and obese (Fa/Fa) Zucker rat hepatocytes

Samples from lean (Fa/+) and obese (Fa/Fa) Zucker rat hepatocytes were examined for the levels of ϵ -PKC in whole cells. The experiments were also carried out on hepatocytes from Zucker rats that had been given BRL 49653 (Fa/+ drug, Fa/Fa drug). The detection procedure used was an ELISA with constant protein loading per well, and an antiserum specific for ϵ -PKC which was produced in the laboratory (see section 2.2.16). All experiments were carried out in quadruplicate with hepatocytes derived from a minimum of three different animals. Results are expressed as mean \pm SEM. * denotes significant difference (two sample Student's *t*-test; $p < 0.05$) between the sample and control (Fa/+).

Figure 5.24: Membrane and cytosol distribution of ϵ -PKC in Zucker rat hepatocytes

Samples from lean (Fa/+) and obese (Fa/Fa) Zucker rat hepatocytes were examined for the distribution of ϵ -PKC between the membrane and the cytosol fractions (see section 2.2.13). The experiments were also carried out on membrane and cytosol samples from Zucker rats that had been given BRL 49653 (Fa/+ drug and Fa/Fa drug). The detection procedure used was an ELISA with constant protein loading per well, and an antiserum specific for ϵ -PKC which was produced in the laboratory (see section 2.2.16). All experiments were carried out in quadruplicate with hepatocytes derived from a minimum of three different animals and the results are expressed as percentage distribution between the two pools. Results are shown as mean \pm SEM. * denotes significant difference (two sample Student's *t*-test; $p < 0.05$) between cytosol and membrane samples.

Levels of epsilon PKC in Zucker rat hepatocytes
Effects of BRL 49653



The level of expression of γ -PKC per milligram of protein was the same in lean (Fa/+) and obese (Fa/Fa) animals (see table 5.3 and figure 5.25) and BRL 49653 significantly increased the level of expression of γ -PKC per milligram of protein in the lean and the obese animals (see figure 5.25 and table 5.3).

When the distribution of γ -PKC between the membrane and cytosol fractions was examined it was found that there was no significant difference in the distribution of the protein in any of the samples other than in the dosed-obese animals where significantly more was found in the cytosol (see table 5.4 and figure 5.26).

The level of expression of ζ -PKC per milligram of protein was the same in lean (Fa/+) and obese (Fa/Fa), and dosed-lean and dosed-obese animals (see table 5.3 and figure 5.27).

When the distribution of ζ -PKC between the membrane and cytosol fractions was examined it was found that there was significantly more ζ -PKC in the membrane and that dosing with BRL 49653 had no effect (see figure 5.28 and table 5.4).

5.4 Discussion

As discussed in Chapters 3 and 4, α -G_{i-2} from Sprague Dawley rat hepatocytes undergoes ligand stimulated and inhibited phosphorylations and these phosphorylations occur at multiple sites on the protein. It was also found that the induction of type I diabetes with streptozotocin caused a change in the phosphorylation characteristics of the protein.

The work carried out in this chapter was to examine whether α -G_{i-2} in hepatocytes derived from lean (Fa/+) and obese (Fa/Fa) Zucker rats also underwent phosphorylation and if the diabetic state of the obese Zuckers affected these events.

It was found that α -G_{i-2} from lean Zucker rats did indeed undergo ligand induced phosphorylation by 8-bromo-cAMP (300 μ M), PMA (100 ng/ml), glucagon (10 nM) and insulin (10 μ M; see section 5.3.2, figure 5.4 and table 5.1). However, in hepatocytes from the obese animals only 8-bromo-cAMP (300 μ M) and PMA (100 ng/ml) were able to affect significantly the levels of phosphorylation (see section 5.3.2, figure 5.4 and table 5.1).

The work of Bushfield *et al.* (1990c) has suggested that α -G_{i-2} from obese Zucker rats was unable to undergo ligand induced phosphorylation as the protein was already fully phosphorylated under basal conditions and this level of phosphorylation explained the loss of G_i inhibition of adenylyl cyclase (Bushfield *et al.*, 1990c). The results presented above for the 8-bromo-cAMP induced phosphorylations of α -G_{i-2} are clearly in disagreement with these findings and no explanation can be offered.

The finding that glucagon stimulated phosphorylation of α -G_{i-2} in the obese animals was no longer significantly different from control (see section 5.3.2, figure 5.4 and table 5.1) was in agreement with the general findings of Bushfield *et al.* (1990c), although they did not test glucagon. The change observed in the glucagon stimulation of

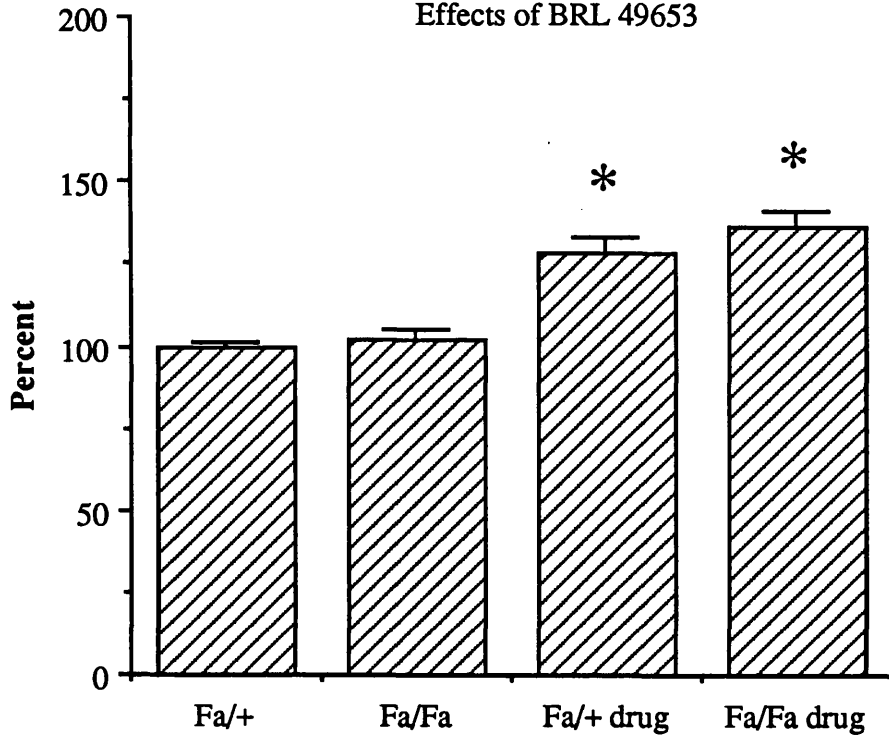
Figure 5.25: Level of γ -PKC present in hepatocytes from lean (Fa/+) and obese (Fa/Fa) Zucker rat hepatocytes

Samples from lean (Fa/+) and obese (Fa/Fa) Zucker rat hepatocytes were examined for the levels of γ -PKC in whole cells. The experiments were also carried out on hepatocytes from Zucker rats that had been given BRL 49653 (Fa/+ drug, Fa/Fa drug). The detection procedure used was an ELISA with constant protein loading per well, and an antiserum specific for γ -PKC which was produced in the laboratory (see section 2.2.16). All experiments were carried out in quadruplicate with hepatocytes derived from a minimum of three different animals. Results are expressed as mean \pm SEM. * denotes significant difference (two sample Student's *t*-test; $p < 0.05$) between the sample and control (Fa/+).

Figure 5.26: Membrane and cytosol distribution of γ -PKC in Zucker rat hepatocytes

Samples from lean (Fa/+) and obese (Fa/Fa) Zucker rat hepatocytes were examined for the distribution of γ -PKC between the membrane and the cytosol fractions (see section 2.2.13). The experiments were also carried out on membrane and cytosol samples from Zucker rats that had been given BRL 49653 (Fa/+ drug and Fa/Fa drug). The detection procedure used was an ELISA with constant protein loading per well, and an antiserum specific for γ -PKC which was produced in the laboratory (see section 2.2.16). All experiments were carried out in quadruplicate with hepatocytes derived from a minimum of three different animals and the results are expressed as percentage distribution between the two pools. Results are shown as mean \pm SEM. * denotes significant difference (two sample Student's *t*-test; $p < 0.05$) between cytosol and membrane samples.

Level of gamma PKC in Zucker rat hepatocytes
Effects of BRL 49653



Percentage membrane cytosol distribution
of gamma PKC

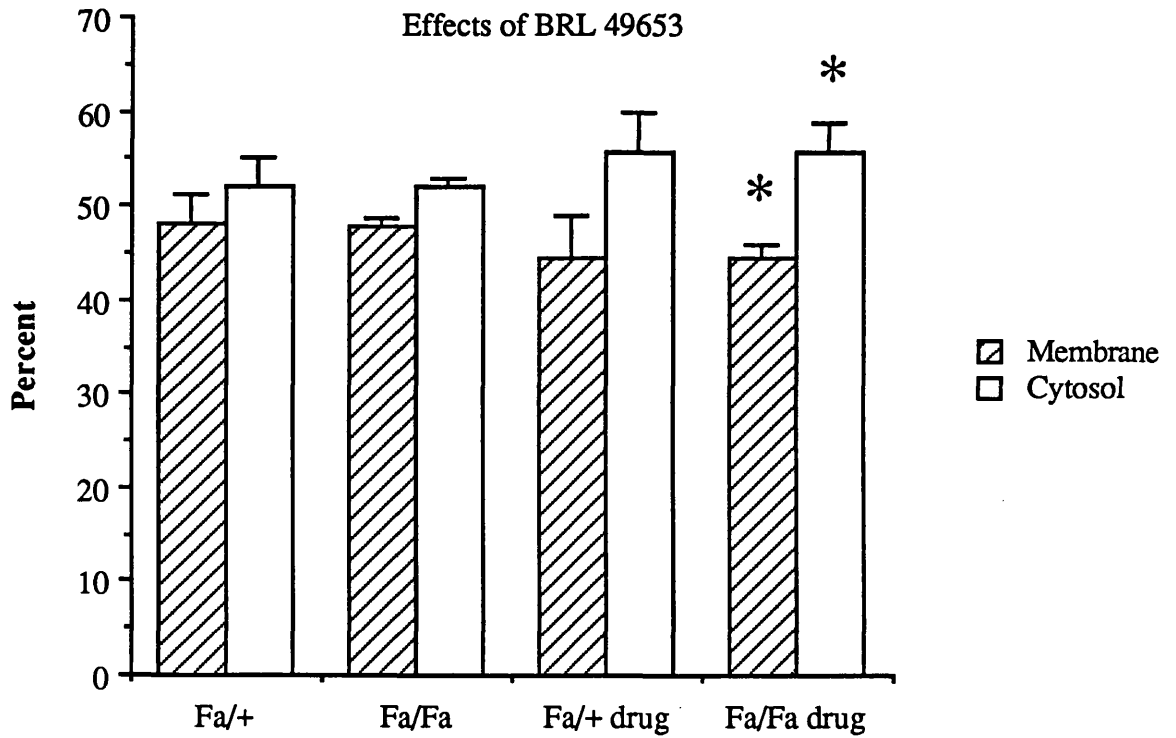
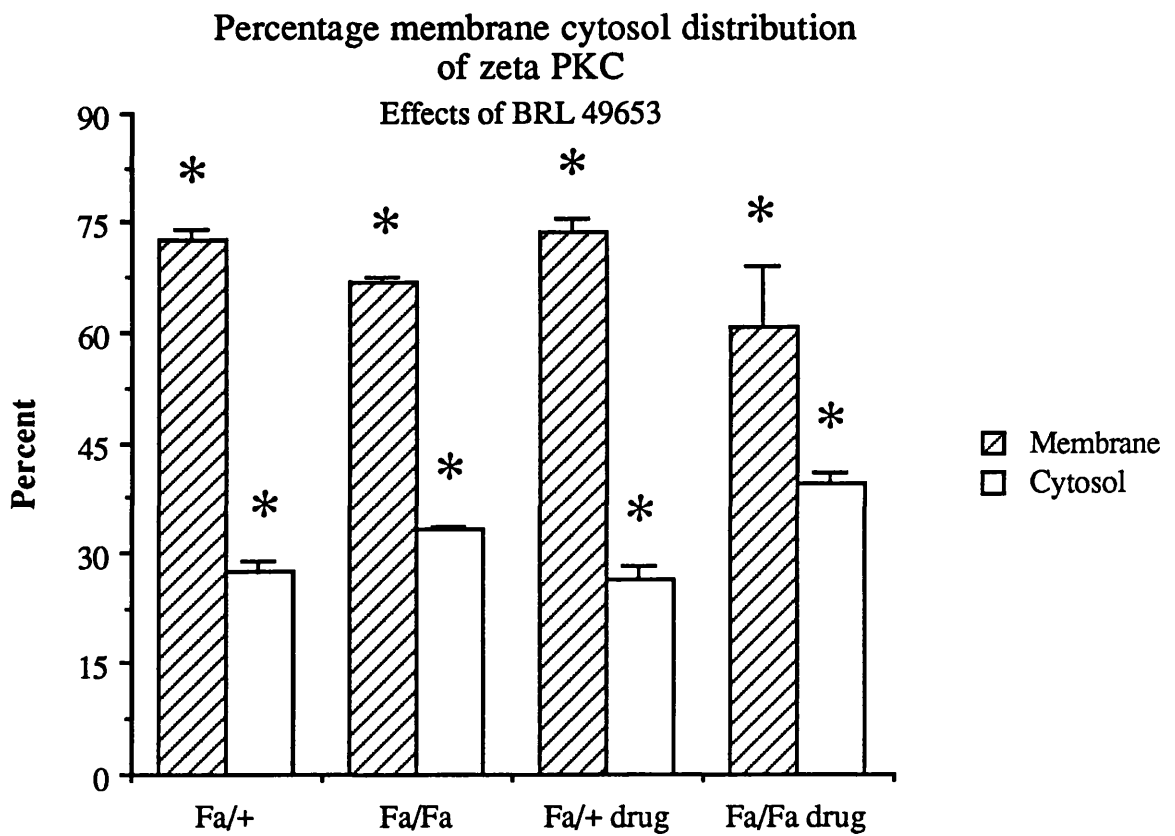
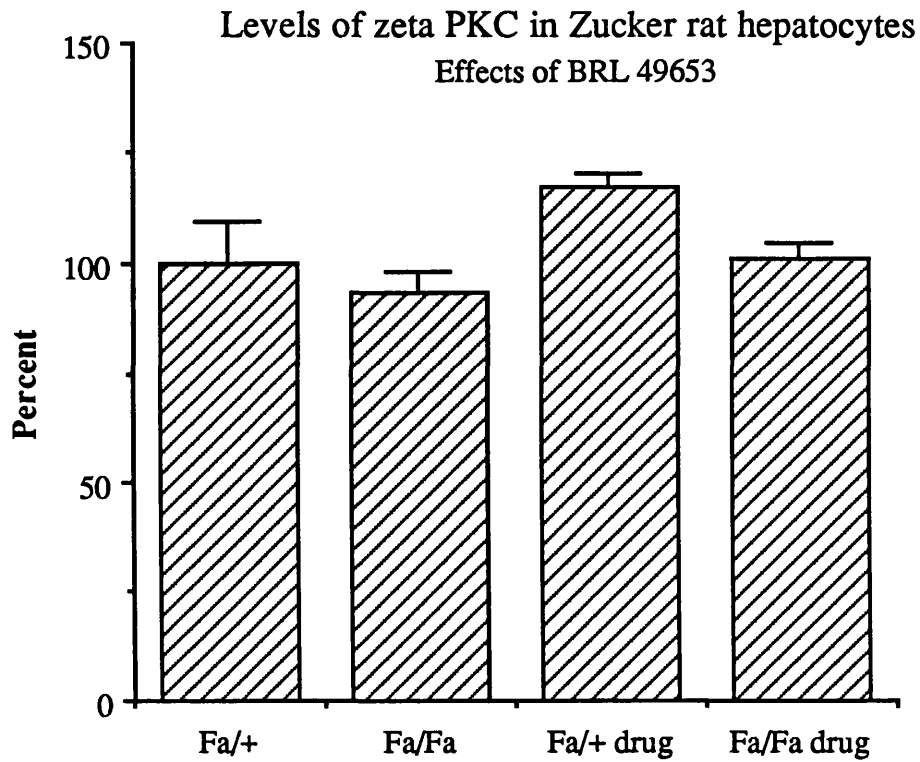


Figure 5.27: Level of ζ -PKC present in hepatocytes from lean (Fa/+) and obese (Fa/Fa) Zucker rat hepatocytes

Samples from lean (Fa/+) and obese (Fa/Fa) Zucker rat hepatocytes were examined for the levels of ζ -PKC in whole cells. The experiments were also carried out on hepatocytes from Zucker rats that had been given BRL 49653 (Fa/+ drug, Fa/Fa drug). The detection procedure used was an ELISA with constant protein loading per well, and an antiserum specific for ζ -PKC which was produced in the laboratory (see section 2.2.16). All experiments were carried out in quadruplicate with hepatocytes derived from a minimum of three different animals. Results are expressed as mean \pm SEM. * denotes significant difference (two sample Student's *t*-test; $p < 0.05$) between the sample and control (Fa/+).

Figure 5.28: Membrane and cytosol distribution of ζ -PKC in Zucker rat hepatocytes

Samples from lean (Fa/+) and obese (Fa/Fa) Zucker rat hepatocytes were examined for the distribution of ζ -PKC between the membrane and the cytosol fractions (see section 2.2.13). The experiments were also carried out on membrane and cytosol samples from Zucker rats that had been given BRL 49653 (Fa/+ drug and Fa/Fa drug). The detection procedure used was an ELISA with constant protein loading per well, and an antiserum specific for ζ -PKC which was produced in the laboratory (see section 2.2.16). All experiments were carried out in quadruplicate with hepatocytes derived from a minimum of three different animals and the results are expressed as percentage distribution between the two pools. Results are shown as mean \pm SEM. * denotes significant difference (two sample Student's *t*-test; $p < 0.05$) between cytosol and membrane samples.



phosphorylation between the lean and the obese animals was not significant and so no real importance can be attached to this finding. This again adds weight to the idea that the dysfunction that was occurring was in some way related to a PKC isoform as it has been shown that glucagon can stimulate both PKC and PKA (Tang & Houslay, 1992) and if part of the dysfunction that occurs in type II diabetes was in the activation of a PKC-isoform then a reduction in the phosphorylation of α -G_{i-2} may be expected but this would be partially masked by the activation of PKA. Alternatively, as discussed for streptozotocin-induced diabetes (see Chapter 4), α -G_{i-2} may have already been phosphorylated possibly as a result of the hyperinsulinaemic condition of the animals and hence further phosphorylation was not possible.

Examination of the level of expression of α -G_{i-2} per milligram of protein in lean and obese Zucker rats by ELISA (see section 5.3.6, figure 5.19 and table 5.3) showed that the hepatocytes of obese animals contained significantly less α -G_{i-2} than those from the lean. Indeed, it was also found that there was significantly more α -G_{i-2} in the membranes of obese animals (see section 5.3.6, table 5.5 and figure 5.20). The decrease in the level of expression of α -G_{i-2} does not affect the comparison of the phosphorylation results between the lean and obese animals as the data in the phosphorylation experiments were normalised to control, unstimulated, hepatocytes. What this result may indicate is that the increase in basal phosphorylation observed in the hepatocytes (Bushfield *et al.*, 1990c) may not reflect an increase in kinase activity but a decrease in the level of available substrate, that is α -G_{i-2}. In addition, the loss of G_i inhibition of adenylyl cyclase action may be because of the decreased level of α -G_{i-2} expression and not as a result of deactivation due to phosphorylation.

As the level of α -G_{i-2} present was compared between lean and obese animals in terms of milligrams of protein then the decrease in α -G_{i-2} expression in the obese animals may not have occurred if the overall protein content has increased. As the obese animals are hyperinsulinaemic (see section 5.1.1) and insulin can stimulate protein synthesis (see section 1.4 and table 1.3; see Hollenberg & Jacobs, 1990) then the decrease in α -G_{i-2} per milligram of protein may be as a result of the stimulation of the synthesis of some other proteins. This idea seems unlikely as no increase in protein synthesis has been reported in the obese Zucker rats, and as the animals also display insulin resistance (see section 5.1.1) then the increased levels of insulin may not be able to stimulate protein synthesis.

From the analysis of tryptic phosphopeptides of α -G_{i-2} it was shown that the stimulation of phosphorylation by PMA and 8-bromo-cAMP in the hepatocytes from lean and obese Zucker rats produced the same peptides, and that these could be identified as C1, C2 and C3 for PMA and vehicle, and C1, C2, C3 and AN for 8-bromo-cAMP (see section 5.3.4, figures 5.12 to 5.17; see Chapter 3 for the identification of peptides). These are the same peptides as produced from ligand stimulated phosphorylations of α -G_{i-2} in Sprague Dawley rat hepatocytes and therefore the PKC-mediated and PKA-dependent

phosphorylation is occurring in Zucker rats is occurring at presumably identical sites (see Chapter 3 and section 3.4). This also indicates that the same α -G_{i-2} phosphorylation system is in operation in the Zucker rats and hence α -G_{i-2} is most probably at the centre of a futile phosphorylation / dephosphorylation cycle (see Houslay, 1991b).

In Sprague Dawley rat hepatocytes it was demonstrated that insulin caused the inhibition of ligand induced phosphorylation of α -G_{i-2} (see Chapter 4). Examination of this effect in Zucker rats revealed that insulin caused a significant inhibition of PMA and glucagon-stimulated phosphorylations in hepatocytes from lean animals and 8-bromo-cAMP and glucagon-stimulated phosphorylation in the obese animals (see section 5.3.2, figure 5.5 and table 5.2). The ability of insulin to inhibit glucagon-stimulated α -G_{i-2} phosphorylation in the lean and the obese animals suggested that although insulin-resistance can be detected in the obese animals the resistance does not effect insulin's actions on α -G_{i-2} phosphorylation which in turn may indicate that α -G_{i-2} is not involved in the insulin signalling that affects glucose metabolism.

The expression of PKC isoforms has been examined in hepatocytes from Sprague Dawley rats that have had type I diabetes induced by streptozotocin (Tang *et al.*, 1993). From these studies it was found that only α , β II, ϵ and ζ isoforms were present in the hepatocytes of untreated animals, and β I, γ , δ and η were not, and the induction of diabetes caused an increase in the expression of β II in the cytoplasm and membrane, and an increase of ϵ in the membrane (Tang *et al.*, 1993). Hence it was possible that some of the changes in the phosphorylation characteristics of α -G_{i-2} observed between the lean and obese Zucker rats may be explained in terms of different levels of expression or distribution of the PKC isoforms. In order to address this the levels of expression and the distribution between membrane and cytosol fractions of some of the PKC-isoforms were examined by ELISA using antisera raised in the laboratory (see section 5.3.7). This was set up as a preliminary study with the realisation that the work would have to be fully quantified by Western blotting. From this work it became apparent that no results could be achieved for α and β PKC-isoforms as the antisera displayed a high level of non-specific binding to the ELISA plates (see table 5.4). This was disappointing as β -PKC expression had already been shown to change in a type I model of diabetes and may therefore play a significant role in insulin signalling (Tang *et al.*, 1993). The antisera for δ , ϵ , γ and ζ isoforms of PKC demonstrated specific binding and the results showed that there was no difference in the level of expression, per milligram of protein, of any of the isoforms in the lean or the obese rats (see section 5.3.7, table 5.3 and figures 5.21, 5.23, 5.25, and 5.27). These results differ from the work of Tang *et al.* (Tang *et al.*, 1993) in that δ and γ PKC were not detected in Sprague Dawley rat hepatocytes and the level of ϵ -PKC expression had increased upon the induction of type I diabetes.

When the distribution between membrane and cytosolic fractions was examined it was found that significantly more δ , ϵ and ζ PKC was in the membrane fraction of the lean

animals and that this distribution was only affected for ϵ -PKC in obese animals where the kinase had translocated from the membrane to the cytosol. These results suggested that ϵ -PKC may play some role in insulin signal transduction as this isoform has been implicated in a type I model (hypoinsulinaemic), where increased expression in the membrane was found (Tang *et al.*, 1993; see section 5.3.7, table 5.4 and figures 5.22, 5.24, 5.26, and 5.28).

As discussed in section 5.1.2, BRL 49653 has a potential use in the treatment of type II, insulin-independent, diabetes. The use of this compound in these studies served two main functions. First, the mode of action of the drug is unknown and it was thought that experiments examining the effect of the drug on the phosphorylation, expression and distribution of α -G_{i-2} and also any effects on PKC distribution and expression, in lean and obese Zucker rats may indicate a method of action; and second, the compound already has recognised beneficial effects in the Zucker rat model of diabetes such as reducing hyperinsulinaemia and restoring insulin sensitivity, so it was therefore thought its use may aid the understanding of how insulin effects the phosphorylation of α -G_{i-2}.

When the effects of chronic dosing of BRL 49653 on α -G_{i-2} expression, and phosphorylation, in hepatocytes from lean Zucker rats was examined it was found that the compound significantly reduced the level of expression to that found in the obese animals and the phosphorylation characteristic now resembled those in the obese animals. It was found that glucagon- and insulin-stimulated phosphorylations were no longer significantly different from control and that the resulting level of phosphorylation was significantly different from non-dosed lean animals (see sections 5.3.3 and 5.3.6, figures 5.8 and 5.19 and tables 5.1 and 5.3). When the inhibitory effects of insulin on ligand induced phosphorylation of α -G_{i-2} was examined it was found that insulin was now only able to significantly inhibit 8-bromo-cAMP stimulated phosphorylation, was no longer able to inhibit PMA induced phosphorylation although the change was not significantly different, and was no longer able to inhibit glucagon stimulated phosphorylation and in this case the change was significantly different (see section 5.3.3, figure 5.9 and table 5.2). Comparisons of the distribution of α -G_{i-2} between the membrane and cytosolic fractions of hepatocytes from lean rats showed that the compound had no effect.

In the obese animals it was found that the chronic dosing with the compound had no effect on the expression of α -G_{i-2} (see section 5.3.6, figure 5.19 and table 5.3) but it did abolish the significant membrane / cytosol distribution of α -G_{i-2} (see section 5.3.6, figure 5.20 and table 5.4). The chronic dosing with compound did not have any significant effect on the phosphorylation characteristics of α -G_{i-2} (see section 5.3.3, figures 5.10 and 5.11, and tables 5.1 and 5.2).

The effect of BRL 49653 on the expression and cellular distribution of PKC isoforms was limited. The only significant effects produced were increased expressions of δ -PKC and γ -PKC in both the lean and obese animals and of ϵ -PKC in lean. The

compound had no effect on the membrane / cytosol distribution of the PKC isoforms in the cell (see section 5.3.7, tables 5.3 and 5.4, and figures 5.21 to 5.28).

From the results presented it appears that BRL 49653 may be producing its effects by either deactivating an isoform of PKC or activating a phosphatase. This idea is supported by the observation that, except for the change in the insulin-mediated inhibition of 8-bromo-cAMP stimulated phosphorylation of α -G_{i-2} in obese Zuckers, the compound only seems to affect phosphorylation events where PKC activation is involved. What the results do show is that as BRL 49653 is able to improve insulin sensitivity and therefore reduce hyperinsulinaemia and improve glucose tolerance in the obese animals and that the function of insulin mediated effects on the phosphorylation of α -G_{i-2} must not be connected with glucose homeostasis but with some other element of insulin signalling. In addition, as the obese Zucker rat is insulin-resistant and it can be shown that insulin can effect the ligand induced phosphorylation of α -G_{i-2} when the cAMP-dependent phosphorylation event is activated, then insulin must still be able to effect cAMP mediated events, again this points to some dysfunction in the PKC-dependent pathway which may be associated with insulin signalling and glucose homeostasis.

Chapter 6

General conclusions

A growing body of evidence is accumulating which suggests that the phosphorylation of heterotrimeric G-proteins (see section 1.2.2) occurs and that it may play a role in regulating the function of these key signalling proteins. In particular, *in vivo* phosphorylation has been reported for α -G_i (isoform not identified), α -G_{i-2} and α -G_z in platelets and hepatocytes (Bushfield *et al.*, 1991; Bushfield *et al.*, 1990b; Carlson *et al.*, 1989; Lounsbury *et al.*, 1991; Lounsbury *et al.*, 1993; Pyne *et al.*, 1989b) and also for α -G_s *in vitro* (Pyne *et al.*, 1992). Indeed, in the hepatocytes it has been shown that the phosphorylation of α -G_{i-2} causes a deactivation of the tonic GTP-mediated inhibitory function of this protein but not receptor-mediated G_i inhibition of adenylyl cyclase (Bushfield *et al.*, 1991; Bushfield *et al.*, 1990b; Pyne *et al.*, 1989b). *In vitro* studies of heterotrimeric G-protein phosphorylation have shown that the phosphorylation causes a decrease in the GTPase activity of the protein and it may be this that causes the change in the G-protein activity (Sauvage *et al.*, 1991).

Prior to this work it had been shown that the phosphorylation of α -G_{i-2} occurred in hepatocytes and it had been suggested that this may occur at two different sites (Bushfield *et al.*, 1990; Bushfield *et al.*, 1990; Bushfield *et al.*, 1991) one of which was PKC-mediated and the other as a result of increased intracellular cAMP levels. In these studies it was definitely shown to be the case with PKC-mediated phosphorylation occurring at one site and a second cAMP-dependent phosphorylation occurring at a second, unidentified site.

Work by Bushfield *et al.* (1991) demonstrated that α -G_{i-2} was at the centre of a futile cycle of phosphorylation and dephosphorylation. The work presented in this thesis has added further details to this cycle and it was shown that the cycle occurred both at the PKC site and the cAMP-dependent site. The cAMP-dependent phosphorylation of α -G_{i-2} also occurred when the cAMP system was not being directly stimulated, that is when either the degradation of cAMP, or the dephosphorylation of α -G_{i-2}, was inhibited then the phosphopeptides maps contained the cAMP-dependent phosphopeptide AN (see Chapter 4). This showed that the phosphorylation of α -G_{i-2} is in a state of dynamic flux which has the advantage that the level of phosphorylation of the protein can be rapidly changed and therefore affect whether the protein is active, and hence possibly affect adenylyl cyclase activity or some other cellular event.

The phosphorylation of α -G_{i-2} by PKC, which is activated by DAG which is produced as part of the inositol phosphate signal transduction system (see sections 1.2.3.2 and 1.2.4.2), may represent another example of cross-talk (see section 1.2.3.3) between the signal transduction systems if α -G_{i-2} is involved in the inhibition of adenylyl cyclase. The result of this phosphorylation would be a reduction in the inhibition of adenylyl cyclase and

this would have two effects. First, is that basal levels of cAMP may increase and second, and possibly more importantly, the removal of the tonic inhibition would mean that the cAMP generating system was sensitised and so able to respond to cAMP generating signals more quickly. Indeed if α -G_{i-2} serves to elicit actions other than the inhibition of adenylyl cyclase activity but some other component of cellular signalling then the result of the phosphorylation may act to sensitise or desensitise the signalling pathway.

Two of the major hormones responsible for altering hepatocytes functions are glucagon and insulin (see sections 4.1.2 and 1.4.1). It had already been demonstrated that glucagon caused an increase in the level of phosphorylation of α -G_{i-2} and these findings were confirmed in this study (Bushfield *et al.*, 1990b). However, in hepatocytes from normal, non-diabetic, Sprague Dawley rats insulin caused a time and dose-dependent inhibition of basal phosphorylation but was unable to inhibit 8-bromo-cAMP or PMA induced phosphorylation. Interestingly, insulin caused an enhancement of the level of phosphorylation produced by glucagon (see Chapter 4). The method by which insulin was effecting such a control over the α -G_{i-2} futile phosphorylation / dephosphorylation cycle was not fully resolved but the data did indicate that insulin may be affecting the cycle at more than one point (see Chapter 4), that is, affecting both phosphorylation and dephosphorylation. This is not unusual for insulin as it has already been shown to stimulate both kinases and phosphatases (see section 1.4.3.1; see Avurch *et al.*, 1990; Dent *et al.*, 1990)

Insulin causes the inhibition of glucose release and a stimulation of the storage of glucose as glycogen and glucagon effectively reverses this process. The effects of glucagon are generated mainly through cAMP dependent mechanisms, although it has also been shown to stimulate PKC activity (Tang & Houslay, 1992; see sections 1.2.4.2 and 4.1.2). As glucagon and insulin have an antagonistic relationship in glucose homeostasis then the effects of one compound may also act to inhibit signal transduction systems controlled by the other and this is effectively what is happening in the glucagon and insulin mediated effects on α -G_{i-2} phosphorylation, that is glucagon caused the phosphorylation of α -G_{i-2} whilst insulin caused a dephosphorylation.

Recently another hormone, amylin, has been implicated in the regulation of glucose metabolism (see section 4.1.2). It has been suggested that amylin attenuates the actions of insulin (see Rink *et al.*, 1993; Westermark *et al.*, 1992) and here it was found that amylin increased basal levels of α -G_{i-2} phosphorylation and blocked insulin's action in the inhibition α -G_{i-2} phosphorylation. The role of amylin in diabetes and glucose metabolism is starting to attract attention and it may be found that in the treatment of type I (insulin-dependent diabetes) that amylin should also be administered (see Rink *et al.*, 1993; Westermark *et al.*, 1992). From the results presented it is clear the amylin does effect the phosphorylation of α -G_{i-2}, although at rather high (10^{-5} M) concentrations, and thus may

play some role in modulating the signal transduction systems in hepatocytes (see Chapter 4).

From the work in Chapter 3 it was found that the phosphorylation of α -G_{i-2} always occurred on serine and that compounds that stimulated PKC activity caused the production of three phosphopeptides on trypsin digestion, namely C1, C2 and C3 (see section 3.3.2 and figures 3.5, 3.6 and 3.16), whilst agents that stimulated the cAMP-pathway produced four phosphopeptides, C1, C2, C3 and AN (see sections 3.3.2 and 4.3.5, and figures 3.7, and 4.23 to 4.31). Although the ligands that stimulated cAMP-dependent phosphorylation of α -G_{i-2} also produced phosphopeptide maps which contained the PKC-dependent phosphopeptides C1, C2, and C3, it was unclear, due to difficulties in quantifying the phosphorylation at the different sites by two-dimensional phosphopeptide mapping, if phosphorylation was occurring at only peptide AN in the presence of cAMP or if phosphorylation was occurring at both sites. However, phosphorylation at the PKC site may have been occurring as it seems that none of the cAMP-dependent phosphorylations were free from PKC activation as a result of cAMP-induced increases in intracellular Ca²⁺ levels which in turn results in the activation of PKC (see Houslay, 1991a; see section 1.2.4.2; Tang & Houslay, 1992).

The *in vitro* phosphorylation of α -G_{i-2} has shown that the protein can be phosphorylated by PKC but not PKA (Lincoln, 1991; Sauvage *et al.*, 1991), so it therefore seems likely that the protein is able to undergo *in vivo* phosphorylation by PKC but not PKA (see section 3.1.1). Hence it is possible that PKC may directly phosphorylate the protein. The phosphorylation motifs for PKC are known, although there is degeneracy and the situation regarding isoform specificities needs to be resolved. However, in conjunction with the trypsin and V8 digests and the secondary digestion of the tryptic peptides with V8, it was possible to predict two potential phosphorylation sites for PKC as serines 47 and 144, with serine 144 being the more favoured based on potential phosphopeptide production on enzymatic cleavage (see Chapter 3). The idea that the protein only possesses one PKC phosphorylation site is supported by the stoichiometry data for PKC mediated ³²P labelling of α -G_{i-2} produced by Bushfield *et al.* (1991).

The identification of the cAMP-dependent site was not possible for two main reasons. First, the data available from enzymatic digests were limited as the phosphorylation process seemed to produce a protein that was less susceptible to V8 cleavage, and second, the identity of the kinase is unknown (see Chapter 3). What can be said is that the phosphorylation site is not likely to be serines 47 or 144, as these serines do not produce phosphopeptides with the necessary mass-charge ratio characteristics. Although it has not been shown *in vitro* that α -G_{i-2} can undergo phosphorylation by PKA (Lincoln, 1991; Sauvage *et al.*, 1991), the work did demonstrate that not only was the phosphorylation cAMP-dependent but that PKA was also involved since PKA inhibitor, HA1004, could prevent cAMP-dependent phosphorylation of α -G_{i-2}, but there is still the

possibility that the inhibitor may have also affected PKC-mediated phosphorylations. The difficulty of digesting α -G_{i-2} that had been phosphorylated by a cAMP-dependent mechanism with V8 indicated that the phosphorylation caused either a conformational change in the protein so that some of the V8 cleavage sites were now masked from the enzyme, or that the phosphorylation occurred at a site near a V8 cleavage site and therefore inhibited a cleavage that was important for the initial digestion of the protein, and the exposure of further V8 cleavage sites to complete digestion.

Both PKC and cAMP-dependent phosphorylations of α -G_{i-2} resulted in the deactivation of the protein and a loss of G_i-mediated inhibition of adenylyl cyclase (Bushfield *et al.*, 1990b). Nevertheless, analysis of both the phosphopeptide mapping data and the stoichiometry data of ³²P labelling of α -G_{i-2}, clearly indicated the presence of two phosphorylation sites. Deactivation of α -G_{i-2} seems to correlate with the phosphorylation of the PKC site (Bushfield *et al.*, 1990b), thus the effect on α -G_{i-2} function due to the phosphorylation at the cAMP-dependent site still has to be found. As the stoichiometry data (Bushfield *et al.*, 1991) and phosphopeptide mapping analysis suggest that phosphorylations occur at both sites on the same protein, then this may indicate that the degree of deactivation of α -G_{i-2} is now greater as the action of two separate phosphatases, or the action of the same phosphatase at two different sites is required to produce a protein that can be activated to inhibit adenylyl cyclase. This may mean that the 'double' phosphorylation of α -G_{i-2} results in an increased level of deactivation of the protein, that is the protein requires a greater degree of dephosphorylation to be in a form that can be activated. Alternatively, the phosphorylation of the PKC site may be required to expose the PKA-dependent site for phosphorylation, or the phosphorylation at the PKA-dependent site may confer stability of the phosphorylated state and hence activation potential of the protein.

Unstimulated hepatocytes show phosphorylation at the PKC site only. This demonstrated that, in unstimulated cells, part of the pool of α -G_{i-2} was inactivated as regards being available to provide tonic inhibition of adenylyl cyclase. This suggested that the cells possess a greater ability to inhibit the activity of adenylyl cyclase than is used. It is possible that this offers an explanation for the mechanism by which insulin exerts a small inhibition on adenylyl activity in intact cells but not in some isolated membranes (see Houslay, 1990; Young *et al.*, 1991). Such a phosphatase driven dephosphorylation of α -G_{i-2} could provide a mechanism for a problem which has taxed investigators for many years.

The idea that the phosphorylation of α -G_{i-2} affects its ability to inhibit adenylyl cyclase came from the observation that the rate of the phosphorylation of α -G_{i-2} is identical to the rate of loss of adenylyl cyclase inhibition in hepatocytes (Bushfield *et al.*, 1990b). It has also been suggested that α -G_i is not involved in the insulin-mediated inhibition of adenylyl cyclase activity because even though α -G_i and the inhibition of adenylyl cyclase are lost in diabetic rats a drug, metformin, which reverses the loss of adenylyl cyclase

inhibition, has no effect on α -G_i levels hence indicating that α -G_i is not responsible for adenylyl cyclase inhibition (Houslay, 1990). As it has been shown that in diabetic rats the level of α -G_{i-2} is reduced and the remaining α -G_{i-2} has undergone increased phosphorylation (Bushfield *et al.*, 1990a; Bushfield *et al.*, 1990b) then a mechanism by which metformin may be working is to decrease the level of phosphorylation of the remaining α -G_{i-2} and therefore restore α -G_{i-2}-mediated inhibition of adenylyl cyclase. Alternatively, if α -G_{i-2} is not involved in adenylyl cyclase inhibition then the function of the phosphorylation events concerning α -G_{i-2} are unknown in terms of the effect on signalling in hepatocytes, although the phosphorylation may still have some effect on α -G_{i-2} function as it has been shown that the phosphorylation of α -G_i can decrease its GTPase activity (Sauvage *et al.*, 1991).

Interestingly, when hepatocytes from non-diabetic Sprague Dawley rats were simultaneously challenged with insulin and glucagon it was found that insulin, instead of inhibiting the phosphorylation event, caused an increase in the level of ³²P incorporated into the protein (see Chapter 4). This was an unexpected effect as it had been found that insulin inhibited most other ligands which promoted cAMP-dependent phosphorylation of α -G_{i-2}. What this effect may again demonstrate is the importance of the control of glucose homeostasis. If cells were exposed to insulin, and therefore glucose release suppressed, and a sudden requirement was made for glucose then this mechanism may provide a method for the rapid reversal of cellular glucose handling. That is, the exposure of cells to both glucagon and insulin caused a greater level of phosphorylation of α -G_{i-2} and therefore attenuated the inhibition of cAMP production which, in turn, might result in an increased adenylyl cyclase activity and an enhancement of the effects of glucagon on glucose metabolism. The existence of this type of mechanism seems unlikely as the involvement of the phosphorylation of α -G_{i-2} in glucose homeostasis is contradicted by the correction of glucose handling by metformin (see Houslay, 1990) and BRL 49653 (see section 5.1.2) in diabetic rats where it has been shown that although the improvements occur there is no effect on either α -G_{i-2} expression, which has been depleted, or on α -G_{i-2} phosphorylation.

If the phosphorylation of α -G_{i-2} does indeed play a role in intracellular signalling, and cellular events mediated by insulin action then some change in α -G_{i-2} may occur in the diabetic condition, and indeed changes in the phosphorylation characteristics and level of expression of α -G_{i-2} in hepatocytes taken from animal models of diabetes have already been reported (Bushfield *et al.*, 1990a; Bushfield *et al.*, 1990b; Bushfield *et al.*, 1990c; Gawler *et al.*, 1987).

To examine further these ideas two animal models of diabetes, namely the streptozotocin induced type I diabetes in Sprague Dawley rats (see section 4.1.1) and the obese Zucker as model of insulin-resistance in type II diabetes (see section 5.1.1) were used. It has already been reported that in both models of diabetes the level of expression of α -G_{i-2} is decreased and its phosphorylation characteristics changed (Bushfield *et al.*, 1990a;

Bushfield *et al.*, 1990b; Bushfield *et al.*, 1990c; Gawler *et al.*, 1987). The changes in expression of α -G_{i-2} observed in the type II model and some of the changes in phosphorylation characteristics found in both models were again confirmed by these studies.

In the type I model it was found that diabetes significantly decreased the levels of phosphorylation induced by 8-bromo-cAMP, PMA and glucagon. Furthermore, insulin no longer inhibited basal phosphorylation levels although the change was not significant (see Chapter 4). When the data on insulin induced inhibition of ligand induced phosphorylations were examined it was found that there was no significant change from the non-diabetic animals, although insulin was now able to inhibit significantly 8-bromo-cAMP induced phosphorylation. The reduced levels of ligand induced phosphorylations may indicate that α -G_{i-2} has already been phosphorylated prior to the start of experiment and the phosphatase activity of the futile phosphorylation / dephosphorylation has decreased, hence no increase in the level of phosphorylation can be achieved. Alternatively, the increased levels of basal phosphorylation may result from the loss of insulin stimulated dephosphorylation as the animal is hypoinsulinaemic. Such increased levels of basal phosphorylation does not appear to make sense in physiological terms if α -G_{i-2} is involved in adenylyl cyclase inhibition as the effect would be to increase the effectiveness of cAMP dependent mechanisms which in turn may compound the glucose metabolism problems.

In the lean Zucker rat, which acted as a control for the type II model obese Zucker rats, it was found that insulin did not affect the basal level of phosphorylation of α -G_{i-2}. Furthermore, 8-bromo-cAMP, PMA and glucagon significantly stimulated the phosphorylation and these results only differed from the non-diabetic Sprague Dawley rats in that insulin did not inhibit basal phosphorylation. In the obese animals the phosphorylation induced by glucagon and insulin were affected to a small extent but the changes were not significant when compared to the lean rats. Examination of the insulin-mediated inhibition of ligand stimulated phosphorylation of α -G_{i-2} showed that in the lean animals insulin inhibited the action of both PMA, and glucagon, and in the obese rats insulin inhibited 8-bromo-cAMP and glucagon (see Chapter 5). These findings contrasted strongly with the studies in Sprague Dawley rat hepatocytes where it was found that the only effect of insulin was to cause an enhancement of the glucagon-mediated stimulation of α -G_{i-2} phosphorylation.

The difference between the phosphorylation characteristics of α -G_{i-2} in the lean Zucker rats and the non-diabetic Sprague Dawley rats was surprising as it was expected that both animals would give a similar result. An explanation may be that as the lean Zucker rats still carries one of the recessive genes which is responsible for obesity then both 'normal' genes are required for the full and correct functioning of the insulin signal transduction system. Alternatively, the difference between the results in the lean Zucker rat and the non-diabetic Sprague Dawley may not reflect the presence of the single copy of the recessive

gene in the Zucker rat but may just show a difference in the two animals' insulin signalling systems.

Although the insulin-resistance in the obese Zucker rat did not significantly effect insulin-dependent modulations of α -G_{i-2} phosphorylation, the fact that insulin was still able to inhibit both 8-bromo-cAMP and glucagon stimulated phosphorylation but no longer the PMA induced phosphorylation, indicated that a fault in the insulin resistant state, and hence possibly part of the control of glucose metabolism, may involve PKC either in its expression or activation. Examination of the level of expression of some of the isoforms of PKC present in hepatocytes revealed that in the isoforms tested (δ , ϵ , γ , and ζ) that the only significant change that occurred was in the distribution of ϵ -PKC between the membrane and cytosol fractions. Interestingly this isoform has also been implicated in changes seen in streptozotocin induced diabetes in Sprague Dawley rats (Tang *et al.*, 1993).

To explore further the relationship between α -G_{i-2} phosphorylation, insulin, and insulin resistance, obese Zucker rats were dosed with the compound BRL 49653 (see section 5.1.2) which is known to have beneficial effects in improving insulin sensitivity and restoring glucose tolerance in animal models of type II diabetes (Cawthorne *et al.*, 1993; Kraegen *et al.*, 1993; Smith *et al.*, 1993; Young *et al.*, 1993). It was found that BRL 49653 changed the phosphorylation characteristics of α -G_{i-2} in lean Zucker rats so that they now resembled those found in the obese. More significantly, it changed the effects of insulin on ligand induced phosphorylation in the lean animals so that they were now approaching the profile seen in the non-diabetic Sprague Dawleys (see Chapters 4 and 5). In the obese animals the dosing with BRL 49653 did not seem to have any significant effect on the phosphorylation of α -G_{i-2} or on insulin's effects on drug induced phosphorylation. These results further support the idea that there may be some residual effect of the one recessive 'obesity' gene in the lean Zucker rats and, more interestingly, that the phosphorylation of α -G_{i-2} is not directly involved in glucose metabolism, because if it were then the changes in the phosphorylations seen between the lean and obese animals should be corrected as BRL 49653 corrects glucose metabolism.

In summary, the phosphorylation of α -G_{i-2} in rat hepatocytes occurs at two different sites, one of which, the PKC site, is most probably serine 144. The effect of such phosphorylations may be to cause a loss of tonic GTP-mediated G_i inhibition of adenylyl cyclase (Bushfield *et al.*, 1991; Bushfield *et al.*, 1990b; Pyne *et al.*, 1989b). Insulin inhibits basal phosphorylation of α -G_{i-2} in the Sprague Dawley rats but not in the Zucker rats. The results from the type II model indicated that insulin resistance may occur as a result of an alteration in the PKC mediated phosphorylation of α -G_{i-2}, although it was also demonstrated that even though the animals were insulin resistant that some of the insulin effects of ligand induced phosphorylations were still active. A study with the compound BRL 49653, which is known to improve insulin sensitivity and glucose handling in animal models of type II diabetes, did not significantly alter the phosphorylation characteristics of

α -G_{i-2} other than to change the phosphorylation events in the control, non-diabetic animals so that they now resembled those found in diabetic obese animals. This drug study did indicate that although changes in α -G_{i-2} phosphorylation did occur in animal models of type II diabetes, and that as these changes could not be corrected by a compound that could improve glucose handling, then the phosphorylation of α -G_{i-2} must be involved in some other aspect of insulin signalling in rat hepatocytes other than glucose homeostasis.

Appendix 1

Phosphate buffered saline (PBS)

0.14 M	NaCl	8.0	g dm ⁻³
2.7 mM	KCl	0.2	g dm ⁻³
1.5 mM	KH ₂ PO ₄	0.2	g dm ⁻³
8.1 mM	Na ₂ HPO ₄	1.15	g dm ⁻³

Appendix 2

Diabetic Sprague Dawley rats

Diabetes was induced in male Sprague-Dawley rats (225 - 250 g) by a single intraperitoneal injection of streptozotocin (50 mg/kg, 0.3 ml) in 0.1 M sodium citrate, pH4.5. Animals were killed three to four days after injection, and were judged to be diabetic if blood glucose levels exceeded 12 mM.

Perfusion buffers

Stock Krebs (1 dm³)

113 mM	NaCl	6.92	g dm ⁻³
4.7 mM	KCl	0.32	g dm ⁻³
1.18 mM	MgSO ₄ .7H ₂ O	0.29	g dm ⁻³
1.18 mM	KH ₂ PO ₄	0.16	g dm ⁻³
25 mM	NaHCO ₃	2.10	g dm ⁻³

Krebs plus EDTA

Stock Krebs (100 ml) plus ethylenediaminetetra-acetic acid (EDTA, a small quantity ~ 0.5 mM).

Krebs plus glucose

Stock Krebs (200 ml) plus 10 mM glucose (0.36 g).

Krebs plus Ca²⁺

Stock Krebs (100 ml) plus 2.5 mM CaCl₂ (27.75 mg).

Heparin solution

1 mg / ml heparin in 0.9% (w/v) NaCl solution.

Appendix 3

Low phosphate Krebs buffers

Stock low phosphate Krebs (1 dm³)

113 mM NaCl	6.92 g dm ⁻³
4.7 mM KCl	0.32 g dm ⁻³
1.18 mM MgSO ₄ .7H ₂ O	0.29 g dm ⁻³
50 μM KH ₂ PO ₄	6.8 mg dm ⁻³
25 mM NaHCO ₃	2.10 g dm ⁻³
25 mM HEPES*	5.96 g dm ⁻³

(*N-2-hydroxyethylpiperazine-N'-2-ethane-sulfonic acid)

Low phosphate Krebs (Incubation buffer)

Stock low phosphate Krebs (200 ml) plus:

2.5% (w/v) Bovine serum albumin (BSA)

2.5 mM CaCl ₂	55.5 mg
10 mM glucose	0.36 g

Siliconisation of conical flasks

To clean, dry, 25 ml conical flasks 10 - 20 ml of dimethyldichlorosilane solution (2% in 1,1,1 trichloroethane; Fisons) was added. The flask was swirled to coat all internal surfaces and the solution transferred to the next flask. The flasks were dried in an oven at 65°C for 30 minutes and then rinsed twice with distilled water before being dried again. The flasks were stored until required.

Appendix 4

Immunoprecipitation buffers

Solubilising buffer

1% (v/v) Triton x100	
10 mM EDTA	1.86 g / 500 ml
100 mM NaH ₂ PO ₄ .2H ₂ O	7.8 g / 500 ml
100 μM Na ₃ VO ₄	9 mg / 500 ml
50 mM HEPES, pH 7.2	7.1 g / 500 ml

[stored at 4°C]

Just before use add:

10	µg/ml	Leupeptin	
10	µg/ml	Aprotinin	
2	mM	Phenylmethyl sulfonyl fluoride (PMSF)*	
10	nM	Okadaic acid (stock [10 ⁻⁴ M] dissolved in dimethyl sulphoxide)	

(* 500 µl PMSF at 35 mg/ml in ethanol to 50 ml solubilising buffer)

Wash buffer

1%	(v/v)	Triton x100	
100	mM	NaCl	5.844 g dm ⁻³
50	mM	NaH ₂ PO ₄ ·2H ₂ O	7.8 g dm ⁻³
50	mM	HEPES, pH 7.2	11.92 g dm ⁻³

[pH when cold]

Wash buffer plus sodium lauryl sulphate (SDS)

Wash buffer plus 0.1% (w/v) sodium lauryl sulphate (SDS)

Appendix 5

Buffers for SDS-PAGE

Lower gel buffer

1.5	M	Tris - HCl, pH8.8	181.65 g dm ⁻³
-----	---	-------------------	---------------------------

Upper gel buffer

0.5	M	Tris - HCl, pH6.8	60.55 g dm ⁻³
-----	---	-------------------	--------------------------

Main gel SDS

1.5	M	Tris - HCl, pH8.8	181.65 g dm ⁻³
10%	(w/v)	sodium lauryl sulphate (SDS)	

Stacking gel SDS

0.5	M	Tris - HCl, pH6.8	60.55 g dm ⁻³
10%	(w/v)	sodium lauryl sulphate (SDS)	

Acrylamide Solution

30%	(w/v)	acrylamide : N,N'-methylenebisacrylamide	
		([37.5 : 1]; [29.29 g/100 ml : 0.78 g/100 ml])	

Running buffer

25 mM	Tris	3.0 g dm ⁻³
192 mM	glycine	14.4 g dm ⁻³
0.1%	(w/v) sodium lauryl sulphate (SDS)	

Main Gel Mix [10%] (two plates)

30 ml	water	
17.25 ml	lower gel buffer	
24 ml	acrylamide solution	
0.92 ml	main gel SDS	
240 µl	10% (w/v) ammonium persulphate	
36 µl	N,N,N',N' - tetramethylethylenediamine (TEMED)	

Stacking Gel

24 ml	water	
9.6 ml	upper gel buffer	
6 ml	acrylamide	
400 µl	stacking gel SDS	
180 µl	10% (w/v) ammonium persulphate	
60 µl	N,N,N',N' - tetramethylethylenediamine (TEMED)	

Laemmli buffer

7.4 ml	water	
2 ml	upper gel buffer	
2 ml	stacking gel SDS	
4 ml	50% (v/v) glycerol	
0.6 ml	2β-mercaptoethanol	
0.001%	(w/v) bromophenol blue	

Appendix 6

Pre-flashing

X-ray film (Fuji RX) was pre-flashed for maximum sensitivity and accuracy (Bonner & Laskey, 1974; Lasey & Mills, 1975; Randerath, 1970) by using an Amersham RPN2051 pre-flash unit. The makers instructions were followed with regards to calibration and use, and are briefly outlined below.

Calibration

The flash gun was switched on and fired three or four times to prime the unit. One sheet of X-ray film was placed on a white background and using a card with a 2 × 5 cm

hole different areas of the film were exposed to the flash with the gun placed at various heights above the card. This process was repeated for a range of heights starting at 10 cm and increasing in 10 cm steps to a height of 1 m. The film was then developed in the normal manner.

The film was scanned using a Shimadzu CS-9000 densitometer set at 540 nm. The machine was set at zero on an unexposed but developed region of the film. Each exposed region of the film was scanned and the exposure that gave an increase of 0.15 absorbance units above back ground was taken as optimum distance for pre-flashing. Under the darkroom conditions used this was found to be 80 cm above the surface of the film.

Pre-flashing

The flash gun was fired three or four times to prime the unit and the gun placed 80 cm above the X-ray film which had been placed on a white background. The gun was fired once and then the film was used in the normal manner.

Appendix 7

Buffers for phospho-peptide and phospho-amino acid analysis

Ammonium bicarbonate solution

50 mM ammonium bicarbonate 400 mg / 100 ml

Electrophoresis buffer (pH 1.9)

50 ml Formic acid (88%)
156 ml Glacial acetic acid
1794 ml Deionized water

Electrophoresis buffer (pH 3.5)

10 ml Pyridine
100 ml Glacial acetic acid
1890 ml Deionized water

Electrophoresis buffer (pH 4.72)

100 ml n-Butanol
50 ml Pyridine
50 ml Glacial acetic acid
1800 ml Deionized water

Phospho-chromatography buffer

750 ml	n-Butanol
500 ml	Pyridine
150 ml	Glacial acetic acid
600 ml	Deionized water

Marker dyes:

5 mg / ml	ϵ - dinitrophenyl (DNP) lysine (yellow, positive marker)
5 mg / ml	DNP-DL-Glutamic acid (yellow, neutral marker)
1 mg/ml	xylene cyanol FF (blue, negative marker)*

(* xylene cyanol FF made up in water containing 30 - 50%
pH 4.72 buffer)

Dyes mixed 1 : 1 : 1 before application.

Appendix 8

Excel Macros

Calculation of mass - charge ratios

The Macro is called from the cell in the next column to the peptide (see end of appendix). The Macro consists of three subroutines; a main routine that calls the other two routines, calculates the mass - charge ratio and produces the final report; a routine that calculates the amino acid composition and charge of the peptide; and a third routine that calculates the peptide mass. Notes in { } brackets represent comments for guidance and not part of the program.

Main control and report subroutine

The function of the subroutine is to call the other routines for the calculation of the constituent amino acids of the peptide and its associated charge, and the routine for the calculation of the peptide's mass. The column heading, A, and row numbers represent the positioning of the program on the Excel spreadsheet.

Once the charge and mass have been calculated this subroutine checks to see if the peptide contains a serine (if it does not this is reported and the calculation stopped) or if it contains more than one serine and hence more than one potential phosphorylation site. If the peptide contains multiple phosphorylation sites the program inserts new lines into the calculation spreadsheet and copies in the peptide sequence. Finally the program calculates the mass - charge ratio and reports the peptide charge, mass and mass - charge ratio. If multiple phosphorylation sites exist then the changes in charge, mass and mass - charge ratio are also reported (see below for example of output).

A

```

1  CalMr
2  =ECHO(FALSE)
3  =CALCULATION(3,FALSE,100,0.001,TRUE,FALSE,TRUE,TRUE,TRUE)
4  =FORMULA("=Mr!Charge(RC[-1])")           {Calls routine to calculate charge}
5  =SELECT("R[0]C[1]")                       {Position for response}
6  =FORMULA("=Mr!MW(RC[-2])") {Calls routine to calculate molecular charge}
7  =SELECT("R[0]C[1]")                       {Position for response}
8  =FORMULA("=RC[-2]*(RC[-1]^(-2/3))*100")   {Calcs. mass - charge ratio}
9  =FORMAT.NUMBER("0.00")
10 =IF(Ser>1)
11 =ALERT("Peptide contains "&Ser&" serines.",2)
12 =FOR("Loop",2,Ser,1)
13 =SELECT("R[1]C[-3]")                       {Lines 10 -32 check to see if the peptide}
14 =INSERT(2)                                  {contains more than one serine. If it does}
15 =SELECT("R[-1]C")                          {then a new line is inserted with a copy of}
16 =COPY()                                       {the peptide. Changes in the charge, mass}
17 =SELECT("R[1]C")                            {and mass - charge ratio are also calculated}
18 =PASTE()                                       {and reported.}
19 =SELECT("RC[1]")
20 =CANCELCOPY()
21 =INSERT(2)
22 =FORMULA("=R[-1]C+1")
23 =SELECT("RC[1]")
24 =INSERT(2)
25 =FORMULA("=R[-1]C-80")
26 =SELECT("RC[1]")
27 =INSERT(2)
28 =FORMULA("=(RC[-2]*(RC[-1]^(-2/3)))*100")
29 =FORMAT.NUMBER("0.00")
30 =NEXT()
31 =ELSE()
32 =END.IF()
33 =CALCULATION(1,FALSE,100,0.001,TRUE,FALSE,TRUE,TRUE,TRUE)
34 =IF(Ser<1)                                   {Lines 34 - 46 check to see if the peptide contains a}
35 =SELECT("RC[-2]")                             {serine and if not reports it.}
36 =FORMULA("")
37 =SELECT("RC[1]")
38 =FORMULA("")
39 =SELECT("RC[1]")
40 =FORMULA("")
41 =SELECT("RC[-3]")
42 =ALERT("There are no serines in this peptide!",3)
43 =ELSE()
44 =END.IF()
45 =ECHO(TRUE)
46 =SELECT("R[1]C[-2]")
47 =RETURN()

```

{End}

Subroutine for the calculation of the constituents and charge of the peptide

This subroutine is called by the above control routine and calculates the amino acid constituents of the peptide and its associated charge. At the end of the calculation the control returns to the main control subroutine and the next section of the program is operated. The column heading, C, and row numbers represent the positioning of the program on the Excel spreadsheet.

C

```
1   Charge
2   =RESULT(1)
3   =SET.NAME("Ala",0)           {Lines 3 - 22 sets the amino acid counters to zero.}
4   =SET.NAME("Arg",0)
5   =SET.NAME("Asn",0)
6   =SET.NAME("Asp",0)
7   =SET.NAME("Cys",0)
8   =SET.NAME("Glu",0)
9   =SET.NAME("Gln",0)
10  =SET.NAME("Gly",0)
11  =SET.NAME("His",0)
12  =SET.NAME("Ile",0)
13  =SET.NAME("Leu",0)
14  =SET.NAME("Lys",0)
15  =SET.NAME("Met",0)
16  =SET.NAME("Phe",0)
17  =SET.NAME("Pro",0)
18  =SET.NAME("Ser",0)
19  =SET.NAME("Thr",0)
20  =SET.NAME("Trp",0)
21  =SET.NAME("Tyr",0)
22  =SET.NAME("Val",0)
23  =ARGUMENT("PEP",2)
24  =LEN(PEP)                    {Number of amino acids in the peptide.}
25  =FOR("Counter",1,C24,1)      {Lines 25 - 107 takes the first amino acid (single}
26  =MID(PEP,Counter,1)          {letter code) and determines which amino acid it }
27  =IF($C$26="A")               {is. When found it adds one to the score of the}
28  =SET.NAME("Ala",Ala+1)       {total number of amino acids of that type found in }
29  =ELSE()                      {the peptide. When line 107 is reached the }
30  =END.IF()                   {program returns to line 25 and the process is}
31  =IF($C$26="R")               {repeated for the next letter. This process}
32  =SET.NAME("Arg",Arg+1)       {continues until all the amino acids in the peptide}
33  =ELSE()                      {have been checked.}
34  =END.IF()
35  =IF($C$26="N")
36  =SET.NAME("Asn",Asn+1)
37  =ELSE()
38  =END.IF()
39  =IF($C$26="D")
40  =SET.NAME("Asp",Asp+1)
41  =ELSE()
42  =END.IF()
43  =IF($C$26="C")
```

```

44 =SET.NAME("Cys",Cys+1)
45 =ELSE()
46 =END.IF()
47 =IF($C$26="E")
48 =SET.NAME("Glu",Glu+1)
49 =ELSE()
50 =END.IF()
51 =IF($C$26="Q")
52 =SET.NAME("Gln",Gln+1)
53 =ELSE()
54 =END.IF()
55 =IF($C$26="G")
56 =SET.NAME("Gly",Gly+1)
57 =ELSE()
58 =END.IF()
59 =IF($C$26="H")
60 =SET.NAME("His",His+1)
61 =ELSE()
62 =END.IF()
63 =IF($C$26="I")
64 =SET.NAME("Ile",Ile+1)
65 =ELSE()
66 =END.IF()
67 =IF($C$26="L")
68 =SET.NAME("Leu",Leu+1)
69 =ELSE()
70 =END.IF()
71 =IF($C$26="K")
72 =SET.NAME("Lys",Lys+1)
73 =ELSE()
74 =END.IF()
75 =IF($C$26="M")
76 =SET.NAME("Met",Met+1)
77 =ELSE()
78 =END.IF()
79 =IF($C$26="F")
80 =SET.NAME("Phe",Phe+1)
81 =ELSE()
82 =END.IF()
83 =IF($C$26="P")
84 =SET.NAME("Pro",Pro+1)
85 =ELSE()
86 =END.IF()
87 =IF($C$26="S")
88 =SET.NAME("Ser",Ser+1)
89 =ELSE()
90 =END.IF()
91 =IF($C$26="T")
92 =SET.NAME("Thr",Thr+1)
93 =ELSE()
94 =END.IF()
95 =IF($C$26="W")
96 =SET.NAME("Trp",Trp+1)

```

```

97 =ELSE()
98 =END.IF()
99 =IF($C$26="Y")
100 =SET.NAME("Tyr",Tyr+1)
101 =ELSE()
102 =END.IF()
103 =IF($C$26="V")
104 =SET.NAME("Val",Val+1)
105 =ELSE()
106 =END.IF()
107 =NEXT()
108 =(Arg*1)+(Cys*-1)+(Lys*1)+(His*1)+((Ser-1)*-1)
109 =RETURN(C108)

```

{Line 108 calculates the charge of the peptide and this value is returned by line 109 to the main control program}

Subroutine for the calculation of the molecular weight of the peptide

This subroutine calculates the mass of the peptide. The column heading, E, and row numbers represent the positioning of the program on the Excel spreadsheet.

	E		
1	MW		
2	=RESULT(1)		
3	=Ala*89	{Lines 3 - 22 calculate the mass of the } {individual amino acids in the peptide based } {on the known numbers of the different } {amino acids calculated in the last } {subroutine.}	
4	=Arg*174		
5	=Asn*132		
6	=Asp*133		
7	=Cys*121		
8	=Glu*147		
9	=Gln*146		
10	=Gly*75		
11	=His*155		
12	=Ile*131		
13	=Leu*131		
14	=Lys*146		
15	=Met*149		
16	=Phe*165		
17	=Pro*115		
18	=Thr*119		
19	=Trp*204		
20	=Tyr*181		
21	=Val*117		
22	=Ser*185		
23	=SUM(E3:E22)		{Calculates mass of peptide}
24	=E23-(18*(LEN(PEP)-1))		{Subtracts the mass of water lost in forming the peptide.}
25	=RETURN(E24)	{Reports the final mass.}	

Calculation and output of results

The Macro is activated from cell C2 on the spread sheet.

C2					
	A	B	C	D	E
1	No.	Peptide	Charge	Mass	Ratio
2	1	MHESKRGD			
3	2	HSSWGMKAA			
4	3	SRE			
5					

After the Macro has run it reports the charge (3), mass (1038) and mass - charge ratio (2.93, [this actually represents the mass - charge ratio multiplied by 100]) of the peptide in cells C2, D2 and E2, respectively.

C3					
	A	B	C	D	E
1	No.	Peptide	Charge	Mass	Ratio
2	1	MHESKRGD	3	1038	2.93
3	2	HSSWGMKAAA			
4	3	SRE			
5					

When the Macro is activated in cell C3 to calculate the mass - charge ratio of the second peptide (HSSWGMKAA) it finds that it contains two serines and this is reported.

C3					
	A	B	C	D	E
1	No.	Pep			
2	1	MH			
3	2	HSS			
4	3	SRE			
5					



Peptide contains 2 serines.

OK

Once the report has been acknowledged the Macro continues with the calculation, inserts a new row and pastes a copy of the peptide in B4. The mass - charge ratios are then reported in the usual fashion with the changes in mass and charge as a result of an extra phosphorylation event being taken into account.

	A	B	C	D	E
1	No.	Peptide	Charge	Mass	Ratio
2	1	MHESKRGD	3	1038	2.93
3	2	HSSWGMKAAA	1	1204	0.88
4		HSSWGMKAAA	2	1124	1.85
5	3	SRE			

Finally the mass charge ratio of the last peptide is calculated by activating the Macro in C5.

	A	B	C	D	E
1	No.	Peptide	Charge	Mass	Ratio
2	1	MHESKRGD	3	1038	2.93
3	2	HSSWGMKAAA	1	1204	0.88
4		HSSWGMKAAA	2	1124	1.85
5	3	SRE	+	470	1.65

Calculation of Mann - Whitney U value

This Excel macro calculates the Mann - Whitney U value for two sets of data in an argument where the data sets are expressed in terms of standard Excel arrays (e.g. A2:E2, A3:F3). The value reported is the U value for which the corresponding p value can be found by using any standard set of statistical tables. The column heading, A, and row numbers represent the positioning of the program on the Excel spreadsheet.

A

```

1  ManWhit
2  =RESULT(1)
3  =ECHO(FALSE)
4  =ARGUMENT("Array1",8)           {Lines 4 and 5 define the argument array}
5  =ARGUMENT("Array2",8)
6  =SET.NAME("U",0)               {Lines 6 - 10 defines names and sets to zero}
7  =SET.NAME("EqualPlace",0)
8  =SET.NAME("low",0)
9  =SET.NAME("UI",0)
10 =SET.NAME("FinalU",0)
11 =COUNT(Array1)                {n1= for Array 1}
12 =COUNT(Array2)                {n2= for Array 2}
13 =SET.NAME("SumRank",0)
14 =SET.NAME("TotalEqual",0)
15 =IF(A11<=A12)
16 =FOR.CELL("TestCell",Array1,TRUE)
17 =SET.NAME("EqualPlace",-0.5)
18 =FOR.CELL("CCell",Array1,Array2,TRUE)
19 =IF(TestCell=CCell)
20 =SET.NAME("EqualPlace",EqualPlace+0.5)
21 =ELSE()
22 =END.IF()
23 =NEXT()

```

```

24 =SET.NAME("TotalEqual",TotalEqual+EqualPlace)
25 =NEXT()
26 =FOR.CELL("CurrentCell",Array1,TRUE)
27 =RANK(CurrentCell,(Array1,Array2),1)
28 =SET.NAME("SumRank",SumRank+A27)
29 =NEXT()
30 =SET.NAME("SumRank",SumRank+TotalEqual)
31 =ELSE()
32 =FOR.CELL("TestCell",Array2,TRUE)
33 =SET.NAME("EqualPlace",-0.5)
34 =FOR.CELL("CCell",Array1,Array2,TRUE)
35 =IF(TestCell=CCell)
36 =SET.NAME("EqualPlace",EqualPlace+0.5)
37 =ELSE()
38 =END.IF()
39 =NEXT()
40 =SET.NAME("TotalEqual",TotalEqual+EqualPlace)
41 =NEXT()
42 =FOR.CELL("CurrentCell",Array2,TRUE)
43 =RANK(CurrentCell,(Array1,Array2),1)
44 =SET.NAME("SumRank",SumRank+A43)
45 =NEXT()
46 =SET.NAME("SumRank",SumRank+TotalEqual)
47 =END.IF()
48 =IF(A11<A12)
49 =SET.NAME("U", U+(A11*A12)+((A11*(A11+1))/2)-SumRank)
50 =SET.NAME("UI",UI+(A11*A12)-A49)
51 =ELSE()
52 =SET.NAME("U", U+(A11*A12)+((A12*(A12+1))/2)-SumRank)
53 =SET.NAME("UI",UI+(A11*A12)-A52)
54 =END.IF()
55 =IF(U<UI)
56 =SET.NAME("FinalU",FinalU+U)
57 =ELSE()
58 =SET.NAME("FinalU",FinalU+UI)
59 =END.IF()
60 =ECHO(TRUE)
61 =RETURN(FinalU)

```

{Lines 15 - 31 ranks the two sets of data and calculates the sum of the ranking if $n_1 \leq n_2$ }

{Lines 32 - 47 ranks the two sets of data and calculates the sum of the ranking if $n_1 > n_2$ }

{Lines 48 - 54 calculates the U values depending on whether $n_1 < n_2$ or $n_1 \geq n_2$ }

{Lines 55 - 61 determine which (U1 or U) is the smallest U value and reports it}

Appendix 9

Buffer A

10 mM	Tris - HCl, pH7.4	1.20 g dm ⁻³
1 mM	EDTA	0.37 g dm ⁻³
1 mM	EGTA	0.37 g dm ⁻³
10 mM	β-glycerophosphate	2.17 g dm ⁻³
2 mM	Benzamidine	0.31 g dm ⁻³
1 mM	Phospho - serine	0.20 g dm ⁻³
1 mM	Phospho - threonine	0.22 g dm ⁻³
0.25 M	Sucrose	25.65 g dm ⁻³

Just before use mix:

25 ml	Buffer A
300 μl	PMSF (17 mg / ml, dissolved in methanol)
25 μl	Aprotinin (stock: 10 mg/ml)
25 μl	Leupeptin (stock: 10 mg/ml)
2.5 μl	Okadaic acid (stock [10 ⁻⁴ M] dissolved in dimethyl sulphoxide)

Appendix 10

Solutions for Western Blotting

Blot Electrode Buffer (BEB)

25 mM	Tris	3.0 g dm ⁻³
192 mM	Glycine	14.4 g dm ⁻³
20% (v/v)	Methanol	200 ml dm ⁻³

Tris - Buffered - Saline - Tween (TSB-T)

10 mM	Tris - HCl, pH 7.4	1.21 g dm ⁻³
140 mM	NaCl	8.18 g dm ⁻³
0.1% (v/v)	Polyoxyethylene sorbitan monolaurat (Tween 20)	

High - Salt - Tris Buffer (HST)

10 mM	Tris - HCl, pH 7.4	1.21 g dm ⁻³
1 M	NaCl	58.4 g dm ⁻³
0.5% (v/v)	Tween 20	

Developing solution

Solution:- 0.4% (w/v) 3-Amino-9-ethylcarbazol (AEC) in dimethyl formamide.

0.4 ml	0.4% (w/v) AEC
9.5 ml	50 mM Sodium acetate pH 5 (pH with glacial acetic acid)
5 μ l	Tween 20
3 μ l	H ₂ O ₂

Ponceau S stain

0.1% (w/v) Ponceau S in 3% (w/v) trichloro-acetic acid.

Appendix 11

Solutions for enzyme - linked immuno - assays (ELISA)

0.1 M sodium carbonate buffer (pH9.6)

Sodium carbonate	1.7 g dm ⁻³
Sodium hydrogen carbonate	2.68 g dm ⁻³

Developing solution

Citric acid buffer (pH6)

18 mM Citric acid	3.78 g dm ⁻³
65 mM Na ₂ HPO ₄	9.23 g dm ⁻³

Developing solution

6 mg	orthophenylenediamine
15 ml	Citric acid buffer (pH6)
5 μ l	H ₂ O ₂

Appendix 12

Calculations of peptides and mass - charge ratios for α -G_{i-2}

Primary sequence of rat α -G_{i-2}

	10	20	30	40	50	
MGCTYSAEDKAAAERSKMIDKNLREDGEKAAREYKLLLLGAGESGKSTIY						50
KQMKIIHEDGYSEEECRQYRAYVYSNTIQSIMAIYKAMGNLQIDFADPQR						100
ADDARQLFALSCAAEEQGMLPEDLSGVIRRLWADHGYQACFGRSREYQLN						150
DSAAYYLNDLERIAQSDYIPTQQDYLRTRYKTTGIVETHFTFKDLHFKMF						200
DYGGQRSEKRWIHC FEGYTAIIFCYALSAYDLVLAEDEEMNRMHESMKL						250
FDSICNNKWFTDTSIILFLNKKDLFEKITSPLTICFPEYTGANKYDEA						300
ASYIQSKFEDLNKRKDTKEIYTHFTCATDTKNYQFYFDAVTDVI IKNNLK						350
DCGLF						355

Possible trypsin and V8 peptides

Using the method outlined in chapter 3 it is possible to predict the serines that possess the best kinase motifs and the peptides that will be produced that contain them on enzymatic cleavage. The table below lists the predicted peptides. (Please see chapter 3 for a more complete explanation.)

Ser	Poss (V8)	Trypsin			Try +V8			Poss(mr)		
		Sequence	c	MW	mr	Sequence	c		MW	mr
16	Y	11A - 21K	3	1299	2.52	15R - 20D	2	829	2.27	N
16	N	11A - 17K	2	812	2.30					
16	N	16S - 21K	2	801	2.32					
16	N	16S - 17K	1	313	2.17					
44	N	30A - 46K	3	1712	2.10					
44	N	33E - 46K	2	1494	1.53					
44	N	36L - 46K	1	1137	0.92					
47	Y	30A - 67R	7	4270	2.66	44S - 58E	4	1779	2.72	Y
47						44S - 59D	4	1894	2.61	N
47						34V - 58E	5	2774	2.53	N
47						34V - 59D	5	2889	2.47	N
47						44S - 63E	4	2331	2.28	N
47						34V - 63E	5	3325	2.24	N
47						44S - 64E	4	2460	2.20	N
47						34V - 64E	5	3454	2.19	N
47						34V - 65E	5	3583	2.14	N
47						44S - 65E	4	2589	2.12	N
47	N	47S - 67R	4	2576	2.13					
47	Y	33E - 67R	6	3972	2.39	44S - 58E	4	1779	2.72	Y
47						44S - 59D	4	1894	2.61	Y
47						34V - 58E	5	2774	2.53	Y
47						34V - 59D	5	2889	2.47	Y
47						44S - 63E	4	2331	2.28	N
47						34V - 63E	5	3325	2.24	N
47						44S - 64E	4	2460	2.20	N
47						34V - 64E	5	3454	2.19	N
47						34V - 65E	5	3583	2.14	N
47						44S - 65E	4	2589	2.12	N
47	Y	36L - 67R	5	3615	2.12	44S - 58E	4	1779	2.72	Y
47						44S - 59D	4	1894	2.61	Y
47						44S - 63E	4	2331	2.28	Y
47						44S - 64E	4	2460	2.20	Y
47						44S - 65E	4	2589	2.12	Y
47	N	36L - 54K	3	2054	1.86					
47	N	36L - 51K	2	1666	1.42					
47	N	47S - 54K	2	1014	1.98					
47	N	47S - 51K	1	627	1.37					
47	N	36L - 51K	2	1666	1.42					

144	Y	106Q - 177R	5	8288	1.22	131L - 146E	4	2694	2.07	Y
144						123D - 146E	4	2809	2.01	Y
144						124L - 159D	4	3328	1.79	Y
144						123D - 159D	4	3443	1.75	Y
144						117Q - 146E	4	3465	1.75	Y
144						116E - 146E	4	3594	1.70	Y
144						124L - 167D	5	5139	1.68	Y
144						135H - 146E	2	1427	1.58	Y
144						117Q - 159D	4	4099	1.56	Y
144						124L - 159D	4	4226	1.53	Y
144						116E - 159D	4	4228	1.53	Y
144						116E - 167D	5	6039	1.51	Y
144						123D - 159D	4	4341	1.50	Y
144						123D - 174D	5	6100	1.50	Y
144						123D - 161E	4	4583	1.45	Y
144						117Q - 174D	5	6756	1.40	Y
144						116E - 174D	5	6885	1.38	Y
144						117Q - 159D	4	4997	1.37	Y
144						116E - 159D	4	5126	1.35	Y
144						117Q - 161E	4	5239	1.33	Y
144						116E - 161E	4	5368	1.30	Y
144						135H - 151D	2	2060	1.24	Y
144						135H - 167D	3	3871	1.22	Y
144						135H - 159D	2	2958	0.97	N
144	Y	130R - 177R	5	5727	1.56	135H - 146E	2	1427	1.58	Y
144						135H - 151D	2	2060	1.24	N
144						135H - 167D	3	3871	1.22	N
144						135H - 174D	3	4717	1.07	N
144						135H - 159D	2	2958	0.97	N
144						135H - 161E	2	3200	0.92	N
144	Y	131L - 177R	4	5571	1.27	135H - 146E	2	1427	1.58	Y
144						135H - 151D	2	2060	1.24	N
144						135H - 159D	2	2958	0.97	N
144						135H - 161E	2	3200	0.92	N
144	N	144S - 177R	3	4129	1.17					
144	N	144S - 162R	2	2400	1.12					
144	N	144S - 145R	1	341	2.05					
144	Y	106Q - 162R	4	6559	1.14	124L - 146E	4	2694	2.07	Y
144						123D - 146E	4	2809	2.01	Y
144						124L - 151D	4	3328	1.79	Y
144						123D - 151D	4	3443	1.75	Y
144						117Q - 146E	4	3465	1.75	Y
144						116E - 146E	4	3594	1.70	Y
144						135H - 146E	2	1427	1.58	Y
144						117Q - 151D	4	4099	1.56	Y
144						124L - 159D	4	4226	1.53	Y
144						116E - 151D	4	4228	1.53	Y
144						123D - 159D	4	4341	1.50	Y
144						123D - 161E	4	4583	1.45	Y
144						117Q - 159D	4	4997	1.37	Y

144						116E - 159D	4	5126	1.35	Y
144						117Q - 161E	4	5239	1.33	Y
144						116E - 161E	4	5368	1.30	Y
144						135H - 151D	2	2060	1.24	Y
144						135H - 159D	2	2958	0.97	N
144	N	106Q - 145R	3	4500	1.10					
144	Y	130R - 162R	4	3998	1.59	135H - 146E	2	1427	1.58	N
144						135H - 151D	2	2060	1.24	N
144						135H - 159D	2	2958	0.97	N
144						135H - 161E	2	3200	0.92	N
144	N	130R - 145R	3	1939	1.93					
144	Y	131L - 162R	3	3842	1.22	135H - 146E	2	1427	1.58	Y
144						135H - 151D	2	2060	1.24	Y
144						135H - 159D	2	2958	0.97	N
144						135H - 161E	2	3200	0.92	N
144	N	131L - 145R	2	1783	1.36					
207	Y	194D - 243R	5	5900	1.53	202V - 217E	4	2040	2.49	Y
207						202V - 232D	3	3565	1.29	N
207						202V - 238E	3	4091	1.17	N
207						202V - 239D	3	4206	1.15	N
207						202V - 208E	1	812	1.15	N
207						202V - 240E	3	4335	1.13	N
207						202V - 241E	3	4465	1.11	N
207	Y	194D - 211K	5	2259	2.90	195L - 208E	2	1731	1.39	N
207						202V - 208E	1	812	1.15	N
207	Y	194D - 210K	4	2131	2.42	195L - 208E	2	1731	1.39	N
207						202V - 208E	1	812	1.15	N
207	Y	194D - 209R	3	2002	1.89	195L - 208E	2	1731	1.39	N
207						202V - 208E	1	812	1.15	N
207	Y	199M - 243R	4	5260	1.32	202V - 217E	4	2040	2.49	Y
207						202V - 232D	3	3565	1.29	N
207						202V - 238E	3	4091	1.17	N
207						202V - 239D	3	4206	1.15	N
207						202V - 208E	1	812	1.15	N
207						202V - 240E	3	4335	1.13	N
207						202V - 241E	3	4465	1.11	N
207	N	207S - 243R	3	4368	1.12					
207	Y	199M - 211K	4	1618	2.90	202V - 208E	1	812	1.15	N
207	Y	199M - 210K	3	1490	2.30	202V - 208E	1	812	1.15	N
207	Y	199M - 209R	2	1362	1.63	202V - 208E	1	812	1.15	N
207	N	207S - 211K	3	727	3.71					
207	N	207S - 210K	2	599	2.82					
207	N	207S - 209R	1	470	1.65					
247	N	244M - 258K	3	1877	1.97					
247	N	244M - 249K	2	842	2.24					
306	Y	297Y - 331K	6	4242	2.29	300A - 319E	5	2452	2.75	Y
306						299E - 319E	5	2581	2.66	Y

306						300A - 316D	4	2093	2.44	Y
306						299E - 316D	4	2222	2.35	Y
306						300A - 329D	5	3605	2.13	N
306						299E - 329D	5	3734	2.08	N
306						300A - 309E	1	1223	0.87	N
306						300A - 310D	1	1338	0.82	N
306						299E - 309E	1	1352	0.82	N
306						299E - 310D	1	1467	0.77	N
306	Y	297Y - 318K	5	2730	2.56	300A - 316D	4	2093	2.44	N
306						299E - 316D	4	2222	2.35	N
306						300A - 309E	1	1223	0.87	N
306						300A - 310D	1	1338	0.82	N
306						299E - 309E	1	1352	0.82	N
306						299E - 310D	1	1467	0.77	N
306	Y	297Y - 315K	4	2385	2.24	300A - 309E	1	1223	0.87	N
306						300A - 310D	1	1338	0.82	N
306						299E - 309E	1	1352	0.82	N
306						299E - 310D	1	1467	0.77	N
306	Y	297Y - 314R	3	2257	1.74	300A - 309E	1	1223	0.87	N
306						300A - 310D	1	1338	0.82	N
306						299E - 309E	1	1352	0.82	N
306						299E - 310D	1	1467	0.77	N
306	Y	297Y - 313K	2	2101	1.22	300A - 309E	1	1223	0.87	N
306						300A - 310D	1	1338	0.82	N
306						299E - 309E	1	1352	0.82	N
306						299E - 310D	1	1467	0.77	N
306	N	297Y - 307K	0	1354	0.00					

Remaining peptides

From the data presented in chapter 3, that is V8 cleavage of the tryptic peptide increases its mass - charge ratio, then it is possible to eliminate all peptides from the above table that are either not cleaved by V8 or whose mass - charge ratio decreases. This leaves the following peptides as candidates. (Please see chapter 3 for a more complete explanation.)

Ser	Poss (V8)	Trypsin			Try +V8			Poss(mr)		
		Sequence	c	MW	mr	Sequence	c		MW	mr
47	Y	30A - 67R	7	4270	2.66	44S - 58E	4	1779	2.72	Y
47	Y	33E - 67R	6	3972	2.39	44S - 58E	4	1779	2.72	Y
47						44S - 59D	4	1894	2.61	Y
47						34V - 58E	5	2774	2.53	Y
47						34V - 59D	5	2889	2.47	Y
47	Y	36L - 67R	5	3615	2.12	44S - 58E	4	1779	2.72	Y
47						44S - 59D	4	1894	2.61	Y
47						44S - 63E	4	2331	2.28	Y
47						44S - 64E	4	2460	2.20	Y
47						44S - 65E	4	2589	2.12	Y
144	Y	106Q - 177R	5	8288	1.22	131L - 146E	4	2694	2.07	Y

144					123D - 146E	4	2809	2.01	Y	
144					124L - 159D	4	3328	1.79	Y	
144					123D - 159D	4	3443	1.75	Y	
144					117Q - 146E	4	3465	1.75	Y	
144					116E - 146E	4	3594	1.70	Y	
144					124L - 167D	5	5139	1.68	Y	
144					135H - 146E	2	1427	1.58	Y	
144					117Q - 159D	4	4099	1.56	Y	
144					124L - 159D	4	4226	1.53	Y	
144					116E - 159D	4	4228	1.53	Y	
144					116E - 167D	5	6039	1.51	Y	
144					123D - 159D	4	4341	1.50	Y	
144					123D - 174D	5	6100	1.50	Y	
144					123D - 161E	4	4583	1.45	Y	
144					117Q - 174D	5	6756	1.40	Y	
144					116E - 174D	5	6885	1.38	Y	
144					117Q - 159D	4	4997	1.37	Y	
144					116E - 159D	4	5126	1.35	Y	
144					117Q - 161E	4	5239	1.33	Y	
144					116E - 161E	4	5368	1.30	Y	
144					135H - 151D	2	2060	1.24	Y	
144					135H - 167D	3	3871	1.22	Y	
144	Y	130R - 177R	5	5727	1.56	135H - 146E	2	1427	1.58	Y
144	Y	131L - 177R	4	5571	1.27	135H - 146E	2	1427	1.58	Y
144	Y	106Q - 162R	4	6559	1.14	124L - 146E	4	2694	2.07	Y
144					123D - 146E	4	2809	2.01	Y	
144					124L - 151D	4	3328	1.79	Y	
144					123D - 151D	4	3443	1.75	Y	
144					117Q - 146E	4	3465	1.75	Y	
144					116E - 146E	4	3594	1.70	Y	
144					135H - 146E	2	1427	1.58	Y	
144					117Q - 151D	4	4099	1.56	Y	
144					124L - 159D	4	4226	1.53	Y	
144					116E - 151D	4	4228	1.53	Y	
144					123D - 159D	4	4341	1.50	Y	
144					123D - 161E	4	4583	1.45	Y	
144					117Q - 159D	4	4997	1.37	Y	
144					116E - 159D	4	5126	1.35	Y	
144					117Q - 161E	4	5239	1.33	Y	
144					116E - 161E	4	5368	1.30	Y	
144					135H - 151D	2	2060	1.24	Y	
144	Y	131L - 162R	3	3842	1.22	135H - 146E	2	1427	1.58	Y
144					135H - 151D	2	2060	1.24	Y	
207	Y	194D - 243R	5	5900	1.53	202V - 217E	4	2040	2.49	Y
207	Y	199M - 243R	4	5260	1.32	202V - 217E	4	2040	2.49	Y
306	Y	297Y - 331K	6	4242	2.29	300A - 319E	5	2452	2.75	Y
306					299E - 319E	5	2581	2.66	Y	
306					300A - 316D	4	2093	2.44	Y	
306					299E - 316D	4	2222	2.35	Y	

Ser = serine number in primary sequence; Poss (V8) = whether the peptide contains a sequence that can be cleaved by V8 (Y = Yes; N = No); Trypsin Sequence = proposed tryptic peptide, number is the position in the primary amino acid sequence, letter the amino acid; c = charge on peptide; MW = molecular weight; mr = mass - charge ratio (multiplied by 100); Try + V8 Sequence = proposed V8 peptide cleaved from corresponding tryptic peptide; Poss (mr) = change in mass - charge ratio of the trypsin peptide upon V8 cleavage, Y = increase, N = decrease. See text in Chapter 3, sections 3.1.2 and 3.1.4, for description of technique for prediction of peptides, and kinase motifs. See sections 2.2.12 and 3.1.4, for description of mass - charge ratio calculations.

Appendix 13

Estimation of α -G_{i-2} loaded per t.l.c. plate

Each t.l.c plate had approximately 100 c.p.m. of ³²P labelled α -G_{i-2} peptides loaded onto it. As this figure was determined by Cerenkov, which has a 50% efficiency, then it is assumed that 200 d.p.m. was applied to the plate. As the time required to process the peptides took approximately one half life (14.3 days) then it is assumed that the loading was in the region of 400 d.p.m. Note: It has been assumed that ³²P is in excess of cold phosphate and no consideration is taken into account for cold labelling.

Using the equations:

$$-\frac{dN}{dt} = \lambda N \qquad \lambda = \frac{0.693}{t_{1/2}}$$

Where $-dN/dt$ = the number of atoms decaying per small increment of time, N = total number of radioactive atoms present at a given time, λ = the decay constant of the isotope and $t_{1/2}$ = half life of ³²P, which equals 14.3 days or 20592 minutes.

Therefore using the above equations and rearranging:

$$N = \frac{400}{(0.693 / 20592)}$$

Therefore:

$$N = 11.8 \times 10^6 \text{ atoms}$$

Avogadro's number = 6.02×10^{23}

Therefore as stoichiometry of labelling is approximately 1 mol ^{32}P / mol $\alpha\text{-G}_{i-2}$ (Bushfield *et al.*, 1990) then there is approximately 20×10^{-18} moles or 20 amoles of $\alpha\text{-G}_{i-2}$.

As 10 - 100 pmoles are required for sequencing then the experiment only produces one ten-millionth of the amount required although the level of peptide actually present are most probably higher it still seems likely that the pmole range will not be reached.

References

- Abdel-Latif, A.A. (1986) *Pharmacol. Rev.* **38** 228-272 Calcium-mobilising receptors, polyphosphoinositides, and the generation of second messengers.
- Ahmad, S., Banville, D., Zhao, Z., Fischer, E.H. & Shen, S.-H. (1993) *PNAS* **90** 2197-2201 A widely expressed human protein-tyrosine phosphatase containing src homology 2 domains.
- Ahn, J., Donner, D.B. & Rosen, O.M. (1993) *J. Biol. Chem.* **268** 7571-7576 Interaction of the human insulin receptor tyrosine kinase from the baculovirus expression system with protein kinase C in a cell-free system.
- Argettsinger, L.S. & Shafer, J.A. (1992) *J. Biol. Chem.* **267** 22095-22101 The reversible and irreversible autophosphorylations of insulin receptor kinase.
- Argos, P. (1989) *Protein structure: a practical approach.* (Ed. T. E. Creighton) 169-191 Predictions of protein structure from gene and amino acid sequences.
- Asano, T. & Hidaka, H. (1984) *J. Pharm. Exp. Ther.* **231** 141-145 Vasodilatory action of HA1004 [N-(2-guanidinoethyl)-5-isoquinolinesulfonamide], a novel calcium antagonist with no effects on cardiac function.
- Avurch, J., Tornqvist, H.E., Gunsalus, J.R., Yurkow, E.J., Kyriakis, J.M. & Price, D.J. (1990) *Handbook of Experimental Pharmacology* (Ed. P. Cuatrecasas) **92** 313-366 Insulin receptor-mediated transmembrane signal.
- Azzi, A., Boscoboinik, D. & Hensey, C. (1992) *Eur. J. Biochem.* **208** 547-557 The protein kinase C family.
- Backer, J.M., Myers, M.J., Sun, X.J., Chin, D.J., Shoelson, S.E., Miralpeix, M. & White, M.F. (1993) *J. Biol. Chem.* **268** 8204-8212 Association of IRS-1 with the insulin receptor and the phosphatidylinositol 3'-kinase. Formation of binary and ternary signaling complexes in intact cells.
- Backer, J.M., Schroeder, G.G., Kahn, C.R., Myers, M.G.J., Wilden, P.A., Cahill, D.A. & White, M.F. (1992) *J. Biol. Chem.* **267** 1367-1374 Insulin stimulation of phosphatidylinositol 3-kinase activity maps to insulin receptor regions required for endogenous substrate phosphorylation.
- Balch, W.E. (1990) *TIBS* **15** 473-472 Small GTP-binding proteins in vesicular transport.
- Baltensperger, K., Kozma, L.M., Cherniack, A.D., Klarlund, J.K., Chawla, A., Banerjee, U. & Czech, M.P. (1993) *Science* **260** 1950-1952 Binding of the Ras activator Son of Sevenless to insulin receptor substrate-1 signaling complexes.
- Banno, Y. & Nozawa, Y. (1987) *Biochem. J.* **248** 95-101 Characterization of partially purified phospholipase C from human platelet membranes.
- Banno, Y., Yada, Y. & Nozawa, Y. (1988) *J. Biol. Chem.* **263** 11459-65 Purification and characterization of membrane-bound phospholipase C specific for phosphoinositides from human platelets.
- Baron, M., Norman, D.G. & Campbell, I.D. (1991) *TIBS* **16** 13-17 Protein modules.

- Baron, V., Kaliman, P., Gautier, N. & Van Obberghen, E. (1992) *J. Biol. Chem.* 267 23290-23294 The insulin receptor activation process involves localized conformational changes.
- Baumgold, J. (1992) *Trends Pharmacol Sci.* 13 339-340 Muscarinic receptor-mediated stimulation of adenylyl cyclase.
- Beavo, J. (1990) Cyclic nucleotide phosphodiesterases: structure, regulation and drug action. (Ed. J. Beavo & M. D. Houslay) 2 3-15 Multiple phosphodiesterase isoenzymes: Background, nomenclature and implications.
- Begum, N., Olefsky, J.M. & Draznin, B. (1993) *J. Biol. Chem.* 268 7917-7922 Mechanism of impaired metabolic signalling by a truncated human insulin receptor - decreased activation of protein phosphatase-1 by insulin.
- Begum, N., Sussman, K.E. & Draznin, B. (1991) *Diabetes* 40 1620-1629 Differential effects of diabetes on adipocyte and liver phosphotyrosine and phosphoserine phosphatase activities.
- Berlot, C.H. & Bourne, H.R. (1992) *Cell* 68 911-922 Identification of effector-activating residues of G α .
- Berridge, M.J. (1987a) *Biochim. Biophys. Acta* 907 33-45 Inositol ligands and cell proliferation.
- Berridge, M.J. (1987b) *Ann. Rev. Biochem.* 56 159-193 Inositol trisphosphates and diacylglycerol: Two interacting second messengers.
- Berridge, M.J. (1993) *Nature* 361 315-325 Inositol trisphosphate and calcium signalling.
- Berridge, M.J. & Irvine, R.F. (1989) *Nature* 341 197-205 Inositol phosphates and cell signalling.
- Berry, M.N. & Friend, D.S. (1969) *J. Cell. Biol.* 43 506-520 High yield preparation of isolated rat liver parenchymal cells.
- Billah, M.M. (1993) *Curr. Opin. Imm.* 5 114-123 Phospholipase D and cell signaling.
- Billah, M.M., Eckel, S., Mullmann, T.J., Egan, R.W. & Siegel, M.I. (1988) *J. Biol. Chem.* 264 17069-17077 Phosphatidylcholine hydrolysis by phospholipase D determines phosphatidate and diglyceride levels in chemotactic peptide-stimulated human neutrophils.
- Birkett, C.R., Foster, K.E., Johnson, L. & Gull, K. (1985) *FEBS Lett.* 187 211-218 Use of monoclonal antibodies to analyse the expression of multi-tubulin families.
- Birnbaumer, L. (1992) *Cell* 71 1069-1072 Receptor-to-effector signalling through G-proteins: Role of $\beta\gamma$ dimers as well as α -subunits.
- Birnbaumer, L., Abramowitz, J. & Brown, A.M. (1990) *Biochim. Biophys. Acta.* 1031 163-224 Receptor-effector coupling by G-proteins.
- Blumberg, P.M., Jaken, S., Konig, B., Sharkey, N.A., Leach, K.L., Jeng, A.Y. & Yeh, E. (1984) *Biochem. Pharm.* 33 933-940 Mechanism of action of phorbol ester tumor promoters: Specific receptors for lipophilic ligands.
- Bokoch, G.M. (1993) *Biochem. J.* 289 17-24 Biology of the Rap proteins, members of the ras superfamily of GTP-binding proteins.

- Bollen, M. & Stalmans, W. (1992) *Crit. Rev. Biochem. Mol. Biol.* 27 227-281 The structure, role, and regulation of type I protein phosphatases.
- Bonner, W.M. & Laskey, R.A. (1974) *Eur. J. Biochem.* 46 83-88 A film detection method for tritium-labelled proteins and nucleic acids in polyacrylamide gels.
- Bottazzo, G.F. (1993) *Diabetes* 42 778-800 Banting Lecture: On the Honey Disease, a dialogue with Socrates [ΠΕΡΙ ΤΟΥ ΜΕΛΙΤΟΣ ΠΑΘΟΥΣ ΔΙΑΛΟΓΟΣ ΣΟΚΡΑΤΗ -].
- Bourne, H.R. & Stryer, L. (1992) *Nature* 358 541-543 The target sets the tempo.
- Bowen, L., Stein, P.P., Stevenson, R. & Shulman, G.I. (1991) *Metabolism* 40 1025-1030 The effect of CP 68,722, a thiozolidinedione derivative, on insulin sensitivity in lean and obese Zucker rats.
- Boyle, W.J., van der Geer, P. & Hunter, T. (1991) *Methods in Enzymology* 201 110-149 Phosphopeptide mapping and phosphoamino acid analysis by two-dimensional separation on thin-layer cellulose plates.
- Brader, M.L. & Dunn, M.F. (1991) *TIBS* 16 341-345 Insulin hexamers: new conformations and applications.
- Bradford, M.M. (1976) *Analytical Biochem.* 72 248-254 A rapid and sensitive method for the quantitation of microgram quantities of protein utilising the principle of protein dye binding.
- Bray, G.A. (1977) *Fed. Proc.* 36 148-153 The Zucker-fatty rat: a review.
- Breddam, K. & Meldal, M. (1992) *Eur. J. Biochem.* 206 103-107 Substrate preferences of glutamic-acid-specific endopeptidases assessed by synthetic peptide substrates based on intramolecular fluorescence quenching.
- Bregman, D.B., Bhattacharyya, N. & Rubin, C.S. (1989) *J. Biol. Chem.* 264 4648-4656 High affinity binding protein for the regulation subunit of cAMP-dependent protein kinase II-β.
- Bregman, D.B., Hirsch, A.H. & Rubin, C.S. (1991) *J. Biol. Chem.* 266 7207-7213 Molecular characterization of bovine brain P75, a high affinity binding protein for the regulatory subunit of cAMP-dependent protein kinase IIβ.
- Burant, C.F., Treutelaar, M.K. & Buse, M.G. (1986) *J. Clin. Invest.* 77 260-270 Diabetes-induced functional and structural changes in insulin receptors from rat skeletal muscle.
- Bushfield, M., Griffiths, S.L., Murphy, G.J., Pyne, N.J., Knowler, J.T., Milligan, G., Parker, P.J., Mollner, S. & Houslay, M.D. (1990a) *Biochem. J.* 271 365-372 Diabetes-induced alterations in the expression, functioning and phosphorylation state of the inhibitory guanine nucleotide regulatory protein Gi-2 in hepatocytes.
- Bushfield, M., Lavan, B.E. & Houslay, M.D. (1991) *Biochem. J.* 274 317-321 Okadaic acid identifies a phosphorylation/dephosphorylation cycle controlling the inhibitory guanine-nucleotide-binding regulatory protein Gi2.
- Bushfield, M., Murphy, G.J., Lavan, B.E., Parker, P.J., Hruby, V.J., Milligan, G. & Houslay, M.D. (1990b) *Biochem. J.* 268 449-457 Hormonal regulation of Gi2 α-subunit phosphorylation in intact hepatocytes.

Bushfield, M., Pyne, N.J. & Houslay, M.D. (1990c) *Eur. J. Biochem.* 192 537-542 Changes in the phosphorylation state of the inhibitory guanine-nucleotide-binding protein Gi-2 in hepatocytes from lean (Fa/Fa) and obese (fa/fa) Zucker rats.

Bushfield, M., Savage, A., Morris, N.J. & Houslay, M.D. (1993) *Biochem. J.* 293 229-236 A mnemonical or negative-co-operativity model for the activation of adenylate cyclase by a common G-protein-coupled calcitonin-gene-related neuropeptide (CGRP)/amylin receptor.

Buss, J.E., Mumby, S.M., Casey, P.J., Gilman, A.G. & Sefton, B.M. (1987) *PNAS* 84 7493-7497 Myristoylated a subunits of gaunine nucleotide-binding regulatory protein.

Camps, M., Hou, C., Sidiropoulos, D., Stock, J.B., Jakobs, K.H. & Gierschik, P. (1992) *Eur. J. Biochem.* 206 821-831 Stimulation of phospholipase C by guanine-nucleotide-binding protein $\beta\gamma$ subunits.

Carbó, N., López-Soriano, F.J. & Argilés, J.M. (1991) *Biosc. Rep.* 11 285-292 Glucose handling by hepatocytes from obese Zucker rats.

Carlson, K.E., Brass, L.F. & Manning, D.R. (1989) *J. Biol. Chem.* 264 13298-13305 Thrombin and phorbol esters cause the selective phosphorylation of a G protein other than Gi in human platelets.

Carpentier, J.L., Gorden, P. & Lew, D.P. (1992) *Exp. Cell Res.* 198 144-149 Calcium ions are required for the intracellular routing of insulin and its receptor.

Carrey, E.A. (1989) *Protein structure: a practical approach.* (Ed. T. E. Creighton) 117-144 Peptide mapping.

Casey, P.J., Fong, H.K.W., Simon, M.I. & Gilman, A.G. (1990) *J. Biol. Chem.* 265 2383-2390 Gz, a gaunine nucleotide binding protein with unique biochemical properties.

Castagna, M. (1987) *Biol. Cell* 59 3-14 Phorbol esters as signal transducers and tumor promoters.

Cawthorne, M.A., Lister, C.A., Holder, J.C., Kirkham, D.M., Young, P.W., Cantello, B.C., Hindley, R.M. & Smith, S.A. (1993) *Diabetes* 42 (Suppl. 1) 204 A (Abstract 654) Anti-hyperglycaemic efficacy of BRL 49653, a highly potent Thiazolidinedione, in animal models of non-insulin dependent diabetes.

Chan, B.L., Chao, M.V. & Saltiel, A.R. (1989) *PNAS USA* 86 1756-1760 Nerve growth factor stimulates the hydrolysis of glycosyl-phosphatidylinositol in PC-12 cells: A mechanism of protein kinase C regulation.

Chin, J.E., Dickens, M., Tavaré, J.M. & Roth, R.A. (1993) *J. Biol. Chem.* 268 6338-6347 Overexpression of protein kinase C isoenzymes α , β I, γ , and ϵ in cells overexpressing the insulin receptor.

Choi, E.-J., Xia, Z., Villacres, E.C. & Storm, D.R. (1993) *Curr. Op. Cell Biol.* 5 269-273 The regulatory diversity of mammalian adenylyl cyclases.

Chothia, C. & Finkelstein, A.V. (1990) *Ann. Rev. Biochem.* 59 1007-1039 The classification and origins of protein folding patterns.

Chou, P.Y. & Fasman, G.D. (1978) *Ann. Rev. Biochem.* 47 251-276 Empirical predictions of protein conformation.

- Cockcroft, S., Baldwin, J.M. & Allan, D. (1984) *J. Biol. Chem.* 221 477-482 The Ca²⁺-activated polyphosphoinositide phosphodiesterase of human and rabbit neutrophil membranes.
- Cockcroft, S. & Thomas, G.M. (1992) *Biochem. J.* 288 1-14 Inositol-lipid-specific phospholipase C isoenzymes and their differential regulation by receptors.
- Cocozza, S., Porcellini, A., Riccardi, G., Monticelli, A., Condorelli, G., Ferrara, A., Pianese, L., C., M., Capaldo, B., Beguinot, F. & Varrone, S. (1992) *Diabetes* 41 521-526 NIDDM associated with mutation in tyrosine kinase domain of insulin receptor gene.
- Cohen, P. (1991) *Methods in Enzymology* 201 389-398 Classification of Protein-serine/threonine phosphatases: identification and quantitation in cell extracts.
- Colca, J.R. & Morton, D.R. (1990) *New Antidiabetic Drugs* (Ed. C. J. Bailey & P. R. Flatt) 255-261 Antihyperglycaemic thiazolidinediones: Ciglitazone and its analogues.
- Conklin, B.R. & Bourne, H.R. (1993) *Cell* 73 631-641 Structural elements of G α subunits that interact with G $\beta\gamma$, receptors, and effectors.
- Considine, R.V. & Caro, J.F. (1993) *J. Cell. Biochem.* 52 8-13 Protein kinase C: Mediator or inhibitor of insulin action?
- Cook, D.L., Satin, L.S. & Hopkins, W.F. (1991) *TINS* 14 411-414 Pancreatic B cells are bursting, but how?
- Cook, S.J. & Wakelam, M.J.O. (1992) *Rev. Physiol. Biochem. Pharm.* 119 13-45 Phospholipases C and D in mitogenic signal transduction.
- Corde, D., Luini, A. & Garattini, S. (1990) *TIPS* 11 471-473 Selectivity of action can be achieved with compounds acting at second messenger targets.
- Crouch, M.F. & Hendry, I.A. (1993) *Cell. Signal.* 5 41-52 Gi α and Gi β are part of a signalling complex in BALB/c3T3 cells: Phosphorylation of Gi β in growth factor-activated fibroblasts.
- Daniel-Issakani, S., Spiegel, A.M. & Strulovici, B. (1989) *J. Biol. Chem.* 264 20240-20247 Lipopolysaccharide response is linked to the GTP binding protein, Gi2, in the promonocytic cell line U937.
- Davis, H.W. & McDonald, J.M. (1990) *Biochem. J.* 270 401-407 Insulin receptor function is inhibited by guanosine 5' - [γ - thiol] triphosphate (GTP[S]).
- DeFronzo, R.A. (1992) *Diabetologia* 35 389-397 Pathogenesis of type 2 (non-insulin dependent) diabetes mellitus.
- Dent, P., Lavoigne, A., Nakielny, S., Caudwell, F.B., Watt, P. & Cohen, P. (1990) *Nature* 348 302-308 The molecular mechanism by which insulin stimulates glycogen synthesis in mammalian skeletal muscle.
- Denton, R.M. (1990) *Nature* 348 286-287 Insulin signalling: Search for the missing link.
- Denton, R.M., Tavaré, J.M., Borthwick, A., Dickens, M., Diggle, T.A., Edgell, N.J., Heesom, K.J., Isaad, T., Lynch, D.F., Moule, S.K., Schmitz-Peiffer, C. & Welsh, G.I. (1992) *Biochem. Soc. Trans.* 20 659-664 Insulin-activated protein kinases in fat and other cells.

Døskeland, S.O., Maronde, E. & Gjertsen, B.T. (1993) *Biochim. et Biophys. Acta.* 1178 249-258 The genetic subtypes of cAMP-dependent protein kinase - functionally different or redundant?

Drapeau, G.R. (1977) *Methods in Enzymology* 47 189-191 Cleavage at glutamic acid with Staphylococcal protease.

Eckel, J., Herberg, L. & Wichelhaus, A. (1993) *Diabetes* 42 (Suppl. 1) A12 (Abstract 39) Expression and function of G-proteins Gs and Gi in ventricular cardiomyocytes from obese Zucker rats.

Egan, S.E. & Weinberg, R.A. (1993) *Nature* 365 781-783 The pathway to signal achievement.

Elliott, K.R.F. & Pogson, C.I. (1977) *Mol. Cell. Biochem.* 16 23-29 Preparation and characterization of isolated parenchymal cells from Guinea pig liver.

Emini, E.A., Hughes, J.V., Perlow, D.S. & Boger, J. (1985) *J. Virol.* 55 836-839 Induction of Hepatitis A virus-neutralizing antibody by specific synthetic peptides.

Exton, J.H. (1990) *J. Biol. Chem.* 265 1-4 Signalling through phosphatidylcholine breakdown.

Feener, E.P., Backer, J.M., King, G.L., Wilden, P.A., Sun, X.J., Kahn, C.R. & White, M.F. (1993) *J. Biol. Chem.* 268 11256-11264 Insulin stimulates serine and tyrosine phosphorylation in the juxtamembrane region of the insulin receptor.

Feng, G.-S., Hui, C.-C. & Pawson, T. (1993) *Science* 259 1607-1611 SH2-containing phosphotyrosine phosphatase as a target of protein-tyrosine kinases.

Ferris, C.D., Haganir, R.L., Supattapone, S. & Snyder, S.H. (1989) *Nature* 342 87-89 Purified Ins(1, 4, 5)P₃ receptor mediates Ca²⁺ flux in reconstituted lipid vesicles.

Findlay, J. & Eliopoulos, E. (1990) *TIPS* 11 492-499 Three-dimensional modelling of G-protein-linked receptors.

Foellmi, L., Wyse, B. & Kletzien, R. (1993) *Diabetes* 42 (Suppl. 1) 144A (Abstract 451) Enhancement of differentiation of preadipocytes from brown fat tissue by an insulin sensitizing agent.

Folli, F., Saad, M.J.A., Backer, J.M. & Kahn, C.R. (1992) *J. Biol. Chem.* 267 22171-22177 Insulin stimulation of phosphatidylinositol 3-kinase activity and association with insulin receptor substrate 1 in liver and muscle of intact rat.

Fong, H.K.W., Yoshimoto, K.K., Eversole-Cire, P. & Simon, M. (1988) *PNAS* 85 3066-3070 Identification of a GTP binding protein α -subunit that lacks the apparent ADP ribosylation site for pertussis toxin

Formisano, P., Sohn, K.-J., Miele, C., Finizio, B., Petruzzello, A., Riccardi, G., Beguinot, L. & Beguinot, F. (1993) *J. Biol. Chem.* 268 5241-5248 Mutation in a conserved motif next to the insulin receptor key autophosphorylation site de-regulates kinase activity and impairs insulin action.

Freeman, R.M., Plutzky, J. & Neel, B.G. (1992) *PNAS* 89 11239-11243 Identification of a human src homology 2-containing protein-tyrosine-phosphatase: A putative homolog of *Drosophila* corkscrew.

- Fujiwara, T., Yoshioka, S., Yoshioka, T., Ushiyama, I. & Horikoshi, H. (1988) *Diabetes* 37 1549-1558 Characterization of new oral antidiabetic agent CS-045: Studies in *KK* and *ob/ob* mice and Zucker fatty rats.
- Fukui, T., Lutz, R.J. & Lowenstein, J.M. (1988) *J. Biol. Chem.* 263 17730-17737 Purification of a phospholipase C from rat liver cytosol that acts on phosphatidylinositol 4,5-bisphosphate and phosphatidylinositol 4-phosphate.
- Fung, B.K.-K., Hurley, J.B. & Stryer, L. (1981) *PNAS* 78 152-156 Flow of information in the light-triggered cyclic nucleotide cascade of vision.
- Gale, N.W., Kaplan, S., Lowenstein, E.J., Schlessinger, J. & Bar-Sagi, D. (1993) *Nature* 363 88-89 Grb2 mediates the EGF-dependent activation of guanine nucleotide exchange on Ras.
- García-Sánz, J.A., Alcántara-Hernández, R., Robles-Flores, M., Torres-Márquez, M.E., Massillon, D., Annabi, B. & Van der Werve, G. (1992) *Biochim. et Biophys. Acta* 1135 221-225 Modulation of protein kinase C of the hormonal responsiveness of hepatocytes from lean (Fa/fa?) and obese (fa/fa) Zucker rats.
- Garnier, J., Osguthorpe, D.J. & Robson, B. (1978) *J. Mol. Biol.* 120 97-120 Analysis of the accuracy and implications of simple methods for predicting the secondary structure of globular proteins.
- Gawler, D., Milligan, G., Spiegel, A.M., Unson, C.G. & Houslay, M.D. (1987) *Nature* 327 229-232 Abolition of the expression of inhibitory guanine nucleotide regulatory protein Gi activity in diabetes.
- Geny, B., Stutchfield, J. & Cockcroft, S. (1989) *Cell. Signal.* 1 165-172 Phorbol ester inhibits polyphosphoinositide phosphodiesterase activity stimulated by either Ca²⁺, fluoride or GTP analogue in HL60 membranes and in permeabilized HL60 cells.
- Gilman, A. (1989) *Harvey Lect.* 90 85 153-172 Transmembrane signaling, G proteins, and adenylyl cyclase.
- Gilman, A.G. (1987) *Ann. Rev. Biochem.* 56 615-650 G proteins: Transducers of receptor generated signals.
- Giorgetti, S., Ballotti, R., Kowalski, C.A., Tartare, S. & Van, O.E. (1993) *J. Biol. Chem.* 268 7358-64 The insulin and insulin-like growth factor-I receptor substrate IRS-1 associates with and activates phosphatidylinositol 3-kinase *in vitro*.
- Giorgino, F., Chen, J.-H. & Smith, R.J. (1992) *Endocrinology* 130 1433-1444 Changes in tyrosine phosphorylation of insulin receptors and a 170,000 molecular weight nonreceptor protein *in vivo* in skeletal muscle of streptozotocin-induced diabetic rats: Effects of insulin and glucose.
- Glaser, K.B., Mobilio, D., Chang, J.Y. & Senko, N. (1993) *TIPS* 14 92-98 Phospholipase A2 enzymes: regulation and inhibition.
- Glatt, C.E. & Snyder, S.H. (1993) *Nature* 363 679-680 Type 5 adenylyl cyclase distribution - reply.
- Goldstein, B.J. (1992) *J. Cell. Biochem.* 48 33-42 Protein-tyrosine phosphatases and the regulation of insulin action.

Goren, H.J. & Boland, D. (1991) *Biochem. Biophys. Res. Commun.* 180 463-9 The 180000 molecular weight plasma membrane insulin receptor substrate is a protein tyrosine phosphatase and is elevated in diabetic plasma membranes.

Goren, H.J., Boland, D. & Fei, Q. (1993) *Cell. Signal.* 5 253-268 Plasma membrane p180, which insulin receptor phosphorylates *in vivo*, is not a tyrosine kinase.

Griffiths, S.L., Knowler, J.T. & Houslay, M.D. (1990) *Eur. J. Biochem.* 193 367-374 Diabetes-induces changes in guanine-nucleotide-regulatory-protein mRNA detected using synthetic oligonucleotide probes.

Grunberger, G. (1991) *Cell. Signal.* 3 171-177 Interplay between insulin signalling and protein kinase C.

Gruppuso, P.A., Boylan, J.M., Levine, B.A. & Ellis, L. (1992) *Biochem. Biophys. Res. Comm.* 189 1457-1463 Insulin receptor tyrosine kinase domain auto-dephosphorylation.

Guillon, G., Mouillac, B. & Savage, A.L. (1992) *Cell. Sign.* 4 11-23 Modulation of hormone-sensitive phospholipase C.

Gundersen, R.E. & Devreotes, P.N. (1990) *Science* 248 591-593 *In vivo* receptor-mediated phosphorylation of a G protein in *Dictyostelium*.

Ha, K.-S. & Exton, J.H. (1993) *J. Biol. Chem.* 268 10534-10539 Differential translocation of protein kinase C isozymes by thrombin and platelet-derived growth factor.

Hadari, Y.R., Tzahar, E., Nadiv, O., Rothenberg, P., Roberts, C.T.J., LeRoith, D., Yarden, Y. & Zick, Y. (1992) *J. Biol. Chem.* 267 17483-17486 Insulin and insulinomimetic agents induce activation of phosphatidylinositol 3'-kinase upon its association with pp185 (IRS-1) in intact rat livers.

Hanks, S.K. & Quinn, A.M. (1991) *Methods in Enzymology* 200 38-62 Protein kinase catalytic domain sequence database: Identification of conserved features of primary structure and classification of family members.

Hardie, D.G., Haystead, T.A.J. & Sim, A.T.R. (1991) *Methods in Enzymology* 201 469-476 Use of Okadaic acid to inhibit protein phosphatases in intact cells.

Häring, H.U. (1991) *Diabetologia* 34 848-861 The insulin receptor: signalling mechanism and contribution to the pathogenesis of insulin resistance.

Harrison, B.C. & Mobly, P.L. (1990) *J. Neurosci. Res.* 25 71-80 Phorbol ester-induced changes in astrocyte morphology: Correlation with protein kinase C activation and protein phosphorylation.

Hauguel, M.S., Peraldi, P., Alengrin, F. & Van, O.E. (1993) *Endocrinology* 132 67-74 Alteration of phosphotyrosine phosphatase activity in tissues from diabetic and pregnant rats

Hawkins, P.T., Berrie, C.P., Morris, A.J. & Downes, C.P. (1986) *Biochem. J.* 243 211-218 Inositol 1, 2-cyclic 4, 5-trisphosphate is not a product of muscarinic receptor stimulated phosphatidyl inositol 4, 5 bisphosphate hydrolysis in rat parotid glands.

Hayashi, H., Kamohara, S., Nishioka, Y., Kanai, F., Miyake, N., Fukui, Y., Shibasaki, F., Takenawa, T. & Ebina, Y. (1992) *J. Biol. Chem.* 267 22575-22580 Insulin treatment stimulates the tyrosine phosphorylation of the α -type 85 kDa subunit of phosphatidylinositol 3-kinase *in vivo*.

Hayashi, H., Miyake, N., Kanai, F., Shibasaki, F., Takenawa, T. & Ebina, Y. (1991) *Biochem. J.* **280** 769-775 Phosphorylation *in vitro* of the 85 kDa subunit of phosphatidylinositol 3-kinase and its possible activation by insulin receptor tyrosine kinase.

Hayashi, H., Nishioka, Y., Kamohara, S., Kanai, F., Ishii, K., Fukui, Y., Shibasaki, F., Takenawa, T., Kido, H., Katsunuma, N. & Ebina, Y. (1993) *J. Biol. Chem.* **268** 7107-7117 The α -type 85 kDa subunit of phosphatidylinositol 3-kinase is phosphorylated at tyrosines 368, 580, and 607 by the insulin receptor.

Haystead, T.A.J., Sim, A.T.R., Carling, D., Honnor, R.C., Tsukitani, Y., Cohen, P. & Hardie, D.G. (1989) *Nature* **337** 78-81 Effects of the tumour promoter okadaic acid on intracellular protein phosphorylation and metabolism.

Hellevuo, K., Yoshimura, M., Kao, M., Hoffman, P.L., Cooper, D.M.F. & Tabakoff, B. (1993) *Biochem. Biophys. Res. Comm.* **192** 311-318 A novel adenylyl cyclase sequence cloned from the human erthroleukemia cell line.

Heyworth, C.M. & Houslay, M.D. (1983) *Biochem. J.* **214** 93-98 Challenge of hepatocytes by glucagon triggers a rapid modulation of adenylyl cyclase activity in isolated membranes.

Hidaka, H. & Hagiwara, M. (1987) *TIPS* **8** 162-163 Pharmacology of the isoquinoline sulfonamide protein kinase C inhibitors.

Hidaka, H., Inagaki, M., Kawamoto, S. & Sasaki, Y. (1984) *Biochem.* **23** 5036-5041 Isoquinolinesulfamides, novel and potent inhibitors of cyclic nucleotidedependent protein kinase and protein kinase C.

Hill, S.J. & Kendall, D.A. (1989) *Cell. Signal.* **1** 135-141 Cross-talk between different receptor - effector systems in the mammalian CNS.

Hirota, K., Hirota, T., Aguilera, G. & Catt, K.J. (1985) *J. Biol. Chem.* **260** 3243-3246 Hormone induced redistribution of calcium-activated phospholipid-dependent protein kinase in pituitary gonadotrophs.

Hofmann, C., Lorenz, K. & Colca, J.R. (1991) *Endocrinology* **129** 1915-1925 Glucose transport deficiency in diabetic animals is corrected by treatment with the oral antihyperglycemic agent pioglitazone.

Hofmann, C.A., Edwards III, C.W., Hillman, R.M. & Colca, J.R. (1992) *Endocrinology* **130** 735-740 Treatment of insulin-resistant mice with the oral antidiabetic agent pioglitazone: Evaluation of liver GLUT2 and phosphoenolpyruvate carboxykinase expression.

Hokin, L.E. & Hokin, M.R. (1955a) *Biochim. Biophys. Acta.* **16** 229-237 Effects of acetylcholine on phosphate turnover in phospholipids of brain cortex *in vitro*.

Hokin, L.E. & Hokin, M.R. (1955b) *Biochim. Biophys. Acta.* **18** 102-110 Effects of acetylcholine on the turnover of phosphoryl units in individual phospholipids of pancreas slices and brain cortex slices.

Hokin-Neaverson, M. (1974) *Biochem. Biophys. Res. Commun.* **58** 763-768 Acetylcholine causes a net decrease in phosphatidylinositol and a net increase in phosphatidic acid in mouse pancreas.

Hollenberg, M.D. & Jacobs, S. (1990) *Handbook of Experimental Pharmacology* (Ed. P. Cuatrecasas) **92** 183-207 Insulin receptor-mediated transmembrane signal.

- Homma, Y., Imaki, J., Nakanishi, O. & Takenawa, T. (1988) *J. Biol. Chem.* 263 6592-6598 Isolation and characterization of two different forms of inositol phospholipid-specific phospholipase C from rat brain.
- Houslay, M.D. (1990) *G Proteins as Mediators of Cellular signalling Processes* (Ed. M. D. Houslay & G. Milligan) 521-553 Insulin and its interaction with G proteins.
- Houslay, M.D. (1991a) *Eur. J. Biochem.* 195 9-27 'Crosstalk': a pivotal role for protein kinase C in modulating relationships between signal transduction pathways.
- Houslay, M.D. (1991b) *Cell. Signal.* 3 1-9 Gi-2 is at the centre of an active phosphorylation / dephosphorylation cycle in hepatocytes: the fine tuning of stimulatory and inhibitory inputs into adenylate cyclase in normal and diabetic states.
- Houslay, M.D., Gawler, D.J., Milligan, G. & Wilson, A. (1989) *Cell. Signal* 1 9-22 Multiple defects occur in the guanine nucleotide regulatory protein system in liver plasma membranes of obese (fa/fa) but not lean (Fa/Fa) Zucker rats: loss of functional Gi and abnormal Gs function.
- Houslay, M.D. & Siddle, K. (1989) *British Medical Bulletin* 45 264-284 Molecular basis of insulin receptor function.
- Huang, C.P., Devanney, J.F. & Kennedy, S.P. (1988a) *Biochem. Biophys. Res. Comm.* 150 1006-1011 Vimentin, a cytoskeletal substrate for protein kinase C.
- Huang, F.L., Yoshida, Y., Nakabayashi, H. & Huang, K.P. (1987) *J. Biol. Chem.* 262 15714-15720 Differential distribution of protein kinase C isozymes in the various regions of brain.
- Huang, K.P. (1989) *TINS* 12 425-432 The mechanism of protein kinase C activation.
- Huang, K.P. & Huang, F.L. (1986) *J. Biol. Chem.* 261 14781-7 Immunochemical characterisation of rat brain protein kinase C.
- Huang, K.P., Huang, F.L., Nakabayashi, H. & Yoshida, Y. (1988b) *J. Biol. Chem.* 263 14839-14845 Biochemical characterisation of rat brain protein kinase C isozymes.
- Hubbard, M.J. & Cohen, P. (1991) *Methods in Enzymology* 201 414-427 Targeting subunits for protein phosphatases.
- Hug, H. & Sarre, T.F. (1993) *Biochem. J.* 291 329-343 Protein kinase C isozymes: divergence in signal transduction.
- Hunter, T. (1991) *Methods in Enzymology* 200 3-37 Protein kinase classification.
- Iismaa, T.P. & Shine, J. (1992) *Curr. Opin. Cell Biol.* 4 195-202 G protein-coupled receptors.
- Ikeda, H., Taketomi, S., Sugiyama, Y., Shimura, Y., Sohda, T., Meguro, K. & Fujita, T. (1990) *Drug Res.* 40 156-162 Effects of pioglitazone on glucose and lipid metabolism in normal and insulin resistant animals.
- Inoguchi, T., Battan, R., Handler, E., Sportsman, J.R., Heath, W. & King, G.L. (1992) *PNAS* 89 11059-11063 Preferential elevation of protein kinase C isoform β II and diacylglycerol levels in the aorta and heart of diabetic rats: Differential reversibility to glycemic control by islet cell transplantation.

- Ionescu, E., Sauter, J.F. & Jeanrenaud, B. (1985) *Am. J. Physiol.* 248 E500-E506 Abnormal oral glucose tolerance in genetically obese (fa/fa) rats.
- Ishii, H., Connolly, T.M., Bross, T.E. & Majerus, P.W. (1986) *PNAS* 83 6397-6401 Inositol cyclic trisphosphate [inositol 1, 2-(cyclic)-4, 5-trisphosphate] is formed upon thrombin stimulation of human platelets.
- Itoh, H., Kozasa, T., Nagata, S., Nakamura, S., Katada, T., Ui, M., Iwai, S., Ohtsuka, E., Kawasaki, H., Suzuki, K. & Kaziro, Y. (1986) *PNAS* 83 3776-3780 Molecular cloning and sequence determination of cDNAs for α subunits of the guanine nucleotide-binding proteins Gs, Gi, and Go from rat brain.
- Itoh, H., Toyama, R., Kozasa, T., Tsukamoto, T., Matsuoka, M. & Kaziro, Y. (1988) *J. Biol. Chem.* 263 6656-6664 Presence of three distinct molecular species of Gi α subunit.
- Iwanishi, M. & Kobayashi, M. (1993) *Metabolism* 42 1017-1021 Effects of Pioglitazone on insulin receptors of skeletal muscles from high-fat-fed rats.
- Jakobs, K.H., Bauer, S. & Watanabe, Y. (1985) *Eur. J. Biochem.* 151 425-430 Modulation of adenylate cyclase of human platelets by phorbol esters: Impairment of the hormone-sensitive inhibitory pathway.
- Jelsema, C.L. & Axelrod, J. (1987) *PNAS* 84 3623-3627 Stimulation of phospholipase A2 activity in bovine rod outer segments: The β subunits of transducin and its inhibition by the α -subunit.
- Jo, H., Cha, B.Y., Davis, H.W. & McDonald, J.M. (1992) *Endo.* 131 2855-2862 Identification, partial purification, and characterisation of two guanosine triphosphate-binding proteins associated with insulin receptors.
- Johnson, L.N. & Barford, D. (1993) *An. Rev. Biophys. Biomol. Struct.* 22 199-232 The effects of phosphorylation on the structure and function of proteins.
- Jones, D.T. & Reed, R.R. (1987) *J. Biol. Chem.* 262 14241-14249 Molecular cloning of five GTP binding protein cDNA species from rat olfactory neuroepithelium.
- Kadowaki, T., Kasuga, M., Akanuma, Y., Ezaki, O. & Takaku, F. (1984) *J. Biol. Chem.* 259 14208-14216 Decreased autophosphorylation of the insulin receptor-kinase in streptozotocin-diabetic rats.
- Kameyama, K., Haga, K., Haga, T., Kontani, K., Katada, T. & Fukada, Y. (1993) *J. Biol. Chem.* 268 7753-7758 Activation by G protein $\beta\gamma$ subunits of β -adrenergic and muscarinic receptor kinase.
- Karplus, P.A. & Schulz, G.E. (1987) *J. Mol. Biol.* 195 701-729 Refined structure of glutathione reductase at 1.54 Å resolution.
- Karplus, P.A. & Schulz, G.E. (1989) *J. Mol. Biol.* 210 163-180 Substrate binding and catalysis by glutathione reductase as derived from refined enzyme: substrate crystal structures at 2Å resolution.
- Kasiske, B.L., O'Donnell, M.P. & Keane, W.F. (1992) *Hypertension Supplement 1*, 19 I110-I115 The Zucker rat model of obesity, insulin resistance, hyperlipidemia, and renal injury.

Katada, T., Gilman, A.G., Watanabe, Y., Bauer, S. & Jakobs, K.H. (1985) *Eur. J. Biochem.* 151 Protein kinase C phosphorylates the inhibitory guanine-nucleotide-binding regulatory component and apparently suppresses its function in hormonal inhibition of adenylate cyclase.

Keller, S.R., Aebersold, R., Garner, C.W. & Lienhard, G.E. (1993) *Biochim-Biophys-Acta.* 1172 323-326 The insulin-elicited 160 kDa phosphotyrosine protein in mouse adipocytes is an insulin receptor substrate 1: identification by cloning.

Keller, S.R. & Lienhard, G.E. (1993) *Molecular Biology of Diabetes* (in press) Structure of insulin receptor substrate 1 and role in insulin signalling as a docking protein for SH2 domain-containing proteins.

Kellerer, M., Obermaier-Kusser, B., Pröfrock, A., Schleicher, E., Seffer, E., Mushack, J., Ermel, B. & Häring, H.U. (1991) *Biochem. J.* 276 103-108 Insulin activates GTP binding to a 40 kDa protein in fat cells.

Kelly, K.L. & Ruderman, N.B. (1993) *J. Biol. Chem.* 268 4391-4398 Insulin-stimulated phosphatidyl 3-kinase.

Kemp, B.E. & Pearson, R.B. (1991) *Biochim. et Biophys. Acta* 1094 67-76 Intracellular regulation of protein kinases and phosphatases.

Kennelly, P.J. & Krebs, E.G. (1991) *J. Biol. Chem.* 266 15555-15558 Consensus sequences as substrate specificity determinants for protein kinases and protein phosphatases.

Kikkawa, H., Ogita, K., Shearman, M.S., Ase, K., Sekiguchi, K., Naor, Z., Kishimoto, A., Nishizuka, Y., Saito, N., Tanaka, C., Ono, Y., Fujii, T. & Igarashi, K. (1988) *ColdSpring Harbor Symposium on Quantitative Biology.* LIII 97-102 The family of protein kinase C: its molecular heterogeneity and differential expression.

Kilgour, E., Anderson, N.G. & Houslay, M.D. (1989) *Biochem. J.* 260 27-36 Activation and phosphorylation of the 'dense-vesicle' high-affinity cyclic-AMP phosphodiesterase by cyclic AMP-dependent protein kinase.

King, P.A., Horton, E.D., Hirshman, M.F. & Horton, E.S. (1992) *J. Clin. Invest.* 90 1568-1575 Insulin resistance in obese Zucker rat (fa/fa) skeletal muscle is associated with the failure of glucose transporter translocation.

Klarlund, J.K., Khalaf, N., Kozma, L. & Czech, M.P. (1993) *J. Biol. Chem.* 268 7646-7649 Activation of protein kinases by insulin and non-hydrolyzable GTP analogs in permeabilized 3T3-L1 adipocytes.

Kobayashi, M., Iwanishi, M., Egawa, K. & Shigeta, Y. (1992) *Diabetes* 41 476-483 Pioglitazone increases insulin sensitivity by activating receptor kinase.

Koch, W.J., Inglese, J., Stone, W.C. & Lefkowitz, R.J. (1993) *J. Biol. Chem.* 268 8256-8260 The binding site for the $\beta\gamma$ subunits of heterotrimeric G proteins on the β -adrenergic receptor kinase.

Kohnken, R.E., Eadie, D.M. & McConnell, D.G. (1981) *J. Biol. Chem.* 256 12510-12516 The light activated GTP dependent cyclic-GMP phosphodiesterase complex of bovine retinal rod outer segments.

Kraegen, E., Oakes, N., Kennedy, C., Sader, S., Laybutt, R. & Chisholm, D. (1993) *Diabetes* 42 (Suppl. 1) 79A (Abstract 257) Effects of BRL 49653 in normal and insulin resistant (high-fat-fed) rats; new information on the modes of action of thiazolidinediones.

- Kraft, A.S. & Anderson, W.B. (1983) *Nature* 301 621-623 Phorbol esters increase the amount of calcium, phospholipid-dependent protein kinase associated with plasma membrane.
- Kreutter, D.K., Andrews, K.M., Gibbs, E.M., Hutson, N.J. & Stevenson, R.W. (1990) *Diabetes* 39 1414-1419 Insulinlike activity of new antidiabetic agent CP 68722 in 3T3-L1 adipocytes.
- Krupinski, J., Rajaram, R., Lakonishok, M., Benovic, J.L. & Cerione, R.A. (1988) *J. Biol. Chem.* 263 12333-12341 Insulin-dependent phosphorylation of GTP-binding proteins in phospholipid vesicles.
- Kuhné, M.R., Pawson, T., Lienhard, G.E. & Feng, G.-S. (1993) *J. Biol. Chem.* 268 11479-11481 The insulin receptor substrate 1 associates with the SH2-containing phosphotyrosine phosphatase Syp.
- Laemmli, U.K. (1970) *Nature* 227 680-685 Cleavage of structural proteins during the assembly of the head of bacteriophage T4.
- Lamb, T.D. & Pugh Jr, E.N. (1992) *TINS* 15 291-298 G-protein cascades: gain and kinetics.
- Lamphere, L., Carpenter, C.L., Sheng, Z.F., Kallen, R.G. & Lienhard, G.E. (1993) (submitted for publication) Activation of phosphatidylinositol 3-kinase in 3T3-L1 adipocytes by association with insulin receptor substrate 1.
- Lasey, R.A. & Mills, A.D. (1975) *Eur. J. Biochem.* 56 335-341 Quantitative film detection of ³H and ¹⁴C in polyacrylamide gels by fluorography.
- Laurenza, A., McHugh Sutkowski, M. & Seamon, K.B. (1989) *TIPS* 10 442-446 Forskolin: Specific stimulator of adenylate cyclase or a diterpene with multiple sites of action?
- Lee, J., O'Hare, T., Pilch, P.F. & Shoelson, S.E. (1993) *J. Biol. Chem.* 268 4092-4098 Insulin receptor autophosphorylation occurs asymmetrically.
- Lefkowitz, R.J. (1992) *Nature* 358 372-372 The subunit story thickens.
- Lerea, C.L., Somers, D.E., Hurley, J.B., Klock, I.B. & Bunt-Milam, H. (1986) *Science* 234 77-80 Identification of specific transducin subunits in retinal rod and cone photoreceptors.
- Levitzki, A. (1988) *TIBS* 13 298-301 Transmembrane signalling to adenylate cyclase in mammalian cells and *Saccharomyces cerevisiae*.
- Li, N., Batzer, A., Daly, R., Yajnik, V., Skolnik, E., Chardin, P., Bar-Sagi, D., Margollis, B. & Schessinger, J. (1993) *Nature* 363 85-88 Guanine-nucleotide-releasing factor hSos1 binds to Grb2 and links receptor tyrosine kinases to Ras signalling.
- Lincoln, T.M. (1991) *Second Messengers Phosphoproteins* 13 99-109 Pertussis toxin-sensitive and insensitive guanine nucleotide binding proteins (G-proteins) are not phosphorylated by cyclic GMP-dependent protein kinase.
- Linder, M.E. & Gilman, A.G. (1992) *Sci. Am.* 267 36-43 G proteins.
- Lounsbury, K.M., Casey, P.J., Brass, L.F. & Manning, D.R. (1991) *J. Biol. Chem.* 266 22051-22056 Phosphorylation of G_z in human platelets.

- Lounsbury, K.M., Schlegel, B., Poncz, M., Brass, L.F. & Manning, D.R. (1993) *J. Biol. Chem.* 268 3494-3498 Analysis of G α by site-directed mutagenesis.
- Luttrell, L., Kilgour, E., Lerner, J. & Romero, G. (1990) *J. Biol. Chem.* 265 16873-16879 A pertussis toxin-sensitive G-protein mediates some aspects of insulin action in BC3H-1 murine myocytes.
- Mann, H.B. & Whitney, D.R. (1947) *Ann. Math. Stat.* 28 50-60 On a test of whether one of two random variables is stochastically larger than the other.
- Martens, G.J.M. (1992) *Prog. Brain Res.* 92 201-214 Molecular biology of G-protein-coupled receptors.
- Masters, S.B., Stroud, R.M. & Bourne, H.R. (1986) *Prot. Eng.* 1 47-54 Family of G protein α chains: amphipathic analysis and predicted structure of functional domains.
- Matsuoka, M., Itoh, H., Kozasa, T. & Kaziro, Y. (1988) *PNAS* 85 5384-5388 Sequence analysis of cDNA and genomic DNA for a putative pertussis toxin insensitive guanine nucleotide binding regulatory protein α subunit.
- May Jr, W.S., Sahyoun, N., Wolf, M. & Cuatrecasas, P. (1985) *Nature* 317 549-551 Role of intracellular calcium mobilisation in the regulation of protein kinase C-mediated membrane processes.
- Mayer, R.J. & Marshall, L.A. (1993) *FASEB J.* 7 339-348 New insights on mammalian phospholipase A2(s); comparison of arachidonoyl-selective and -nonselective enzymes.
- McCaleb, M.L. & Sredy, J. (1992) *Metabolism* 41 522-525 Metabolic abnormalities of the hyperglycemic obese Zucker rat.
- McClain, D.A. (1990) *J. Biol. Chem.* 265 21363-21367 Endocytosis of insulin receptors is not required for activation or deactivation of the hormone response.
- McKnight, G.S., Cadd, G.G., Clegg, C.H., Otten, A.D. & Correll, L.A. (1988) *Cold Spring Harbor Symposia on Quantitative Biology* LIII 111-119 Expression of wild-type and mutant subunits of the cAMP-dependent protein kinase.
- McPherson, R.K., Gibbs, E.M., Treadway, J.L. & Stevenson, R.W. (1993) *Diabetes* 42 (Suppl. 1) 36A (Abstract 105) Englitazone effects signal transduction and metabolic response to insulin and glucagon in isolated rat hepatocytes.
- Meyerovitch, J., Backer, J.M., Csermely, P., Shoelson, S.E. & Kahn, C.R. (1992) *Biochemistry* 31 10338-10344 Insulin differentially regulates protein phosphotyrosine phosphatase activity in rat hepatoma cells
- Michell, R.H. (1975) *Biochim. Biophys. Acta* 415 81-147 Inositol phospholipids and cell surface receptor function.
- Michell, R.M. (1987) *Brit. Med. J.* 295 1320-1323 How do receptors at the cell surface send signals to the cell interior?
- Milligan, G., Mitchell, F.M., Mullaney, I., McClue, S.J. & McKenzie, F.R. (1990) *Symp. Soc. Exp. Biol.* 44 157-172 The role and specificity of guanine nucleotide binding proteins in receptor-effector coupling.

- Moises, R.S. & Heidenreich, K.A. (1990) *J. Cell. Phys.* 144 538-545 Pertussis toxin catalyzed ADP-ribosylation of a 41 kDa G-protein impairs insulin-stimulated glucose metabolism in BC3H-1 myocytes.
- Mooney, R.A. & Bordwell, K.L. (1992) *J. Biol. Chem.* 267 14054-14060 Differential dephosphorylation of the insulin receptor and its 160-kDa substrate (pp160) in rat adipocytes.
- Morris, N.J., Bushfield, M., Lavan, B.E. & Houslay, M.D. (1994) (Submitted for publication) The phosphorylation of the inhibitory guanine nucleotide regulatory protein Gi-2 can occur at multiple sites in intact rat hepatocytes.
- Myers, M.G. & White, M.F. (1993) *Diabetes* 42 643-650 The new elements of insulin signaling: Insulin receptor substrate-1 and proteins with SH2 domains.
- Myers, M.J., Sun, X.J., Cheatham, B., Jachna, B.R., Glasheen, E.M., Backer, J.M. & White, M.F. (1993) *Endocrinology* 132 1421-1430 IRS-1 is a common element in insulin and insulin-like growth factor-I signaling to the phosphatidylinositol 3'-kinase
- Nakadate, T., Jeng, A.J. & Blumberg, P.M. (1988) *Biochem. Pharm.* 37 1541-1545 Comparison of protein kinase C functional assays to clarify mechanism of inhibitor action.
- Nathan, D.M. (1993) *New Eng. J. Med.* 328 1676-1685 Long term complications of diabetes mellitus,
- Neer, E.J. & Clapham, D.E. (1988) *Nature* 333 129-134 Roles of G protein subunits in transmembrane signalling.
- Neubig, R.R. & Thomsen, W.J. (1989) *BioEssays* 11 136-141 How does a key fit a flexible lock? Structure and dynamics of receptor function.
- Nishimura, H., Kuzuya, H., Okamoto, M., Yamada, K., Kosaki, A., Takechi, T., Inoue, G., Kono, S. & Imura, H. (1989) *Am. Phys. Soc.* E624-E630 Postreceptor defect in insulin action in streptozotocin-induced diabetic rats.
- Nishizuka, Y. (1984) *Nature* 308 693-698 The role of protein kinase C in cell surface signal transduction and tumour promotion.
- Nishizuka, Y. (1986) *Science* 233 305-312 Studies and perspectives of protein kinase C.
- O'Flahery, J.T. (1987) *Biochem. Pharmacol.* 36 407-412 Phospholipid metabolism and stimulus-response coupling.
- O'Rahilly, S. & Moller, D.E. (1992) *Clin. Endocrinol. (Oxf)* 36 121-32 Mutant insulin receptors in syndromes of insulin resistance.
- Offord, R.E. (1966) *Nature* 21 591-593 Electro-phoretic mobilities of peptides on paper and their use in the determination of amide groups.
- Okamoto, M., Hayashi, T., Kono, S., Inoue, G., Kubota, M., Okamoto, M., Kuzuya, H. & Imura, H. (1993) *Biochem. J.* 290 327-333 Specific activity of phosphatidylinositol 3-kinase is increased by insulin stimulation.
- Olefsky, J.M. (1990) *Diabetes* 39 1009-1016 The insulin receptor, a multifunctional protein.

- Olianas, M.C. & Onali, P. (1986) *J. Neurochem.* 47 890-897 Phorbol esters increase GTP-dependent adenylate cyclase activity in rat brain striatal membranes.
- Ono, Y., Fujii, T., Ogita, K., Kikkawa, U., Igarashi, K. & Nishizuka, Y. (1988) *J. Biol. Chem.* 263 6927-6932 The structure, expression, and properties of additional members of the protein kinase C family.
- Orellana, S.A., Amieux, P.S., Zhao, X. & McKnight, G.S. (1993) *J. Biol. Chem.* 268 6843-6846 Mutations in the catalytic subunit of the cAMP-dependent protein kinase interfere with the holoenzyme formation without disrupting inhibition by protein kinase inhibitor.
- Osborne, N.N., Broyden, N.J., Barnett, N.L. & Morris, N.J. (1991) *J. Neurochem.* 57 594-604 Protein kinase C (α and β) immunoreactivity in rabbit and rat retina. Effect of phorbol esters and transmitter agonists on immunoreactivity and the translocation of the enzyme from cytosolic to membrane compartments.
- Osborne, N.N., Tobin, A.B. & Ghazi, H. (1988) *Neurochem. Res.* 13 177-191 Role of inositol trisphosphate as a second messenger in signal transduction processes: An Essay.
- Parenti, M., Viganó, A., Newman, C.M.H., Milligan, G. & Magee, A.I. (1993) *Biochem. J.* 291 349-353 A novel N-terminal motif for palmitoylation of G-protein α subunits.
- Pearson, R.B. & Kemp, B.E. (1991) *Methods in Enzymology* 200 62-81 Protein kinase phosphorylation site sequences and consensus specificity motifs: tabulations.
- Pelech, S.L. & Vance, D.E. (1989) *TIBS* 14 28-30 Signal Transduction via phosphatidylcholine cycles.
- Pillion, D.J., Kim, S.J., Kim, H. & Meezan, E. (1992) *Am. J. Med. Sci.* 303 40-52 Insulin signal transduction: the role of protein phosphorylation.
- Pleroni, J.P., Miller, D., Premont, R.T. & Iyengar, R. (1993) *Nature* 363 679-679 Type 5 adenylyl cyclase distribution.
- Pot, D.A. & Dixon, J.E. (1992) *Biochim. et Biophys. Acta* 1136 35-43 A thousand and two protein tyrosine phosphatases.
- Putney, J.W., Takemura, H., Hughes, A.R., Horstman, D.A. & Thastrup, O. (1989) *FASEB J.* 3 1899-1905 How do IP regulate Ca^{2+} signalling.
- Pyne, N.J., Freissmuth, M. & Palmer, S. (1992) *Biochem. J.* 285 333-338 Phosphorylation of the spliced variant forms of the recombinant stimulatory guanine-nucleotide-binding protein ($G_{\alpha s}$) by protein kinase C.
- Pyne, N.J., Heyworth, C.M., Balfour, N.W. & Hoslay, M.D. (1989a) *Biochem. Biophys. Res. Comm.* 165 251-256 Insulin affects the ability of G_i to be ADP-ribosylated but does not elicit its phosphorylation in intact hepatocytes.
- Pyne, N.J., Murphy, G.J., Milligan, G. & Hoslay, M.D. (1989b) *FEBS Lett.* 243 77-82 Treatment of intact hepatocytes with either phorbol ester TPA or glucagon elicits the phosphorylation and functional inactivation of the inhibitory guanine nucleotide regulatory protein G_i .
- Rana, R.S. & Hokin, L.E. (1990) *Physiological Rev.* 70 115-164 Role of phosphoinositides in transmembrane signalling.

- Randerath, K. (1970) *Anal. Biochem.* 34 188-205 An evaluation of film detection methods for weak β emitters, particularly tritium.
- Rebecchi, M.J. & Rosen, O.M. (1987) *J. Biol. Chem.* 262 12526-32 Purification of a phosphoinositide-specific phospholipase C from bovine brain.
- Regoli, D. & Nantel, F. (1990) *TIPS* 11 400-401 Direct activation of G-proteins.
- Reichlin, M. (1980) *Methods in Enzymology* 70 159-166 Use of glutaraldehyde as a coupling agent for proteins and peptides.
- Reithmann, C., Gierschik, P. & Jakobs, K.H. (1990) *Symp. Soc. Exp. Biol.* 44 207-224 Stimulation and inhibition of adenylyl cyclase.
- Rice, K.M., Turnbow, M.A. & Garner, C.W. (1993) *Biochem. Biophys. Res. Commun.* 190 961-7 Insulin stimulates the degradation of IRS-1 in 3T3-L1 adipocytes.
- Rink, T.J., Beaumont, K., Koda, J. & Young, A. (1993) *TIPS* 14 113-118 Structure and biology of amylin.
- Robertson, R.P., Seaquist, E.R. & Walseth, T.F. (1991) *Diabetes* 40 1-6 Perspectives in diabetes: G proteins and modulation of insulin secretion.
- Rodbell, M. (1985) *TIBS* 10 461-464 Programmable messenger: A new theory of hormone action.
- Rodbell, M. (1992) *Current Topics in Cellular Regulation* (Ed. E. R. Stadtman, P. B. Chock, & A. Levitzki) 32 1-47 The role of GTP-binding proteins in signal transduction: from the sublimely simple to the conceptually complex.
- Rodbell, M., Birnbaumer, L., Pohl, S.L. & Krans, H.M.J. (1971) *J. Biol. Chem.* 246 1877-1882 The glucagon adenylyl cyclase system in plasma membrane of rat liver.
- Romero, G. (1991) *Cell Biol. Int. Rep.* 15 827-852 Inositolglycans and cellular signalling.
- Ross, E.M. & Gilman, A.G. (1980) *Ann. Rev. Biochem.* 49 533-564 Biochemical properties of hormone sensitive adenylate cyclase.
- Rothenberg, P.L. & Kahn, C.R. (1988) *J. Biol. Chem.* 263 15546-15552 Insulin inhibits pertussis toxin-catalyzed ADP-ribosylation of G-proteins.
- Rothenberg, P.L., White, M.F., Kahn, C.R. & Jacobs, S. (1990) *Handbook of Experimental Pharmacology* (Ed. P. Cuatrecasas) 92 209-230 The insulin receptor tyrosine kinase.
- Rozakis-Adcock, M., Fernley, R., Wade, J., Pawson, T. & Bowtell, D. (1993) *Nature* 363 83-85 The SH2 and SH3 domains of mammalian Grb2 couple the EGF receptor to the Ras activator mSos1.
- Ruoff, G. (1993) *J. Family Practice.* 36 329-335 The management of non-insulin-dependent diabetes mellitus in the elderly.
- Sagi-Eisenberg, R. (1989) *TIBS* 14 355-357 Open question: GTP binding proteins as possible targets for protein kinase C action.
- Sali, A., Overington, J.P., Johnson, M.S. & Blundell, T.L. (1990) *TIBS* 15 235-240 From comparisons of protein sequences and structures to protein modelling and design.

- Saltiel, A.R., Cuatrecasas, P. & Jacobs, S. (1990) Handbook of Experimental Pharmacology (Ed. P. Cuatrecasas) 92 290-311 Second messengers of insulin action.
- Sandouk, T., Reda, D. & Hofmann, C. (1993) Endocrinology 133 352-359 The antidiabetic agent pioglitazone increases expression of glucose transporters in 3T3-F442A cells by increasing messenger ribonucleic acid transcript stability.
- Sasaki, Y., Zhang, X.F., Nishiyama, M., Avruch, J. & Wands, J.R. (1993) J. Biol. Chem. 268 3805-3806 Expression and phosphorylation of insulin receptor substrate 1 during rat liver regeneration.
- Sauvage, C., Rumigny, J.-F. & Maitre, M. (1991) Mol. Cell. Biochem. 107 65-77 Purification and characterisation of G proteins from human brain: modification of GTPase activity upon phosphorylation.
- Schmidt, C.J., Thomas, T.C., Levine, M.A. & Neer, E.J. (1992) J. Biol. Chem. 267 13807-13810 Specificity of G protein β and γ subunit interactions.
- Schulz, I., Thevenod, F. & Dehlinger-Kremer, M. (1989) Cell. Calcium 10 325-336 Modulation of intracellular free Ca^{2+} concentration by $\text{Ins}(1,4,5)\text{P}_3$ sensitive and insensitive non-mitochondrial Ca^{2+} pools.
- Sechi, L.A., Griffin, C.A., Grady, E.F., Grunfeld, C., Kalinyak, J.E. & Schambelan, M. (1992) Diabetes 41 1113-1118 Tissue-specific regulation of insulin receptor mRNA levels in rats with STZ-induced diabetes.
- Sellinger, O.Z. & Wolfson, M.F. (1991) Biochim. et Biophys. Acta. 1080 110-118 Carboxymethylation affects the proteolysis of myelin basic protein by *Staphylococcus aureus* V8 proteinase.
- Senogles, S.E., Spiegel, A.M., Padrell, E., Iyengar, R. & Caron, M.G. (1990) J. Biol. Chem. 265 4507-4514 Specificity of receptor-G protein interactions.
- Sharkey, N.A., Leach, K.L. & Blumberg, P.M. (1984) PNAS 81 607-610 Competitive inhibition of diacylglycerol of specific phorbol esters.
- Sherman, W.M., Katz, A.L., Cutler, C.L., Withers, R.T. & Ivy, J.L. (1988) Am. J. Physiol. 255 E374-E382 Glucose transport: locus of muscle insulin resistance in obese Zucker rats.
- Shoelson, S.E., Chatterjee, S., Chaudhuri, M. & White, M.F. (1992) PNAS 89 2027-2031 YMXM motifs of IRS-1 define substrate specificity of the insulin receptor kinase.
- Simmonds, W.F., Goldsmith, P.K., Codina, J., Unson, C.G. & Spiegel, A.M. (1989) PNAS 86 7809-7813 Gi_2 mediates α_2 -adrenergic inhibition of adenylyl cyclase in platelet membranes: *In situ* identification with $\text{G}\alpha$ C-terminal antibodies.
- Skolnik, E.Y., Batzer, A., Li, N., Lee, C.-H., Lowenstein, E., Mohammadi, M., Margolis, B. & Schlessinger, J. (1993a) Science 260 1953-1955 The function of GRB2 in linking the insulin receptor to Ras signalling pathways.
- Skolnik, E.Y., Lee, C.H., Batzer, A., Vicentini, L.M., Zhou, M., Daly, R., Myers, M.J.J., Backer, J.M., Ullrich, A., White, M.F. & Schlessinger, J. (1993b) EMBO-J. 12 1929-1936 The SH2/SH3 domain-containing protein GRB2 interacts with tyrosine-phosphorylated IRS1 and Shc: implications for insulin control of ras signalling.

- Sliker, L.J., Roberts, E.F., Shaw, W.N. & Johnson, W.T. (1990) *Diabetes* 39 619-625 Effect of streptozocin-induced diabetes on insulin-receptor tyrosine kinase activity in obese Zucker rats.
- Smith, D.M., King, M.J. & Sale, G.J. (1988) *Biochem. J.* 250 509-519 Two systems *in vitro* that show insulin-stimulated serine kinase activity towards the insulin receptor.
- Smith, S.A., Cawthorne, M.A., Coyle, P.J., Holder, J.C., Kirkham, D., Lister, C.A., Murphy, G.J. & Young, P.W. (1993) *Diabetologia* 36 (Suppl. 1) A184 (Abstract) BRL 49653 normalises glycaemic control in Zucker (fa/fa) rats by improving hepatic and peripheral tissue sensitivity to insulin.
- Smrcka, A.V. & Sternweis, P.C. (1993) *J. Biol. Chem.* 268 9667-9674 Regulation of purified subtypes of phosphatidylinositol-specific phospholipase C β by G proteins α and $\beta\gamma$ subunits.
- Smyth, D.G. (1967) *Methods in Enzymology* 11 214-231 Techniques in enzymatic hydrolysis.
- Somerharju, P., Paridon, P.V. & Wirtz, K.W.A. (1983) *Biochem. Biophys. Acta.* 731 186-195 Phosphatidyl inositol transfer protein from bovine brain substrate specificity and membrane binding properties.
- Sørensen, S.B., Sørensen, T.L. & Breddam, K. (1991) *FEBS Lett.* 294 195-197 Fragmentation of proteins by *S. aureus* strain V8 protease: ammonium bicarbonate strongly inhibits the enzyme but does not improve the selectivity for glutamic acid.
- Spiegel, A.M., Backlund, P.S., Butrynski, J.E., Jones, T.L.Z. & Simonds, W.F. (1991) *TIBS* 16 338-341 The G protein connection: molecular basis of membrane association.
- Srivastava, S.K. & Singh, U.S. (1990) *Biochem. Biophys. Res. Comm.* 173 501-506 Insulin activates guanosine 5' - [γ - thiol] triphosphate (GTP γ S) binding to a novel GTP-binding, Gir, from human placenta.
- Stabel, S. & Parker, P.J. (1993) *Intracellular Messengers* (Ed. C. W. Taylor) 167-198 Protein kinase C.
- Stern, J.S., Johnson, P.R., Batchelor, B.R., Zucker, L.M. & Hirsch, J. (1975) *Am. J. Physiol.* 228 543-548 Pancreatic insulin release and peripheral tissue resistance in Zucker obese rats fed high- and low-carbohydrate diets.
- Sternweis, P.C. & Smrcka, A.V. (1992) *TIBS* 17 502-506 Regulation of phospholipase C by G proteins.
- Stevenson, R.W., Hutson, N.J., Krupp, M.N., Volkmann, R.A., Holland, G.F., Egger, J.F., McPherson, R.K., Hall, K.L., Danbury, B.H., Gibbs, E.M. & Kreutter, D.K. (1990) *Diabetes* 39 1218-1227 Actions of novel antidiabetic agent englitazone in hyperglycemic hyperinsulinemic ob/ob mice.
- Streb, H., Irvine, R.F., Berridge, M.J. & Schulz, I. (1983) *Nature* 306 67-69 Release of Ca²⁺ from non-mitochondrial stores in pancreatic acinar cells by Ins(1, 4, 5)P₃.
- Strittmatter, S.M., Valenzuela, D., Kennedy, T.E., Neer, E.J. & Fishman, M.C. (1990) *Nature* 344 836-841 Go is a major growth cone protein subject to regulation by GAP-43.
- Stutchfield, J. & Cockcroft, S. (1988) *Biochem. J.* 250 375-382 Guanine nucleotides stimulate polyphosphoinositide phosphodiesterase and exocytotic secretion from HL60 cells permeabilized with streptolysin O.

- Styer, L. & Bourne, H.R. (1986) *Ann. Rev. Cell Biol.* 2 391-419 G proteins: A family of signal transducers.
- Sung, C.K. & Goldfine, I.D. (1992) *Biochem. Biophys. Res. Comm.* 189 1024-1030 Phosphatidylinositol-3-kinase is a non-tyrosine phosphorylated member of the insulin receptor complex.
- Supattapone, S., Worley, P.F., Baraban, J.M. & Snyder, S.H. (1988) *J. Biol. Chem.* 263 1530-1534 Solubilisation, purification, and characterisation of an Inositol Trisphosphate receptor.
- Suter, S.L., Nolan, J.L., Wallace, P., Gumbiner, B. & Olefsky, J.M. (1992) *Diabetes Care* 15 193-199 Metabolic effects of new oral hypoglycemic agent CS-045 in NIDDM subjects.
- Sutherland, E.W. & Rall, A. (1960) *Pharmacol. Rev.* 12 265-286 The relationship of adenosine 3' 5' phosphate and phosphorylase to the action of catecholamines and other hormones.
- Tang, E.K. & Houslay, M.D. (1992) *Biochem. J.* 283 341-346 Glucagon, vasopressin and angiotensin all elicit a rapid, transient increase in hepatocyte protein kinase C activity.
- Tang, E.K., Parker, P.J., Beattie, J. & Houslay, M.D. (1993) *FEBS Lett.* 326 117-123 Diabetes induces selective alterations in the expression of protein kinase C isoforms in hepatocytes.
- Tang, W.J. & Gilman, A.G. (1991) *Science* 254 1500-1503 Type-specific regulation of adenylyl cyclase by G protein beta gamma subunits.
- Tang, W.J. & Gilman, A.G. (1992) *Cell* 70 869-872 Adenylyl cyclases.
- Tapley, P.M. & Murray, A.W. (1984) *Biochem. Biophys. Res. Comm.* 122 158-164 Modulation of Ca²⁺ activated, phospholipid- dependent protein kinase in platelets treated with tumor- promoting phorbol ester.
- Tattersall, R.B. & Gale, E.A.M. (1990) *The new patient.* Churchill Livingstone
- Tavaré, J.M., O'Brien, R.M., Siddle, K. & Denton, R.M. (1988) *Biochem. J.* 253 783-788 Analysis of insulin-receptor phosphorylation sites in intact cells by two-dimensional phosphopeptide mapping,
- Taylor, C.W. (1990) *Biochem. J.* 272 1-13 The role of G proteins in transmembrane signalling.
- Taylor, S.S., Buechler, J.A. & Yonemoto, W. (1990) *Ann. Rev. Biochem.* 59 971-1005 cAMP-dependent protein kinase: framework for a diverse family of regulatory enzymes.
- Tobe, K., Matuoka, K., Tamemoto, H., Ueki, K., Kaburagi, Y., Asai, S., Noguchi, T., Matsuda, M., Tanaka, S., Hattori, S., Fukui, Y., Akanuma, Y., Yazaki, Y., Takenawa, T. & Kadowaki, T. (1993) *J. Biol. Chem.* 268 11167-11171 Insulin stimulates association of insulin receptor substrate-1 with the protein abundant Src homology growth factor receptor-bound protein-2.
- Towbin, H., Staehelin, T. & Gordon, J. (1979) *PNAS* 76 4350-4354 Electrophoretic transfer of proteins from polyacrylamide gels to nitrocellulose: Procedure and some applications.

- Triscari, J., Stern, J.S., Johnson, P.R. & Sullivan, A.C. (1979) *Metabolism* 28 183-189 Carbohydrate metabolism in lean and obese Zucker rats.
- Van der Werve, G., Zaninetti, D., Lang, U., Vallotton, M.B. & Jeanrenaud, B. (1987) *Diabetes* 36 310-314 Identification of a major defect in insulin-resistant tissues of genetically obese (fa/fa) Zucker rats: Impaired protein kinase C.
- Wang, C.-C. & Tsou, C.-L. (1991) *TIBS* 16 279-281 The insulin A and B chains contain sufficient structural information to form the native molecule.
- Wang, J.L., Corbett, J.A., Marshall, C.A. & McDaniel, M.L. (1993) *J. Biol. Chem* 268 7785-7791 Glucose-induced insulin secretion from purified β -cells.
- Wang, Y., Scott, J.D., McKnight, G.S. & Krebs, E.G. (1991) *PNAS* 88 2446-2450 A constitutively active holoenzyme form of the cAMP-dependent protein kinase.
- Watkins, P.J., Drury, P.L. & Taylor, K.W. (1990) *Diabetes and its management*. Blackwell Scientific Publications
- Weinstein, S.P., Holand, A., O'Boyle, E. & Haber, R.S. (1993) *Metabolism* 42 1365-1369 Effects of thiazolidinediones on glucocorticoid-induced insulin resistance and GLUT4 glucose transporter expression in rat skeletal muscle.
- Westermarck, P., Johnson, K.H., O'Brien, T.D. & Betsholtz, C. (1992) *Diabetologia* 35 297-303 Islet amyloid polypeptide - a novel controversy in diabetic research.
- Williamson, F.A. & Morre, D.J. (1976) *Biochem. Biophys. Res. Commun.* 68 1201-1205 Distribution of phosphatidyl inositol biosynthetic activities among cell fraction from rat liver.

Wilson, D.B., Connolly, T.M., Bross, T.E., Majerus, P.W., Sherman, W.R., Tyler, A.N., Rubin, L.J. & Brown, J.E. (1985) *J. Biol. Chem.* 260 13496-13501 Isolation and characterisation of the inositol cyclic phosphate products of polyphosphoinositide cleavage by phospholipase C: physiological effects in permeabilized platelets and limulus photoreceptor cells.

Wolf, M., LeVine III, H., May Jr, W.S., Cuatrecasas, P. & Sahyoun, N. (1985) *Nature* 317 546-549 A model for intracellular translocation of protein kinase C involving synergism between Ca²⁺ and phorbol esters.

Woodgett, J.R. (1991) *Methods in Enzymology* 200 564-577 cDNA cloning and properties of glycogen synthase kinase-3.

Yamane, H.K. & Fung, B.K.-K. (1993) *Ann. rev. Pharm. Tox.* 32 201-241 Covalent modifications of G-proteins.

Yatomi, Y., Arata, Y., Tada, S., Kume, S. & Ui, M. (1992) *Eur. J. Biochem.* 205 1003-1009 Phosphorylation of the inhibitory guanine-nucleotide-binding protein as a possible mechanism of inhibition by protein kinase C of agonist-induced Ca²⁺ mobilization in human platelet.

Yoshimura, M. & Cooper, M.F. (1993) *J. Biol. Chem.* 268 4604-4607 Type-specific stimulation of adenylylcyclase by protein kinase C.

Young, P., Kirkham, D.M., Murphy, G.J. & Cawthorne, M.A. (1991) *Diabetologia* 34 565-569 Evaluation of inhibitory guanine nucleotide regulatory protein Gi function in hepatocytes and liver membranes from obese Zucker (fa/fa) rats and their lean littermates.

Young, P.W., Cawthorne, M.A., Coyle, P.J., Holder, J.C., Holman, G.D., Kozka, I.J., Kirkham, D. & Smith, S.A. (1993) *Diabetologia* 36 (Suppl. 1) A75 (Abstract) Chronic treatment of ob/ob mice with BRL 49653 enhances insulin-stimulated translocation of GLUT4 to the adipocyte cell surface.

Zucker, L.M. & Antoniades, H.N. (1972) *Endocrinology* 90 1320-1330 Insulin and obesity in the Zucker genetically obese rat "fatty".

Zucker, L.M. & Zucker, T.F. (1961) *J. Hered.* 52 275-278 Fatty, a new mutation in the rat.

